INHIBITION OF T-CELL RESPONSES BY MICROBES AND IMMUNE CELLS

Thesis Submitted by

Lorena Preciado Llanes

For

The degree of Doctor of Philosophy

Infection & Immunity Department

Faculty of Medical School

November 2013

ABSTRACT

Some antigens can induce B-cell activation and antibody production without 'T cell help' and hence are called T-independent (TI) antigens. Similarly to bacterial capsular polysaccharides, anti-IgD-conjugated dextran (α-δ-DEX) is a TI type 2 mimic which stimulates B lymphocytes by cross-linking of numerous B-cell receptor molecules. This thesis demonstrates that α-δ-DEX-activated B-cells directly inhibit TCR-induced $CD4^+$ T-cell proliferation and activation *in vitro*. Experiments performed with purified cell populations excluded the possibility of α-δ-DEX acting directly on $CD4^+$ T lymphocytes and confirmed that B lymphocytes exposed to α-δ-DEX for a period of 24 hours become activated and acquire a suppressive phenotype. Interestingly, these suppressor B-cells appear to be effective even when they are present at numbers below the physiological T:B ratio. Although the exact mechanism of action remains obscure, this is the first evidence of TI type 2 antigen activated B-cells mediating inhibition of activation and proliferation of helper T lymphocytes.

Neisseria meningitidis is a bacterium which rarely causes invasive disease and sepsis, but perpetuates colonisation in the nasopharynx by avoiding immune recognition and killing. Because several *N. meningitidis* constituents are TI type 2 antigens and/or provide second signals to B-cells *via* TLRs, it was hypothesized that paraformaldehyde fixed meningococcus could exert immunomodulatory properties. A deep suppression of $CD4^+$ T-cell responses occurred when αCD3-stimulated PBMCs where incubated with small meningococci counts (ratios between 0.1 to 10:1 bacteria per cell). A clear T_H1 cytokine profile and IL-10 secretion was observed in supernatants from these cultures. Interestingly, outer membrane vesicles (OMVs) from *N. meningitidis* and *N. lactamica* replicated the suppression phenomenon induced by the whole organism. Bacterial capsule, lipooligosaccharides and Opa are not responsible for the suppressive effect. Depletion of B-cells, monocytes or NK cells does not reverse the meningococcus-mediated inhibition in PBMC cultures.

Several bacterial components stimulate nitric oxide (NO) production, however *N. meningitidis* can counteract the bactericidal effect of reactive nitrogen intermediates by a partial denitrification pathway. Since NO is also produced as a result of TCR engagement, it was investigated whether NO donation or inhibition could influence $CD4^+$ T-cell responses. A novel specific eNOS inhibitor (Cavtratin) derived from the caveolin-1 structure was tested for the first time in PBMC cultures. Cavtratin concentrations of 10 and 15 μM increases proliferation of $CD4^+$ T lymphocytes and reduce the percentage of cell death in the PBMC culture after anti-CD3 stimulation.

ACKNOWLEDGEMENTS

This piece of work would not have been possible without the encouragement and support from many people.

- My supervisors Prof. Robert C Read and Prof. Andrew Heath for their invaluable support, patience, motivation and guidance during this scientific journey that was completely new to me back in 2009. In particular, I would like to thank them for instilling in me confidence and courage to complete my PhD. Because they cared about my professional success and helped me to get involved into the scientific environment. I will miss the lengthy meetings and millions of emails back and forward between us.
- To CONACyT and SEP in Mexico for funding me. I do appreciate the effort is done in my country to send students abroad and I do believe I will be able to pay back to them with work in the future.
- To all the volunteers who kindly donated blood for my experiments. In particular, all the staff in OPAT at the Royal Hallamshire Hospital. They always welcomed me with a smile and made my Tuesdays and Thursdays early mornings less painful.
- To Sue Newton and Kay Hopkinson at the Flow Cytometry Facilities. They were essential staff members in my battle against the LSRII and the always broken red laser.
- My colleagues and friends from the research office and labs in L-floor….it was such a nice break to relax and have funny conversations with everyone! They made my daily work more enjoyable, even considering all the jokes about me being Mexican. Particularly, I would like to thank to my close friends Martin “Martinico”, Laura, Risat, Jones, Ed, Paul Collini, Dr. Jon Shaw and Cathy. Also to those friends who have already changed directions away from Sheffield but whom were essential for my “survival” in those early years: Jay, James, Luke and Kimberley. It does not matter that they sometimes ran away from me because they did not want to donate some blood for my experiments!
- To everyone in the Mexican and Latin American Society for creating a little Mexico here in Sheffield. Our parties, dancing and food are beyond comparison. I never been so proud to be Mexican!
- To my “almost“ sisters Fernanda, Laura and Tessabelle. To Fer and Lau because they became my family here in UK. Those trips made en “la vacacion” and the Saturdays shopping at Meadowhall or having nice simple meals (maybe some gorditas!), were critical to put me back on my feet when I was feeling lonely or sad...”nos tomamos un poptel?”. To my favourite

Maltese ever Tessa. For her crazy shouting, her spontaneous laugh, her support at the lab and her unquestionable friendship since 2008. She was my very first friend in the UK.....ILLALLU! Hope we will have some more adventures to share at the house with “dangerous stairs”.

- To David, for his motivating words and all the help he gave me unconditionally in the last year. You has taught me how to get passion for living and enjoy the world. I really hope we get more adventures together (not Flow cytometry!). Te quiero con todo my heart!
- Lastly but with all my love, I dedicate my PhD to my parents. Those Sundays at 5pm on Skype were my very special family moment. Without my parent’s unconditional love and support it would have been impossible to achieve this. I do appreciate all the sacrifices they have made for me. Gracias mami, because regardless of the distance you have always been there to love me and take care of me. You are my model of devotion, dedication, compassion and fortitude. Gracias papi, for your patience and unconditional support. You have given me wings to go around the world and have never said no when I needed you. I will be always thankful and I will be there for you when you need me back. Thank you both for being an example of life for me.

“We are made wise not by the recollection of our past,

but by the responsibility for our future...”

George Bernard Shaw

CONTENTS

LIST OF FIGURES

CHAPTER 1

CHAPTER 2

CHAPTER 3

CHAPTER 4

CHAPTER 5

LIST OF TABLES

LIST OF ABBREVIATIONS

α-δ-dex	Anti-IgD conjugated dextran
APC	Antigen presenting cell
BCR	B-cell receptor
Breg	B regulatory cell
CBA	Cytokine bead array
CFSE	Carboxyfluorescein diacetate succinimidyl ester
ConA	Concanavalin A
DMSO	Dimethyl sulfoxide
E.coli	*Escherichia coli*
FACS	Fluorescence activated cell sorting
FSC-A	Forward scatter area
GSNO	*S*-nitrosoglutathione
IgD	Immunoglobulin class D
IgM	Immunoglobulin class M
IFN-γ	Interferon gamma
IL	Interleukin
L-NAME	Nω-Nitro-L-arginine methyl ester hydrochloride
L-NMMA	NG-monomethyl L-arginine citrate
LOS	Lipooligosaccharides
LPS	Lipopolysaccharide
MFI	Median fluorescence intensity
MHC	Major histocompatibility complex proteins
MID	*Moraxella* IgD-binding protein
N. meningitidis	*Neisseria meningitidis*
NF-κβ	Nuclear factor kappa beta
NO	Nitric oxide
NOS	Nitric oxide synthase
Opa	Opacity associated adhesin
PBMC	Peripheral blood mononuclear cells
PBS	Phosphate buffered saline
SEB	*Staphylococcus* enterotoxin B
SEM	Standard error of the mean
SSC-A	Side scatter area
S. pneumoniae	*Streptococcus pneumoniae*
TCR	T-cell receptor
TD	T-cell dependent
T_H	Helper T-cell
T_H1	Helper T-cell subset 1
T_H2	Helper T-cell subset 2
TI	T-cell independent
TLR	Toll-like receptors
TNF-α	Factor de necrosis tumoral alfa
Treg	T regulatory cell
µl	Microliter
µM	Micromolar
µg	Microgram

CHAPTER 1:

INTRODUCTION

1.1 ADAPTIVE IMMUNE RESPONSES

1.1.1 Innate and adaptive immune system

Since the early 1890s, two distinctive immune systems were identified: the innate and the adaptive. The innate immune response is a rapid first line of defence, recruits immune cells and triggers inflammation at the site of infection. Dendritic cells, macrophages, monocytes, neutrophils, eosinophils, basophils, mast cells and natural killers all play a role in the innate immunity. Most of the cells from this system recognise and pick up common microbial constituents through pattern recognition receptors, such as Toll-like receptors, scavenger receptors, mannose and glucan receptors (Janeway & Medzhitov 2002). Apart from the well known phagocytosis, secreted preformed molecules such as antimicrobial enzymes (lysozyme, phospholipase A_2), antimicrobial peptides (defensins, cathelicidins and histatins) and the complement system, are mechanisms that the innate system uses for the lysis of microorganisms.

In contrast, the adaptive immune system evolves during the lifetime of an individual, specifically targeting pathogens or its products and providing long-term protection (immunological memory). Adaptive immune responses are initiated in peripheral lymphoid tissues where antigen presenting cells (APCs) or free antigens become in contact and induce activation of T and B lymphocytes, respectively. T and B lymphocytes are the effector cell types of the adaptive immune system. T-cells produce regulatory pro/anti-inflammatory cytokines and lyse infected cells, whereas B-cells are specialised in producing antibodies.

Even though the adaptive and innate immune systems are functionally different, they work together in a sequence of events integrating a complex cooperation network to mount the offensive against invasive microorganisms.

1.1.2 T lymphocytes

T lymphocytes undergo their maturation and differentiation in the thymus, where self-reactive cells will be eliminated whilst functional competent cells capable of recognising foreign antigens are selected and allowed to mature (Carpenter & Bosselut 2010).

T lymphocytes recognise antigens and become activated by engagement of their T-cell receptor (TCR). TCR is a complex of membrane proteins, composed of ligand-sensing subunits (α and β)

which determine the affinity for antigens and three proximal CD3 signalling dimers (γε, δε and ζζ) (Call et al. 2002; Janeway 1992). It is in the thymus where the gene rearrangement of α and β chains occurs by random association of genes, resulting in a large TCR diversity (10^{15}) against antigens (Delves & Roitt 2000).

Through a major histocompatibility complex (MHC), APCs will expose antigenic peptides to T-cells and trigger the TCR-dependent intracellular signalling that leads to activation, proliferation and differentiation into effector T-cells (section 1.1.4). T-cells can also be activated by certain mitogens which non-specifically bind to TCR but induce proliferation of T-cells. For example, phytohaemagglutinin (PHA), concanavalin A (ConA) and superantigens such as staphylococcal enterotoxin B (SEB).

1.1.2.1 T-cell subsets

Based on the expression of surface markers and their function, Dong & Martinez (2010) have described 10 distinctive T-cell subsets: Naive, Helper, Cytotoxic, Regulatory (Treg), Natural killer T (NKT), Memory, CD8αα, γδ T, Exhausted and Anergic. Although it was originally considered that T-cells will differentiate into only one effector subset, nowadays many T-cells have been characterised and reported to evolve from one phenotype to another or to be a mixture of two subsets. Such quality has received the name of "T-cell plasticity" (Hirahara et al. 2013). In this section however, we will only revise some of the major populations.

Depending on their restriction to bind to MHC class I or II is that thymocytes differentiate into $CD8^+$ or $CD4^+$, respectively (Carpenter & Bosselut 2010). Naive T lymphocytes (either $CD4^+$ or $CD8^+$) are cells that have not encountered their specific antigen yet; they have just left the thymus and started traffic towards lymphoid tissue. Once in contact with the antigen they become effector cells and preferentially migrate to peripheral tissues. The function of $CD8^+$ Cytotoxic T-cells is to kill infected cells expressing pathogenic molecules on the surface of MHC class I. Cytotoxic T-cells destroy infected cells by inducing apoptosis via death-receptors ligation (mainly Fas) and by delivering cytotoxic granules (containing granzymes and perforin) into endosomes which get released in the cytoplasm of the affected cell (Harari et al. 2009; Russell & Ley 2002; Rouvier et al. 1993). In contrast, $CD4^+$ Helper T-cells recognise molecules on MHC class II and their function is not to kill but to regulate other immune cells.

Depending on the cytokines they produce and their function, Helper $CD4^+$ T lymphocytes can further differentiate into T_H1, T_H2, T_H9, T_H17, T_H22, T_{FH} (follicular) or iTreg (antigen-induced Treg) .

Whether a T_H differentiates along any of these pathways is influenced by many factors, such as: the amount, type and affinity of antigen recognition, the APC which presents the antigen, the cytokine environment, and direct DNA or histones modifications (epigenetics) (Hirahara et al. 2013; Kaiko et al. 2008).

After exposure to two different antigens, Del Prete et al (1991) corroborated the existence of two opposite T Helper populations in humans: T_H1 and T_H2, which were previously described in mouse (Mosmann & Sad 1996; Mosmann et al. 1986). T_H1 are characterised by IL-2, IFN-γ and TNF-β production, thus evoking a cell-mediated immunity and phagocyte-dependent inflammation. T_H2 secrete IL-4, IL-5, IL-6, IL-9, IL-10 and IL-13 which promote IgE antibody production. IFN-γ, IL-12 and TGF-β drives T_H1 development, whilst IL-4 induces T_H2 differentiation. After commitment into one lineage, cytokines produced by one pathway will switch off the cytokine gene transcription of the other pathway (Nakamura et al. 1997). For example, IL-4 from T_H2 cells promotes a T_H2 response but inhibits expression of the IL-12 receptor crucial for T_H1 cells; whereas IFN-γ from T_H1 inhibits T_H2 responsiveness. Cell mediated T_H1 responses are mainly involved in the clearance of intracellular organisms and in the pathogenesis of organ autoimmune diseases (delayed hypersensitivity responses). Humoral T_H2 responses have been associated with allergic disorders such as asthma (Akdis et al. 2004; Walker et al. 1991) and are important for the clearance of extracellular pathogens. It has been suggested that if naive T-cells get primed by dendritic cells they will tend to a T_H1 differentiation; whilst priming by B-cells will lead a predominant T_H2 lineage (Hilkens et al. 1997; Macaulay et al. 1997; Stockinger et al. 1996; Heufler et al. 1996). However, the T_H1/T_H2 outcome seems to be more complex, as a reciprocal feedback occurs between the T-cell and the antigen presenting cell (Rissoan et al. 1999).

T_H17 cells were identified by the production of large quantities of the pro-inflammatory cytokine IL-17 (IL-17A and IL-17F), IL-21 and also by the induction of many chemokines (Bettelli et al. 2008; Park et al. 2005). The simultaneous presence of TGF-β and IL-6 initiates T_H17 differentiation, but it is IL-23 and IL-21 that maintain their development. In contrast, products of the T_H1 and T_H2 lineages (IL-12, IL-4 and IFN-γ) block T_H17 development (Harrington et al. 2005; Park et al. 2005). Since the T_H17 subset also secretes IL-6, IL-1β, TNF-α and nitric oxide; T_H17 cells have been implicated in autoimmune diseases involving neutrophil recruitment, metalloproteinases activity and subsequent tissue inflammation, such as encephalomyelitis (Bettelli et al. 2008; Park et al. 2005; Langrish et al. 2005).

Firstly described by the Sakaguchi group (1995), T-regulatory cells (Treg) have acquired major importance in the last decade due to their role as downregulators of immune responses and

maintenance of self-tolerance, as lack of Tregs in the periphery results in T-cell mediated autoimmunity and allergic disorders (Sakaguchi et al. 2008). Foxp3 was found to be the transcription factor responsible of the development and suppressive function in Tregs (Fontenot et al. 2003). Tregs can be naturally created in thymus or induced in periphery from naive T_H. A Treg suppressive phenotype with induction of Foxp3 in naive helper cells can be achieved in the presence of IL-2 together with TGF-β1 and can be synergized by retinoic acid produced by dendritic cells in the gut (Benson et al. 2007; Marie et al. 2005; Fantini et al. 2004). Activated Tregs express high amounts of the surface receptors CD25 (IL-2Rα) and CTLA-4 (Shevach 2009). After antigen-stimulation Tregs mediate suppression by secretion of anti-inflammatory cytokines (IL-10, TGF-β, IL-35), by repression of IL-2, IL-4 and IFN-γ, by cell cycle arrest, by inducing anergy or by cytolisis (Shevach 2009; Sakaguchi et al. 2008; Taylor et al. 2006).

Follicular Helper T-cells (T_{FH}) only produce small amounts of cytokines but are specialised in travelling to lymphoid nodes and germinal centres to provide support to B-cells in the production of IgA and IgG antibodies (Breitfeld et al. 2000). Thus, T_{FH} are associated to the expression of several molecules important for B-cell co-stimulation ($CXCR5^{high}$, $ICOS^{high}$, $PD1^{high}$, $BTLA^{high}$, $CD200^{high}$, $SLAM^{low}$). A type I Interferon signalling in dendritic cells and T-B interactions with expression of the transcription factor Bcl6 drive T_{FH} development (Johnston et al. 2009; Cucak et al. 2009).

T_H9 is a recently identified T-helper subset that preferentially secretes IL-9 (Dardalhon et al. 2008), which is involved in the resistance against parasites but is pathologically present in allergic airway and gut diseases (Staudt et al. 2010). Although they also produce IL-10, no suppressive properties have been observed in this population (Dardalhon et al. 2008). T_H9 differentiation is initiated by a combination of TGF-β and IL-4 (Stassen et al. 2012), but it is the expression of the transcription factor Interferon regulatory factor 4 (IFR4) that leads IL-9 production in these cells (Staudt et al. 2010). *In vivo*, IL-9 enhances the activity of mast cells, induces mucus and chemokine production in lung epithelial cells, expands the B-cell subset 1 and increases secretion of IgE and IgG (Stassen et al. 2012).

Finally, the T_H22 subset is characterised by their large IL-22 secretion and moderate amounts of IL-10, IL-13 and TNF-α (Eyerich et al. 2009; Trifari et al. 2009). IL-1β and IL-23 lead to the development of IL-22 producing T-cells from naive T-cells (Trifari et al. 2009). IL-22 is a member of the IL-10 family, which in combination with TNF-α seem to play an important role in the activation of keratinocytes. Thus, is believed to influence regenerative and inflammatory responses in skin conditions, such as psoriaris (Eyerich et al. 2009 Trifari et al. 2009).

Even though each of the T_H subsets are represented by key regulators or features, recent evidence has shown that it is not infrequent for one cell to contain more than one key regulator or marker. Indeed, this 'subset' approach might be over-simplistic and underestimates the plasticity of T_H cells (Hirahara et al. 2013). Moreover, balance between subsets of T-helper is delicate and broken balance (such as less Tregs and more Th1 or Th2) can lead to disease (Akdis et al. 2004). Some publications suggest that the strong activation signals overcome the downregulation of Tregs and so they propose it will be possible to treat allergic disorders by increasing Tregs and decreasing Th2 simulatenously (Ling et al. 2004).

Figure 1.1 illustrates an overview of some of the effector Helper T-cells.

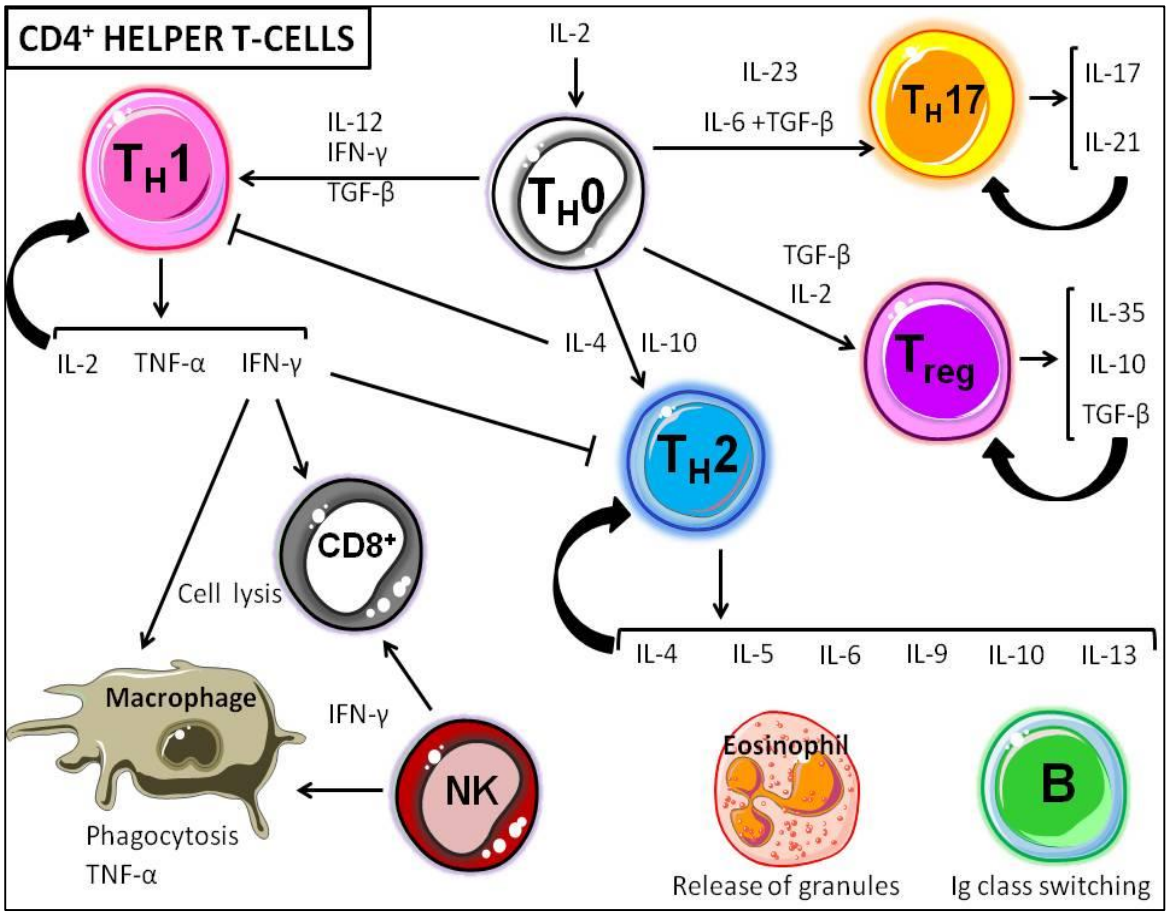

Figure 1.1: Major CD4⁺ T-cell subsets and their cytokines.

Upon antigen presentation and in the presence of IL-2, T_H0 cells polarize into one of the several T_H subsets. Depending on the cytokines present at the environment, T_H0 can differentiate into T_H1, T_H2, T_H17 or Treg among others. Cytokines produced by these subsets will have secondary effects on cells from the innate and adaptive immune system.

T_H = Helper CD4⁺ T-cell; CD8⁺= Cytotoxic CD8⁺ T-cell; Treg= T-regulatory cell; B= B-cell; NK= Natural killer cell.

1.1.3 B lymphocytes

B lymphocytes are produced and differentiated in the bone marrow through the immature stages pro-B and pre-B where the rearrangement of immunoglobulin genes occurs until reaching complete maturity (Delves & Roitt 2000). Auto-reactive B lymphocytes are eliminated in the bone marrow, while mature effective B lymphocytes are sent to the circulation to finally home in peripheral lymphoid tissue.

B lymphocytes are well known by their ability to produce antibodies that directly neutralise the pathogenic action or antibodies which opsonise the microorganism facilitating phagocytosis and complement-mediated killing. Antibodies can be induced by previous infections or vaccination and play an important role in secondary responses. B lymphocytes can also perform as APCs displaying the antigen to T-cells and driving their differentiation (section 1.1.4), in particular late at the primary response or in a secondary response (Rivera et al. 2001). In this respect, recent evidence has elucidated the importance of B-cells as regulators of T-cells.

B-cells can modulate the intensity and quality of the T-cell response to antigens via antibody-independent mechanisms, such as secretion of cytokines or direct cell-contact (co-stimulatory molecules). Upon antigen recognition, effector B-cells can secrete cytokines which lead to polarization of naive $CD4^+$ T lymphocytes into T_H1 or T_H2 (section 1.1.2.1). The importance of B regulation has been recognised in several T-cell mediated autoimmune disorders, either by influencing T_H differentiation, T-cell activation or the number of Treg (Lund & Randall 2010). Moreover, B-cells have been considered essential effectors in the regulation of T-cell expansion (Crawford et al. 2006; Linton et al. 2003), T-cell re-activation and generation of long-term T-cell memory against certain virus (Whitmire et al. 2009; Iijima et al. 2008; Thomsen et al. 1996). A mouse model of encephalomyelitis which depleted B-cells before and after the instalment of the disease, determined a biphasic therapeutic role of B-cells capable of suppressing or exacerbating auto-reactive T-cells over the course of the autoimmune disease (Matsushita et al. 2008).

1.1.3.1 B-cell subsets

B effector-1 cells (Be-1) secrete IFN-γ, IL-12, IL-10, IL-6 and TNF-α which enhance T_H1 differentiation and further production of T_H1 cytokines. Be-1 cells are present in mucosal tissue, pleural and peritoneal cavities, and their differentiation is not driven by T lymphocytes (Lund & Randall 2010; Harris et al. 2000).

In contrast, B effector-2 cells (Be-2) secrete IL-2, Lymphotoxin-α, IL-4 and IL-13 in large concentrations, but minimal amounts of IL-10, TNFα and IL-6 (Lund & Randall 2010; Harris et al. 2000). Thus, Be-2 cells can act as APCs and exert a preferential T_H2 differentiation (Macaulay et al. 1997). Be-2 cells are the main B population found in peripheral lymphoid organs and their development is dependent on T cells that produce IL-4 and engagement of CD40 as well as CD80/CD86 molecules (Harris et al. 2005) (section 1.1.4.3).

B-regulatory cells (Bregs or B10) are a newly accepted subset of B-cells with immunoregulatory/immunosuppressive properties (Mauri & Bosma 2012), present in small numbers in spleen and peritoneal cavity but rare in blood or lymph nodes (Matsushita et al. 2008). The inhibitory function of Bregs is mediated to a great extent through IL-10 secretion (Bouaziz et al. 2010; Fillatreau et al. 2002). However, TGF-β1 production, cell-contact suppression via CD40 or CD80/86 molecules, dampening of dendritic cell activity and neutralising antibodies against harmful factors are also well supported mechanisms of downregulation (Blair et al. 2010; Mizoguchi & Bhan 2006). IL-10 is a suppressive cytokine which blocks T_H1 polarization by suppressing IL-12, also downregulates pro-inflammatory cytokines (TNF-α, IL-1, IL-6 and IL-8) produced by neutrophils, macrophages and other ganulocytes, and suppresses antigen presentation (Asadullah et al. 2003). An interaction T-B cell is essential to occur, as the main stimulus for IL-10 production in Bregs is provided by CD40 engagement (Blair et al. 2010). Nowadays, Bregs have been phenotypically identified by a combination of markers, such as $CD5^+$ $CD19^{high}$ $CD24^{high}$ $CD38^{high}$ $CD1d^+$ (Mauri & Bosma 2012; Blair et al. 2010; Yanaba et al. 2008).

Plasma cells are terminally differentiated end-stage cells, they do not divide and their lifespan is between few days up to months. Their main function is antibody production and these cells lack many of their development transcription factors and the receptors for antigen presentation (Calame 2001). XBP-1 and Blimp-1 are key transcription factors for the differentiation of B-cells into antibody-secreting plasma cells within lymph nodes (Reimold et al. 2001; Turner et al. 1994).

Memory B-cells are mature long-lived cells mainly originated at the germinal centres and which can be re-activated to become plasma cells after secondary challenge. Their main feature is to go under Ig class switching (section 1.1.3.2) and produce highly specific antibodies for a long period of time. Development of a memory B-cell requires T-cell co-stimulation or 'help', particularly through binding of their CD40 receptor (sections 1.1.4.3 and 1.1.5.1) and by some T-derived cytokines such as IL-4, IL-5 and IL-6. Although markers for this subset seem to be highly heterogeneous, loss of IgD and expression of CD27 and/or IgG can be considered good indicators

of B-cell memory. Achievement and maintenance of memory is driven by several factors, such as the antigen's characteristics and the strength of the immune response (Yoshida et al. 2010).

Figure 1.2 illustrates the cytokine profile and the action of these B-cell subsets.

1.1.3.2 Antibodies

Antibodies (secreted immunoglobulins) are proteins produced by the terminally differentiated and effector B lymphocyte or plasma cell (section 1.1.3.1). Although some antibodies can directly neutralise pathogens or toxins, others coat the surface of the pathogen to facilitate phagocytosis (opsonisation) or induce complement activation to destroy bacteria by permeabilising the cell-wall.

Based on their heavy chain, five different classes of immunoglobulins (Ig) with different biological properties are produced. IgM is the first class expressed by immature B lymphocytes in bone marrow, is the most widely secreted Ig in primary antibody responses. IgD is expressed on the cell surface together with IgM, and denotes B-cell maturity to respond to antigen in peripheral lymphoid organs (naive B-cells). IgG is secreted in large quantities in secondary humoral responses, activates the complement system and is the only one capable to confer passive immunity to fetus by crossing the placenta barrier. IgA is the most abundant in saliva, tears, milk, respiratory and gut secretions. Secreted IgE binds to the surface of mast cells and basophils as passive receptor of antigens, leading to their activation and secretion of histamine and cytokines.

In germinal centres, upon activation of B lymphocytes by the antigen, membrane IgD is lost and B-cells can either produce just IgM or 'class switch' to other Ig class. Class switching occurs followed by DNA recombination and somatic hypermutation (point mutations), which together aim to produce new IgG, IgA or IgE with higher affinity for a specific antigen and memory cells (Shih et al. 2002; Liu et al. 1996). Indeed, this secondary antibody response lasts longer and results in higher titers.

1.1.3.3 B-cell receptor engagement

The B-cell receptor (BCR) is comprised by a membrane bound immunoglobulin which confers the antigen recognition and two adjacent subunits (Igα and Igβ) in charge of downstream signalling. Diverse specificities of the antigen receptors are produced by gene rearrangements during the early developmental stages of the lymphocyte, but further diversity takes place by splicing as B-

cells continue to mature (Delves & Roitt 2000). The BCR of mature B lymphocytes is composed by membrane-bound IgD and IgM, but is the former the one that has been attributed with the most of the signalling properties (Geisberger et al. 2006; Kim & Reth 1995).

B cells become activated via BCR cross-linking after encountering an antigen. The outcome of the

BCR engagement is influenced by a combination of factors, such as positive and negative regulators or co-stimulatory molecules, the abundance of the antigen, the antigenic epitopes and the extension of the BCR cross-linking. Moreover, it has been proposed that the strength of the BCR signal received by the antigen sets a threshold of susceptibility to self-reactivity that varies in each individual (Grimaldi et al. 2005).

The intracellular cascade after BCR engagement starts with the phosphorylation of the Igα and Igβ tyrosine-based activation motifs (ITAMs) by protein kinases of the Src family. This event recruits and activates Syk, a tyrosine kinase that activates other targets such as BLNK, phospholipase C-γ and the Bruton's tyrosine kinase (Btk). This leads to inositol triphosphate (IP_3) production and subsequent Ca^{2+} release, which activates the protein kinase C cascade and downstream nuclear transcription factors, such as NF-κβ and the nuclear factor of activated T-cells (NFAT) (Dal Porto et al. 2004). The mitogen activated protein kinase (MAPK) is a Ca^{2+}-independent downstream pathway also involved after BCR engagement, especially though its member ERK (Gauld et al. 2002).

BCR is further modulated by a co-receptor complex formed by CD19, CD22 and FcγRIIB (Grimaldi et al. 2005). CD19 is a transmembrane glycoprotein which stays in proximity with BCR, gets phosphorylated upon BCR engagement and helps IgM/IgD receptor-antigen microclusters formation (Depoil et al. 2008). CD19 works as an adaptor-like protein, initiates activation of phosphatidylinositol 3-kinase (PI-3K) needed for Ca^{2+} mobilisation and also establishes BCR-mediated Btk activation (Fujimoto et al. 2000; Buhl & Cambier 1999; Tuveson et al. 1993). In contrast, CD22 has tyrosine-based inactivation motifs (ITIMs) which if get activated by Lyn (a member of *Src* family), they result in inhibition of BCR signalling (Cornall et al. 1998). With a similar Lyn mechanism as CD22, FcγRIIb is another negative regulator of antigen-induced B-cell activation, acting by limiting Ca^{2+} mobilisation and preventing IP_3 accumulation (Nakamura et al. 2000).

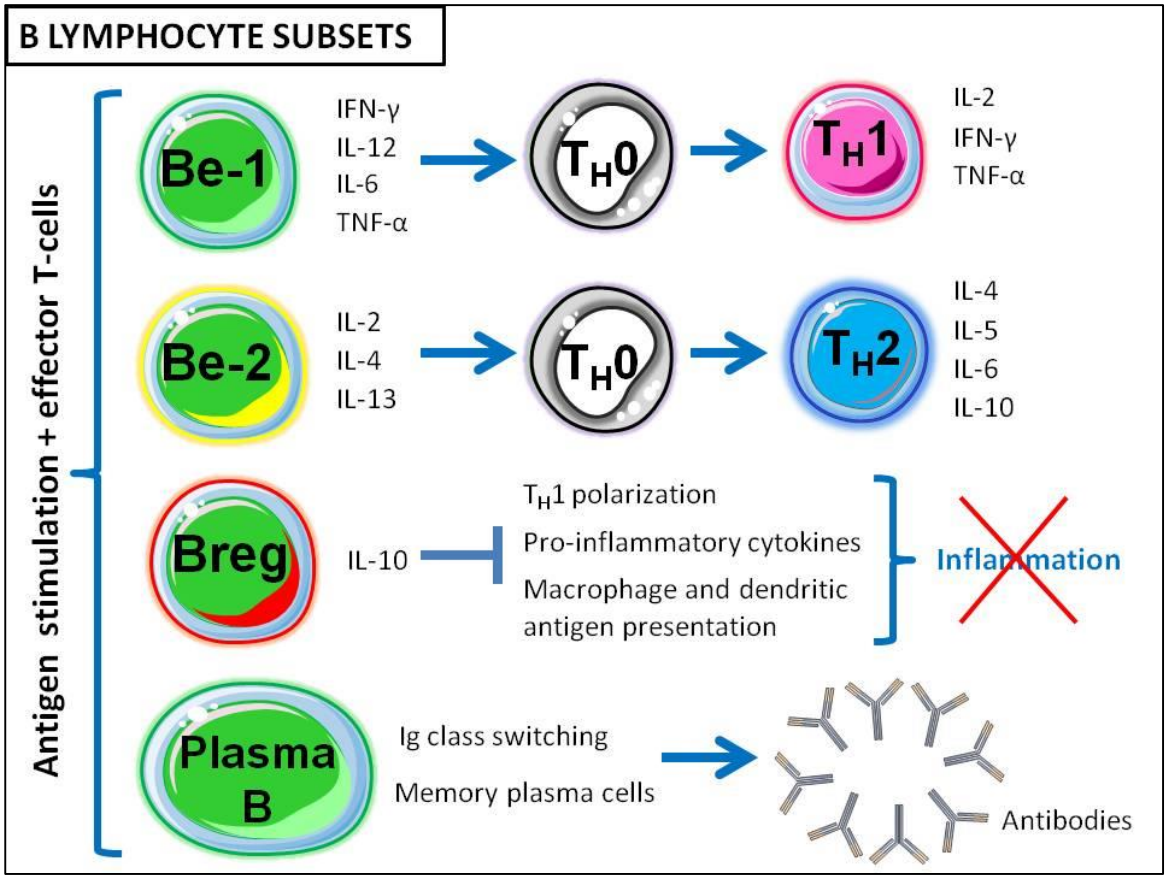

Figure 1.2: Major B-cell subsets and their role.

Upon antigen recognition or contact with effector T-cells, B lymphocytes become effector cells. Cytokines produced by the subsets Be-1 and Be-2 induce polarization of T-cells into T_H1 and T_H2, respectively. Breg exerts inhibitory properties mainly *via* IL-10 secretion. Antibody production and immune memory are the major roles of plasmatic B-cells.

Be= Effector B-cell; Breg= B-regulatory cell; T_H = Helper $CD4^+$ T-cell.

1.1.4 Interactions between antigen presenting cells and T lymphocytes

For a T lymphocyte to become activated, it requires to be exposed to its TCR specific antigen and a series of co-stimulatory signals. Antigen presenting cells (APCs) will accomplish this task by taking up the pathogen (section 1.1.4.1) and then processing it into peptides that can be displayed in MHC molecules on the cell surface (section 1.1.4.2). Once the MHC bound peptide gets in contact with the antigen-binding site of the TCR, several molecules will intervene to stabilise the interaction and to provide further co-stimulation to the T-cell (section 1.1.4.3). Finally, T-cell signal transduction pathways will be initiated to produce transcription factors needed for T-cell activation and differentiation (section 1.1.4.4).

1.1.4.1 Pathogen recognition by APCs

Dendritic cells, macrophages and monocytes are all APCs specialised in the phagocytosis and destruction of pathogens but incapable of developing immunological memory. APCs take up the antigen by either phagocytosis (complement-mediated), macropinocytosis (liquid egulfment) or by using signalling receptors.

APCs recognise pathogens though a set of constitutively expressed pattern recognition receptors (PRRs). Common microbial constituents known as pathogen-associated molecular patterns (PAMPs) are molecules detected by PRRs. From all the PRRs, Toll-like receptors (TLRs) are the best characterised and can be found in several immune cells, such as dendritic cells, macrophages, B lymphocytes and even some subsets of T lymphocytes. TLRs can be expressed extracellularly or associated to intracellular vesicles, but upon antigen recognition all lead downstream signalling cascades via one of the 4 adapters (MyD88, TRIF, TRAM or TIRAP). In humans, 10 different TLRs have been identified and categorised depending on the molecules they target. For example the extracellular located TLR-1, TLR-2 and TLR-6 mainly bind to lipoproteins; whilst TLR-3 TLR-7, TLR-8 and TLR-9 are intracellular and bind to double or single stranded nucleic acids (Akira et al. 2006). Of relevance is the extracellular TLR-4 which recognises LPS and heat shock proteins, both involved in the pathogenesis of sepsis (Lu et al. 2008; Leon et al. 2008). From the TLR adapter molecules MyD88 is the most common to all TLRs, although combinations among the other adapters are also common. In general, TLRs pathways culminate with the activation of NF-κβ and MAP kinase, which in turn induce transcription of pro-inflammatory cytokines (Kawai & Akira 2011).

As mentioned previously, B-cells can function as competent APCs (Chesnut & Grey 1981) priming naive T-cells preferentially with proteins (Constant et al. 1995) and being almost as effective as dendritic cells (Cassell & Schwartz 1994). In contrast to the innate APCs, B-cells recognise and perform endocytosis of the antigen through their BCR. Indeed, B lymphocytes do not phagocytose the antigen and only use the TLRs as accessory activation signals (section 1.1.5.2.1). Furthermore, it has been published that the same TLR stimulation results in a distinctive cytokine profile between dendritic cells and B-cells, as they seem to prefer distinct signalling pathways (Barr et al. 2007).

1.1.4.2 Processing of antigen and its expression on MHC molecules

Once the antigen is internalised by the APC, pathogens will get degraded into small peptides that can be bound to MHC molecules. Finally, the complex antigen-MHC is exported to the cell surface.

The two MHC molecules differ in their cellular distribution, structure and function. MHC class I is contained in every cell type in the body, apart from erythrocytes; whilst MHC class II is restricted to dendritic cells, macrophages, monocytes and B-cells. MHC class I molecules bind to peptides from intracellular pathogens that have been degraded in the cytosol by the proteasome, for example viruses (Grommé & Neefjes 2002). In contrast, MHC class II bind to peptides from extracellular pathogens that have been degraded by digestive enzymes in endocytic acidified vesicles, such as most bacteria (Villadangos 2001). In the case of B-cells, the cross-linked BCR is rapidly internalised into early endosomes and finally transported to reach the MHC class II loading compartments (Cheng et al. 1999).

APCs expressing MHC class I will present the antigen to $CD8^+$ Cytotoxic T lymphocytes, whereas the ones with MHC class II will present to $CD4^+$ Helper T lymphocytes. Although B lymphocytes and macrophages constitutively express high levels of MHC class II, dendritic cells are the most specialised in antigen processing and presentation to naive T-cells. Dendritic cells can present on MHC class I or II molecules, are able to phagocyte any pathogen and constitutively express co-stimulatory molecules for T-cells.

1.1.4.3 TCR activation and the need of co-stimulatory molecules

The activation process starts when an APC become in physical contact with a T lymphocyte, so the first activation signal is provided when the MHC bound peptide is recognised by its specific TCR. As mentioned in section 1.1.2, TCR is formed by the antigen binding region (chains α and β) in co-

expression with the CD3 signalling dimers (γε, δε and ζζ). Upon TCR ligation, protein kinases become activated and trigger production of transcription factors (section 1.1.4.4).

Beyond the binding between MHC and TCR, a second signal via several co-stimulatory ligands/receptors pairs and adhesion molecules is required to achieve complete T-cell activation, differentiation and expansion (Schwartz 1990; Huet et al. 1987). If no specific binding occurs between the MHC-bound peptide and the TCR, the cells will rapidly dissociate. However, if the TCR has encounter a compatible antigen then TCR signalling will be triggered (1^{st} signal) and additional co-stimulation (2^{nd} signal) will take place to make the interaction more durable. If only the first TCR signal is provided the T lymphocyte will enter into anergy/tolerance; indeed, naive lymphocyte must engage both antigen and co-stimulatory ligands on the same APC. A reciprocal constant regulation between APCs and T lymphocytes occurs through co-stimulatory molecules and cytokines.

During the contact between APC and T-cell, TCR-CD3 complexes cluster on the cell surface to be in close contact with MHC molecules, facilitating also intracellular kinases to interact with the cytoplasmic domains (Dustin 2008; Monks et al. 1998). Simultaneously, the co-receptors CD8 and CD4 bind to the invariant lateral region of the MHC class I and II, respectively. Since CD4/CD8 are physically associated to the TCR, their binding helps in stabilising the MHC-TCR interaction (Janeway 1992). In addition, the intracellular adhesion molecule 1 (ICAM-1) is known to be central to achieve a persistent polarization between APC and naive T lymphocyte (Dustin 2008).

Just after the specific antigen-TCR ligation takes place, T Helper lymphocytes upregulate expression of the integral membrane protein CD154 (also known as CD40 ligand or CD40L). CD40L binds to the transmembrane glycoprotein CD40 present on dendritic cells and B lymphocytes. This provides a feedback signal to boost their maturation increasing their antigen presentation capacity, to perpetuate APCs survival and to induce cytokine production (Quezada et al. 2004). Moreover, CD40 engagement enhances clonal expansion of B-cells, triggers their Ig class switching and generates long-lived/memory plasma cells (Elgueta et al. 2009; Garside et al. 1998; Allen et al. 1993). As discussed in section 1.1.5.1, is this cognate interaction what defines a T-dependent B-cell response. Reciprocally, the APC will upregulate co-stimulatory molecules to induce T_H differentiation, proliferation and cytokine production. Therefore, blocking of CD40L with a monoclonal antibody results in deep suppression of T responses via diverse mechanisms; for example, by abolishing the CD40-dependent IL-12 production from APCs (Stuber et al. 1996). Manipulation of the CD40/CD40L has been studied for the treatment of autoimmune disorders, to enhance tolerance in transplants and to target cancer cells (Elgueta et al. 2009; Quezada et al.

2004). In addition to the above mentioned, the OX40L molecule upregulated on B-cells after CD40 ligation, has been implicated in T-cell expansion, survival and T_H2 development (Linton et al. 2003; Gramaglia et al. 2000).

CD28 is expressed constitutively on most of the $CD4^+$ Helper T-cells and on 50% of the $CD8^+$ Cytotoxic T-cells. CD28 is a strong co-stimulatory molecule for T-cells as gets involved with the TCR signalling to boost proliferation, cytokine production (particularly IL-2) and resistance to apoptosis (Rudd et al. 2009; Jenkins et al. 1991; Linsley et al. 1991). In support, CD28 deficient mice suffer ablated T-dependent antigen responses (Green et al. 1994). When CD28 binds to its pair of ligands B7-1 (CD80) and B7-2 (CD86) on the surface of APCs (Linsley et al. 1991), it becomes activated by phosphorylation at its cytoplasmic domain, leading to a very similar tyrosine kinases activation pathway as the TCR (Rudd et al. 2009) (section 1.1.4.4).

Cytotoxic T lymphocyte-associated antigen 4 (CTLA-4) is the second molecule that also binds to B-7 ligands (Linsley, Brady, Urnes, et al. 1991). It is not expressed on resting T lymphocytes but in activated ones and resides in intracellular membranes before migrating to the cell surface after TCR ligation (Rudd et al. 2009). CTLA-4 has higher affinity than the CD28 interaction (Linsley, Brady, Urnes, et al. 1991), so acts as an important negative feedback system by blocking CD28-dependent stimulation (Linsley et al. 1992). Apart from blocking CD28 binding it has been proposed that CTLA-4 exerts its inhibitory effects by other means. For example, it might limit the physical contact between T lymphocyte and APC by affecting T-cell adhesion or by reversing the TCR-induced signals (Rudd et al. 2009).

Program death-1 (PD-1), is also a member of the CD28 family which is upregulated in activated T lymphocytes. PD-1 can bind to two B7 homologs: PD-L1 (B7-H1) and PD-1L2 (B7-DC). PD-1 is an immunoinhibitory receptor, engagement of PD-1 by both of its ligands leads to suppression of CD3-mediated T-cell proliferation by stopping the cell cycle progression, not by apoptosis (Latchman et al. 2001; Freeman et al. 2000). PD-1 blocks activation of PI-3K, an important molecule needed to provide enough intracellular glucose during the proliferation stage (Riley 2009). The PD-1 pathway might also act by reducing production of cytokines, in particular the key T_H1 cytokine IL-2. Therefore, it is believed that PD-1 is involved in controlling tolerance, blocking activation of self-reactive T lymphocytes (Riley 2009; Latchman et al. 2001).

Inducible co-stimulator (ICOS), another member of the CD28 family, is a co-stimulatory molecule expressed upon T-cell activation. In contrast to CD28, ICOS stimulation fails to induce long-term T-cell expansion because does not induce IL-2 production (Hutloff et al. 1999). Rather than in T-

cell priming, ICOS might be more important in later stages of the response or in those scenarios where T clonal expansion has to be limited (Riley & June 2005).

The B- and T-lymphocyte attenuator (BTLA) is the last member of the CD28 family, expressed on T and B lymphocytes. BTLA binds to the tumour necrosis factor herpes virus entry mediator expressed on APCs, including naive B-cells (Sedy et al. 2005). BTLA exerts inhibitory properties similar to PD-1 and CTLA-4, attenuating T-cell proliferation dependent on IL-2 production (Watanabe et al. 2003) and reducing phosphorylation of Syk after BCR cross-linking in B-cells (Vendel et al. 2009).

1.1.4.4 T-cell downstream activation

Similar to the activation process occurred after BCR cross-linking (section 1.1.3.3.), TCR ligation results in signal transduction pathways involving a pathway of mitogenic tyrosine kinases (MAPKs).

Immediately after TCR ligation, ITAMs motifs at the CD3 and CD28 cytoplasmic tails get phosphorylated by Lck, resulting in the ZAP-70 recruitment to the membrane, binding and activation. ZAP-70 is a tyrosine kinase member of the Syk family that phosphorylates a couple of adapter proteins (LAT and SLP-76), which in turn phosphorylate the phospholipase C-γ. Activated phospholipase C-γ leads to inositol triphosphate (IP_3) production and subsequent internal Ca^{2+} release. Simultaneously, diacylglycerol (DAG) recruits protein kinase C and leads to Ras activation pathway. Finally, the transcription factors NF-κβ, NFAT and AP-1 induce gene transcription (Smith-Garvin et al. 2009).

At the end, is this gene transcription that determines the fate of a T lymphocyte towards an effector cytokine producing cell, a memory cell or simply apoptosis.

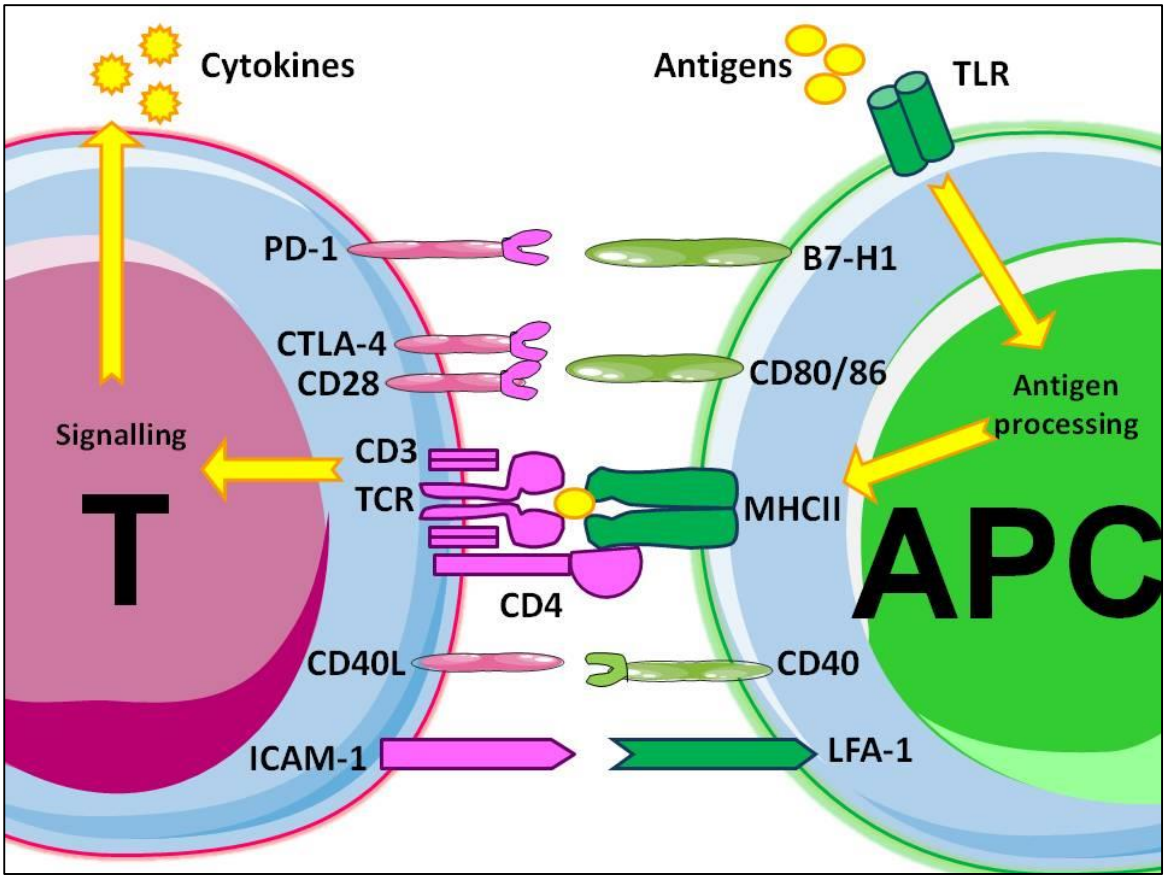

Figure 1.3: Major molecules involved at the interaction between CD4+ T-cell and APC.

APCs recognise and capture the antigenic particles trough pattern recognition receptors, such as TLRs. The antigen is then processed and presented to $CD4^+$ T lymphocytes on a MHCII molecule. The TCR/CD3 complex recognises the antigenic particle and initiates intracellular signalling. Second signals *via* several co-stimulatory ligands/receptors pairs and adhesion molecules are required to achieve complete T-cell activation. At this point, some molecules could provide regulatory signals, inhibiting T-cell responses rather than activating, for example CTLA-4 and PD-1. Production of cytokines is the final result of the interaction between T-cells and APCs.

1.1.5 T-Dependent and T-Independent B-cell responses

1.1.5.1 T-dependent (TD) responses

As mentioned in section 1.1.4, cell-contact between a T-cell and an APC is required to trigger activation of T lymphocytes, T_H differentiation and clonal expansion. Similarly, B lymphocytes cannot be fully activated by the antigenic cross-link of their BCR only and require reciprocal 'T cell help' to develop into plasma and memory cells. The interaction between a helper T-cell and a B-cell specific for the same antigen ('cognate interaction') is what delivers a second signal to naive B lymphocytes. Via co-stimulatory molecules and cytokines, T-cells induce B-cell differentiation into short-lived antibody producing plasma cells ('T-dependent humoral response') or into long-lived memory cells (McHeyzer-Williams & McHeyzer-Williams 2005). Be-2 cells are the major B-cell subset involved in T-dependent (TD) responses (section 1.1.3.1).

From the secondary co-stimulatory signals which induce Ig class switching, the most important comes from the CD40-CD40L interaction between the B-cell and the Helper T-cell (Allen et al. 1993) (section 1.1.4.3). CD40 engagement recruits the adapter proteins TRAFs, which lead cluster and activation of several kinases followed by downstream signalling through MAPK or NF-κβ and finally gene transcription (Elgueta et al. 2009).

In addition to CD40, other molecules such as the B-cell activating factor (BAFF), OX40L (CD252) and the inducible costimulator ligand (ICOSL) play a role for the cognate priming of B-cells (McHeyzer-Williams & McHeyzer-Williams 2005). Cytokines IL-4, IL-21, IFN-γ and IL-10 are also involved in the class switching to IgG, IgA and IgE; whilst IL-5, IL-6 and IL-2 are more involved in the maintenance of specific Ig producing cells (Ozaki et al. 2002; Cerutti et al. 1998; Takeda et al. 1996; McHeyzer-Williams 1989; Sonoda et al. 1989). Moreover, Pasare & Medzhitov (2005) describe a critical role of TLRs in TD antigen-specific antibodies, suggesting that TLR activation is essential for the production of some Ig classes (especially IgG and IgM).

Overall, TD antigens require a large number of secondary signals but generate B lymphocytes with the potential to develop immunological memory and to mount secondary antibody responses.

1.1.5.2 T-independent (TI) responses

Few antigens are capable of inducing antibody production without 'T cell help' and hence are called T-independent (TI) antigens (Mond et al. 1995). These antigens do not require cognate

interactions to induce fully B-cell activation and a rapid but short-lasting antibody production (in particular IgM).

Be-1 cells (section 1.1.3.1) are usually classified as effectors of TI responses, although some evidence has demonstrated that they are also capable of performing some TD responses and secrete IgA and IgG isotypes (Herzenberg 2000).

TI antigens are further classified as type 1 (TI-1) and type 2 (TI-2) antigens on the basis of their antigenic properties and the way they stimulate B lymphocytes (Mond et al. 1995).

1.1.5.2.1 TI type 1 antigens

In large concentrations these antigens act as mitogens, inducing non-antigen specific polyclonal B-cell activation and antibody production, even in neonates (Mond et al. 1995). The typical examples include bacterial lipopolysaccharides (LPS) and bacterial DNA, which cross-link the BCR (1st signal) but can be also be recognised by TLRs (2nd signal) expressed on B lymphocytes (Bekeredjian-Ding & Jego 2009) (sections 1.1.4 and 1.1.5.2.2). LPS activate B lymphocytes through TLR-4 signalling (Chow et al. 1999), while bacterial DNA does it via TLR-9 (Ruprecht & Lanzavecchia 2006).

LPS can directly exert polyclonal B-cell proliferation and IgM antibody production (Goud et al. 1990; Dziarski 1982; Coutinho et al. 1974). More importantly, LPS-activated B-cells can gain T-cell modulatory properties depending on the LPS amount they are exposed to. Low LPS concentrations direct T_H2 polarization, whereas high concentrations induce IFN-γ and IL-10 secreting T-cells that resemble a Treg phenotype (Xu et al. 2008).

1.1.5.2.1 TI type 2 antigens

TI type 2 antigens consist of large, flexible, slowly degraded molecules with highly repetitive identical antigenic epitopes, which can also activate the complement cascade (Mond et al. 1995; Dintzis et al. 1983). TI type 2 antigens activate mature B lymphocytes only, thus they fail to induce an immune response in neonates. Polysaccharides from the bacterial capsule and from the cell wall are the classic example of TI type 2 antigens, but other examples include dextran and Ficoll (Mond et al. 1995).

The major activation signal starts when the antigen cross-links several BCR simultaneously, in a multivalent manner. Dintzis et al. (1983) found that a minimum of 20 epitopes distributed in a two dimensional spacing of 5-10nm should be contained in a molecule in order to be TI immunogenic.

This translates into a minimum of 10 BCR bound to a single ligand to achieve B-cell stimulation (Sulzer & Perelson 1997). As reviewed in section 1.1.3.3, BCR engagement is followed by protein tyrosine kynase activity and subsequent activation of Btk, dependent on PI-3K (Li et al. 1997). Because Btk allows extracellular calcium to enter into the cell (Fluckiger et al. 1998), it plays an important role in BCR signal transduction, proliferation and IgM responses (Khan 2001; Khan et al. 1995). TI type 2 antigens generate multivalent Ig clusters that attract and activate several Btk molecules, thus resulting in persistent calcium influxes and subsequent recruitment of nuclear transcription factors, such as NF-κβ (Bajpai et al. 2000; Vos et al. 2000). The fact that TI type 2 antigens require functional Btk involvement is what differentiates them from the TI type 1 group (Rawlings et al. 1993).

BCR cross-linking with TI type 2 antigens might be enough to induce B-cell proliferation, but a second signal is essential to trigger antibody production (Vos et al. 2000). TLRs expressed in human B-cells can recognise bacterial components (section 1.1.4.1) and indeed provide a secondary aid for B-cell proliferation, differentiation, Ig class switching and migration (homing) to specific lymphoid tissue (Bekeredjian-Ding & Jego 2009). For example, addition of TLR-2 and/or TLR-9 agonists together with BCR engagement (anti-Ig) resulted in enhanced IL-10 secretion, extensive sustained B-cell proliferation and Ig class switching (Liang et al. 2011; Bouaziz et al. 2010; Ruprecht & Lanzavecchia 2006). Moreover, TLR activity via MyD88 was found to be as strong stimuli as Btk to induce secretion of pathogen-specific IgM (Alugupalli et al. 2007). However, it has been shown that the effects of TLRs stimulation vary depending on the B-cell subset, their phenotypic receptors and the tissue where they home (Ganley-Leal et al. 2006).

Moreover, T-cells can be recruited and respond to the presence of multivalent antigens (Siliciano et al. 1985), secreting cytokines that influence Ig production (Pike & Nossal 1984). The Snapper group has demonstrated that T_H-derived IL-2, IL-3, IL-4, IL-5, IL-6, IL-10 and IFN-γ can modulate Ig secretion after TI type 2 stimulation (Vos et al. 2000).

In conclusion, TI type 2 antigens which are also recognised by TLRs and/or induce secretion of cytokines by other leukocytes or dendritic cells, will successfully lead secondary intracellular pathways to enhance B-cell activity, differentiation and Ig class switch. There is also some evidence from model systems that Ig responses against capsular polysaccharides vary depending if the polysaccharides are presented on whole organisms or in a purified form (Khan et al. 2004). A publication has reported that TI type 2 responses can even generate a big pool of memory-like B-cells with the special feature of becoming downregulated in their secondary response by IgG

antibodies specific to the immunising antigen, thus avoiding antibody overproduction (Obukhanych & Nussenzweig 2006).

1.2 *NEISSERIA MENINGITIDIS*

1.2.1 Generalities and epidemiology

Neisseria meningitidis (*N. meningitidis*, meningococcus) is an encapsulated diploccocus gram negative β-Proteobacterium which exclusively infects humans and is the leading cause of bacterial meningitis. Bacterial meningitis has a prevalence of 4 to 6 cases per 100,000 adults and from those, 80% are caused by *N. meningitidis* or *S. pneumoniae* (van de Beek et al. 2006). Morbidity rates for meningococcal meningitis are reported as 3 to 7%, representing 1.2 million cases per annum worldwide with a prevalence of 1-12 cases/100,000 (1,000/100,000 in African epidemics) (Stephens et al. 2007; Rosenstein et al. 2001). After the vaccine introduction, the incidence of meningococcal disease in the UK remains low (2.05 cases/100,000) ("Health Protection Agency" 2012). Adolescents (15-24 years old) and infants between 3 and 7 months have the highest rate of disease (Stephens et al. 2007).

The first official description of meningococcal meningitidis occurred in 1805 when Vieusseux reported an outbreak of cerebrospinal fever in Geneva (Vieusseux 1806). However, it was not until 1887 that Anton Weichselbaum first isolated the bacterium from the cerebrospinal fluid of a patient with meningitis, calling this organism *Diplococcus intracellularis* (Weichselbaum 1887). It was in 1909 when C. Dopter first reported the presence of the meningococcus in the human nasopharynx (Dopter 1909).

Twelve serogroups have been established based on the immunochemistry of the capsular polysaccharides, but only six (A, B, C, X, W and Y) are responsible of causing more than the 90% of meningococcal invasive disease worldwide (Harrison et al. 2013; Stephens et al. 2007). Of these 12 serogroups, pathogenic strains from the groups A, B, C and X have been fully sequenced.

Serogroup A shows a tendency to cause large-scale epidemics in developing countries, being the zone of the African "meningitis belt" the one with the highest prevalence of the disease in kids aged between 7 and 14 years. In contrast, serogroups B, C and Y are associated with sporadic disease or severe outbreaks in North America, Zealand, South America and Europe. Serogroup B is endemic in industrialised countries, it is responsible for 30-40% of all meningococcal disease cases in the United States, 30–80% in the European Union and some epidemic outbreaks in Latin-American countries (WHO 2012; Harrison et al. 2009). Global incidence of meningococcus B has been estimated at 20 000 and 80 000 cases per year, accounting for 2000–8000 deaths annually

(Stephens et al. 2007; Rosenstein et al. 2001). Most serogroup B cases are sporadic and a long-lasting hyperendemic wave of disease may occur.

Further characterisation of *N. meningitidis* serotypes has been accomplished on the basis of multilocus sequence typing, a modern technique performed through DNA sequencing in housekeeping genes (Maiden et al., 1998). Genes such as *PorA, PorB, NadA, fHBP, GNA2132* and *FetA* are included in this mapping (Harrison et al. 2009; Caugant 2008).

1.2.2 Colonisation and meningococcal disease

The human nasopharynx is the only natural reservoir for *N. meningitidis*, so spread of the bacterium occurs person to person by droplets of respiratory tract secretions. Whether or not the infection is acquired, depends on the type of contact with the carrier, the virulence of the strain, its effective evasion of the immune system response and the genetic susceptibility of the host. At the colonisation stage, meningococci proliferate on the surface of human non-ciliated epithelial cells, forming small microcolonies at the site of initial attachment (Rosenstein et al. 2001). In most cases, the organism is carried asymptomatically in the nasopharynx. Between 10 and 30% of healthy individuals will carry *N. meningitidis* in the upper respiratory tract at any time (Caugant et al. 1994). The duration of the carriage state can be chronic, intermittent or transient. Most of the times, the colonisation is transient and ends up in elimination of the meningococcus**.** Generation of natural immunity is thought to be the result of cumulative immunising episodes by recurrent meningococci colonisation in nasopharynx. Thus, natural generation of protective IgG serum bactericidal antibodies (SBA) against the colonising strain is accomplished (Robinson et al. 2002)**.**

Occasionally, in the presence of certain factors that impair the integrity of the nasopharyngeal mucosa or when immune mechanisms against the bacteria are unsuccessful, *N. meningitidis* can gain entry to the blood stream. Meningococci can penetrate the epithelial barrier by moving through epithelial or endothelial cell junctions, by transcytosis or being carried across the epithelial and endothelial barriers inside immune cells such as monocytes.

Meningococcal disease usually occurs within 1–14 days post-acquisition of the bacterium, but its diagnosis is often missed or confused because the early stages of disease mimic common viral infections such as influenza. Once in the blood stream, bacteria can multiply and cause diverse forms of meningococcal disease (Figure 1.4). Meningococcal meningitis is the most common disease form and occurs when the bacterium cross the blood-brain barrier to establish in the

meninges. Classical clinical features in adults include fever, severe headache, nausea/vomiting, dislike of bright lights, neck stiffness, drowsiness, altered mental status (Glasgow scale below 14) and a non-specific or maculo-papular rash (van de Beek et al. 2004). Less severe infections such as purulent or immune arthritis, pneumonia, purulent pericarditis, conjunctivitis, otitis, sinusitis and genitourinary infections are less common.

Meningococcal sepsis is the most severe and life-threatening form of the disease. It is characterised by an abrupt onset of fever and a non-blanching petechial or purpuric rash that may progress to purpura fulminans, followed by a rapid onset of hypotension and acute adrenal haemorrhage. Meningococcemia is triggered by activation of the complement and the excessive release of pro-inflammatory cytokines, among which TNF-α, IFN-γ, IL-1β, IL-6, IL-8 and IL-12p70 play a crucial role (Hellerud et al. 2008; Van Deuren et al. 1995). Carrol et al. (2005) found that this initial pro-inflammatory profile is altered in patients with severe meningococcal sepsis as higher levels of the anti-inflammatory IL-1R are present in blood, perhaps as a manner of downregulation and counterbalance. Fulminant meningococcal septicaemia is characterised by a rapid proliferation of the meningococci in circulation, with bacterial numbers up to 10^5–10^8/mL and high levels of meningococcal endotoxin (10^1–10^3 EU/mL) (Hellerud et al. 2008; Stephens et al. 2007). Septic patients with high endotoxin concentrations will suffer disseminated intravascular coagulation due to activation of the coagulation system and concomitant down regulation of the fibrinolytic system. Later, progressive circulatory collapse and severe coagulopathy can result in multiple organ failure, thrombosis, necrosis and death within a few hours (Hellerud et al. 2008; Stephens et al. 2007). Despite the use of antibiotics fatality rates for meningococcal disease are still high (3 to 15%), rising up to 40% in the case of meningococcal septic shock (van de Beek et al. 2004). Up to 25% of the survivors are left with permanent sequelae, including hearing loss, motor nerve deficits, visual impairment, cognitive impairment and limb amputations as result of necrosis (Stephens et al. 2007).

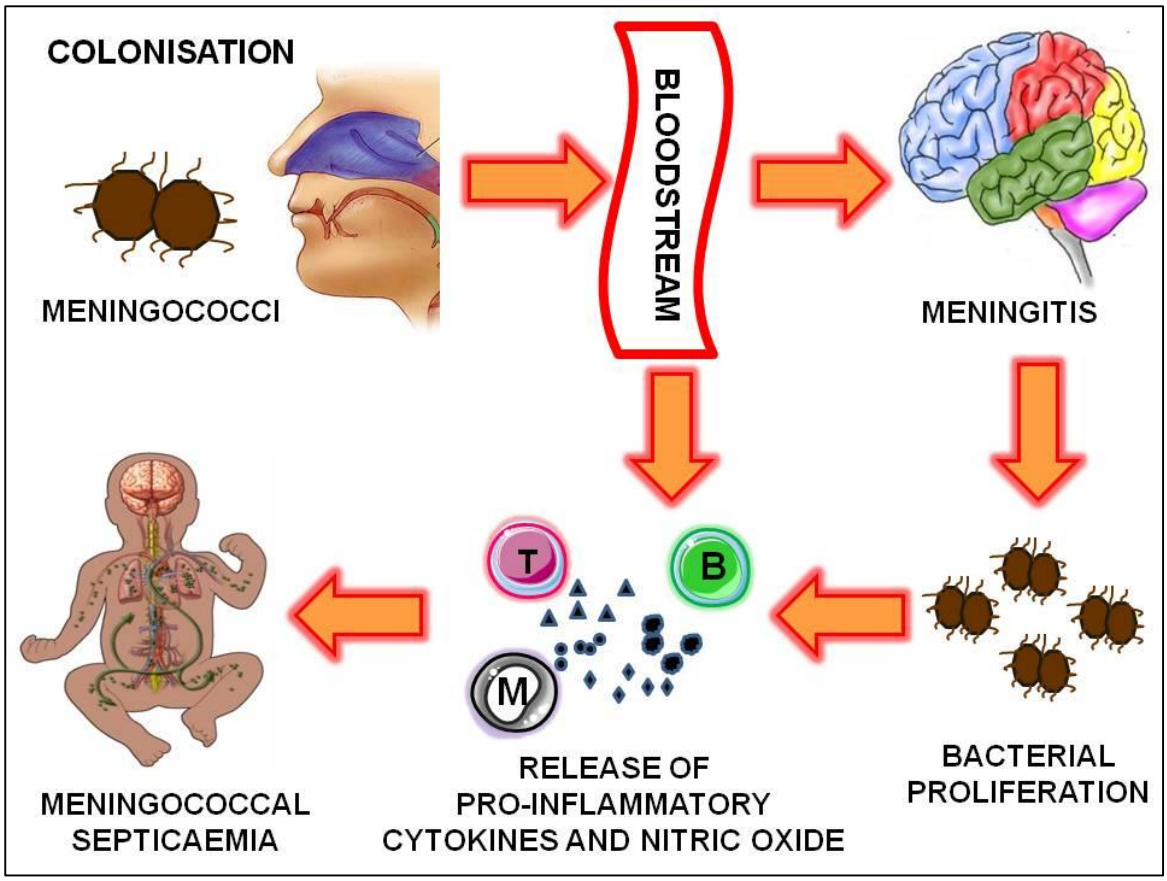

Figure 1.4: Progression of meningococcal disease.

Meningococci colonise the nasopharynx and remains silent avoiding killing by the immune system (carriage stage). Occasionally, the bacterium crosses into the bloodstream and causes meningococcal disease, meningitis and/or meningococcal septicaemia. Release of pro-inflammatory cytokines and nitric oxide play an important role in the severity of the disease.

1.2.3 Diagnosis, treatment and vaccination

Although the clinical presentation of meningococcal meningitis is well known, early diagnosis in infants can be difficult due to a late onset of the classical symptoms and because the course of the disease is not always the same. Hence, a hazardous lumbar puncture with isolation of the pathogen will be required to confirm a meningococcal meningitis case (van de Beek et al. 2006). Recently, suspected cases of meningococcal disease have been definitively confirmed and typed by PCR (Corless et al. 2001; Maiden et al. 1998) or multilocus sequence typing (Maiden et al. 1998).

Parenteral benzylpenicillin should be given in suspected meningococcal disease (meningitis with non-blanching rash or meningococcal septicaemia) (Health Protection Agency 2012). Once confirmed, the antibiotic therapy includes a third-generation cephalosporin (ceftriaxone or cefotaxime) with or without adjunctive dexamethasone (Theilen et al. 2008). Intensive care is needed to restore electrolytes imbalance and monitor neurological, cardiovascular and respiratory functions in those patients suffering septic shock.

Due to the severity of the disease and its unpredictable course, prevention through vaccination is the best option to control the disease by *N. meningitidis*. In the 1960's, the first successful vaccines based on meningococci capsular polysaccharides against serogroups A, C, W and Y were administrated. However, these vaccines resulted to be poorly immunogenic in children under 2 years old as they only elicited a T-independent type 2 response, with no memory and with low antibodies titers (section 1.1.5.2.1). Thus, the susceptibility to meningococcus is higher in infants and young children than adults.

Conjugated vaccines combining capsular polysaccharides with a protein were manufactured to overcome this problem and to achieve an effective T-dependent long-lasting response (section 1.1.5.1). The MenC vaccine was the first of this type to be introduced and be successful against the serogroup C, proving to be effective to induce long-term protection in 1 year old children and with a single dose (Miller et al. 2002). Nowadays, two conjugated tetravalent vaccines against the serogroups A, C, Y and W have been licensed and are effective in infants. MenACWY-D (Sanofi Pasteur) contains polysaccharides of the 4 serogroups conjugated to diphtheria toxid (Pace et al. 2009). MenACWY-CRM (Novartis) is made from oligosaccharides from the capsule but linked to a diphtheria mutant carrier protein (CRM-197) and with the addition of an adjuvant (aluminum phosphate) (Pace et al. 2009; Snape et al. 2008). Recently, a conjugated vaccine against the same serogroups but using tetanus toxoid (MenACWY-TT) suggested a slightly broader effectiveness when compared to MenACWY-CRM (Knuf et al. 2013). Another vaccine of this type has been

manufactured to control epidemic outbreaks of the *N. meningitidis* serogroup A in the African 'meningitis belt' region. MenAfriVac is affordable, has shown to be safe until now and is now part of an extensive vaccination campaign (WHO 2013).

Regardless of the success of these conjugated vaccines, a polysaccharide-based approach against the serogroup B is impossible to use, as the major component of its serogroup capsule is a common carbohydrate (α2-8-linked N-acetyl neuramic acid) present in mammalian brain cells (Serrato et al. 2004; Gotschlich et al. 1969). The fact that this polysaccharide is poorly immunogenic, plus the risk of eliciting autoimmunity against this component on the host cells, has prevented the development of a MenB vaccine under the conventional approach (Tan et al. 2010).

Novel vaccines against the serogroup B have been under development based on certain proteins contained within the *Neisseria* outer membrane vesicles (OMVs) (section 1.2.4.6). Although they have been effective in controlling epidemics caused by a single strain like the one that occurred in New Zealand (Holst et al. 2009), these vaccines represent major problems owing to the high variability of the immunodominant components (Urwin et al. 2004). Indeed, within a vaccine formulation it will be necessary to include multiple variants of a single antigen to account for its diversity; for example different types of PorA protein (Tan et al. 2010). New engineered approaches have been additive into the effort of improving OMVs vaccines against MenB. The identification of immunogenic candidates by the reverse vaccinology technique (Pizza et al. 2000) is possibly the main example. Released in January 2013, Bexsero (Novartis) is the newest successful vaccine formulation which is immunogenic in infants, children, adolescents and adults. Bexsero contains 3 antigens identified by reverse vaccinology: adhesin A (NadA), factor H‑binding protein (fHbp) and neisserial heparin binding antigen (NHBA), in addition to OMVs from the New Zealand vaccine containing PorA P1.4 (Gorringe & Pajón 2012; Giuliani et al. 2006). This vaccine has been already licensed in Australia and Europe but not yet in the UK. The JCVI has advice that toddler routine vaccination with Bexsero is unlikely to be cost effective in the UK, as it will only reduce up to half of the cases in infants and does not prevent acquisition of the bacterium in adolescents (JCVI 2013).

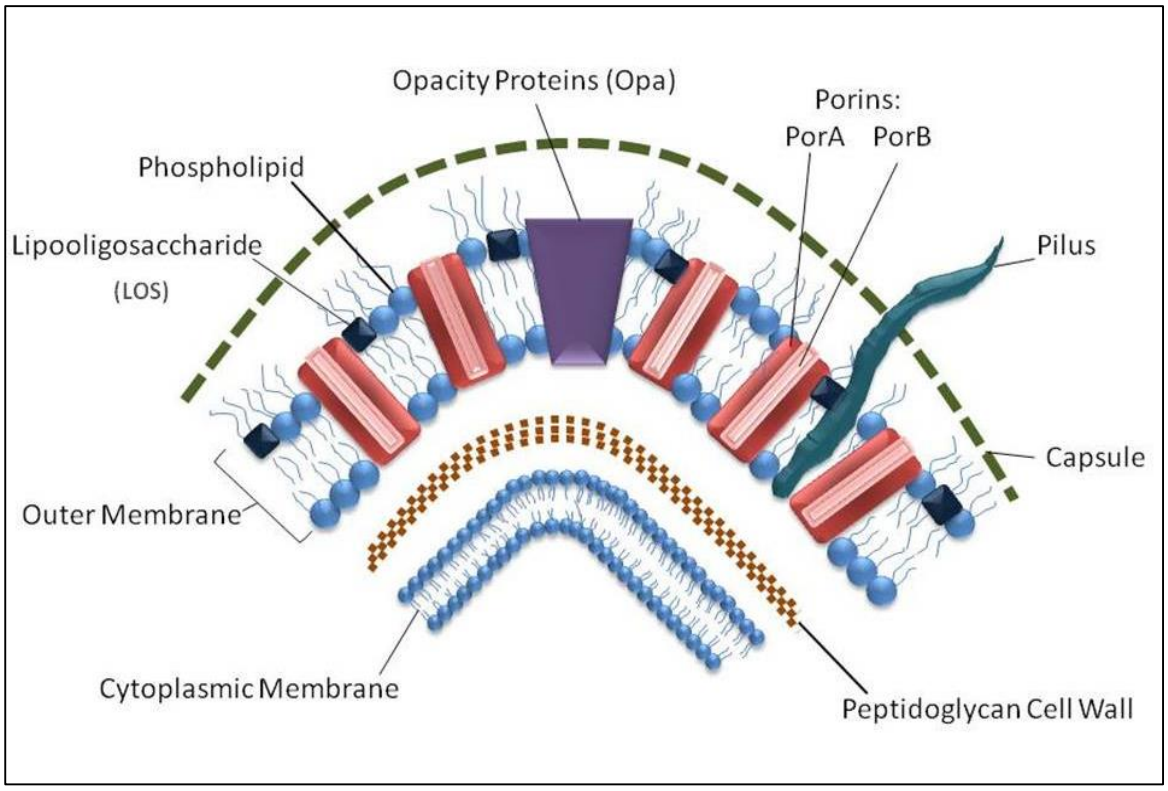

Figure 1.5: Schematic representation of the major outer membrane constituents of *N. meningitidis*.

1.2.4 Main virulence and immunogenic factors of *N. meningitidis*

The main *N. meningitidis* components and a schematic representation of its Gram negative structure is presented in Figure 1.5.

1.2.4.1 Capsule polysaccharide

The majority of serogroup B, C, Y and W135 isolates have a capsule composed of polysialic acid and derivatives (Gotschlich et al. 1969). However, the meningococcus capsule has to be absent to effectively adhere and colonise epithelial cells in the nasopharynx (Claus et al., 2002). Non-capsulated organisms have been isolated from the nasopharynx of carriers (Claus et al. 2002); whereas isolates from blood and cerebrospinal fluid from patients with meningococcal disease are almost exclusively capsulated (Cartwright et al. 1987). This dichotomy can be explained by the meningococcus ability of switching on/off the capsular polysaccharide expression via a genetic modification within the *SiaD* and *SiA* genes (Hammerschmidt et al. 1996). The capsule plays an important role in invasive meningococcal disease, as once in the bloodstream the capsule protects the microorganism from phagocytosis and from being destroyed by the complement system (section 1.2.5).

1.2.4.2 Lipooligosaccharyde

Lipooligosaccharyde (LOS) constitutes 50% of the meningococcal outer membrane. It is composed of a hydrophobic lipid A anchored to the membrane and linked to a short hydrophilic chain of 8-12 saccharide units exposed on the surface. Although LOS is indifferently referred to as LPS by many authors, meningococcus lacks of a repeating O-polysaccharide region present in enteric LPS (Zughaier et al. 2004; Brandtzaeg et al. 2001). Protein LpxA is responsible for adding the O-linked 3-OH fatty acid to UDP-N-acetylglucosamine, which is the first step in the lipid A synthesis (Steeghs et al. 1997).

Twelve different immunotypes have been detected based on the LOS structure, being the immunotypes L3, L7 and L9 the most associated with rapid progressive meningitis and septicaemia due to serogroups B and C; whereas the L1, L8 and L10 immunotypes are mainly seen in carriers (Mackinnon et al. 1993). This can be explained by the aggressive immunotypes inducing higher levels of TNF-α and IL-6 as compared with other immunotypes (Braun et al. 2002). Moreover, several immunotypes can mask their terminal lactosamine by adding sialic acid on their LOS

structure, a condition that reduces antibody opsonisation and complement activity (Estabrook et al. 1997).

The lipid A from LOS is the endotoxin which triggers a strong systemic inflammation responsible of many of the clinical features in bacterial septicaemia, such as coagulopathy, endothelial disruption, hypotension and organ failure. The presence of LOS in blood can be recognised by the soluble LPS-binding protein, by the membrane receptor CD14 and by the TLR-4. In monocytes, macrophages and granulocytes, CD14 together with TLR-4 and the soluble TLR-4 associated protein MD-2, form a complex to recognise LPS (Zughaier et al. 2004). But it is the TIR domain of the TLR-4 that triggers intracellular signalling through adaptor proteins. Signalling via the adaptor MyD88 activates transcription factors NFκβ and MAPK, resulting in production of pro-inflammatory cytokines TNF-α, IL-6, IL-8 and IL-12p (Lu et al. 2008). On the other side, signalling through the adaptor TRIF induces interferon type I transcription, important for antibacterial and antiviral responses (Lu et al. 2008). LOS variations from different strains can influence the magnitude of the TLR signalling and the cytokine output (Pridmore et al. 2003). Similarly to the observation in monocytes, infection by meningococci induces maturation and secretion of IL-6, IL-8 and TNF-α from dendritic cells (Unkmeir, Kämmerer, et al. 2002; Kolb-Mäurer et al. 2001).
Pro-inflammatory cytokines such as TNF-α, IL-1β, IL-6 and IL-8 are extremely upregulated in patients with meningococcal septicaemia and high plasmatic levels of LPS/LOS. But as a counter-balance, the anti-inflammatory cytokines IL-10 and IL-1 receptor antagonist (IL-1RA) are also elevated in those patients (Brandtzaeg et al. 2001). Thus, the balance among these cytokines and the compartment in which they are being secreted (blood or cerebrospinal fluid) play an important role in the clinical prognosis.

1.2.4.3 Pili and adhesins

Adherence of capsulate meningoccoci to nonciliated columnar cells in the nasopharynx is dependent on and driven by long thin homopolymeric flexible filaments type IV pili, which extend from the inner membrane to the bacterial surface (Carbonnelle et al. 2009). Pilus is crucial to the niche specialisation of the meningococci because it mediates tropism, specifically for human respiratory tract epithelia (Virji et al. 1991; Rayner et al. 1995; Stephens & McGee 1981). Constant binding and retraction of the pilus allows a form of bacterial movement called “twitching motility” whereby bacteria crawl over a surface to spread along the apical cell surface (Lee et al. 2005). Although it was first suggested that pilus binds to the membrane cofactor protein CD46 expressed on all human cells except erythrocytes, it was later discover that other CD46-independent binding

mechanisms exist (Källström et al. 1997; Kirchner et al. 2005). Type IV pilus is also involved in the bacteria-bacteria interaction and in the formation of the polarity complex (cytoplasmic proteins and adhesins) on microvascular endothelial cells (Coureuil et al. 2009). It creates a 'cortical plaque' that protects bacterial colonies from the blood flow shear and induces opening of cell-cell junctions (Lécuyer et al. 2012; Merz et al. 1999). In addition, pili are essential for natural competence and DNA transformation; antigenic variations in pili allow *N. meningitidis* to colonise different niches and avoid clearance (Nassif et al. 1994).

Apart from pili, Opa and Opc are considered major meningococcal adhesins (section 1.2.4.4); whereas *Neisseria* hia homolog A (NhhA) (Scarselli et al. 2006), HrpA (Schmitt et al. 2007) and Neisserial adhesin A (NadA) (Franzoso et al. 2008) are referred as minor adhesins.

1.2.4.4 Outer Membrane Proteins: Opa and Opc

After the pili initial attachment, the opacity associated adhesin proteins Opa and Opc generate a tight secondary binding that lead to meningococci engulfment or transcytosis throughout host cells (Sadarangani et al. 2011; Carbonnelle et al. 2009). They participate in the meningococcus internalisation and synergise the action of pili (Rowe et al. 2007). Opa is an eight-stranded transmembrane β-barrel structure with four surface-exposed loops; while Opc is a 10-stranded β-barrel molecule with five surface-exposed loops.

Opc facilitates bacterial adhesion and invasion of epithelial cells and brain-derived endothelial cells by interacting with heparan sulfate proteoglycans (HSPGs) (de Vries et al. 1998), integrins, cytoskeletal proteins and the extracellular matrix proteins vitronectin and fibronectin (Unkmeir, Latsch, et al. 2002).

Opa is a highly diverse protein because *N. meningitidis* contains 4 different *opa* alleles with the capacity of going through phase variation (Sadarangani et al. 2011). Although Opa can also bind to HSPGs, the majority of Opa variants bind to carcinoembryonic antigen-related cell adhesion molecules (CEACAMs) (Carbonnelle et al. 2009; Gray-Owen et al. 1997). The CEACAMs are members of the immunoglobulin superfamily with cell adhesion properties (Beauchemin et al. 1999). From the group, CEACAM1, CEACAM3, CEACAM5 and CEACAM6 have been shown to bind to *Neisseria spp* Opa variants (Bos et al. 2002). CEACAM3 is expressed only on neutrophils and CEACAM5 exclusively on epithelial cells; whereas CEACAM 6 is expressed on both. CEACAM1 is widely found on epithelial and endothelial cells, as well as on granulocytes and activated lymphocytes (Sadarangani et al. 2011). In the presence of pro-inflammatory cytokines, such as TNF-α and IL-2, CEACAM expression become upregulated in endothelial cells, activated $CD4^+$ T -

cells, $CD19^+$ B-cells and NK-cells (Muenzner et al. 2000; Kammerer et al. 1998). Since high levels of CEACAM1 are also induced upon TCR-crosslinking, it has been suggested to be involved in T-cell signalling and proliferation (Nagaishi et al. 2006; Kammerer et al. 1998). CEACAM1 can express a long cytoplasmic tail with an inhibitory motif (ITIM), thus Opa-CEACAM1 binding has been associated to T-cell suppression (Lee et al. 2008; Nagaishi et al. 2006; Nakajima et al. 2002; Boulton & Gray-Owen 2002). However, T-cell co-stimulation has been reported to occur in the presence of Opa or if a monoclonal antibody is directed against CEACAM1 (Donda et al. 2000; Kammerer et al. 1998; Wiertz et al. 1996). Indeed, the outcome seems to depend on the balance among CEACAM1 splice variants (long or short cytoplasmic tail), the amounts of bacterial Opa proteins and the cellular environment (Nagaishi et al. 2006; Muenzner et al. 2000).

1.2.4.5 Outer Membrane Proteins: PorA and Por B

The porins PorA and PorB are the most abundant outer membrane proteins, with PorB being the most important of the two. Meningococcus is capable of expressing the two porin proteins simultaneously: Por A (class 1) and one of two mutually exclusive PorB2 or PorB3. A *N. meningitidis* classification into serosubtypes is done based on the phase-variable PorA, whilst serotypes are based on PorB (Frasch et al. 1985). Porins are located in the bacterial outer membrane to allow small hydrophilic nutrients to diffuse into the cell, and they might be also be involved in bacterial up-take by re-arranging the cytoskeleton.

PorA binds a complement inhibitor to reduce complement-mediated bactericidal activity and thus improving bacterial survival in plasma (Jarva et al. 2005). PorB targets host cells to localise within the mitochondrial inner membrane, it binds to the voltage-dependent anion channel and thus can modify the mitochondrial membrane potential. Both pro-apoptotic (Kozjak-Pavlovic et al. 2009) and anti-apoptotic (Massari et al. 2000) effects have been associated to PorB.

Both porins are immunogenic, enhance expression of CD86 on APCs and induce TLR-2/TLR-1 downstream signalling through MyD88 (Massari et al. 2006; Wetzler 1994); therefore have been used in the past as vaccine adjuvants to enhance T-dependent responses (Fusco et al. 1997).

1.2.4.6 Outer Membrane Vesicles

During log-phase growth and as a virulence mechanism, *N. meningitidis* releases into the surrounding medium blebs or vesicles from its outer membrane. Outer membrane vesicles (OMVs) are primarily composed by LOS (50%), in addition to outer-membrane proteins, phospholipids and capsular polysaccharides (Rosenstein et al. 2001). Indeed, released OMVs from

rapidly growing meningococci contributes to the very high plasmatic levels of endotoxin (LOS/LPS), which characterise fatal meningococcal septicaemia (Namork & Brandtzaeg 2002; Brandtzaeg et al. 1989).

The biological effects of OMVs are similar to the ones of purified meningococcal LPS, as OMVs induce secretion of TNF-α, IL-6 and procoagulant activity in a dose-dependent manner (Bjerre et al. 2000). If LOS is removed from the vesicles, the non-LOS components will be still able to generate a pro-inflammatory response (TNF-α, IL-1β and IFN-γ), although much higher concentrations of the vesicles will be required (Hellerud et al. 2008; Sprong et al. 2001).

Several studies have shown that proteins contained within OMVs are good immunogenic candidates (section 1.2.3) and that whole OMVs can be safely used in vaccine preparations after LOS removal, either by detergent-extraction or using LOS-deficient engineered strains (van de Waterbeemd et al. 2012). Although is well known that porins are the major inducers of bactericidal antibodies, Marzoa et al. (2012) suggests that protein complexes formed by porins and accessory proteins (RmpM, CxChap or FetA) offer the advantage of preserving the conformational structure seen in native OMVs. This principle facilitates exposure of epitopes and indeed promotes a more efficient immune response, with complement activation and opsonophagocytosis.

1.2.4.7 Bacterial genome and phase variation

N. meningitidis has one of the most dynamic genomes studied so far, possessing many hundreds of repetitive elements and phase variable genes, plus the ability of performing horizontal DNA transfer (Tettelin et al. 2000; Caugant 2008). Interestingly, meningococci have acquired DNA from commensal *Neisseria spp*., from other bacteria (e.g. *Haemophilus*) and from phages. Genome plasticity and phenotype diversity result in evolution of a pool of genes implicated in cellular invasion or virulence of the strain, as well as in a differential survival of variant genotypes within a clonal complex over an extended time period (Buckee et al. 2008). Buckee et al. (2008) proposes a selective model built on the assumption that strains with slight differences in transmissibility and which could co-infect a host, are in constant competition. Hence, a small subset of the most transmissible strain will persist during long-term and will become the central persisting genotype. It has been previously observed that populations of carried meningococci comprise multiple lineages, whereas meningococcal isolates from cases of invasive disease typically contain a limited subset of lineages (Jolley et al., 2005; Yazdankhah et al., 2004). The meningococcus serogroup B wild type strain MC58 has a genome of 2,272,351 bp and 2158 predicted coding regions with an average G-C content of 51.5%. It has 2158 ORFs identified, from which 71% are similar to ORFs

from g-Proteobacteria (mainly *H. influenzae*) suggesting a common ancestor for these two microorganisms (Tettelin et al. 2000). Genome analysis shows that strain MC58 has a far greater number of phase-variable genes and contains several putative phage-derived ORF's (Masignani et al. 2001). Several phase variation events take place during *N. meningitidis* infection, including modifications to LOS, outer membrane proteins and pilin, as well as on/off expression of the capsule (van der Woude & Bäumler 2004).

1.2.5 *N. meningitidis* is capable of evading some immune responses.

N. meningitidis must evade the immune system to invade host cells and induce systemic disease. The presence of a capsule is fundamental to many of the bacterial survival mechanisms. Meningococcus capsule limits the adhesion with phagocytic cells and impairs complement-mediated killing by blocking antibody binding and complement deposition; thus reducing opsonisation and subsequent phagocytosis by macrophages and dendritic cells (McNeil and Virji, 1997; Read et al., 1996).

In addition to the capsule, LOS is an important mechanism to escape innate immune responses. Meningococci strains containing sialylated LOS phenotypes avoid immune recognition by anti-LOS antibodies and they become protected against complement-mediated bacteriolysis (Estabrook et al. 1997). When LOS are sialylated, phagocytosis and phagocytic killing become restricted, most likely because sialylation masks Opa and Opc proteins and reduce their interactions with polymorphonuclears, monocytes and dendritic cells (Unkmeir, Latsch, et al. 2002; McNeil & Virji 1997).

In order to survive and replicate inside epithelial cells, meningococcus overcome the action of bactericidal lysosomes. The meningococcal IgA1 protease prevents phagosomal maturation and bacterial lysis by cleaving and reducing the amount of lysosome-associated membrane proteins (LAMPs) and affecting other lysosome structures (Ayala et al. 1998). In addition, IgA1 proteases degrade immunoglobulins produced in mucosal surfaces.

Phase variation of many of the *N. meningitidis* genes may confer it advantage to escape from the recognition by the immune system (section 1.2.4.7). For example, a recent publication has found a phase variant of PorA with reduced levels of surface expression that allows the bacterium to avoid killing by specific PorA bactericidal antibodies (Tauseef et al. 2013).

1.2.6 *N. meningitidis* and nitric oxide

Nitric (NO) has been directly implicated in the pathogenesis of septic shock because it increases vascular permeability, reduces cardiac contractility and generates hypotension with hyporesponsiveness to systemic vasoconstrictors (Petros et al. 1994). In this context, high levels of NO, nitrate and nitrite have been detected in blood and cerebrospinal fluid from patients with severe meningococcal disease and sepsis (Wong et al. 1996; Kornelisse et al. 1996; Petros et al. 1994).

In addition to its vasodilator properties, NO is well known as a bactericidal molecule (section 1.3.3). Mononuclear cells, but mostly macrophages are responsible of the NO overproduction during infections. Within the nasopharynx at the site of *N. meningitidis* colonisation, mononuclear cells and macrophages account for between 14-18% of the total cells (Pipkorn et al. 1988). Indeed, the nitric oxide output is particularly high due to the presence of NO producer cells and the abundance of commensal organisms colonising the nasopharynx (Busch et al. 2000; Lundberg & Weitzberg 1999).

Bacterial LOS/LPS and pro-inflammatory cytokines, are the main stimuli for NO production during bacterial infections. However, NO production is not always dependent on the amount of LPS and is more correlated to the source of LPS, free calcium levels and the cell type (Azenabor et al. 2009; Zughaier et al. 2004). IFN-γ is the major stimulus for NO production from macrophages (Ding et al. 1988). In meningococcal disease TNF-α, IFN-γ and IL-1β are recognised major stimuli for the induction of NO production in different cell types (Kwon et al. 2001; Taylor et al. 1998; de Vera et al. 1996). Vice versa, local variations in NO levels can alter the pattern of the cytokines secreted by macrophages. For instance, macrophages treated with small amounts of an NO donor secreted less IL-10 but more IL-12 and TNF-α in comparison with the non-treated control. Since infection with *N. meningitidis* reduces the overall amount of NO present in the environment by a denitrification system (section 1.2.6.1), it is expected for the NO-related cytokines to suffer modifications (Stevanin et al. 2007).

1.2.6.1 *N. meningitidis* has a partial denitrification system

Several pathogens have evolved a variety of strategies to counteract the bactericidal effect of the reactive nitrogen intermediates of their host cell. Microbes can inhibit NO synthesis by blocking or reducing the enzymes or substrates necessary for NO production, by presenting a LPS phase-

variant that no longer induces NO, and by repairing DNA damage caused by reactive nitrogen products (Chakravortty & Hensel 2003; Eriksson et al. 2000; Cowley et al. 1996).

N. meningitidis posses a developed partial denitrification system, that allows the reduction of soluble nitrite into nitric oxide and finally into non-bactericidal N_2O. Moreover, this denitrification system seems physiologically relevant to enhance meningococcus survival during mucosal colonisation and within macrophages. Since meningococcus is likely to encounter microenvironments rich in NO but reduced in oxygen, the bacterium has become adapted to support growth by using the denitrification pathway (Anjum et al. 2002). Denitrification is a respiratory process which involves the use of nitrogen oxides as alternative electron acceptors under oxygen-limited conditions (Rock et al. 2005). The *N. meningitidis* denitrification system is comprised of two stages, each catalysed by a distinct enzyme (Barth et al. 2009; Anjum et al. 2002; Berks et al. 1995). Within the process, the substrates at each step can serve as electron acceptors to supplement bacterial growth:

1. NO_2 to NO, by the nitrite reductase (AniA).
2. NO to N_2O, by the nitric oxide reductase (NorB).

AniA was first identified in *Neisseria gonorroheae*, as a copper-containing inducible nitrite reductase which is attached to the outer membrane and reside in the periplasm (Boulanger & Murphy 2002). It is coded by the gene *aniA* (NMB1623) (Tettelin et al. 2000) and its expression is induced by anaerobiosis (Householder et al. 1999). The homologue of the fumarate and nitrate reductase regulator (FNR) is a transcriptional regulator that controls the expression of 11 genes involved in anaerobic respiration and carbon metabolism, and has been demonstrated to act as a transcriptional activator for the expression of *aniA* (Lissenden et al. 2000). FNR is normally regarded as an oxygen-sensitive activator protein, but has been shown to be sensitive to NO by reaction of its [4Fe-4S]2+ cluster with NO (Cruz-Ramos et al. 2002). Reaction of FNR with NO lowers the affinity of FNR to its DNA binding sequence, then FNR become inactivated and is no longer able to induce aniA transcription.

Gene *norB* (NMB1623) codes for the nitric oxide reductase NorB, which is part of the superfamily of haem/copper cytochrome oxidases (Householder et al. 2000; van der Oost et al. 1994). NorB is bound to the membrane and its structure consists of 12 transmembrane helices that contain six invariant histidines at defined positions. Using electrons derived from soluble electron donors and as part of the respiratory chain, NorB catalyses the reduction of two molecules of NO to N_2O and water. Although NorB is expressed in all the *Neisseria spp.*, the meningococcal reductase activity is one of the most powerful (Barth et al. 2009). NorB is the major player within the denitrification

system because has a dual role in both the protection against the bactericidal effect of macrophage-derived NO and the utilisation of internally generated NO as part of a bacterial metabolic pathway. As compared with wild type strains, *norB* mutants are killed more by macrophages in the early stage of infection (Stevanin et al. 2005). Furthermore, NorB together with PorB prevent macrophage apoptosis and prolong survival of the phagocyted meningococci (Tunbridge et al. 2006). In infected macrophages, NorB activity and the subsequent reduction in NO levels results in high concentrations of NO-regulated pro-inflammatory cytokines such as TNF-α, IL-12 and CCL5 (Stevanin et al. 2007).

NsrR (NMB0437) codes for the NO-sensitive repressor protein (NsrR) member of the Rrf2 family of putative transcription regulators (Tettelin et al. 2000). The NsrR regulon of *N. meningitidis* contains only a very small number of genes and regulates the transcription of the two denitrification genes, aniA and norB in a NO-dependent manner (Heurlier et al. 2008; Rock et al. 2007). When the concentration of NO is very low NsrR binds to DNA and repress gene expression, in particular *norB*. In contrast, concentrations above ~1μM cause the protein to dissociate from the DNA, allowing the expression of the detoxification genes (Heurlier et al. 2008). In this context, to ensure that AniA does not overproduce NO from nitrate, *aniA* expression is tightly regulated by both FNR and NsrR (Heurlier et al. 2008; Rock et al. 2007).

1.3 NITRIC OXIDE

Nitric oxide (NO) is a simple diatomic gas, composed of one atom of nitrogen and one atom of oxygen. NO is poorly soluble in water, does not go undergo hydration reaction and as an uncharged molecule is capable of traversing cellular membranes, making it freely diffusible. In addition, NO contains an unpaired electron and is therefore a highly reactive free radical.

The biological synthesis of NO was first studied by the Ignarro (Ignarro et al. 1987) and Mocada groups (Palmer et al. 1987), when they identified that the Endothelium Derived Relaxant Factor (EDRF) which exhibited vasorelaxant properties was in fact NO. It was in 1992 when NO was named the molecule of the year, after discovering its role as biological messenger in many physiological and pathological conditions (Gibaldi 1993; Culotta & Koshland 1992). In biological tissues the half life of NO is only 3-5 seconds, owing to the propensity of the molecule to rapidly react with the metal centres (free iron, iron within iron-sulphur centres, or iron within haemproteins) and with the superoxide radical (O_2-) (Ignarro et al. 1993). In aqueous solution, in the presence of oxygen, NO is oxidised almost entirely to nitrite (NO_2-) with very low levels of nitrate (NO_3-) (Ignarro et al. 1993). Under mildly acidic conditions, NO_2- can be reduced to NO and the same cycle continues.

1.3.1 Production of NO

In mammalian organisms, NO is produced by the family of enzymes called nitric oxide synthases (NOS). In the presence of NADPH and O_2 serving as co-substrates, NOS oxidize one molecule of L-arginine to produce N^w-OH-L-arginine as an intermediate, which is further oxidized to yield one molecule of NO and L-citrulline (Knowles & Moncada 1994).

Three different cytoplasmatic isoforms of NOS are defined: the 157kD neuronal NOS (nNOS or NOS1), the 135kD inducible NOS (iNOS or NOS2) and the 140kD endothelial NOS (eNOS or NOS3). Each isoform is well conserved among species (80-94% identity) but have fewer similarities between the isoforms in any given species (50-60%) (Knowles & Moncada 1994).

Each NOS polypeptide consists of an N-terminal oxygenase domain and a C-terminal reductase domain, separated by a 30-40 amino acids long recognition sequence for calmodulin, a Ca_2^+ binding protein (Bredt & Snyder 1990). Dimerisation is needed to achieve the active state of all three NOS and involves the interaction between the oxygenase domains and the formation of the

active-site pocket for binding of L-arginine and haem (Stuehr 1997; Masters et al. 1996). The binding regions of calmodulin act as a hinge between the N-terminal oxidase and C-terminal reductase. In this manner, calmodulin binding triggers electron transfer to the haem group by bringing the domains into alignment (Abu-Soud et al. 1994). nNOS and eNOS are constitutively expressed and dependent in their activity on increased intracellular Ca_2^+ fluxes (Salerno et al. 1997). In contrast, iNOS requires a stimulus to be expressed and is considered Ca_2^+ independent. Whilst nNOS and eNOS produce small amounts of NO during short periods of time, iNOS has the ability to produce large quantities and remain permanently active due to a tight irreversible calmodulin-Ca_2^+ binding (Salerno et al. 1997) (Figure 1.6 and Table 1.1).

Among cells from various peripheral tissues and brain, basal levels of each of the three NOS mRNAs and proteins expressed are different in their sizes and sequences, suggesting the possibility that these variants are produced by alternative splicing (Park et al. 2000).

iNOS is mainly present within macrophages, dendritic and natural killers cells (Bogdan 2001). Although various bacterial components (via TLR recognition) and several cytokines induce activation of the iNOS promoter (Bogdan 2001), the combination of LPS, TNF-α, IFN-γ and IL-1β remain known as the major stimuli (Xie et al. 1992). Transcriptional activation of the human iNOS gene requires the presence of cytokine responsive elements and inducible NFκβ elements upstream of the gene (Taylor et al. 1998). Among the iNOS inhibitors, TGF-β and the T_H2 cytokine IL-4 are recognised as the most potent (Bogdan 2001). iNOS has been found to be elevated in bacterial meningitis and iNOS-derived NO has been suggested to be involved in the disruption of the blood-brain barrier and in the secretion of pro-inflammatory cytokines (Winkler et al. 2001).

eNOS is located as a membrane-anchored protein in the Golgi apparatus and in plasmalemmal vesicles (caveolae), and is heavily expressed by vascular endothelial cells and T-cell lines (Bogdan 2001). eNOS is reversibly inhibited by *S*-nitrosylation (section 1.3.2) in resting cells, being targeted to caveolae by reversible thiopalmitoylation of eNOS Cys15 and Cys26. But after agonist stimulation, eNOS undergoes denitrosylation and is transported to internal membrane structures (Erwin et al. 2006). Such translocation to the cytoplasmic compartment is indispensable for eNOS denitrosylation and requires the presence of the CD8-transmembrane domain (CD8-Myr) (Erwin et al. 2006). Later on, the membrane-associated eNOS is re-nitrosylated and returns to its basal state. eNOS-derived NO has been thoroughly studied within cardiovascular conditions for many years, whereas the implication of eNOS in T-cell activation and TCR signalling has been just recently pointed out (section 1.3.7).

The role of nNOS is almost exclusively limited to the central and peripheral nervous systems as is widely expressed in neurons, spinal cord, sympathetic and adrenal ganglia (Knowles & Moncada 1994). nNOS-derived NO plays a role in synaptic plasticity, acts as a neurotransmitter and controls blood pressure in the brain (Garthwaite 2008).

1.3.2 *S*-Nitrosylation

In the presence of a strongly oxidizing cofactor, the NO radical is covalently attached with cysteine thiol residues of proteins, peptides or amino acids, forming stable low molecular weight-*S*-nitrosothiol (SNO) compounds (Stamler et al. 1992). The *S*-nitrosylation process provides a route through which NO-derived bioactivity is not restricted to the site of its production and represents a form of reversible post-translational modification of proteins. *S*-nitrosylation is implicated in NOS regulation and diverse cell responses, such as activation of soluble guanylate cyclase and cGMP production, transcriptional activity of NFκβ and the regulation of caspases and other apoptotic factors (Hess et al. 2005; M. W. Foster et al. 2009).

A related chemical event is “transnitrosation”, which involves the heterolytic cleavage of the S-nitrosothiol bond to yield nitrosium (NO^+) that is later transferred to another thiol (Arnelle & Stamler 1995). The major example of this, is the selectively denitrosylation of *S*- nitrosoglutathione (GSNO) by the glutathione-dependent alcohol dehydrogenase or GSNO reductase, which is capable of catalyzing the NADH/NADPH-dependent degradation of GSNO to GSSG and ammonia (Jensen et al. 1998). The predominant low molecular weight *S*-nitrosothiol GSNO works as a reservoir of NO within cells and is maintained in balance by the action of its GSNO reductase.

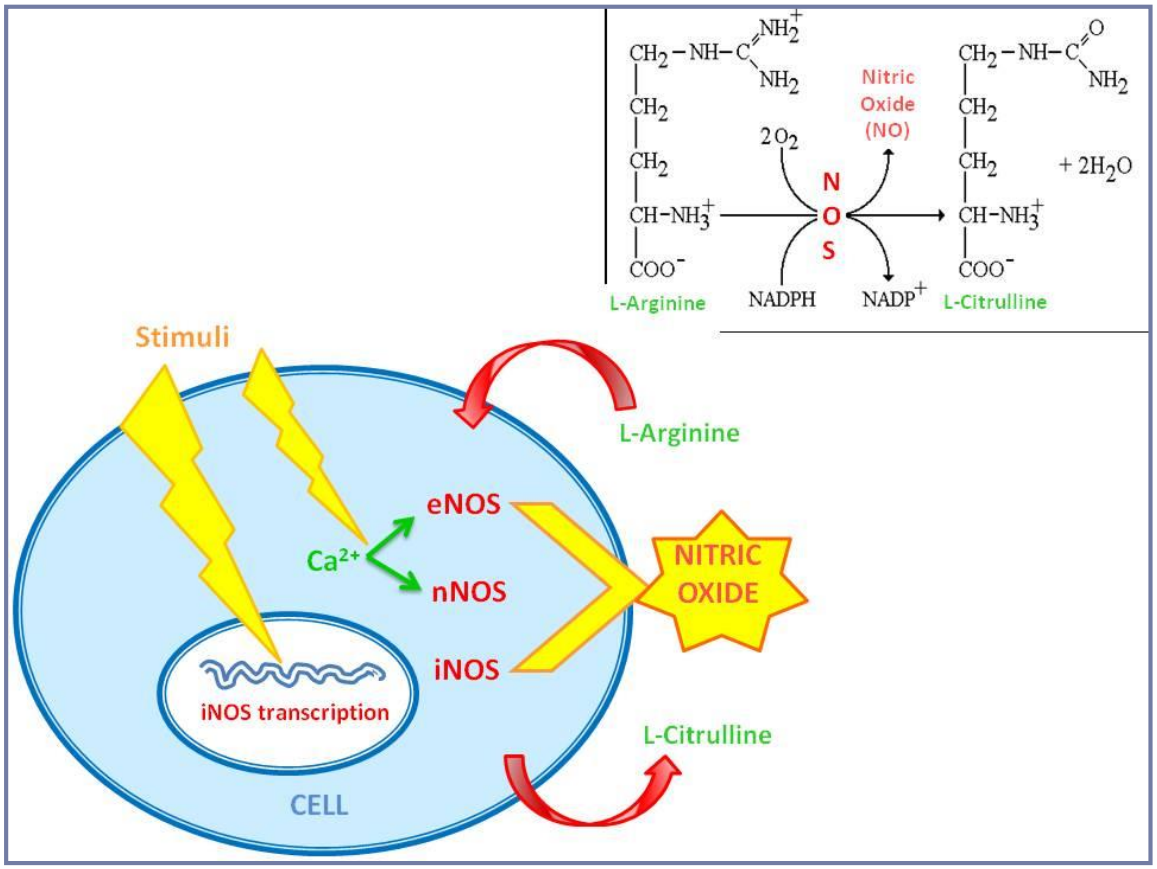

Figure1.6: Nitric oxide (NO) production.

Nitric oxide is produced by the family of nitric oxide synthases (NOS), which catalyze the oxidation of L-ariginine into L-citrulline. Endothelial NOS (eNOS) and neuronal NOS (nNOS) are constitutively expressed within cells and require Ca_2^+ for its activity. In contrast, transcription of the inducible NOS (iNOS) requires external stimuli and is not Ca_2^+/dependent.

Table 1.1: Features of human Nitric Oxide Synthases (NOS)

Nitric Oxide Synthases	Gene locus	Cellular expression (Subcellular localisation)	Stimuli for induction	Role of the NO produced
nNOS (NOS1)	12q 24.2-31	Neuronal cells and myocytes (Cytosol, endoplasmic reticulum, postsynaptic densities, sarcolemma)	Constitutively expressed and Ca2+ dependent	Neurotransmitter/neuromodulator in both the central and the peripheral nervous systems.
iNOS (NOS2)	17q 11.2-12	Macrophages (Phagosomes), dendritic cells and NK cells	Cytokines, cellular activation, TLR engagement, etc	Cytotoxic or cytostatic effector in the immune system. Not typically expressed in resting cells, must be induced by cytokines or microbial products.
eNOS (NOS3)	7q 35-36	Endothelial cells, cardiomyocytes and platelets (Golgi apparatus, plasmalemmal caveolae)	Constitutively expressed and Ca2+ dependent	Vasodilator in the cardiovascular system.

1.3.3 Bactericidal activity of NO

NO is well known as a bactericidal agent because exerts inhibitory, cytotoxic and genotoxic effects on microorganisms. NO has been shown to inhibit cellular respiration by reversible inhibition of cytochrome c oxidase (complex IV in the mitochondrial respiratory chain) (Cleeter et al. 1994); mobilises intracellular zinc targeting DNA-binding zinc metalloproteins (Schapiro et al. 2003) and cause deamination of deoxynucleotides resulting in DNA mutations (Wink et al. 1991).

Antimicrobial properties have been attributed to the various reaction products of NO or reactive nitrogen intermediates, such as NONOates, *S*-nitrosothiols, peroxynitrite, nitrite and nitrous acid. Interaction between reactive oxygen species and reactive nitrogen species seems to play a synergistic role in respiratory burst and NO synthesis. During a response against infection, high concentrations of NO and O_2^- radicals can interact to increase their bactericidal actions. The rapid reaction of NO with O_2^- generates peroxynitrite ($ONOO^-$), an effective potent oxidizing compound for SH groups, lipids and DNA, capable of causing nitration of tyrosine residues of proteins (Vazquez-Torres et al. 1995). With the oxygen intermediate H_2O_2, NO can be synergized to cause double-stranded DNA breakage, bacterial Fe_2^+ release, depletion of the antioxidant glutathione and death in *E. coli* (Pacelli et al. 1995).

1.3.4 NO as a regulator of intracellular pathways

Through *S*-nitrosylation (section 1.3.2) NO has been implicated in numerous physiological conditions, especially as intracellular messenger modulating a large number of downstream signalling pathways (Figure 1.7). Nitrosylation/denitrosylation as a redox switch, are dynamically regulated and can lead to activation of some proteins but inhibition of others (Stamler et al. 2001).

The main example of intracellular signalling is the NO binding to the ferrous state of the heme prosthetic group of the β1 subunit of soluble guanylyl cyclase (sGC), which results in the consequent production of guanosine 3',5'-cyclic monophosphate (cGMP). An increase in cGMP causes downstream activation of cGMP-dependent protein kinase (PKG) and further mitochondrial hyperpolarisation (Friebe & Koesling 2003).

Studies have demonstrated that NF-kβ sites are essential in the promoter region of the *iNOS* gene to induce its transcription (de Vera et al. 1996). Because both activation and inhibition of NF-kβ have been observed in response to NO, evidence suggests that high levels of NO may perform a

negative feedback on NF-kβ; whereas low levels enhance the TNF-α or PMA induced NF-kβ DNA-binding activity and transactivation (Janssen-Heininger et al. 2000). Proposed mechanisms for NF-kβ inhibition are *S*-nitrosylation on the p-50 protein that would obstruct NF-kβ binding to DNA (DelaTorre et al. 1997) and *S*-nitrosylation of the subunit IKKβ at the IKK complex (Reynaert et al. 2004). Similarly, the presence of eNOS causes *S*-nitrosylation at the TIR domain of MyD88, resulting in negative functioning by retarding MyD88-dependent signalling events, such as the NF-kβ and TNF pathways. Thus, S-nitrosylation of TIR may represent a control for the acute-phase inflammatory responses (Into et al. 2008).

1.3.5 Involvement of NO in mitochondrial respiration and function

Since NO is also produced within the mitochondria, some studies have suggested that eNOS may be targeted to the mitochondrial outer membrane (Gao et al. 2004), or that a specific mitochondrial NOS (mtNOS) isoform may exist at the mitochondrial inner membrane (Giulivi et al. 1998). NO has an important role in controlling mitochondrial biogenesis and cellular respiration.

Long exposure to eNOS-derived NO has been found to be responsible of triggering mitochondrial biogenesis, due to its ability to generate cGMP which interacts with the main mitochondrial regulators (Nisoli et al. 2003). Nisoli et al. (2004) reported that this NO/cGMP-dependent mitochondrial biogenesis increases O_2 consumption, cellular respiration and ATP content. In support, $eNOS^{-/-}$ mice presented a metabolic syndrome phenotype characterised by low mitochondrial numbers, small mitochondrial size, reduced energy expendure, obsesity and insulin resistance(Nisoli et al. 2004; Nisoli et al. 2003).

NO has been recognised as a controller for mitochondrial respiration because the respiratory chain offers 40 different potential metal target sites among the four respiratory complexes (Brown 2001; Henry & Guissani 1999). Donation of NO causes an immediate oxygen-dependent inhibition of respiration and ATP synthesis in a variety of cells (Brown 2001). A reversible inhibition of complex I is driven by *S*-nitrosylation of essential thiols (Brown 2001; Henry & Guissani 1999). The complex IV (cytochrome *c* oxidase) is also reversibly inhibited when NO competes with oxygen at the oxygen binding site of cytochrome *c* oxidase (Brown & Cooper 1994). In contrast, peroxynitrite irreversibly inhibits mitochondrial respiration by causing oxidative damage to all the respiratory complexes, disrupts the inner mitochondrial membrane potential, induces permeability transition and calcium release with ROS accumulation (Kim et al. 2001; Ghafourifar et al. 1999). Such reversible/irreversible nature of the respiratory chain inhibition, will mainly depend on the

relation between NO and oxygen and on how long the complex has been repressed. Beltrán et al. (2000) proposed that under conditions of cellular stress, inhibition of cytochrome *c* by NO may exert an early protective action on mitochondria by reversal of the ATP synthase, maintaining the mitochondrial transmembrane potential and avoiding its collapse.

1.3.6 NO involvement in cell death

NO has been described as a bifunctional modulator either stimulating or inhibiting apoptosis (Figure 1.7).

The NO anti-apoptotic effect involves several mechanisms, such as cGMP-dependent cyclic nucleotides (Dimmeler et al. 1998), upregulation of the anti-apoptotic protein Bcl-2 (Genaro et al. 1995), upregulation of heat shock proteins (Kim et al. 2001), inactivation of caspases by *S*-nitrosylation (Mannick et al. 2001) and inhibition of Fas-induced apoptosis (Mannick et al. 1997). *S*-nitrosylation on catalytic sites of caspase members is a well known example where NO exhibits anti-apoptotic properties. In resting cells the majority of mitochondrial Caspase-3 and Caspase-9 are normally inhibited by *S*-nitrosylation, preventing their auto-activation inside the mitochondria and an uncontrolled apoptotic activity (Mannick et al. 2001). Fas is able to reverse the effect, stimulating denitrosylation at the caspase active-site thiol ("thiolation") (Mannick et al. 2001; Mannick et al. 1999). A similar example of apoptosis downregulation, occurs on the apoptosis signal-regulating kinase 1 (ASK1); S-nitrosylation of ASK1 inhibits further binding to its substrate kinases (Park et al. 2004).

The pro-apoptotic NO effect has been attributed to several mechanisms, such as direct DNA damage (Kim et al. 2001), activation and expression of the tumour suppressor gene p53 (Messmer et al. 1994), proteasome inhibition (Glockzin et al. 1999) and lipid peroxidation (Ghafourifar et al. 1999). NO induces mitochondria hyperpolarisation and reactive oxygen species production (Perl et al. 2004). At high concentrations NO induces changes in the mitochondrial transmembrane potential, leading to cell necrosis by inhibiting cytochrome c activity and releasing it from the mitochondria into the cytosol (Brookes et al. 2000; Ghafourifar et al. 1999; Ushmorov et al. 1999). Peroxynitrite (ONOO-) also promotes irreversible mitochondrial damage and the opening of the permeability transition pore, allowing calcium and cytochrome *c* release (Ghafourifar et al. 1999). Finally, cytochrome *c* release can result in apoptosis by the activation of caspases -8, -3 and -9 (Ushmorov et al. 1999; Chlichlia et al. 1998; Melino et al. 1997). Intracellular NO can also signal apoptosis by *S*-nitrosylation of GAPDH, triggering its binding with the E3 ubiquitin ligase (Siah1)

and making it more stable to degrade nuclear proteins (Hara et al. 2005). Other example of NO leading to apoptosis is the conversion of the inactive guanosine diphosphate-bound Ras to the active form guanosin triphosphate-bound (Williams et al. 2003). At last and depending on the ATP storages, cells make a death decision either for apoptosis (ATP-dependent) or necrosis.

The switch between apoptotic or anti-apoptotic effects is probably cell type dependent and seems to be influenced by the concentrations of NO and the time of exposure to NO donors (Kim et al. 2001). NO at low concentrations (<1 µM) and for short periods is considered anti-apoptotic and may inhibit cytochrome oxidase *c* in a reversible manner; whereas high levels of NO (>1 µM) and for a prolonged exposure may generate an irreversible inhibition of respiration and severe mitochondrial damage (Brown 2001; Melino et al. 1997; Cleeter et al. 1994). Depending on the concentration, GSNO is also capable of controlling the apoptosis switch that occurs during the natural selection of thymocytes. Low intracellular concentrations of GSNO (<0.6 mmol/L) promotes acidification of thymocyte lysosomes and triggers apoptosis; whilst higher concentrations (>2 mmol/L) prevent apoptosis of thymocytes (Sandau & Brüne 1996).

1.3.7 T lymphocytes and NO.

Within the immune system and under both healthy and pathological conditions, nitrosylation/denitrosylation reactions have been reported to influence cell proliferation, differentiation, activation and apoptosis of immune cells (Hess et al. 2005; M. W. Foster et al. 2009).

In T-cells, TCR cross-linking via CD3/CD28 co-stimulation results in a series of mitochondrial events: 1) Mitochondrial hyperpolarisation; 2) Elevation of cytoplasmatic and mitochondrial Ca_2^+; 3) reactive oxygen intermediates (ROI) production; and 4) Expression of constitutive NOS with the corresponding NO production (Sena et al. 2013; Ibiza et al. 2006; Perl et al. 2004; Nagy et al. 2003) (Figure 1.8).

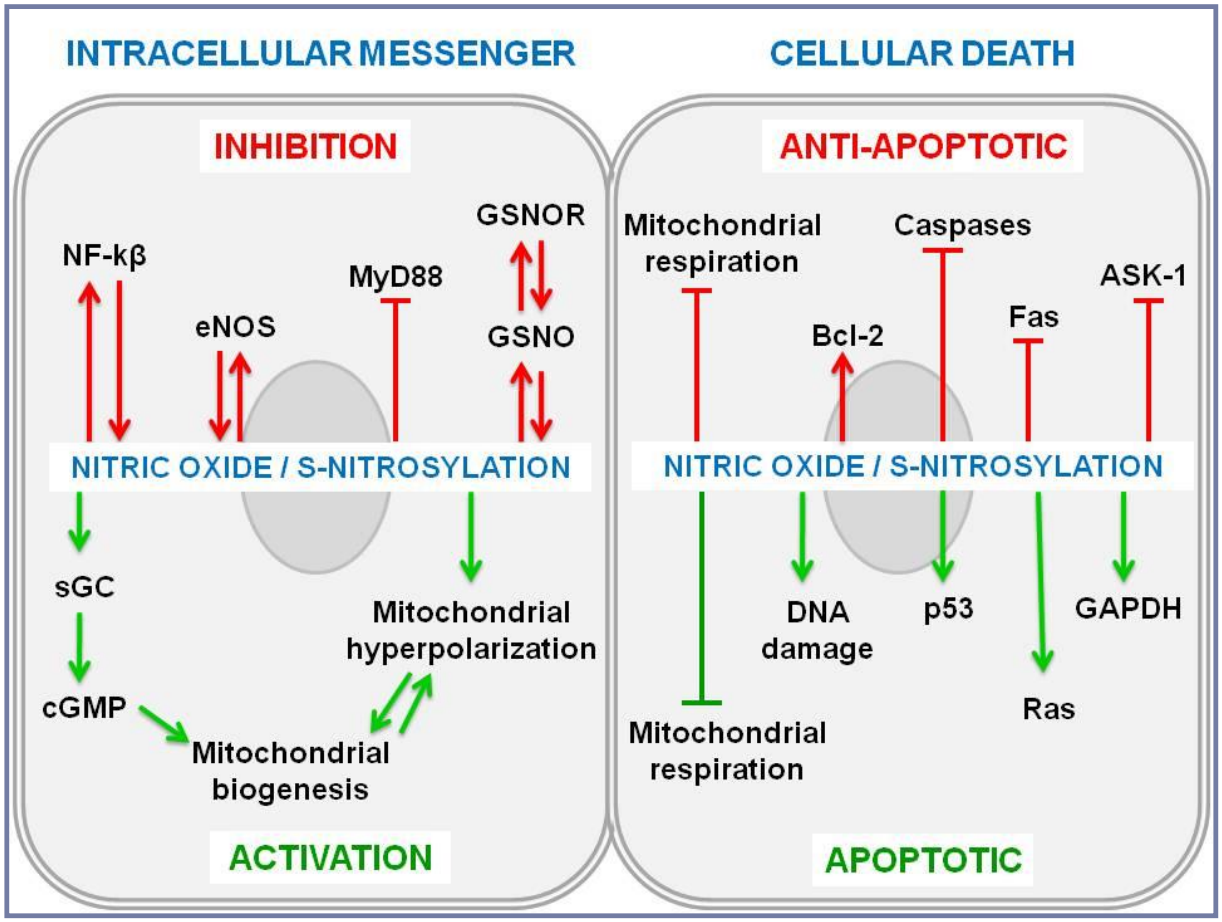

Figure 1.7: The dual role of NO in cell signalling and apoptosis.

NO is able to regulate intracellular processes *via* the signalling molecule cGMP and through nitrosylation of proteins. NO leads to activation or inhibition of diverse pathways and becomes regulated through feedback loops. From these, GSNO and activation of sGC are the major feedback signals. Depending on NO concentrations, both apoptotic and anti-apoptotic effects have been observed. Nitrosylation of caspases and inhibition of the Fas pathway represent the main mechanisms for avoiding apoptosis, whilst inhibition of mitochondrial respiration is the key event for NO-induced apoptosis.

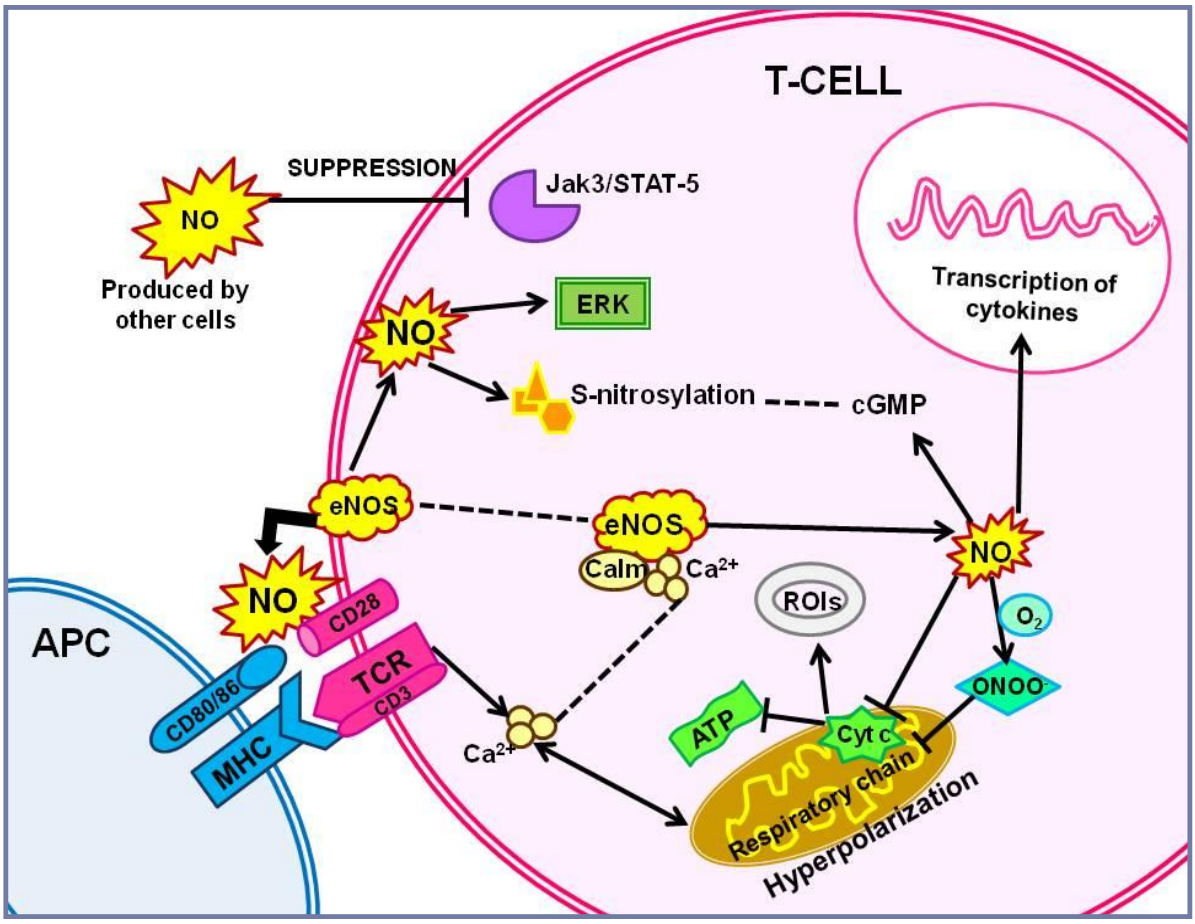

Figure 1.8: NO production and activity at the moment of TCR cross-linking.

TCR cross-linking leads to NO production, mitochondrial hyperpolarysation, ROIs production and increased intracellular Ca_2^+. NO is produced in the cytoplasm by eNOS, which requires Ca_2^+ and calmodulin (calm) for its activation. NO produced is mainly involved within the mitochondrial hyperpolarysation and reversible inhibits the respiratory chain, causing ATP depletion and ROIs production. In addition, NO regulates several proteins by S-nitrosylation, induces transcription of some cytokines and is present at the immunological synapse. However, NO produced by other cells (such as macrophages) could lead to suppression of T-cell proliferation and activation. Reaction of NO with O_2 generates $ONOO^-$, which cause irreversible damage to the respiratory complex.

Nagy et al. (2003) demonstrated that treatment of activated T lymphocytes with a NO donor (NOC-18, 600μM) increased cytosolic and mitochondrial Ca_2^+ levels, ROI generation and mitochondrial hyperpolarisation. In contrast, inhibition of NO by a specific NO chelator (C-PTIO) caused a deeply inhibitory effect on mitochondrial hyperpolarisation and ROI production, also blocking elevation of cytoplasmatic and mitochondrial Ca_2^+ levels. Therefore it is likely that TCR-activation-induced mitochondrial hyperpolarisation is mediated through NO and that NO is primarily regulated by Ca_2^+ and ROIs.

Cytoplasmic and mitochondrial Ca_2^+ levels increase rapidly five to ten minutes after TCR cross-linking, lasting at least 48 hours (Imboden & Weiss 1987). Ca_2^+ works as an intracellular messenger activating some molecules, such as protein kinase C, calmodulin and the calmodulin-dependent protein kinase (Premack & Gardner 1992). As mentioned in section 1.3.1, intracellular presence of Ca_2^+ and subsequent calmodulin binding are essential to achieve an active state on the constitutively expressed NOS. Thus, is not surprising to find the constitutive eNOS as the dominant producer of NO in T-cells (Ibiza et al. 2006; Nagy et al. 2003). Reiling et al. (1996) and Nagy et al. (2003) confirmed the presence of eNOS and nNOS but absence of iNOS in primary human B and T lymphocytes. eNOS undergoes a rapid specific and sustained activation in response to the TCR engagement and in a Ca_2^+-dependent manner via the PI3K-Akt pathway through phosphorylation of Ser (Ibiza et al. 2006; Fulton et al. 1999). eNOS protein levels increased up to 15-fold by CD3/CD28 co-stimulation, and a six-fold increment of NO levels was detected in T-cells activated via CD3/CD28 co-stimulation for a period of 24 hours (Nagy et al. 2003; Reiling et al. 1996).

In peripheral lymphocytes, a transitory increment in the mitochondrial transmembrane potential occurs in two contradictory scenarios, either triggered by cellular activation or as an early event in apoptosis (Perl et al. 2004). Mitochondrial hyperpolarisation is followed by just a transient inhibition of F0F1-ATPase, ATP depletion and sensitisation to necrosis (Gergely et al. 2002). However, in pathological conditions like systemic lupus erythematosus, an elevated and constant Ca_2^+ flux into the mitochondria induces persistent mitochondrial hyperpolarisation and disruption of the mitochondrial transmembrane potential (Nagy et al. 2004; Gergely et al. 2002) Finally, this leads to ROI overproduction, ATP depletion, spontaneous apoptosis and necrosis (Nagy et al. 2004). Using human Jurkat cells, Banki et al. (1999) showed that mitochondrial hyperpolarisation together with an increment in ROIs accumulation precedes Fas-induced apoptosis.

Forty minutes after TCR engagement, either by superantigens or CD3/CD28 co-stimulation, NO can be found at a concentration of 20 nM in highly purified T lymphoblasts and primary human T lymphocytes (Ibiza et al. 2006). eNOS is normally present in the Golgi apparatus but is translocated

to the membrane when contact between T-cell and antigen presenting cell occurs, remaining at that site for at least 30 min (Ibiza et al. 2006). The onsite production of NO by eNOS promotes and synergizes phosphorylation of the CD3ζ chain and ZAP-70, followed by downstream phosphorylation of the ERK pathway (section 1.1.4.4). T lymphoblasts from eNOS-deficient mice and T-cells incubated with a NOS inhibitor (N-nitro-L-arginine, 500 μM) did not maintain ERK activation (Ibiza et al. 2006). eNOS-derived NO acts on the redox-active Cys residue 118 at the Golgi-localised N-Ras, achieving its activation and the consequent downstream activation of the ERK pathway towards cell death (Ibiza et al. 2008; Lander et al. 1997). The C118 residue is so critical that mutations on this site leads to impaired activation of N-Ras and abolish TCR-dependent apoptosis (Ibiza et al. 2008).

In addition to the involvement in TCR activation and mitochondrial hyperpolarisation, NO has been suggested to be a regulator for the cytokines balance among T_H1 and T_H2 cells. As mentioned in section 1.2.6, NO production can be induced by the main T_H1 cytokine IFN-γ (van der Veen, Dietlin, Pen, et al. 2000). Niedbala et al. (1999) established that high concentrations of a NO donor (SNAP, 500 μM) lead to suppression of IFN-γ production by T_H1 cells whereas low concentrations of SNAP (10 μM) increase IFN-γ. Within this model, culture of a T_H1 cell line in the presence of IL-12 and SNAP (10 μM) enhanced even more the IFN-γ production; however little or no effect was seen on the T_H2 line or on proliferation of both T_H1 and T_H2 cells. The explanation to this phenomenon came in a later work that showed how low levels of NO selectively enhance IL-12Rβ2 via a cGMP-dependent mechanism during T_H1 differentiation (Niedbala et al. 2002; Niedbala et al. 2006). Similarly, overexpression of eNOS increased IFN-γ production while reduced IL-2 production (Ibiza et al. 2006). On the other hand, Gomes et al. (2006) demonstrated that incubation of T_H2 lymphocytes with NO donors generates high levels of intracellular cGMP, which trigger a sustained Ca_2^+ response and subsequent expression of the T_H2 cytokine IL-4. Controversial results were reported earlier by (Nukaya et al. 1995), who found that addition of a NO donor (SNP, 0.1μM) was enough to inhibit IL-4 production in the T_H2 clone, but did not inhibit IL-2 production in T_H1 cells. Moreover, T_H2 cells were more susceptible to detrimental NO effects and suffered more inhibition of DNA synthesis in comparison with the T_H1 clone (Nukaya et al. 1995).

Other studies have suggested that NO may regulate T-cell function but is not T_H1/T_H2 selective, neither for proliferation nor for cytokine production (Macphail et al. 2003; van der Veen et al. 1999; Bauer et al. 1997). Van der Veen et al. (1999) did not find any significant difference on the *in vitro* secretion of T_H1 or T_H2 cytokines when a NO donor was added to T_H1 and T_H2 clones activated with an anti-CD3 antibody. In an *in vivo* model where mice were injected in the footpad with carrageenin to induce local inflammation, Ianaro et al. (1994) observed that cells obtained

from the draining lymph node from injected mice with carrageenin plus a NOS inhibitor (L-NMMA) developed a different pattern of cytokine production but not T_H1 or T_H2 specific. In comparison with carrageenin controls, cells which were exposed to L-NMMA showed reduced secretion of IL-1, IL-2, IL-6 and IFN-γ but increased IL-10 production. Surprinsingly, L-NMMA did reduce local edema formation although almost no effect was seen on the number of cells at the inflammation site, IL-4, TNF-α or TGF-β levels. Macphail et al. (2003) proposes that the effects seen on T_H1 and T_H2 lymphocytes depend mainly on the exposure time to NO. Incubation with NO donors prior to stimulation abolishes proliferation of both T_H populations in a time-dependent manner. Simultaneously, reduction of IL-2 mRNA, IL-13 mRNA and IFN-γ mRNA is observed as time of NO exposure increases (Macphail et al. 2003).

NO has also been associated with T-cell suppression because NO production from macrophages (van der Veen, Dietlin, Dixon Gray, et al. 2000; Bingisser et al. 1998; Strickland et al. 1996; Isobe & Nakashima 1992) suppressor monocytes (Slaney et al. 2011) and myeloid-derived suppressor cells (Movahedi et al. 2008; Mazzoni et al. 2002) causes inhibition of T-cell proliferation via NO-dependent dephosphorylation of intracellular signalling molecules or proteins. Bingisser et al. (1998) and Mazzoni et al. (2002) describe that NO induces a reversible type of T-cell anergy by reducing phosphorylation of tyrosine residues in Jak3/STAT5, an essential molecule for proliferation and cycle progression in activated T-cells (Moriggl et al. 1999). Even in presence of mesenchymal stem cells which generally suppress T-cell proliferation, addition of a NOS inhibitor (L-NAME) restored not only the T-cell proliferation but also Stat5 phosphorylation (Sato et al. 2007). Similarly, Strickland et al. (1996) observed that alveolar macrophage-derived NO reversibly blocks downstream phosphorylation of the IL-2 receptor associated proteins. van der Veen et al. (1999), also reported that the NO donor SNAP at a concentration of up to 0.1mM inhibited the proliferation of T_H1 and T_H2 clones; whereas higher concentrations induced apoptosis of both cellular subtypes. In prostate cancer, the immunosuppression/anergy of $CD8^+$ tumor-infiltrating cytotoxic lymphocytes against cancer cells was reverted by inhibiting the activity of the enzyme arginase I and by adding NOS inhibitors (Bronte et al. 2005). The suppressive effect on T-cells could be indirectly related to the L-arginine deprivation caused by an increased NOS enzymatic activity. Choi et al. (2009) reported that in the absence of L-arginine T-cells cannot be activated, proliferate or produce cytokines efficiently.

Valenti et al. (2005) suggest that NO blocks T-cell proliferation by arresting the cells in late G1 phase of the cell cycle, just before DNA synthesis. These cells will be committed to apoptosis or necrosis if the harmful NO stimulus persists, as the protein p53 starts to accumulate (Valenti et al. 2005). Niedbala et al. (2002) reinforced that T-cell exposure to high concentrations of NO (NOC-

18 >100μM) consistently increased the level of apoptosis; whilst low concentrations (NOC-18 <10μM) enhanced the differentiation of the of $CD8^+$ cytotoxic T-cells. Earlier work reported that a NOS inhibitor (L-NMMA) protected mature T lymphocytes from TCR-triggered death by reducing the TCR-stimulated expression of functional Fas ligand and thus stopping the downstream apoptosis signalling (Williams et al. 1998).

1.3.8 Paradoxical effect of nitric oxide in bacterial toxin induced-disease

For some time glucocorticoids have been used in the treatment of toxic shock syndrome, due to its ability to prevent NO production induced by *Staphylococcus aureus* toxins or LPS (Zembowicz & Vane 1992). However, animal models that studied the effect of NO in *Staphylococcal enterotoxin* B-induced shock and LPS-induced cytotoxicity derived controversial conclusions.

Some authors reported that administration of a NOS inhibitor affords a protective effect against endotoxemia, preventing hypotension and secondary organ failure (Kilbourn et al. 1990). In contrast, others demonstrated that endogenous NO is beneficial and that NOS inhibition increases thrombosis and mortality rates in T-cell-dependent shock induced by superantigens (Florquin et al. 1994; Shultz & Raij 1992; Billiar et al. 1990). Florquin et al. (1994) showed that NOS inhibition with L-NAME enhanced IFN-γ and TNF-α production, inducing lethal prothrombotic events in mice. This observation together with the fact that IFN-γ and TNF-α normally induces NO synthesis, denotes that NO might downregulate IFN-γ and TNF-α to counteract their prothrombotic properties (Florquin et al. 1994). To overcome this problem, Jaimes et al. (2001) propose that prevention of glomerular thrombosis and restitution of vascular tone can be achieved *in vivo* with concomitant administration of a NO and TNF-α inhibitors. Sundrani et al. (2000) observed that superfusion of a non-selective NOS inhibitor is deleterious in septic rats because increases leukocyte rolling and leukocyte adhesion (Grisham et al. 1998); resulting in long lasting stickier leukocytes that can block the microvasculature. In the other hand, Brás et al. (1997) found that administration of NO donors to mice injected with *Staphylococcal enterotoxin* B have contradictory effects, inducing thymic clonal expansion of $CD4^+$ thymocytes but inhibiting proliferation of peripheral T_H1 lymphocytes. Presence of NO donors delay *Staphylococcal enterotoxin* B-triggered apoptosis and replenish the pool of thymocytes (Brás et al. 1997).

1.4 AIMS OF THIS PROJECT

Well established models of B-cell stimulation using T-independent antigens have been reported in the literature. The finding that became of big interest in our lab was that combination of T-independent type 2 mimics with TCR T-cell stimulation (anti-CD3 $\pm$ anti-CD28), unexpectedly results in suppression of T-cell proliferation and activation within a PBMC culture. The work described in Chapter 3 aims to identify the cells involved in the T cell suppression caused by TI-2 mimics and if possible to identify the mechanism of action.

N. meningitidis is a bacterium which rarely causes invasive disease and sepsis, but perpetuates colonisation in the nasopharynx by avoiding immune recognition and killing. Because several *N. meningitidis* constituents are TI type 2 antigens and/or provide second signals to B-cells *via* TLR, it was hypothesized that paraformaldehyde fixed meningococcus could exert immunomodulatory properties. Chapter 4 aims to explore this possibility and intends to elucidate bacterial constituents that could function as immunosuppressor molecules.

Several bacterial components stimulate nitric oxide production; however *N. meningitidis* can counteract the bactericidal effect of reactive nitrogen intermediates by a partial denitrification pathway. Nitric oxide is produced in T-cells as a result of TCR engagement. Fluctuations of NO concentrations have been associated to activation or inhibition of several intracellular pathways, which lead to either proliferation or apoptosis. Chapter 5 investigates whether NO donation or inhibition could influence $CD4^+$ T-cell responses and provide a link with bacterial infections.

It is expected that the knowledge generated from this project will help to understand those bacterial infections that initiate colonisation and evade the immune the system. In particular, those bacteria which remain ‘silent’ in the host before inducing severe and rapidly progressive systemic infections, such as sepsis.

CHAPTER 2:

METHODOLOGY

2.1 ISOLATION OF PERIPHERAL BLOOD MONONUCLEAR CELLS

For all experiments, an amount of peripheral blood was taken from the cubital vein of adult healthy volunteers and collected into 50 ml tubes containing heparin (10 IU of heparin per ml of blood). At room temperature, blood was diluted 1:1 with sterile PBS and slowly poured onto half the volume of lymphocyte separation medium (Lymphoprep™, BioWhittaker, Lonza, UK). Centrifugation at 400 rcf, ACCN=0, Brake=0, 20°C for 35 min allowed layers formation. The layer of peripheral blood mononuclear cells (PBMCs), located at the interface between the lymphocyte separation buffer and the plasma, was carefully removed with a plastic pasteur pipette. Plasma was also removed and stored on ice for cell culture media preparation.

Collected PBMCs were washed four times with 20ml sterile chilled PBS (centrifugation at 600 rcf, ACCN=8, Brake=8, 4°C, 10 min). After discarding supernantant, the final pellet was resuspended in 1 ml of cell culture media preparation: RPMI 1640 media (BioWhittaker, Lonza, UK) containing 20% autologous plasma and supplemented with 2 mM L-Glutamine (Lonza, UK). On the basis of tryptan blue (0.1%, Sigma, UK), live PBMCs were counted with an improved Neubauer chamber, and were further resuspended in the RPMI preparation to obtain a final concentration of 1×10^7 cells per ml.

Students and members of the staff at the Medical School from Sheffield University and the Royal Hallamshire Hospital gave informed consent and participated as voluntary blood donors. The procedure was approved by the Central Office for Research Ethics.

2.2 ISOLATION OF PRIMARY CELL TYPES

2.2.1 Enrichment of cell populations

In all cases, negative selection was preferred to purify cell populations from PBMCs. Without using columns but using antibody complexes linked to magnetic particles (EasySep™, Stemcell Technologies), cross-linked undesired cells remained attached to the magnet while desired cells were found free in the supernatant.

Briefly the procedure is as follows, cells were placed in a sterile polystyrene round-bottom tube and resuspended in the recommended medium RoboSep™ (sterile PBS + 2% fetal bovine serum + 1 mM EDTA, calcium and magnesium free). Subsequent incubation for 10-15 min with the provided antibody cocktail, targeted the phenotypic antigens from all the undesired PBMCs (Table 2.1). At this stage, the magnetic dextran nanoparticles were added and incubated for further 5-10 min to allow formation of magnetic antibody complexes. Before magnetic separation, the mixture was gently mixed with a pipette and more RoboSep medium was added according to manufacturer's instructions. The EasyPlate EasySep magnet™ was preferred over other magnets because it allows maximal recovery out from small numbers of cells. After 10 min on the plate magnet, supernatants were collected from the wells and washed with RPMI media to obtain a cell pellet. Following manufacturer's instructions, $\geq$95% pure and viable cell populations were obtained.

Table 2.1: Enrichment of cell populations.

Cell population to be purified	**Negative selection Kit (**EasySep™ Stemcell Technologies**)**	**Antibodies contained in the cocktail (anti-)**
$CD4^+$ T-cells	Human CD4+ T-cell enrichment kit. Cat# 19052	CD8, CD14, CD16, CD19, CD20, CD36, CD56, CD66b, CD123, TCRγ/δ and glycophorin A
B-cells	Human B-cell enrichment kit. Cat# 19054	CD2, CD3, CD14, CD16, CD36, CD43, CD56, CD66b and glycophorin A
Monocytes	Human Monocyte enrichment kit. Cat#19059	CD2, CD3, CD16, CD19, CD20, CD56, CD66b, CD123 and glycophorin A

2.2.2 Depletion of cell populations

Cell depletions were achieved by performing a positive selection on the undesired cell type. The cell fraction to be depleted was labeled with antibody complexes linked to magnetic particles (EasySep®, Stemcell Technologies) and remained attached to the magnet, while the unlabelled PBMCs were collected from the supernatant.

Similarly to the enrichment procedure, PBMCs were incubated for 15 minutes with the antibody of interest and then labeled with magnetic dextran nanoparticles for 10 minutes. Next, the sample tube was placed in the magnet and left on the side for 10 minutes. Finally, the depleted fraction was poured out from the tube whilst the targeted undesired cells remained attached to the sides of the magnet. This last step was repeated twice in order to increase purity of the depleted fraction. Table 2.2 contains a full description of the depletion kits used for this procedure.

Almost absolute cell removal was achieved ($\geq$99%) by following manufacturer's depletion procedure.

Table 2.2: Depletion of cell populations.

Cell population to be depleted	**Positive selection Kit (**EasySep™ Stemcell Technologies**)**	**Antibodies contained in the cocktail (anti-)**
B-cells	HLA B-cell positive selection kit. Cat# 18454HLA	CD19 and CD20
Monocytes	Human CD14 selection kit. Cat#18058	CD14
NK cells	Human CD56 selection kit. Cat #18055	CD56

2.3 STIMULATION OF T AND B-CELLS

2.3.1 Stimulation of T-cells

2.3.1.1 anti-CD3

Purified anti-human CD3 antibody (αCD3) (Invitrogen, UK) was used to achieve T-cell activation by direct binding with the cell surface CD3 molecule and subsequent engagement of the TCR (Geppert & Lipsky 1987). More effective than free αCD3 is plate-bound αCD3, perhaps because the tissue culture flat bottom provides a physical platform upon which the purified antibody can be easily exposed to T-cells and be cross-linked (Vayuvegula et al. 1990).

A 48-well tissue culture plate was pre-coated with 0.1-0.3 µg/ml of αCD3 in sterile PBS, allowing incubation at 4°C for at least 18 hours to achieve plate binding. Prior to performing the assay, wells containing the immobilised αCD3 were carefully washed 3 times with sterile PBS.

It was demonstrated previously in our lab (J.B. Wing and R.A. Foster, unpublished data), that these concentrations of plate-bound αCD3 stimulate $CD4^+$ T-cells sufficiently to prime them. The resultant proliferation and activation are suboptimal and so allow detecting changes in both directions.

2.3.1.2 Concanavalin A

Concanavalin A (ConA) is a lectin extracted from castor beans, which interacts with receptors containing mannose carbohydrates. ConA provides a non-specific mitogenic effect on CD4 and CD8 T-cells, but only in presence of accessory cell contact (Chatila et al. 1987).

At a final concentration of 5 µg/ml, ConA (Sigma, UK) was directly added to wells containing 500µl of cell culture media and 1 $x10^6$ PBMCs.

2.3.1.3 *S. aureus* Enterotoxin B

Staphylococcus aureus enterotoxin B (SEB) was selected for being a classical superantigen TCR agonist in humans. Superantigens are proteins of bacterial or viral origin which engage a particular region of the variable chain at the TCR (Vβ domain), located outside the peptide-binding groove (Choi et al. 1989). Thus, regardless the antigen specificity of the receptor, superantigens are able stimulate up to 20% of the total T-cell population depending on the Vβ family against which the superantigen is reactive to.

At a final concentration of 400 ng/ml SEB (Sigma, UK) was directly added to wells containing 500µl of cell culture media and 1 $x10^6$ PBMCs.

2.3.1.4 αCD3/αCD28 Dynabeads

Evidence suggests that highly purified primary T-cells are unresponsive to solid-phase bound αCD3 alone (Palacios 1985). However, simultaneous cross-linking of the CD28 molecule with a monoclonal antibody augments T-cell stimulation by providing a helper signal. An anti-CD28 antibody (αCD28) will mimic the CD80/86 co-stimulation, even in absence of accessory cells (Jenkins et al. 1991; Baroja et al. 1988).

Therefore, in every assay performed with purified T lymphocytes, Dynabeads® Human T-Activator CD3/CD28 (Invitrogen, UK) were preferred over the usual plate-bound αCD3. Dynabeads® Human T-Activator CD3/CD28 are magnetic beads coated with anti-CD3 and anti-CD28 monoclonal antibodies that mimic *in vivo* T-cell activation from antigen presenting cells and provide an effective TCR signalling.

Prior addition of enriched T-cells (1 x10^6 per well), Dynabeads® Human T-Activator CD3/CD28 were washed once with PBS, resuspended in RPMI 1640 media and added directly to the cell culture well at a ratio of 1:1 bead per T-cell.

2.3.2 B-cell stimulation with T-independent mimics

2.3.2.1 Anti-IgD-conjugated dextran

Anti-IgD-conjugated dextran (α-δ-dex) is a T-independent type II mimic (section 1.1.5.2.1) which consists of multivalent anti-IgD antibodies conjugated to a dextran molecule (Rehe et al. 1990; Brunswick et al. 1988). When prepared as previously described (Peçanha et al. 1993; Snapper et al. 1992), a concentration of 1 μg/ml was sufficient for B-cell stimulation when added directly to a well containing 1 x10^6 PBMCs (R. a Foster et al. 2009).

For this work, α-δ-dex was manufactured and kindly provided by Dr. Andrew Lees, Biosynexus (Gaithersburg, MD, USA).

2.3.2.2 *Moraxella* IgD-binding protein

The high molecular weight adhesin surface protein *Moraxella* IgD-binding protein (MID) displays a high affinity for soluble and surface-bound IgD (Forsgren et al. 2001). The tetrameric MID sequence containing the amino acid residues 962 to 1200, has been detected as the essential IgD binding subunit of this protein (Nordström et al. 2002). A truncated protein containing the amino acids $MID^{962\text{-}1200}$ has been shown to induce B-cell activation and proliferation in a T-independent fashion. Concentrations of 0.5-1 μg/ml are enough to detect an effect in peripheral blood lymphocytes (Nordström et al. 2006).

For this work, $MID^{962\text{-}1200}$ (from now on only referred as MID) was manufactured and kindly provided by Kristian Riesbeck (Lund University, Sweden).

2.4 PROLIFERATION ASSAY

To quantify proliferation of T and B cells, a protocol based on carboxyfluorescein diacetate succinimidyl ester (CFSE) was applied. CFSE is a non-fluorescent molecule which passively diffuses into cells and reacts with intracellular amines. Inside the cells, its succinimidyl ester group is hydrolyzed by non-specific esterases to become a fluorescent conjugate. The dye is then retained and divides equally between daughter cells upon division cycles (Lyons & Parish 1994). Thus, CFSE labeling allows identification of cell populations which have undergone multiple rounds of meiosis, being possible to track up to 10 generations (Lyons 2000).

According to manufacturer's instructions (Molecular Probes, Invitrogen, UK), a 10 mM stock CFSE solution was prepared with 90 µl of sterile high quality DMSO and stored frozen in aliquots. From these, a 0.1mM CFSE solution was prepared on the day with sterile PBS. Following extraction, washing and resuspension of PBMCs in RPMI (section 2.1), 20 µl of the CFSE solution was added per 1 x 10^7 cells per ml, obtaining a final CFSE concentration of 2 µM. Immediately after, PBMCs were incubated at 37^{o}C for 10 min in the dark. Next, the reaction was quenched with an equal volume of cold autologous plasma and incubated for other 10 min at room temperature in the dark. After centrifugation (600 rcf, 20^{o}C for 10 min) and decanting of supernatant, pellets were washed three times with 10 ml of the RPMI preparation (section 2.1). The resultant pellet was then resuspended in 1ml of RPMI and cells were counted as described before (section 2.1). Finally, 1 x10^6 PBMCs were added to 48-well flat-bottomed cell culture plates (TC treated, sterile; Costar, UK) in a final volume of 500 µl of RPMI preparation per well, allowing cell incubation (37^{o}C, 5% CO_2) until further flow cytometric analysis.

In flow cytometry, the sequential halving of CFSE fluorescence intensity is represented as an histogram with series of distributions or peaks, which can be analysed using a proliferation analysis package from a specialised software (FlowJo 7.6®). All proliferation results and graphs were reported as division index, which is defined as the average number of divisions undergone in the starting population, including undivided cells (section 2.5.5).

2.5 ANALYSIS OF SAMPLES BY MULTICOLOR FLOW CYTOMETRY

Except where otherwise noted, cells were seeded at 1 x 10^6 cells per well in a final volume of 500µl of RPMI preparation and incubated at 37°C, 5% CO_2 in a humidified atmosphere for 96 hours before harvesting. Incubation of PBMCs for 4 days has previously demonstrated to be enough to detect maximal cell proliferation and activation, before excessive numbers of cells die and the culture media become exhausted (J.B. Wing and R.A. Foster, unpublished data).

2.5.1 Flow Cytometer LSRII

For all samples, FACS analysis was done with the LSRII flow cytometer (BDbiosciences, UK). The BD LSRII™ is fully configurable and comes with 4 lasers (UV, violet, blue and red), allowing analysis up to 13 fluorochromes simultaneously. Along the project, multicolour panels were design to assess several phenotypic, activation and viability parameters simultaneously. Table 2.3 shows the instrument settings at the Core Flow Cytometry facilities at the University of Sheffield.

In every experiment, digital acquisition and experimental layout was performed with the FACS DIVA™ software (BDbiosciences, UK).

Table 2.3: BD LSRII Flow Cytometer customised setup

Laser	Excitation channel (nm)	Filters
UV	355	450/50
		530/30
Violet	405	450/50
		525/50
Blue	488	530/30
		575/26
		610/20
		660/20
		695/40
		780/60
Red	633	660/20
		730/45
		780/60

2.5.2 Extracellular staining for phenotypic and activation markers

An extracellular staining was required to label surface molecules that determine cell phenotype and expression of activation markers. Table 2.4 provides a full description of the antibodies and their fluorochromes.

Cells were harvested from the 48-well plates and transferred into 1.1 ml racked micro test tubes (Elkay Laboratories, UK) for immunofluorescence labeling. Then, samples were washed three times with Fluorescence Activated Cell Sorting (FACS) buffer [PBS supplemented with 0.1% bovine serum albumin (First Link, UK)].

1 x 10^6 cells were stained with 1 µl (approx 0.025 µg) of each of the desired antibodies into 80 µl of FACS buffer, which also contained a cell viability dye (section 2.6.1). After incubation for 1 hour in the dark at 4^{o}C, cells were washed three times with FACS buffer to remove unbound antibodies. Finally, samples were fixed with 300 µl of 2% paraformaldehyde and analysed by flow cytometry.

2.5.3 Intracellular staining

Only in a couple of experiments (sections 5.4.3 and 5.5.4), an intracellular staining protocol was carried out to assess expression of Foxp3 within T-cells. APC-Foxp3 antibody (eBioscience, UK) together with a Foxp3 staining buffer kit (eBioscience, UK), were used according to manufacturer's instructions at a concentration of 0.5 µg per 1 x 10^6 cells.

2.5.4 Selection of fluorochromes

Seeking for the best possible combination of fluorophores to investigate T and B-cells interactions within a single assay, an extensive optimisation of multicolour panels has been carried out in our lab. Along this research work, further optimisation and modifications to the initial multicolour matrix were made to cover the aims of this project (Table 2.4).

Table 2.4: Description of the fluorescently-labeled antibodies used.

Molecule	Antigen Location	Fluorochrome	FACS Channel	Supplier
CD4	EC	Allophycocyanin conjugate (APC)	Red 660/20	Invitrogen
CD4	EC	PerCP Cy 5.5	Blue 695/40	eBioscence
CD19	EC	PE Cy-7	Blue 780/60	Invitrogen
CD20	EC	APC	Red 660/20	eBioscence
CD14	EC	Pacific blue conjugate (PB)	Violet 450/50	Invitrogen
CD56	EC	Brilliant Violet 510	Violet 525/50	Biolegend
CD25	EC	R- Phycoerythrin (PE)	Blue 575/26	eBioscence
CD86	EC	PE Alexa-700	Blue 695/40	Invitrogen
IgD	EC	PE	Blue 575/26	Invitrogen
Foxp3	IC	APC	Red 660/20	eBioscence
Free amines	IC	LIVE/DEAD® Fixable Blue Dead Cell Stain (UV dead/live)	UV 450/50	Molecular probes-Invitrogen
Nucleic acids	IC	TOPRO-3	Red 660/20	Molecular probes-Invitrogen
Phospholipid phosphatidylserine	IC	Annexin-V	Blue 575/26	BD Pharmingen

EC= extracellular; IC= intracellular.

2.5.5 Post-acquisition analysis

Collected data was analysed with the FlowJo 7.6® Windows software (TreeStar Inc, USA), a powerful, fast and reliable program dedicated to digital analysis of FACS data.

As in any polychromatic flow cytometry matrix, compensation was necessary to correct for spectral overlap. Compensation was done post-hoc with the dedicated tool of FlowJo 7.6 software, in conjunction with anti-mouse Ig, κ compensation beads (CompBeads, BDbiosciences, UK), isotype controls and cell based single staining in the cases of CFSE, UV Live/Dead, Annexin-V and TO-PRO-3. After compensation, biexponential transformation (logicle implementation) improved visualisation and clustering of populations with negative values. Such transformation causes the scale to compress in the lower range so distributions around zero are seen, thus the comparison in between low and high fluorescence looks more precise.

Applying a consequential gating strategy to all individual experiments, the different cell populations were established in the following order:

Gating cells (FSC-Area *versus* SSC-Area) > Doublet discrimination and singlets inclusion (FSC-Area *versus* FSC-Height) > selection of live cells by gating on the UV Live/Dead low population > Gating on CD14 negative cells to exclude $CD14^+$ monocytes > and finally, gating of T-cells ($CD4^+$ $CD19^-$) and B cells ($CD19^+$ $CD4^-$) (Figure 2.1).

Cell proliferation was evaluated by the CFSE method (section 2.4) using a proliferation platform also contained within the FlowJo 7.6 software. The tool provides constant 'best-fit' gates for a CFSE histogram, but has the advantage of being adjustable for the numbers of peaks (cell generations), the peak 0 (generation 0), the ratios between adjacent peaks and the width of each peak. For this project, division index was the proliferation parameter chosen to report as it reflects what the entire system is doing, including the non-responding cells (i.e., includes the cells in peak 0 that never divided) (section 2.4).

2.6 VIABILITY ASSAYS

2.6.1 Cell death

As a routine, the viability dye LIVE/DEAD® Fixable Blue Dead Cell Stain Kit for UV excitation (Molecular Probes, Invitrogen, UK) was included in every experiment to monitor cell death. Such dye reacts with free amines, yielding intense fluorescence from cells with compromised membranes in which the dye reacts with free amines both in the cell interior and on the cell surface. In contrast, viable cells will show relatively dim staining as the dye's reactivity is restricted to the cell-surface amines (Perfetto et al. 2006). On this basis, results were expressed as percentage of live cells.

To reconstitute the reactive dye, 50 µl of DMSO were added directly to the vial and small aliquots were frozen for future use. On the day the stock was diluted 1:500 in FACS buffer. Subsequently, all fluorochromes included in the extracellular staining panel (section 2.5.2) were incorporated into this FACS/fixable blue solution.

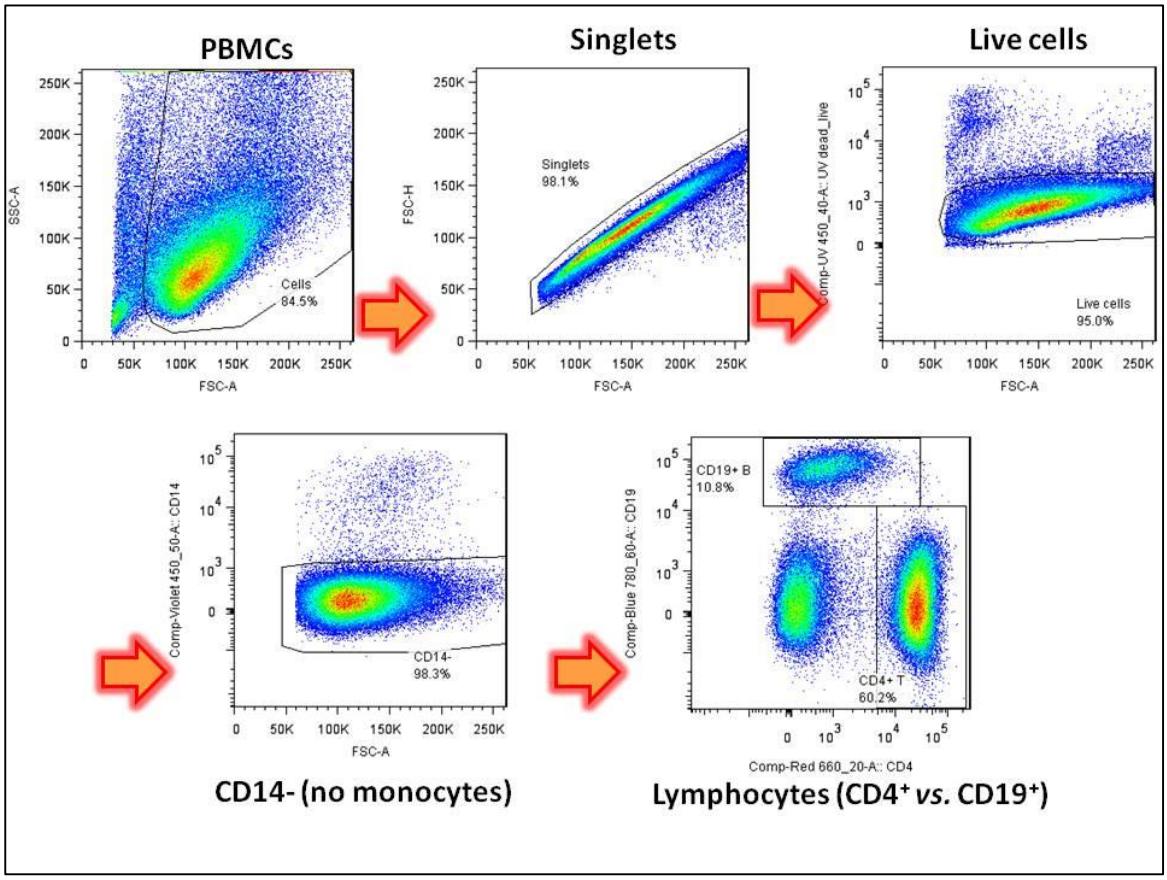

Figure 2.1: Sequential gating strategy.

Example of the gating strategy applied to detect the different cell populations. Gating cells (FSC-Area *versus* SSC-Area) > Doublet discrimination and singlets inclusion (FSC-Area *versus* FSC-Height) > selection of live cells by gating on the dye live/dead > Gating on CD14 negative cells to exclude $CD14^+$ monocytes > and finally, gating of T-cells ($CD4^+$ $CD19^-$) and B cells ($CD19^+$ $CD4^-$).

Plots are representative of a single donor stimulated with αCD3. Results are given in % of cells within each gate.

2.6.1 Apoptosis

For more specific and sensitive viability assays, apoptosis was evaluated after 24, 48, 72 and/or 96 hour incubation. Detection of membrane disruption as an indicator of cell death was conducted by using simultaneous staining with Annexin-V and TO-PRO-3 (Vermes et al. 2000). Loss of plasma membrane integrity occurs as an early event in apoptotic cells, and is characterised by the translocation of phospholipid phosphatidylserine (PS) residues from the inner to the outer leaflet of the plasma membrane. Annexin-V is a Ca^{2+} dependent phospholipid-binding protein with high affinity for those externalised PS and thus serves for detection of early apoptotic cells (Vermes et al. 1995). TO-PRO-3 is a cell-impairment cyanine single dye which has strong affinity for DNA. Thus, when the cell membrane integrity is broken and becomes leaky, TOPRO-3 incorporates with the nuclear DNA and becomes fluorescent (Matsuzaki et al. 1997). Positive cells for TO-PRO-3 are indicative of going through late apoptosis or necrosis; however, does not distinguish between both stages (Vermes et al. 2000).

After the usual extracellular staining protocol (section 2.5.2) but without fixation, 4 µl of Annexin-V antibody (BD Pharmingen, UK) into 80 µl of 1X Annexin binding buffer (BD Pharmingen, UK) were added to each sample. Incubation in the dark for 30 min at room temperature was enough to allow binding. A 100nM stock solution of TO-PRO-3 (Molecular probes, UK) was prepared into 1X Annexin binding buffer. Immediately prior to flow cytometry analysis, 200 µl of this TO-PRO-3 solution was added to each sample.

2.7 CYTOKINE ANALYSIS

Measurement of cytokines in collected supernatants was carried out using Cytometric Bead Array (CBA) Flexsets (Becton Dickinson FACS array™) according to manufacturer's instructions. Results were collected on a BD FACSArray using BD FACSArray software for acquisition and FCAP array software (Soft Flow) for analysis. Results were reported as median fluorescence intensity and cytokine concentration (pg/ml).

Run and analysis of samples was carried out by the technical support team (Sue Clark and Kay Hopkinson) at the Flow Cytometry facilities, Medical School, University of Sheffield.

2.8 BACTERIAL STRAINS AND DERIVED COMPONENTS

2.8.1 *Neisseria meningitidis*

2.8.1.1 Strains

Different strains of the bacterium *N. meningitidis* were used along this project:

a) Wild type serogroup B meningococci (strain MC58):
The MC58 strain was originally isolated in 1991 from a confirmed case of meningococcal meningitis in the UK (McGuinness et al. 1991) and its genome was later fully sequenced (Tettelin et al. 2000).

b) LPS-deficient mutant and its parental strain H44/76:
An LPS deficient strain was kindly provided and manufactured by Dr. Peter van der Ley (National Institute of Public Health, The Netherlands). Briefly, the mutant was constructed as an *lpxA*-knockout by inserting a kanamycin-resistance cassette at position 293 in the *lpxA* gene contained in a plasmid. The resulting plasmid (pLAK33) was linearised and transformed to strain H44/76 (Steeghs et al. 1998). For this project, absence of the *lpxA* gen was further confirmed in our lab by selection of kanamycin resistant colonies and PCR of the *lxpA* fragment (section 4.5).
Similar to MC58, the wild type serogroup B meningococci H44/76 strain was initially isolated in Norway from patients with invasive meningococcal infection (Holten 1979).

c) Opa-deficient serogroup B (strains MC58/h18.18-Opa-1 and ¢2):
The MC58 Opa-deficient strain is a capsulated piliated variant from MC58/h18.18, which was isolated through a procedure of receptor-overlay colony blots using soluble CEACAM-1Fc constructs (Bradley et al. 2005; Virji et al. 1995).
The ¢2 Opa-deficient strain was also included in our assays (characterised by Virji et al. (1995). ¢2 is a meningococcus Opa negative variant from the MC58 group (B15:P1.7,16) which lacks of capsule by mutation, but expresses Opc and Pili.
Absence of Opa proteins from both strains was previously confirmed in our lab by immunoblotting (J Laver and L Green).

In our lab, frozen stocks of viable bacteria were maintained in cryopreservation fluid (Protect™, TSC) at -80°C until their use.

2.8.1.2 Bacterial growth

The frozen bacteria stocks were allowed to thaw and then streaked over Columbia blood agar (CBA) plates. In case of the LPS-deficient mutant, CBA plates were supplemented with kanamycin (50 µg/ml) for antibiotic selection. Streak plates were incubated at 37°C, 5% CO_2 for 16-20 hours, when bacterial colonies reach a macroscopic size of approximately 2-3 mm.

Mueller-Hinton Broth (MHB) (Oxoid, UK) was prepared by adding 21 g of powdered MHB to 1 L of distillated water. The suspension was mixed and sterilised by autoclaving at 120°C for 15 min and stored in glass bottles at room temperature. Individual bacterial colonies (between 6 and 8 colonies) were randomly taken from the plate and inoculated into 10 ml of MHB. The tube was then incubated at 37°C under a 5% CO_2 condition and with mild agitation provided by a plate mixer.

In case of these three strains, mid-log phase culture was reached in about 2.5 or 3 hours with an average absorbance (OD_{600nm})= 0.3 to 0.4

2.8.1.3 Stock preparation for experiments

The mid-log phase culture was pelleted and washed 3 times with sterile PBS. Fixation was performed by adding 2% paraformaldehyde solution and incubating for 25 minutes. The number of colony forming units (cfu) per ml was determined by the Miles and Misra technique. A stock solution of 5 $x10^8$ bacteria/ml was prepared in PBS or RPMI culture media. Aliquots were frozen at -20°C and defrosted on the day of the experiment.

2.8.2 *Streptococcus pneumoniae*

The *Streptococcus pneumoniae* virulent serotype 2 strain D39, was chosen due to its widely accepted use in research as a model strain to study pathogenicity. Strain D39 was obtained from a clinical isolate in 1916, but not sequenced until 2007 (Lanie et al. 2007).

We thank Dr. David Dockrell (Medical School, the University of Sheffield) for providing us with the strain.

2.8.2.1 Bacterial growth

The frozen bacteria stocks were allowed to thaw and then streaked over CBA plates containing horse blood. Plates were incubated over night at 37^{O}C and 5% CO_2.

From the plate, around 6-7 colonies of *S. pneumoniae* D39 were selected and inoculated into 20 ml of Brain-Heart Infusion (BHI) broth supplemented with 20% heat inactivated fetal calf serum. Mid-log phase was typically reached at 5 or 6 hours incubation with mild agitation at 37^{O}C and 5% CO_2. An average absorbance (OD_{610nm}) of around 0.5-0.6 was reached in about 4 hours.

2.8.1.3 Stock preparation for experiments

Same as described for *N. meningitidis* (section 2.8.1.3).

2.8.3 *Escherichia coli*

The non-pathogenic *Escherichia coli* serotype O6 biotype 1 strain (ATCC 25922) (ATCC 2012) was used in this project.

We thank Dr. Mark Thomas (Medical School, the University of Sheffield) for providing us with the strain.

2.8.3.1 Bacterial growth

The frozen bacteria stocks were allowed to thaw and then streaked over LB plates. Plates were incubated over night at 37^{O}C and 5% CO_2.

From the plate, around 6-7 colonies of *E. coli* 25922 were selected and inoculated into 20 ml of MHB broth. With mild agitation at 37^{O}C and 5% CO_2, mid-log phase was typically reached at 2 hours with an average absorbance (OD_{610nm}) of around 0.5-0.6.

2.8.3.3 Stock preparation for experiments

Same as described for *N. meningitidis* (section 2.8.1.3).

2.8.4 Outer membrane vesicles

Outer membrane vesicles (OMVs) are 'blebs' from the bacterial outer membrane (Rosenstein et al. 2001) (section 1.2.4.6).

Purified OMVs from both *N. meningitidis* (MC58 strain) and *Neisseria lactamica* (strain NL1009) were produced and kindly donated by Andrew Gorringe (Health Protection Agency UK) (Gorringe et al. 2009; Oliver et al. 2002).

2.9 NITRIC OXIDE (NO) DONATION AND INHIBITION

2.9.1 Nitric Oxide donor

2,2'-(Hydroxynitrosohydrazino)bis-ethanamine or NOC-18 (Sigma-Aldrich, UK) was selected as the NO donor in our system because it is a stable NO-amine complex that spontaneously releases 2 molecules of NO under physiological conditions. NOC-18 is a slow NO generator, with a half life of 21 hours at 37^{o}C and under a pH of 7.4.

According to manufacturer's instructions NOC-18 was diluted into 0.1 M NaOH and stored in aliquots, frozen and protected from light. A titration of the compound was performed from 1µM to 1000 µM, selecting 300 µM as optimal concentration for not causing cellular death and keeping a maximal effect (section 5.4.1).

2.9.2 Nitric Oxide synthases inhibitors

Two widely used arginine analogues, Nω-Nitro-L-arginine methyl ester hydrochloride (L-NAME) and NG-monomethyl L-arginine citrate (L-NMMA) were selected as inhibitors of NO synthases. L-arginine analogues work by competitive interaction with the substrate L-arginine, binding at the NOS catalytic site, avoiding L-arginine uptake by the enzyme and further NO formation (Rees et al. 1990) (Kerwin & Heller 1994). Indeed, L-NAME and L-NMMA are capable of blocking NO production from the three NO synthases (iNOS, eNOS and nNOS).

Following manufacturer's instructions (Sigma-Aldrich, UK), L-NAME and L-NMMA solutions were freshly prepared and diluted into RPMI. A titration of L-NAME was performed from 0.5 mM to 10 mM, choosing 10 mM as optimal concentration for showing the maximal inhibitory effect.

2.9.3 Cavtratin Peptide

The caveolin-1-derived peptide named cavtratin and designed by (Bucci et al. 2000), contains the amino acids sequence (82-101) corresponding to the scaffolding domain of caveolin-1 (DGIWKASFTTFTVTKYWFYR), attached to the antennapedia internalisation sequence (RQIKIWFQNRRMKWKK). Amino acids 82-101 from the caveolin-1 sequence have been shown to interact directly with eNOS and block its catalytic activity via inhibition of calmodulin binding (Bucci et al. 2000; Kwok et al. 2009; Ju et al. 1997).

The peptide was customised and manufactured by Genecust (Luxembourg) with a purity >80%. Additionally, a second peptide was manufactured containing the caveolin-1 domain but lacking internalisation sequence (SI Biologics, United Kingdom).

According to manufactures instructions, both peptides were resuspended in DMSO and stored in small aliquots frozen.

2.10 Statistical Analysis

Graphics and statistical analysis were performed using the GraphPad Prism 5® software.

Experiments with only two groups were compared by a paired student *t*- test, while experiments containing more than 2 groups were compared by one way ANOVA or paired ANOVA. In addition, the post-tests Dunnett's (when compared to a control data set) and Bonferroni's (selected pairs comparisons) were applied.

In all cases, significance was defined by a p value ≤ 0.05 and the following significance intervals: * p= 0.01-0.05, ** p= 0.001-0.01, *** p= ≤ 0.001. Along this work, graphics are shown as means and standard errors of the mean (SEM).

CHAPTER 3:

HUMAN B-CELL ACTIVATION WITH A POLYCLONAL T-INDEPENDENT TYPE 2 ANTIGEN MIMIC INHIBITS TCR-INDUCED T-CELL PROLIFERATION AND ACTIVATION.

3.1 INTRODUCTION

Section 1.1.4 has explained in detail how T and B lymphocytes interact in synergy with each other to coordinate immune responses against pathogens. Normally, the TCR will bind to a compatible antigen-MHC complex on B-cells, triggering intracellular pathways within T lymphocytes and ultimately producing the up or downregulation of surface antigens and cytokines which can in turn regulate B-cell and other immune cells. Simultaneously and *via* co-stimulatory molecules such as CD40, B lymphocytes will gain T-cell 'help' for further activation, expansion and production of memory B-cells or antibody producing plasma cells.

There are two broad types of antigen, distinguished by the necessity for T-cell 'help' to be delivered to B-cells before the B-cells can respond properly. Responses to T-dependent (TD) antigens require T-cell 'help' by engagement of the CD40 molecule on B-cells by the CD40 ligand (CD154) on T-cells (cognate 'help') (section 1.1.5.1). In contrast, T-independent (TI) antigens activate B-cells in the absence of T-cell 'help' (section 1.1.5.2).

TI antigens are further classified as type 1 and type 2 (section 1.1.5.2). TI type 1 antigens such as bacterial cell wall components induce polyclonal B-cell responses *via* cross-linking TLRs along with the B-cell receptor (BCR). TI type 2 antigens are large molecules with repeating epitopes (as polysaccharides), which extensively cross-link surface immunoglobulins within the BCR.

Anti-IgD-conjugated dextran (α-δ-DEX) is a model TI type 2 antigen that stimulates B lymphocytes by cross-linking of numerous B-cell receptor molecules in a similar manner to bacterial capsular polysaccharides (Peçanha et al. 1993). α-δ-DEX consists of multivalent anti-IgD antibodies covalently linked to a high molecular weight dextran molecule (Brunswick et al. 1988). α-δ-DEX is a potent stimulator of resting B cells which can be used in cellular function assays as a polyclonal B-cell mitogen and activator (Peçanha et al. 1991), although does not initiate immunoglobulin production or isotype switching (Snapper & Mond 1996).

It has been previously demonstrated that α-δ-DEX induces effective activation and proliferation of B-cells in a PBMC culture and that such response can be strongly synergistic if simultaneous bystander T-cell help occurs (R. a Foster et al. 2009; Snapper et al. 1995).

The finding that became of big interest in our lab was that combination of α-δ-DEX with TCR T-cell stimulation (anti-CD3 $\pm$ anti-CD28), unexpectedly results in suppression of T-cell proliferation and activation within a PBMC culture. In comparison with the control sample containing TCR activators

only, additional B-cell stimulation with α-δ-DEX reduced the division index and expression of activation markers of $CD4^+$ T-cells (Figure 3.1) (J.B. Wing and R.A. Foster, unpublished data).

In the recent years before the start of this PhD project, several experiments carried out by a colleague in our lab (Dr. J.B. Wing, unpublished data) aimed at identifying the mechanism of action by which TI type 2 analogous compounds (α-δ-DEX and MID) could restrain T-cell proliferation and activation. Among of the most relevant observations made, was the fact that both $CD4^+$ and $CD8^+$ T lymphocytes appeared to be inhibited by TI stimulation. An extensive cytokine analysis also revealed that samples with TCR stimulation plus α-δ-DEX had reduced supernatant concentrations of IL-5, IL-10, IL-13, IL-17 and TNF-α as compared with the samples with TCR stimulation only. Levels of IFN-γ remained unaffected across the board, while release of IL-1β was highly induced by α-δ-DEX even on its own (Figure 3.2). Although the precise role of B-cells in inducing this suppression remained uncertain, activation-induced T-cell death and involvement of T-regulatory cells were excluded as possible mechanisms of action (J.B. Wing, unpublished data).

The work described in this chapter aimed to further identify the cells involved in the T cell suppression caused by TI-2 mimics and if possible to identify the mechanism of action.

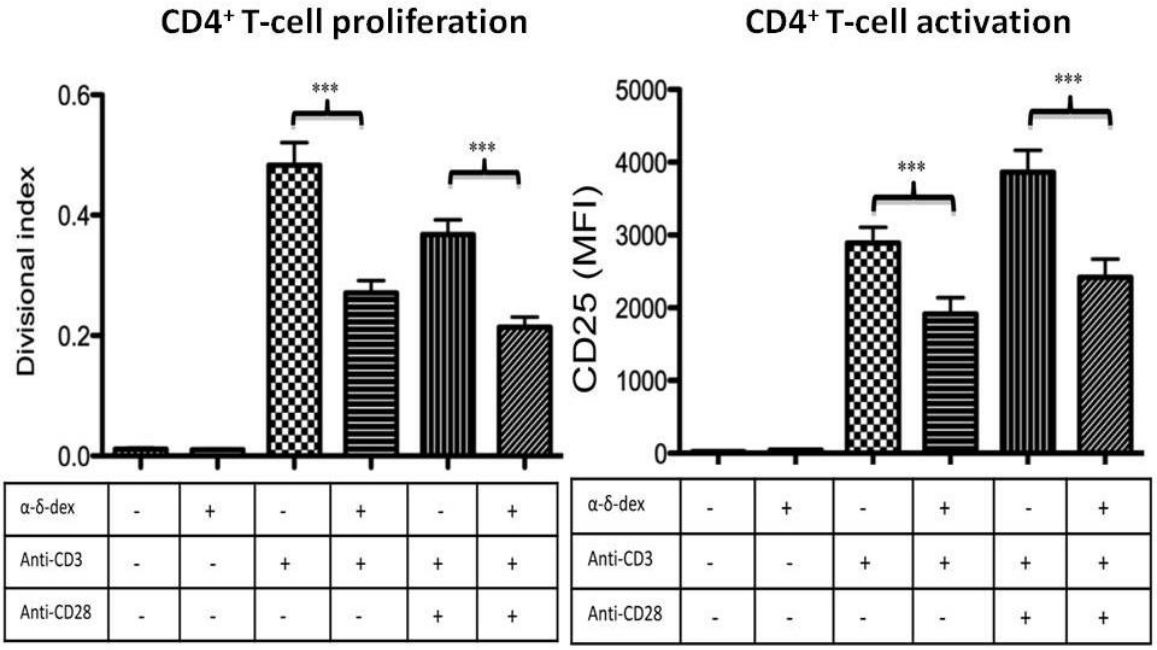

Figure 3.1: T-cell proliferation and activation by TCR receptor stimulation is suppressed by α-δ-dex stimulation of B-cells (J.B. Wing, unpublished data)**.**

PBMCs were extracted from human blood and stimulated for 96 hours with plate bound αCD3 ± αCD28 and/or the TI-II antigen mimic, α-δ-dex. Proliferation of $CD4^+$ T-cells was reported as division index; while expression of the CD25 marker as median fluorescence intensity (MFI) represented T-cell activation. Bars represent means and SEM, n=53. ANOVA, Bonferroni's selected pairs. *$p \leq 0.05$, **$p \leq 0.01$, ***$p \leq 0.001$.

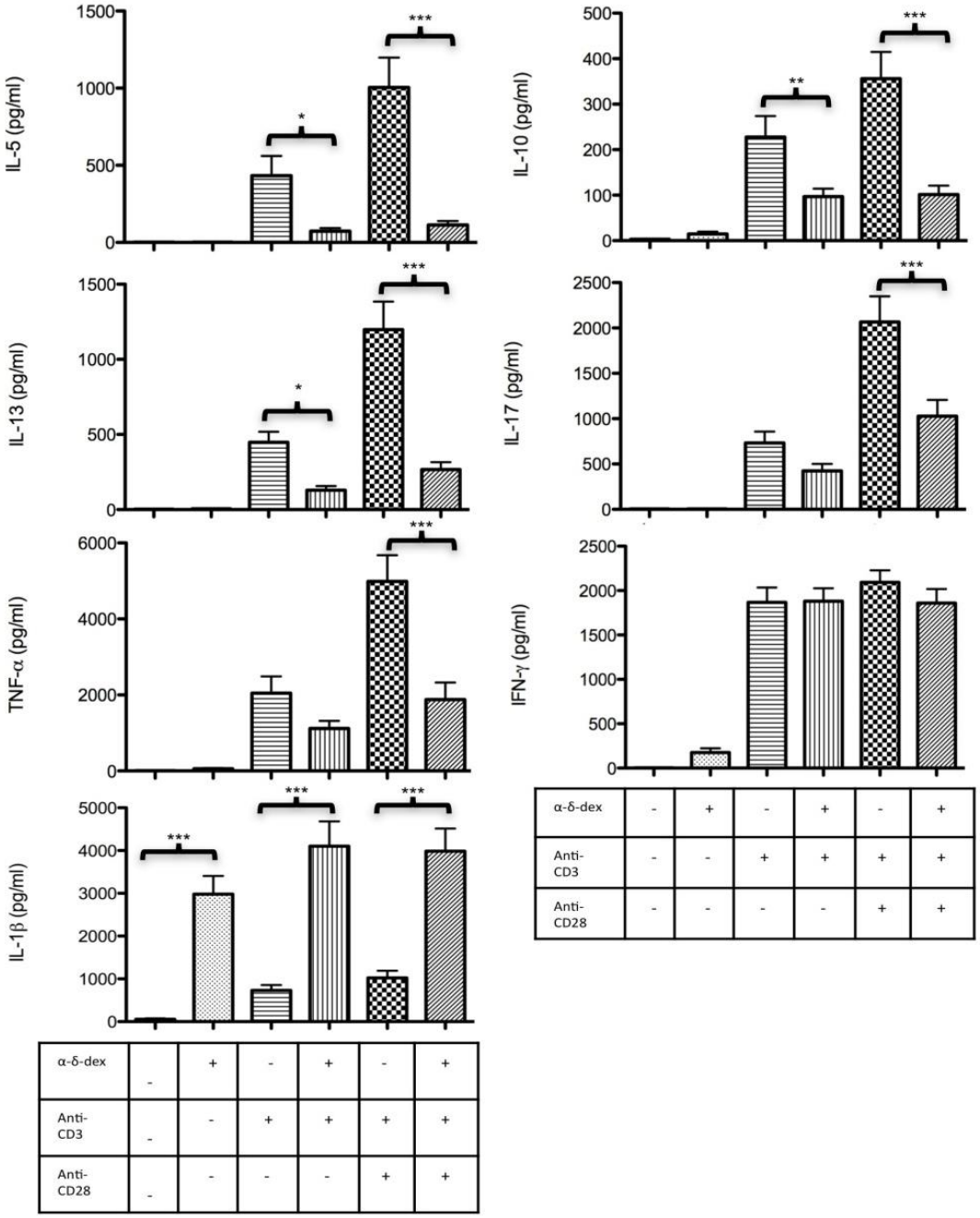

Figure 3.2: TI type 2 activation of B-cells blocks release of several T-cell cytokines (J.B. Wing, unpublished data)**.**

PBMCs were extracted from human blood and stimulated for 96 hours with plate bound anti-CD3 ± anti-CD28 and/or the TI type 2 antigen mimic, α-δ-dex. Supernatants were then collected and cytokines assayed by Cytometric Bead Array. Bars represent means and SEM, n=22. Paired ANOVA, Bonferroni's Multiple Comparison Test. *$p \leq 0.05$, **$p \leq 0.01$, ***$p \leq 0.001$.

3.2 GENERAL METHODOLOGY

PBMCs were isolated from fresh heparinised blood by centrifugation with lymphocyte separation media and removal of the buffy coat (section 2.1). Cells were washed 3 times and resuspended in RPMI media supplemented with L-glutamine and 20% of autologous plasma. PBMCs were then stained with the proliferation dye CFSE (section 2.4), followed by 3 washes to remove the excess dye. Finally, cells were enumerated by hemocytometer and added to 48-well plates at a concentration of $1x10^6$ cells per well in a final volume of 500 µl RPMI preparation.

T-cells were stimulated with 0.1-0.3 µg/ml plate-bound anti-CD3 (section 2.3.1.1) or with anti-CD3/CD28 dynabeads (section 2.3.1.4) in the case of enriched $CD4^+$ T-cells. TI type 2 B-cell stimulation was provided by 1 µg/ml α-∂-DEX (section 2.3.2.1) or 2 µg/ml MID (section 2.3.2.2), in the presence or absence of T-cell stimulators. The negative control for all experiments consisted of PBMCs in the complete absence of stimuli, cells which will not divide or become activated at all. On the other hand, the positive control was represented by the sample containing T-cell stimulators (plate bound αCD3 or αCD3/αCD28 dynabeads) which will induce a constant T-cell division and large expression of the surface activation marker.

Except where otherwise noted, cells were incubated at 37°C and 5% CO_2 in a humidified atmosphere for 96 hours before harvesting.

Extracellular immunofluorescence staining for flow cytometric analysis was performed by incubating $1x10^6$ PBMCs with the relevant antibodies (section 2.5.2). The sequential gating strategy excluded doublets, dead cells and monocytes ($CD14^+$) from the analysis, allowing identification of live T and B lymphocytes ($CD4^+$ and $CD19^+$ respectively) (section 2.5.5).

Employing a CFSE dilution method (section 2.4), proliferation was reported as the average number of cell divisions (division index) for T and B-cell populations. Median fluorescence intensity (MFI) of the surface markers CD25 and CD86 represented T and B-cell activation, respectively. CD25 is the α-chain of the IL-2 receptor, which gets over-expressed during T-cell activation and in a dependent manner to the presence of IL-2 (Robb et al. 1984). Thus, measurement of CD25 is widely used as an activation marker in T lymphocytes. Similarly, expression of the B7 molecule CD86 is known to be enhanced on activated B lymphocytes after CD40 ligation (Elgueta et al. 2009).

See Figure 3.3 for a simplified methodology flow chart.

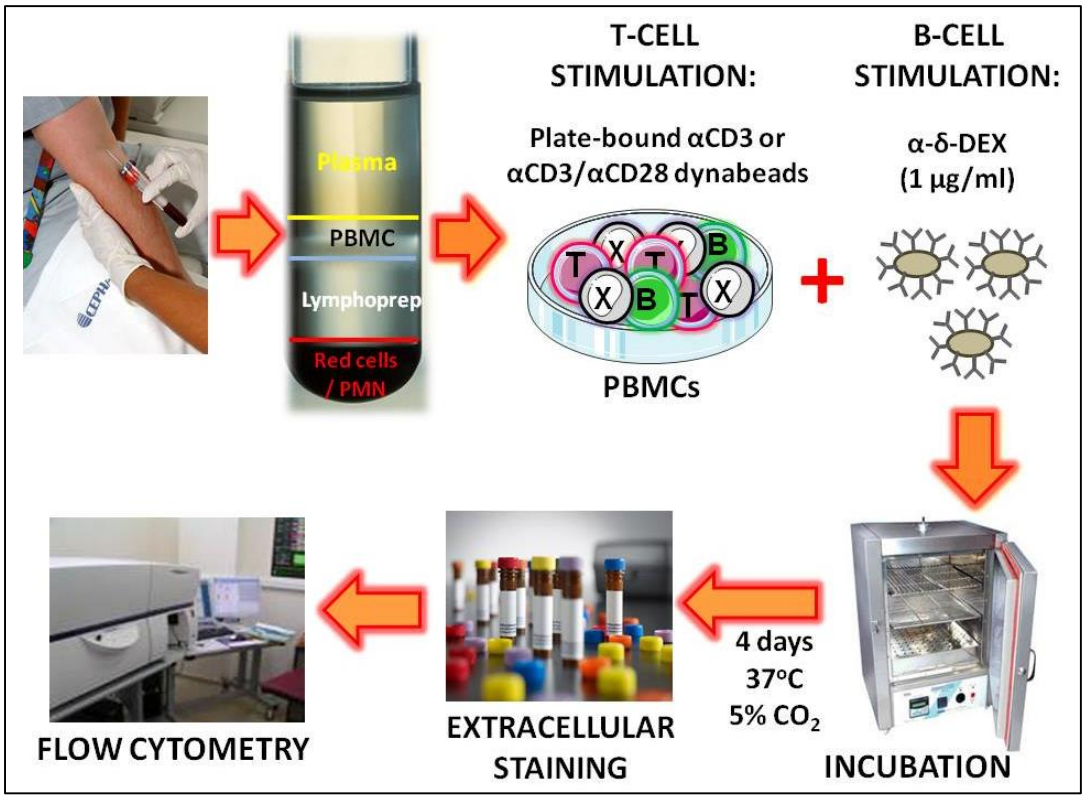

Figure 3.3: Schematic diagram of the general methodology applied applied in Chapter 3.

Human PBMCs were isolated from peripheral blood using Lymphoprep™ density gradient centrifugation. T-cells were stimulated with anti-CD3 (αCD3) or anti-CD3 + anti-CD28 (αCD3 + αCD28) coated dynabeads, while B-cells received TI type 2 stimulation with α-ð-DEX or MID. Cells were plated and incubated for 96 hours at 37°C and 5% CO_2. Finally, samples were stained with the desired fluorescently-labeled antibodies and analysed by flow cytometry.

3.3 T-INDEPENDENT TYPE 2 STIMULATION OF B-CELLS INHIBITS T-CELL ACTIVATION AND PROLIFERATION

This section aimed to reproduce the observation previously recorded in our lab, in which addition of α-δ-DEX in the presence of a T-cell stimulus (plate-bound αCD3) resulted in proliferation and activation of B-cells but suppression of T-cell responses to CD3 cross-linking (section 3.1).

Figure 3.4-A shows the proliferation index of $CD19^+$ B lymphocytes that have been exposed to α-δ-DEX for 96 hours, in the presence or absence of αCD3. As expected, α-δ-DEX alone induced a substantial B-cell proliferation as compared with the negative control (non-stimulated PBMCs). Moreover, a synergistic effect was observed when both α-δ-DEX and αCD3 were present, possibly due to activated T-cells that provided cognate co-stimulation (T-cell help) to B-cells.

Figure 3.4-B represents the level of B-cell activation reported by CD86 expression. The same trend can be seen here, demonstrating how α-δ-DEX achieves B-cell activation on its own but the presence of a T-cell stimulus results in a boost for such B-cell response.

The finding of greatest relevance to this thesis, however, occurred on $CD4^+$ T-cells. In comparison with the group containing αCD3 only in which T-cells proliferated as expected *via* TCR cross-linking, the group exposed to αCD3 and α-δ-DEX showed at least a 50% reduction of their division index (Figure 3.5-A). There was a corresponding, dramatic fall in the expression of the activation marker CD25 by T-cells (Figure 3.5-B) in those samples containing both stimuli. It is important to mention that α-δ-DEX on its own did not have any effect on $CD4^+$ T-cell proliferation or activation.

Thus it was possible to reproduce the observation made by previous colleagues in our laboratory, in which TI type 2 stimulation with α-δ-DEX activates B lymphocytes but inversely inhibits αCD3-derived T-cell responses (Figure 3.6).

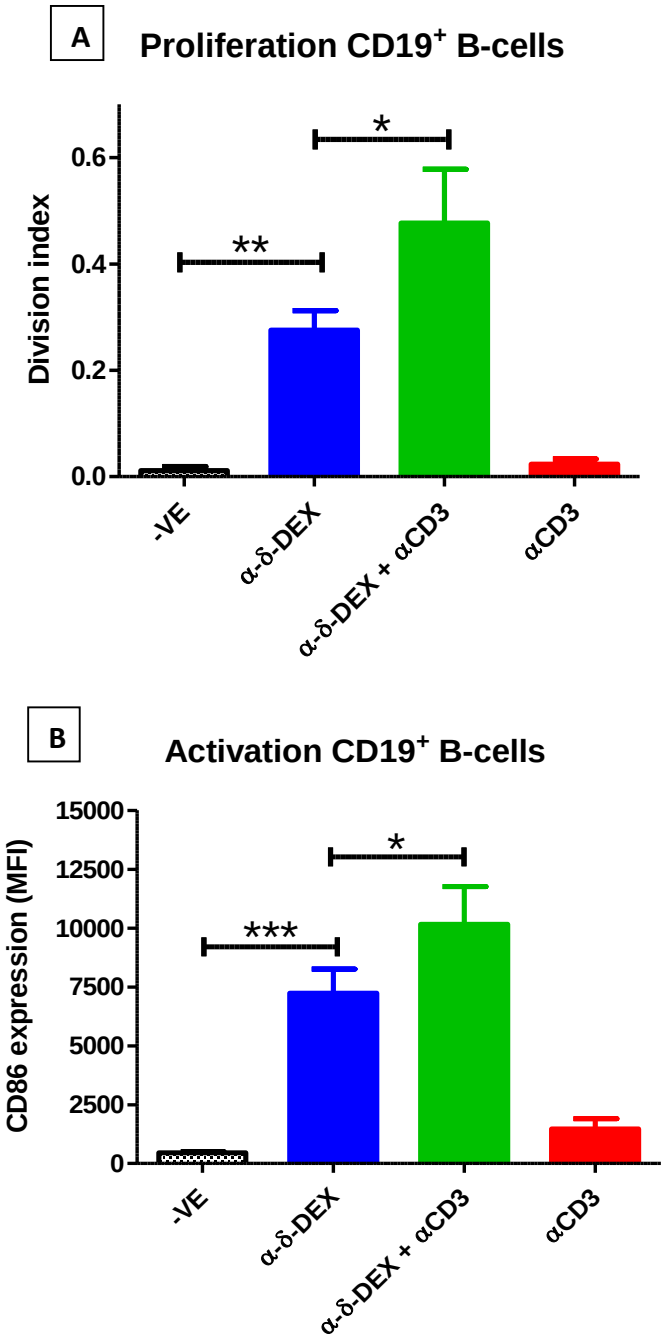

Figure 3.4: CD19⁺ B-cell proliferation and activation are induced by the TI type II mimic α-δ-DEX.

A. Proliferation CD19⁺ B-cells, reported as division index. **B. Activation CD19⁺ B-cells**, expression of the CD86 marker as median fluorescence intensity (MFI). Bars represent means and SEM, n=8. Paired ANOVA, Bonferroni's Multiple Comparison Test. *$p \leq 0.05$, **$p \leq 0.01$, ***$p \leq 0.001$.

-VE= negative control, non-stimulated PBMCs. α-δ-DEX= B-cell stimulation, 1 µg/ml. αCD3 = T-cell stimulation, plate-bound 0.1 µg/ml.

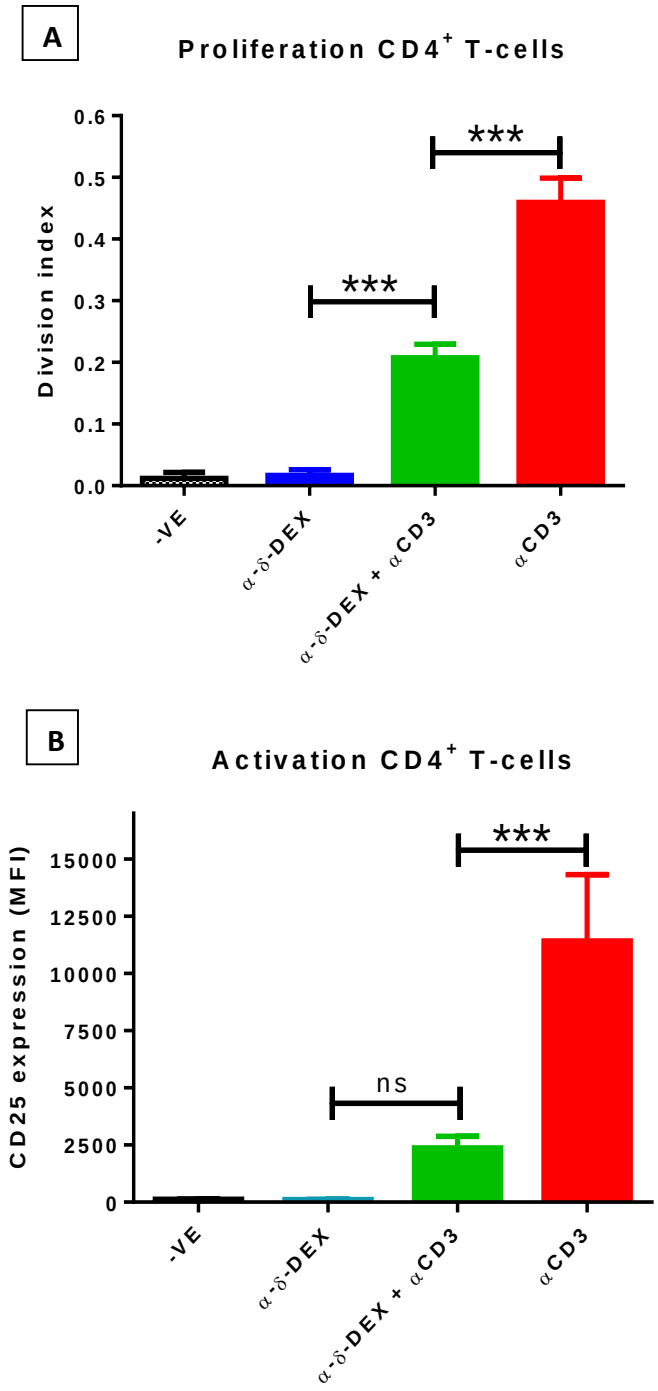

Figure 3.5: CD4⁺ T-cell activation and proliferation by TCR receptor stimulation is suppressed by α-ð-DEX stimulation of B-cells.

A. Proliferation CD4⁺ T-cells, reported as division index. **B. Activation CD4⁺ T-cells**, expression of the CD25 marker as median fluorescence intensity (MFI). Bars represent means and SEM, n=8. Paired ANOVA, Bonferroni's Multiple Comparison Test. *$p \leq 0.05$, **$p \leq 0.01$, ***$p \leq 0.001$.

-VE= negative control, non-stimulated PBMCs. α-δ-DEX= B-cell stimulation, 1 µg/ml. αCD3 = T-cell stimulation, plate-bound 0.1 µg/ml.

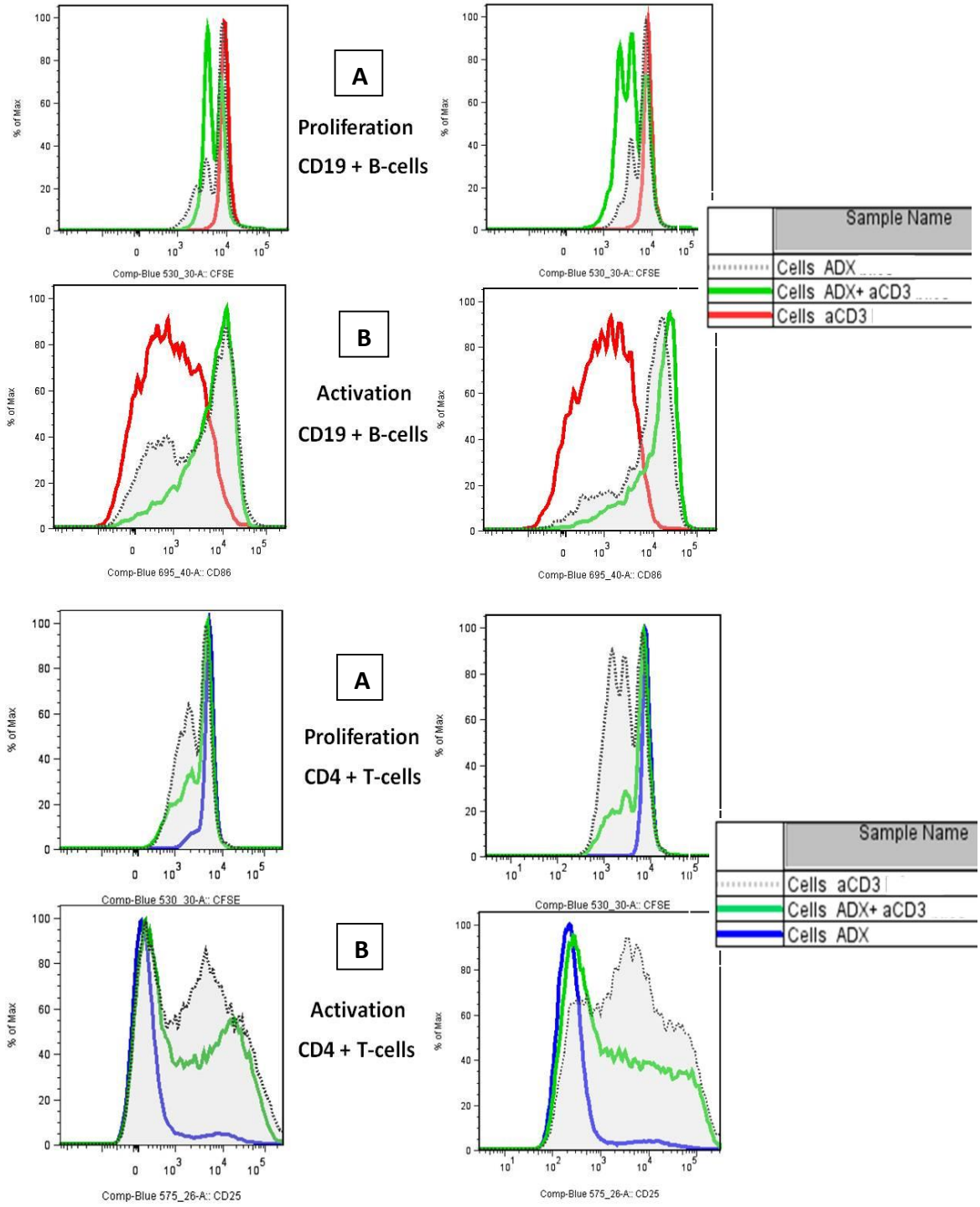

Figure 3.6: Examples of overlaid histograms presenting B and T cell responses following incubation with various stimuli.

A. Proliferation assessed by the CFSE dilution method, the x axis represents intensity of CFSE fluorescence and the y axis % of maximum. **B. Activation as MFI of activation markers,** the x axis represents intensity of CD25-PE or CD86-PE Alexa700 fluorescence, while the y axis % of maximum. Representative examples from 4 different experiments and 4 different donors.

3.4 CD80, CD86 AND IL-1 DO NOT APPEAR TO PLAY A ROLE AS SUPPRESSOR MOLECULES

From the molecules at the immunological synapse, it is well known that binding of the B7 ligands CD80/CD86 to CTLA-4 expressed on the surface of activated T lymphocytes mediates a suppressive activity on these cells (Linsley et al. 1992) (section 1.1.4.3). Thus, a blocking experiment was designed in order to investigate if an engagement between CD80/CD86 and CTLA-4 was responsible for the inhibition.

Blockade of the CD80 and CD86 molecules was carried out with low endotoxin, azide free purified monoclonal antibodies, αCD80 (Biolegend, clone 2D10) and αCD86 (Biolegend, clone IT2.2) respectively. At concentrations of 10 µg/ml, these monoclonal antibodies were added directly to the wells containing αCD3-stimulated PBMCs plus α-δ-DEX and incubated over a 96 hour period.

Although this experiment is representative of only 2 donors, there is no evidence that blocking of CD80 or CD86 could overcome the T-cell suppression induced by α-δ-DEX. As shown in Figure 3.7, not even a slight recovery was detected on T-cell proliferation or activation in the presence of these monoclonal antibodies.

In addition and in relation to the previous finding that IL-1β release was highly induced by α-δ-DEX (Figure 3.1), we aimed to block this cytokine using recombinant IL-1 receptor antagonist (IL-1RA). The protein IL-1RA naturally competes with IL-1β for binding to the IL-1 receptor, preventing downstream signalling and subsequent inflammatory effects mediated *via* IL-1β (Goldbach-Mansky 2012).

IL-1RA was produced and kindly provided by Dr. Martin Nicklin (Medical School, the University of Sheffield). Based on personal communication and advice with Dr. Nicklin, IL-1RA at a final concentration of 10 ng/ml was added to the well containing PBMCs stimulated with αCD3 and α-δ-DEX.

As shown in Figure 3.7, IL-1RA was also unable to restore T-cell proliferation and activation if α-δ-DEX was present in the cell culture.

Even though the sample size is small for this set of conditions, it can be suggested that CD80, CD86 and the IL-1 receptor do not play an essential role in the α-δ-DEX inhibitory phenomenon.

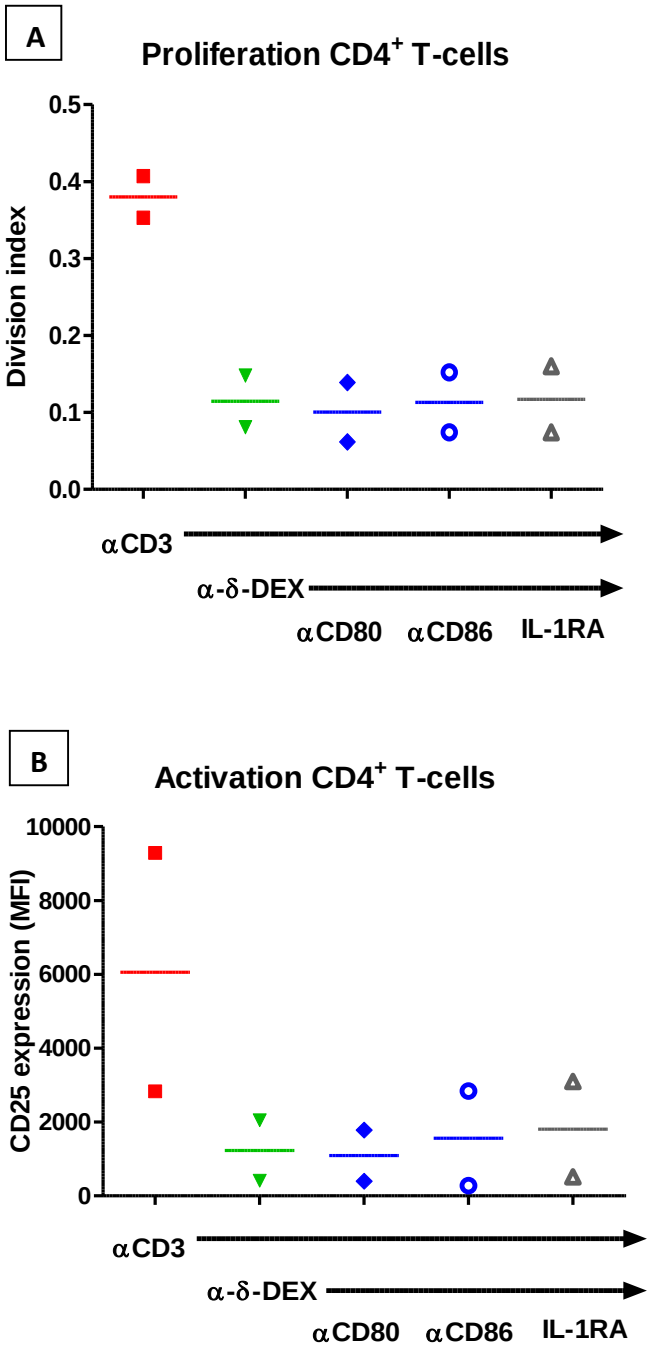

Figure 3.7: Blockade of the B-cell molecules CD80 and CD86 does not restore the suppression induced by α-δ-DEX on CD4⁺ T lymphocytes. Similarly, blockade of IL-1 receptor does not reestablish normal T-cell proliferation or activation.

A. Proliferation CD4⁺ T-cells, reported as division index. **B. Activation CD4⁺ T-cells**, expression of the CD25 marker as median fluorescence intensity (MFI). Lines represent means, n=2. PBMCs were stimulated with αCD3 (plate-bound 0.1 µg/ml), in the presence of α-δ-DEX (1 µg/ml) and one of the following: purified anti-CD80 (10 µg/ml), purified anti-CD86 (10 µg/ml) or IL-1 receptor antagonist (IL-1RA, 10 ng/ml). The group containing αCD3 only represents our positive control (red squares), while the group containing αCD3+ α-δ-DEX (green triangles) provides the baseline of suppression to compare against.

3.5 A POSSIBLE MINOR EFFECT OF INTERLEUKIN-10 (IL-10)

Although a previous cytokine analysis from supernatants did not reveal an increase in IL-10 production after α-δ-DEX stimulation (Figure 3.1), the impact of this T-cell down-regulatory cytokine as a possible mechanism of suppression in our system was further examined.

For this set of experiments IL-10 blocking was performed using a functional grade anti-IL-10 monoclonal antibody (αIL-10, eBioscence clone JES3-9D7), added directly to the wells containing αCD3 and α-δ-DEX. Three different concentrations of αIL-10 were tested (5, 10, 20 μg/ml) and compared against the isotype control (Rat IgG1, 20 μg/ml) or the positive control (αCD3-stimulated).

The addition of αIL10 may have had a small effect in reversing the suppression of T cell proliferation caused by α-δ-DEX, but this was only statistically significant at one of the three concentrations assessed (10μg/ml). Even in this case T cell proliferation remained significantly suppressed in comparison with the αCD3 control group (Figure 3.8-A)

An αIL-10 blockade benefit was unclear for T-cell activation, since not even a partial recovery was found on expression of CD25 for any of the dose groups when compared with the isotype control (Figure 3.8-B). In contrast, αIL10 caused a substantial increase in CD25 expression by αCD3-stimulated B cells in the absence of α-δ-DEX (Figure 3.8-B).

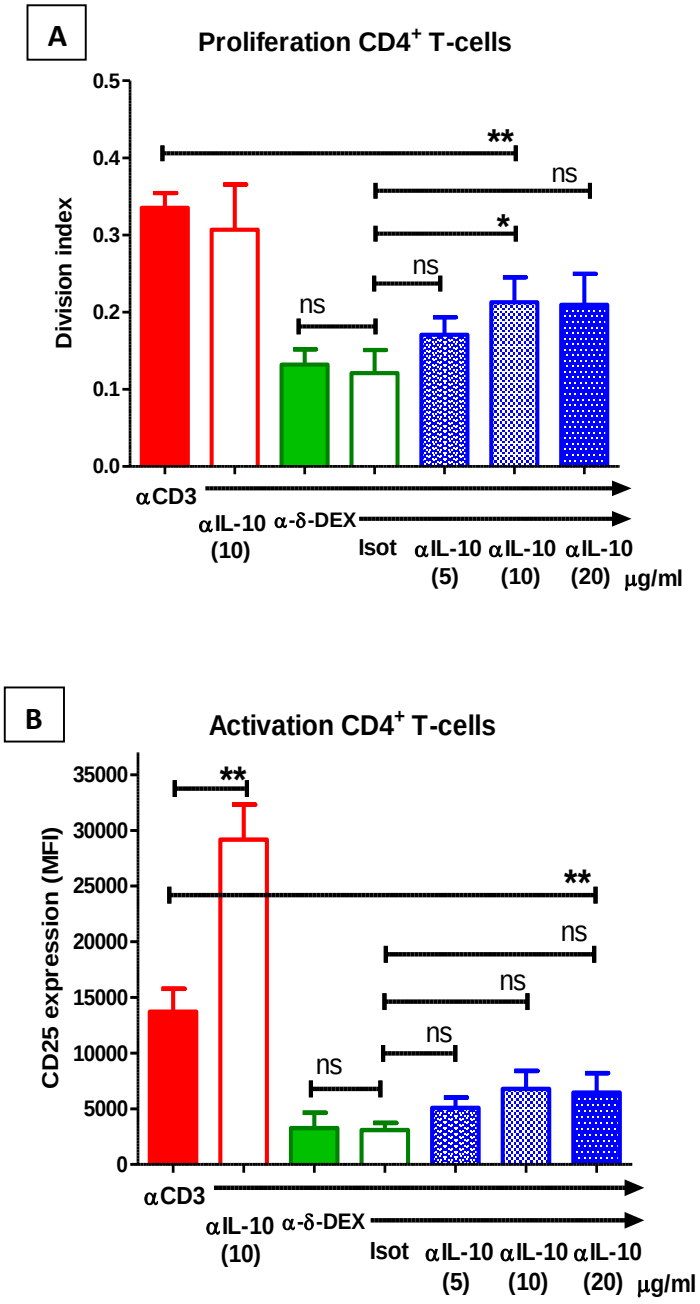

Figure 3.8: A possible minor effect of IL-10 in the α-δ-DEX inhibitory effect.

A. Proliferation CD4⁺ T-cells, reported as division index. **B. Activation CD4⁺ T-cells**, expression of the CD25 marker as median fluorescence intensity (MFI). Bars represent means and SEM, n=6. Paired ANOVA, Dunnett's Multiple Comparison Test (*vs.* αCD3 or αCD3+α-δ-DEX+isotype). *$p \leq 0.05$, **$p \leq 0.01$, ***$p \leq 0.001$, ns= not significant.

PBMCs were stimulated with αCD3 (plate-bound 0.1 µg/ml), in the presence of α-δ-DEX (1 µg/ml) and one of the following: αIL-10 at 5, 10 or 20 µg/ml (blue bars) or the isotype control at 20 µg/ml (Isot, green empty bar). The group containing αCD3 only represents the positive control (red filled bar), while the group containing αCD3+ α-δ-DEX (green filled bar) provides the baseline of suppression to compare against. The additional control sample (n= 3) containing αCD3+αIL-10 at 10 µg/ml is also shown (empty red bar).

3.6 α-δ-DEX DOES NOT HAVE A DIRECT SUPPRESSIVE EFFECT ON PURIFIED CD4$^+$ T-CELLS

Although α-δ-DEX should bind to and affect only cells expressing IgD, we wanted to be certain there was no direct effect on T lymphocytes. To address this question, a simple experiment was carried out with purified CD4$^+$ T-cells.

Primary human CD4$^+$ T-cells were enriched from PBMCs using a negative selection kit (section 2.2.1), obtaining a final purity greater than 95% in all cases (Figure 3.9). As mentioned in section 2.3.1.4, αCD3/αCD28 dynabeads were preferred over plate-bound αCD3 to induce cell proliferation and activation on purified populations. A ratio of 1:1 dynabead per cell was sufficient to provide a good baseline to assess changes on T-cell division index and CD25 expression, thus it was chosen as our positive control.

Figure 3.10 provides strong evidence that addition of α-δ-DEX had not direct effect on T lymphocytes. Neither proliferation nor activation of purified CD4$^+$ T-cells were diminished in the presence of α-δ-DEX over 4 days of incubation.

Therefore it can be concluded that in the absence of accessory cells, α-δ-DEX does have any suppressor effect on CD4$^+$ T-cells.

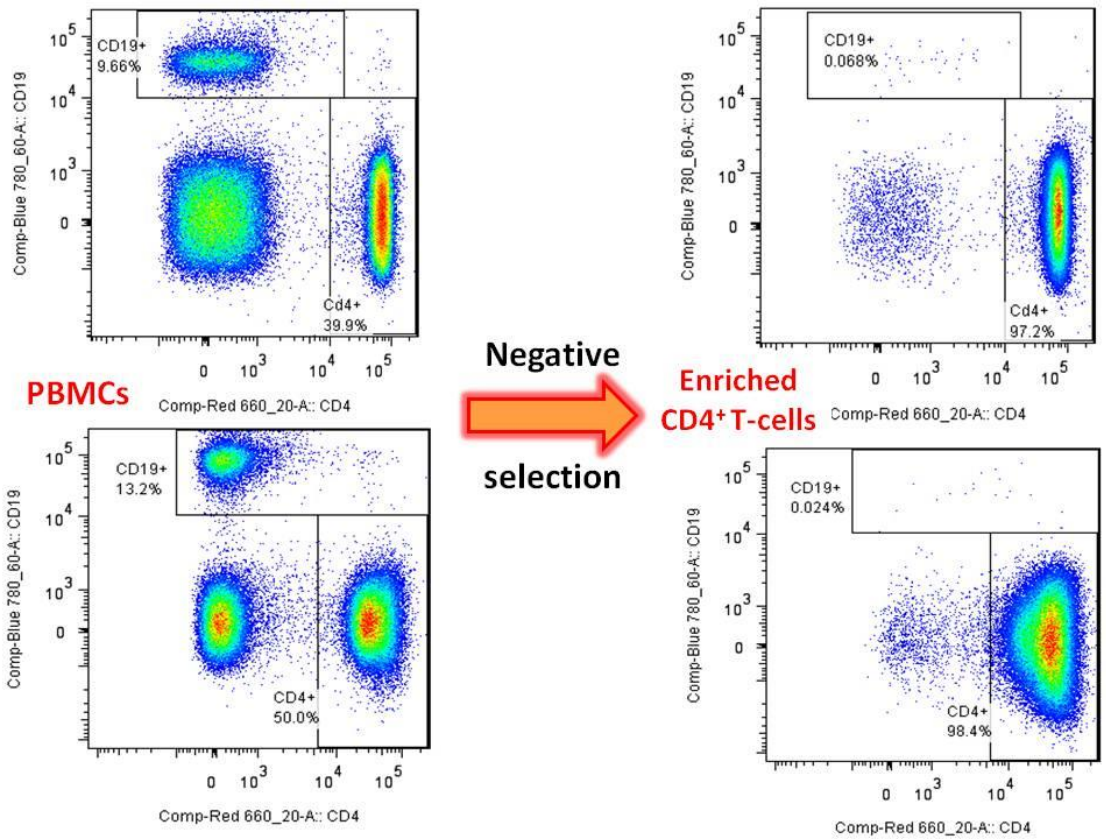

Figure 3.9: Dot plot examples of primary human enriched CD4⁺ T-cells illustrating purity greater than 95%.

Purified CD4⁺ T lymphocytes were obtained from PBMCs by negative selection. After a sequential gating strategy for exclusion of doublets and dead cells, dot plots illustrate the final gating for selection of CD4⁺ cells (*x*- axis= CD4-APC) *vs.*CD19⁺ cells (*y*- axis = CD19 PE Cy-7). Plots are representative examples from 2 donors.

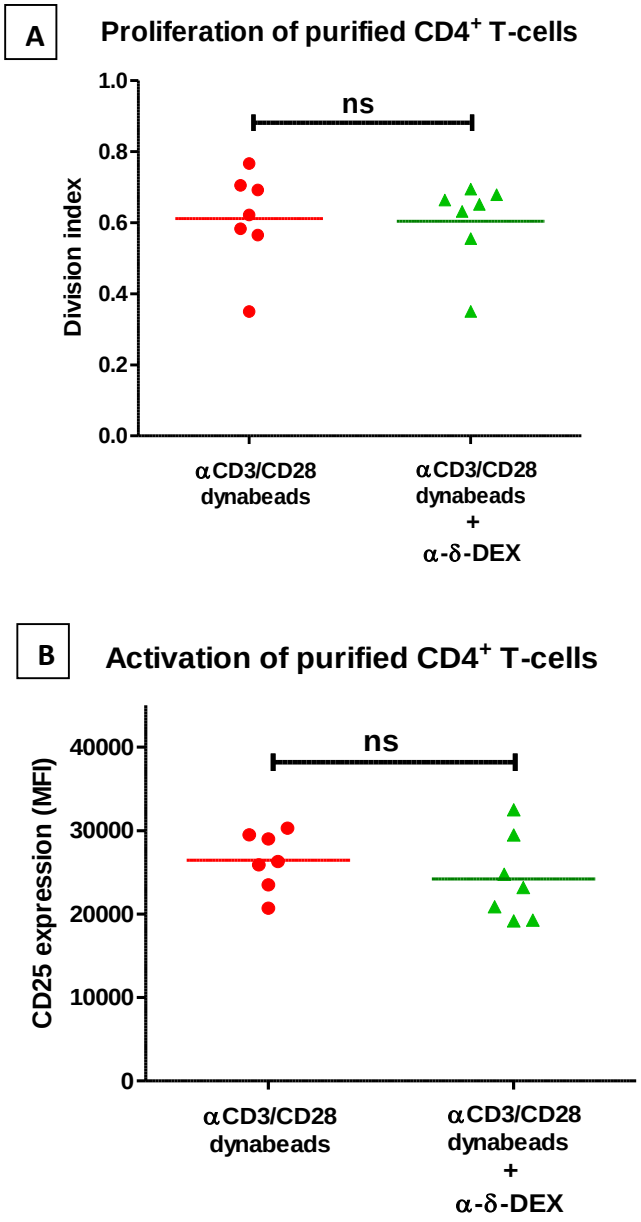

Figure 3.10: α-δ-DEX does not have a direct suppressive effect on purified CD4⁺ T-cells.

A. Proliferation of enriched CD4⁺T-cells, reported as division index. **B. Activation of enriched CD4⁺ T-cells**, expression of the CD25 marker as median fluorescence intensity (MFI). Bars represent means, n=7. Paired student *t*-test, ns= not significant.

Primary CD4⁺ T-cells were enriched by negative selection from PBMCs and stimulated with αCD3/αCD28 dynabeads (1:1 ratio beads:cells), in the absence or presence of α-δ-DEX (1 µg/ml).

3.7 Purified B-cells are Capable of Suppressing T-cell Proliferation But only when Primed with α-δ-DEX

Having excluded the possibility that α-δ-DEX could affect T-cells directly (section 3.6), we aimed to investigate whether activated B-cells exposed to α-δ-DEX could subsequently suppress $CD4^+$ T-cells.

As in the previous experiment, purified negative selected $CD4^+$ T-cells were obtained from whole PBMCs on day 0. Similarly, $CD19^+$ and/or $CD20^+$ B-cells were enriched on the same day using also a negative selection principle (section 2.2.1). In the conditions containing both populations, T and B-cells were seeded at an approximate 6 to 1 ratio, up to 1 x 10^6 cells per well in total. These T-cell : B-cell proportions were ultimately chosen based on the proportions of these lymphocytic populations found in whole peripheral blood, 72.6% (54.90-84.03%) $CD3^+$ T-cells and 11% (4.0-20%) $CD19^+$ or $CD20^+$ B-cells (Bisset et al. 2004). Figure 3.11 shows how optimisation of the protocol was achieved and how the initial T:B ratios were more or less maintained over 4 days of incubation. For this experiment, αCD3/αCD28 Dynabeads were used again for T-cell stimulation and as positive control. In all conditions, 1 x10^6 beads were placed in each well on day 0 just prior to T-cells. From the moment T-cells were enriched and stimulated (day 0), 96 hours of incubation took place before analysis.

Preliminary experiments accomplished to optimise T and B-cell ratios, raised the suspicion that direct administration of α-δ-DEX to pure T and B-cells will not show a suppressive effect (data not shown). Therefore two main conditions were tested: Purified T-cells plus B-cells both isolated on day 0 in the presence or absence of α-δ-DEX; and T-cells isolated (on day 0) plus pre-activated B-cells isolated on day 1 from PBMCs exposed to α-δ-DEX over 24 hours. For a schematic representation of this protocol, see Figure 3.12.

From the data in Figure 3.13-A and in comparison with the control group containing only stimulated $CD4^+$ T-cells, it is evident that α-δ-DEX was unable of generating an inhibitory effect when the culture contained only purified non-stimulated B and T-cells. However, when B-cells were first primed with α-δ-DEX in the presence of whole PBMCs, those pre-activated B-cells acquired a suppressive phenotype that markedly decreased T-cell proliferation. More importantly, since the activation beads were present in the well 24 hours before the primed cells were co-cultured with T-cells (Figure 3.12), it can be inferred that those pre-activated B-cells were powerful enough to restrict cell division that had already started.

Irrespective of whether B-cells were pre-activated with α-δ-DEX there was no change on $CD4^+$ T-cell activation as measured by CD25 expression in relation to the control group (Figure 3.13-B). This might be explained, by the fact that over-expression of activation markers is an early phenomenon, so the presence of a T-cell stimulus for 24 hours prior co-culture with pre-activated B-cells could had been sufficient for starting an unstoppable activation cascade.

These findings suggest that accessory cells are required during the α-δ-DEX stimulation stage to induce a suppressive phenotype on B lymphocytes but once the phenotype is acquired then enriched B-cells are sufficient to inhibit T-cell proliferation.

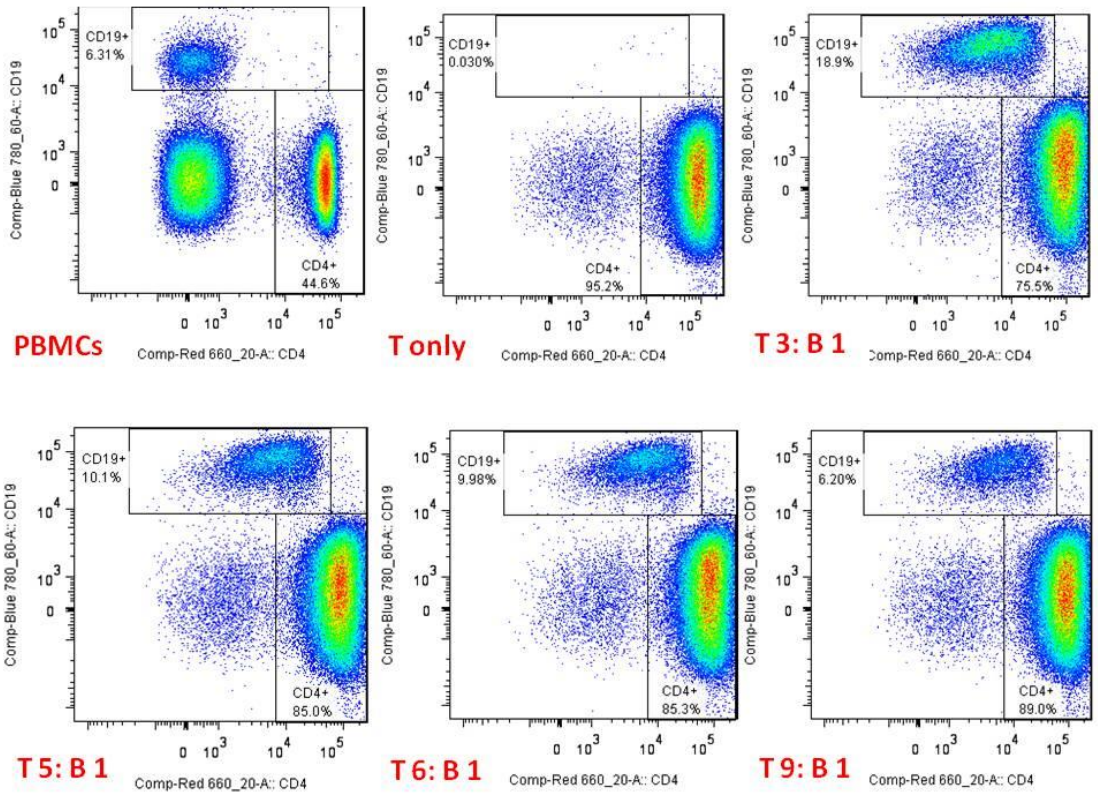

Figure 3.11: Dot plot examples illustrating different ratios between enriched CD4$^+$ T and CD19$^+$ B lymphocytes.

Purified CD4$^+$ T and B lymphocytes were obtained from PBMCs by negative selection on day 0 and cultured over 4 days. Labels represent T:B ratios at which the cells were seeded on day 0, while the plots show the proportion of both populations after 4 days in incubation. After a sequential gating strategy for exclusion of doublets and dead cells, these dot plots illustrate the final gating for selection of CD4$^+$ T cells (*x*- axis= CD4-APC) and CD19$^+$ B cells (*y*- axis = CD19 PE Cy-7).

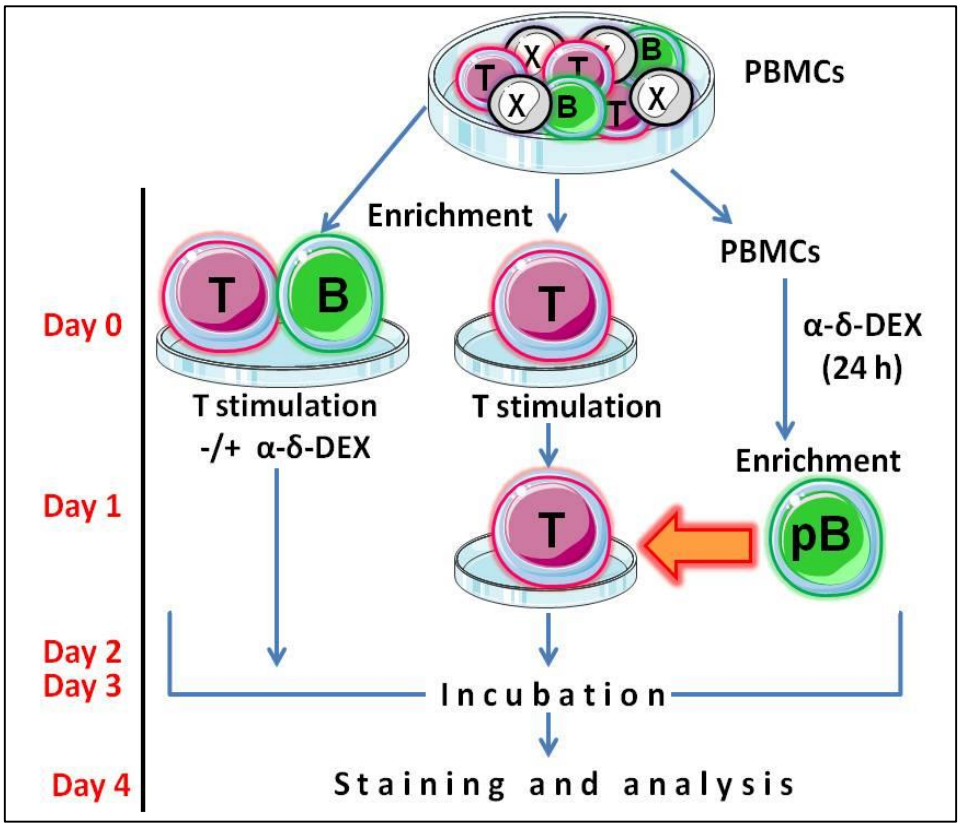

Figure 3.12: Schematic representation of the experimental protocol involving purified T and B lymphocytes in the presence of α-δ-DEX.

1st condition: Enriched $CD4^+$ T and B lymphocytes were obtained from PBMCs on day 0, following co-culture and stimulation with αCD3/αCD28 dynabeads plus/minus α-δ-DEX over 4 days. 2nd condition: PBMCs were stimulated with α-δ-DEX over a 24 hours period. At this time, 'pre-activated' B-cells were enriched and transferred to a well containing purified $CD4^+$ T-cells isolated on day 0 and which already contained αCD3/αCD28 dynabeads. Finally, 3 more days were allowed in co-culture before analysis. Although is not illustrated within this schema, a well containing only enriched T-cells plus αCD3/αCD28 dynabeads was used a positive control.

T= $CD4^+$ T-cell, B= B-cell, pB= α-δ-DEX pre-activated B-cell, X= accessory cell.

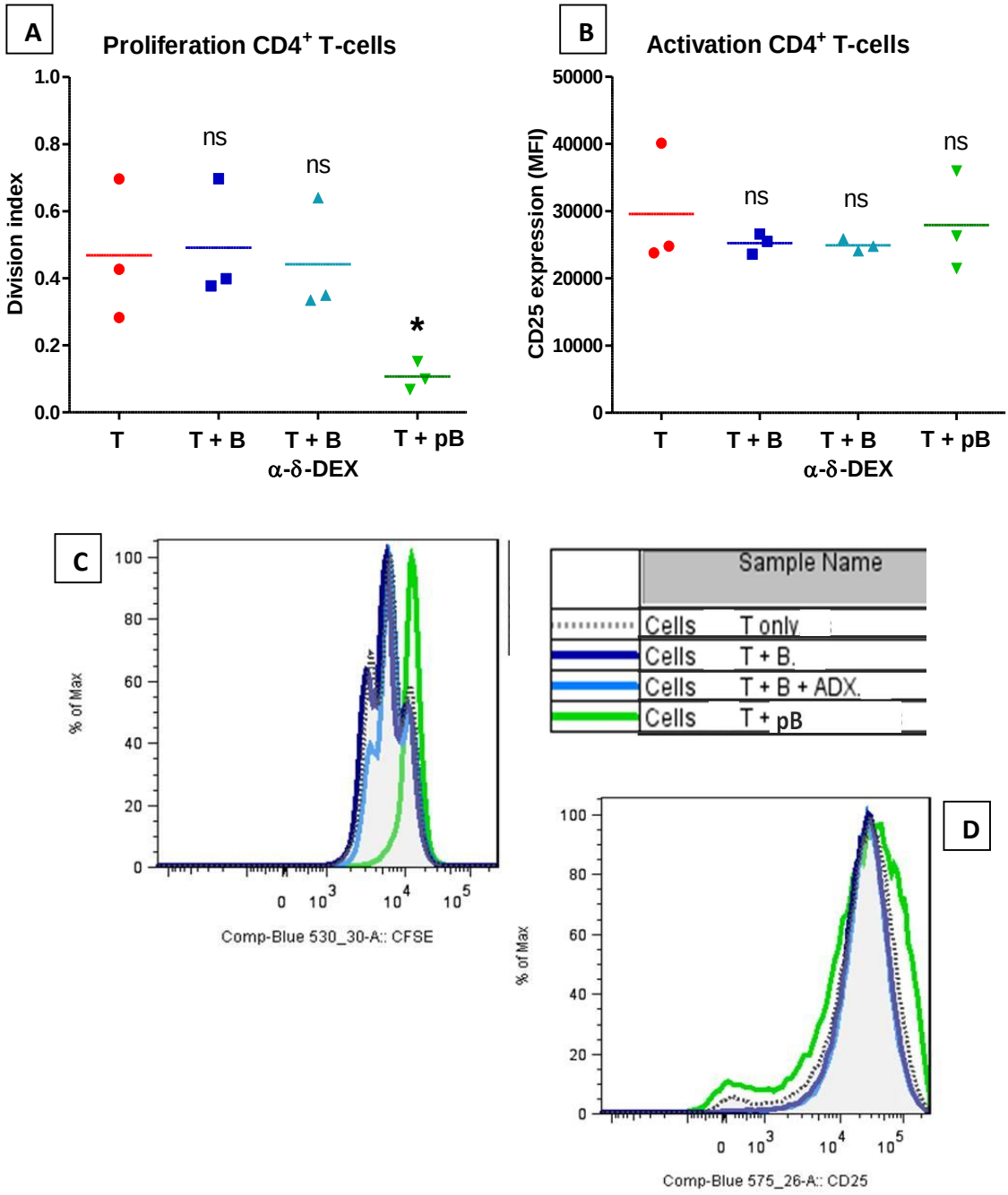

Figure 3.13: B-cells are capable of suppressing proliferation of purified CD4⁺ T-cells, but only when primed with α-δ-DEX.
A. Proliferation of enriched CD4⁺ T-cells, reported as division index. **B. Activation of enriched CD4⁺ T-cells**, expression of the CD25 marker as median fluorescence intensity (MFI). Bars represent means, n=3. Paired ANOVA, Dunnett's Multiple Comparison Test (*vs.* T); *$p \leq 0.05$, ns= not significant. All conditions were stimulated with αCD3/αCD28 dynabeads (1:1 ratio). Primary CD4⁺ T and B lymphocytes were enriched by negative selection from PBMCs. In red, control group containing T-cells alone. In blue, co-cultures of T and B-cells without and with α-δ-DEX. In green, co-culture of T and pre-activated B-cells, after 24 hours exposure to α-δ-DEX. T= CD4⁺ T-cell, B= B-cell, pB= α-δ-DEX pre-activated B-cell. **C and D. Histograms of representative examples. C. CD4+ T-cell proliferation assessed by the CFSE dilution method**, the x axis represents intensity of CFSE fluorescence and the y axis % of maximum. **D. Activation as MFI of activation marker CD25,** the x axis represents intensity of CD25-PE, while the y axis % of maximum

3.8 THE SUPPRESSIVE EFFECT OF α-δ-DEX PRE-ACTIVATED B-CELLS IS CONTACT DEPENDENT

As reported in section 3.7, 24 hours incubation with α-δ-DEX in the presence of PBMCs was sufficient to achieve B-cell stimulation and subsequent suppression of purified T-cells. To attempt to determine whether B-cell mediated this suppression through cell-cell contact or *via* a soluble mediator a supernatant transfer experiment was designed.

After 24 hours incubation (day 1), supernatants from non-stimulated or α-δ-DEX-stimulated PBMCs were transferred to wells containing purified $CD4^+$ T lymphocytes and αCD3/αCD28 dynabeads. As an extra control and to exclude the possibility that α-δ-DEX could exhaust any cell culture media component, the supernatant from a well without cells and just RPMI preparation plus α-δ-DEX was also transferred. In all conditions, only 200 µl of supernatant were transferred to avoid that the culture media became exhausted faster over the remaining 3 days of incubation. The additional 300 µl of the usual RPMI preparation, to complete a final volume of 500 µl, were already present in the well from day 0 when purified $CD4^+$ T-cells were seeded. In total, from when T-cells were enriched and stimulated (day 0), 4 days of incubation passed before flow cytometric analysis. For a better understanding of the overall experimental protocol refer to Figure 3.14.

Within this experiment, purified $CD4^+$ T-cells were also co-cultured with either non pre-activated B-cells or α-δ-DEX pre-activated B-cells, both enriched from PBMCs on day 1. In the same way as previous experiments, the overall purity for enriched populations was kept equal to or above 95% and the starting ratio was 6:1 T-cells:B-cells (Figure 3.15).

From Figure 3.16-A which presents the proliferation of purified $CD4^+$ T lymphocytes, we were able to re-assure that purified α-δ-DEX pre-activated B-cells are able of restraining T-cell division in co-culture, as there was a significant difference between the non pre-activated and pre-activated groups. Unexpectedly, co-culture with B lymphocytes taken from unstimulated PBMCs resulted in a small but significant fall in the number of cell divisions in comparison with the positive control group containing only enriched $CD4^+$ T-cells. Some possible explanations could be given about these non pre-activated B-cells which also decreased T-cell proliferation (discussed in section 3.16).

Similar to the observation in section 3.7, T-cell activation did not differ between unstimulated and pre-activated B lymphocytes or against the control sample containing only T-cells. (Figure 3.16-B).

To confirm the fact that α-δ-DEX acts through a B-cell-contact mechanism, no significant differences were found in any of the groups receiving supernatants. Division index and expression of CD25 remained unaffected, even after transfer of the supernatant coming from an α-δ-DEX-stimulated sample (Figure 3.16).

Simultaneous analysis of the marker CD86 expressed on B-lymphocytes reassures that 24 hour incubation with α-δ-DEX is enough to activate B-lymphocytes. In comparison with enriched B-cells that were not exposed to the TI mimic, pre-activated B-cells had a 2.5 fold increment on the expression of CD86 on day 4 of the experiment (Figure 3.16-C). A relevant finding was that these α-δ-DEX pre-activated B-cells did not proliferate (data not shown).

In summary, such evidence supports that cell-contact is required to suppress T-cell responses and suggests that no soluble factor seems to be responsible for the effect. Moreover, these results consolidate the fact that α-δ-DEX priming in the presence of accessory cells generates a special B-cell phenotype sufficient to deeply inhibiting T-cell proliferation.

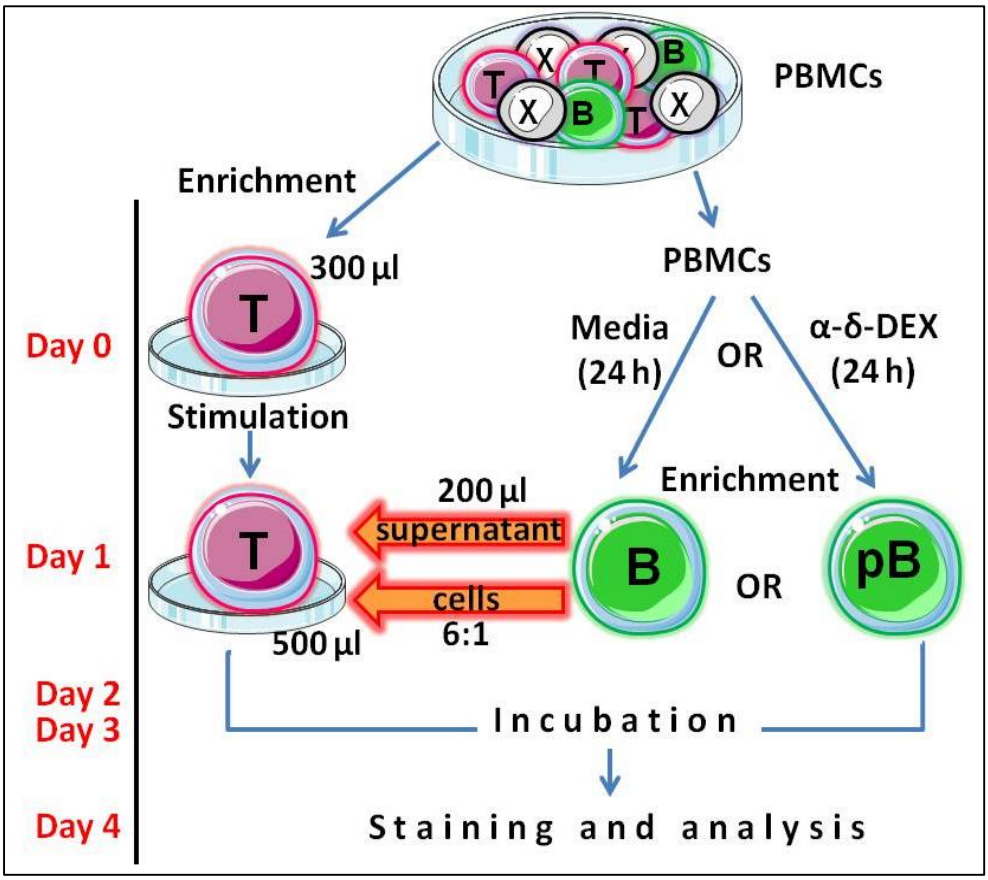

Figure 3.14: Schematic representation of supernatant transfer experiment involving α-δ-DEX.

Enriched $CD4^+$ T lymphocytes were obtained from PBMCs on day 0, following stimulation with αCD3/αCD28 dynabeads. On the same day, PBMCs were incubated in the presence or absence of α-δ-DEX. After a 24 hours incubation, non pre-activated B-cells and pre-activated B-cells were enriched and co-cultured with the purified $CD4^+$ T-cells. In parallel, 200 µl of supernatants from those wells containing PBMCs plus/minus α-δ-DEX were transferred to purified $CD4^+$ T-cells that already had 300 µl of RPMI preparation. Although is not illustrated within this schema, in addition to the usual control group including T-cells only and αCD3/αCD28 dynabeads, a single well containing no cells but only RPMI media and α-δ-DEX functioned as a secondary control.

T= $CD4^+$ T-cell, B= B-cell, pB= α-δ-DEX pre-activated B-cell, X= accessory cell.

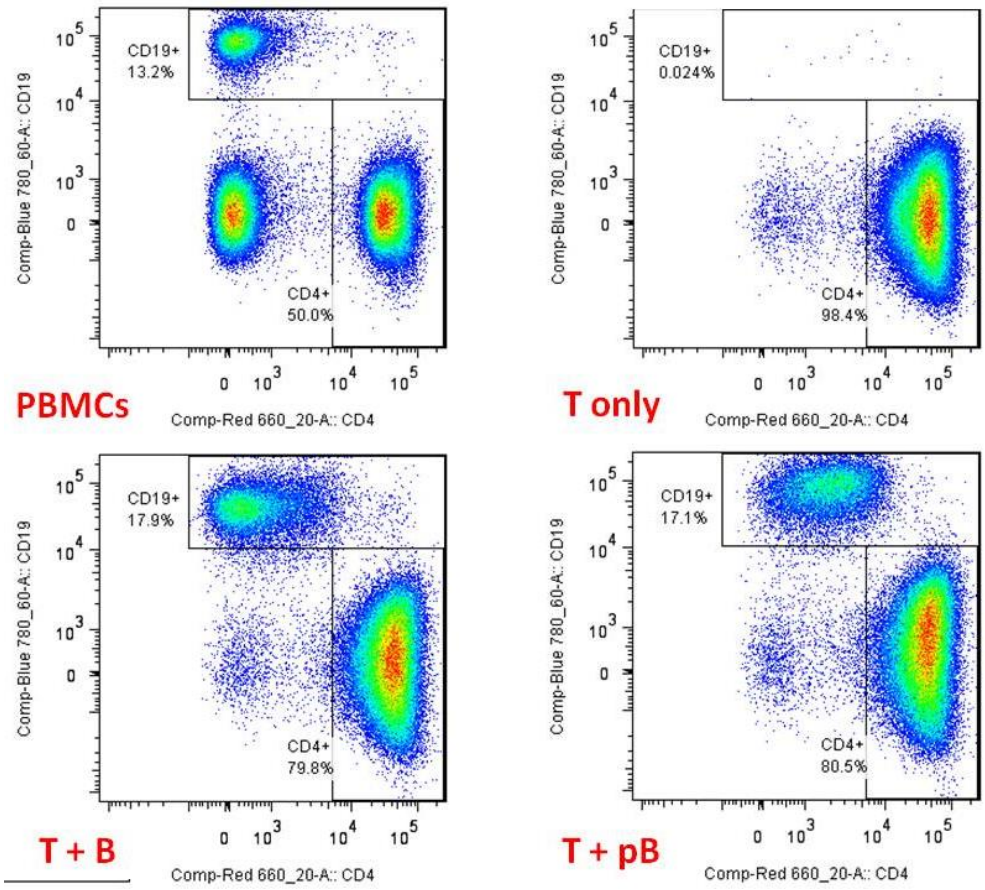

Figure 3.15: Dot plot examples demonstrating enriched CD4⁺ T-cells in co-culture with non-stimulated or α-δ-DEX pre-activated CD19⁺ B-cells.

Purified CD4⁺ T and CD19⁺ B lymphocytes were obtained separately from PBMCs by negative selection and co-cultured at an approximate 6 to 1 ratio. After a sequential gating strategy for exclusion of doublets and dead cells, dot plots illustrate the final gating for selection of CD4⁺ T cells (*x*- axis= CD4-APC) and CD19⁺ B cells (*y*- axis = CD19 PE Cy-7). Note that purity of both T+B lymphocytes exceeds 95% in both conditions.

T= CD4⁺ T-cell, B= B-cell, pB= α-δ-DEX pre-activated B-cell.

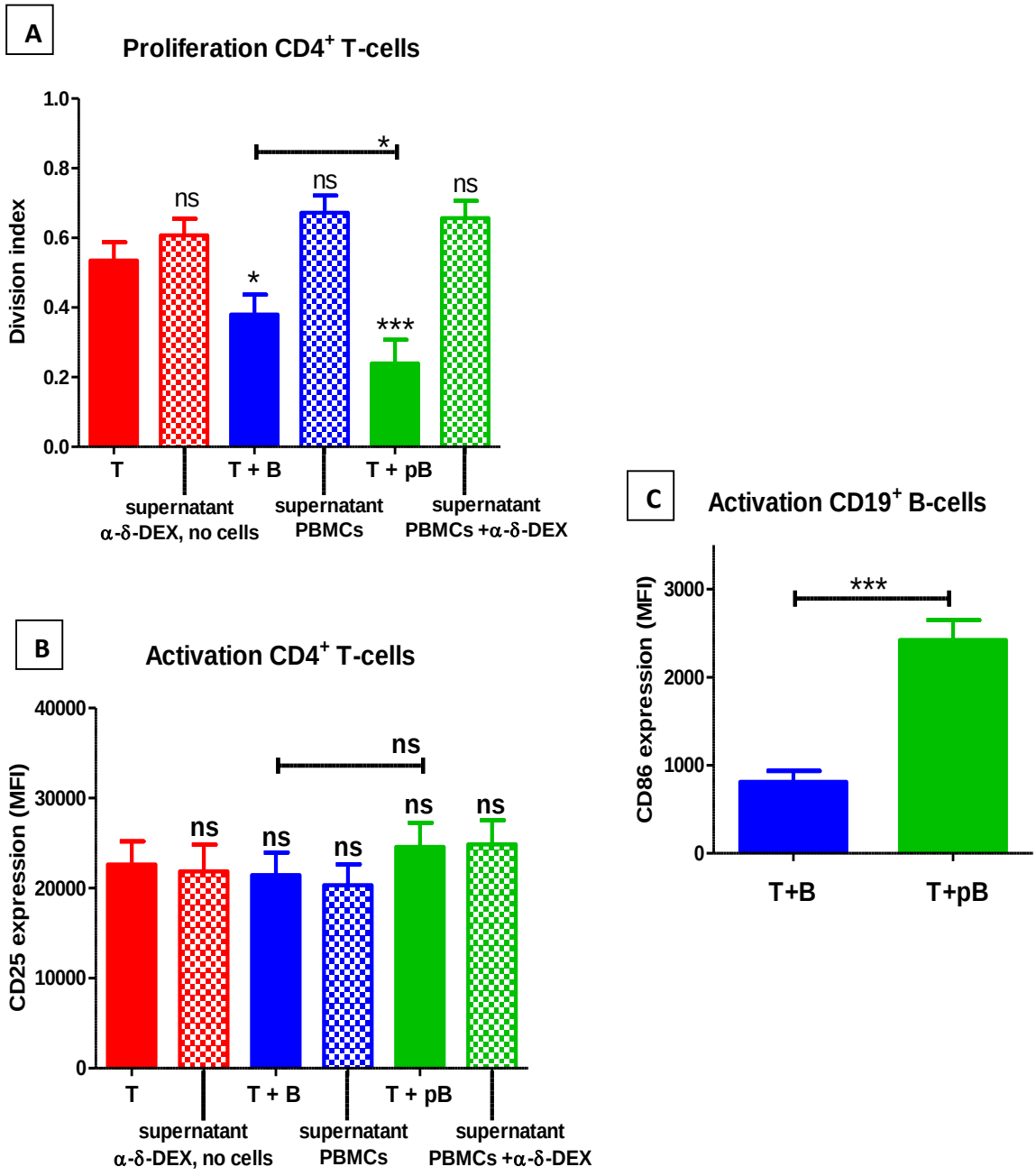

Figure 3.16: α-δ-DEX pre-activated B-cells suppress proliferation of purified CD4⁺ T-cells by a cell contact dependent mechanism.

A. Proliferation of enriched CD4⁺ T-cells, reported as division index. **B. Activation of enriched CD4⁺ T-cells**, expression of the CD25 marker as median fluorescence intensity (MFI). **C. Activation CD19⁺ B-cells**, expression of the CD86 marker as median fluorescence intensity (MFI). Bars represent means and SEM, n=8. Paired ANOVA, Dunnett's (*vs.* T) and Bonferroni's Multiple Comparison Test; *$p \leq 0.05$, **$p \leq 0.01$, ***$p \leq 0.001$, ns= not significant. Primary CD4⁺ T and B lymphocytes were enriched by negative selection from PBMCs and all conditions were stimulated with αCD3/αCD28 dynabeads. In red (solid bar), control group containing T-cells alone. In blue (solid bar), co-culture of T and non pre-activated B-cells. In green (solid bar), co-culture of T and α-δ-DEX pre-activated B-cells. Square bars represent the wells containing T-cells plus the respective PBMCs supernatant, with and without α-δ-DEX. T= CD4⁺ T-cell, B= B-cell, pB= α-δ-DEX pre-activated B-cell.

3.9 TI-II MIMICS STILL HAVE AN EFFECT ON B-CELL DEPLETED PBMCS

Moraxella IgD-binding protein (MID) is an outer membrane protein with specific affinity for human IgD (Forsgren et al. 2001). A truncated form of this protein containing the amino acid residues 962-1200 binds to soluble and membrane IgD, inducing B-cell activation and proliferation in a culture of peripheral blood lymphocytes (Nordström et al. 2006; Nordström et al. 2002). It had previously been reported by colleagues in our lab that MID shares very similar T-cell inhibitory properties to the ones described for α-δ-DEX (J.B. Wing, unpublished data), suggesting in this manner a generic TI phenomenon rather than an isolated α-δ-DEX property. Therefore, to establish that only B-cells were capable to respond to TI type II stimulation and subsequently restrain $CD4^+$ T responses, B-cell depleted PBMCs were exposed to α-δ-DEX and MID. The use of MID would also help to exclude the possibility that the α-δ-DEX preparation had a contaminant or that the effect was unspecific *via* FcR or the dextran molecule.

3.9.1 α-δ-DEX suppresses T-cell responses even in B-cell depleted PBMCs, although the effect is stronger when B lymphocytes are present.

Almost absolute B-cell removal from PBMCs (<1% $CD19^+$ cells left) was achieved from day 0 (sections 2.2.2 and 3.10) and remained following incubation over 4 days with or without α-δ-DEX (1 μg/ml). In parallel, whole PBMCs were exposed to the same TI stimuli and used as control groups.

Figure 3.17 compares B-cell depleted groups against whole PBMCs, showing proliferation and activation of $CD4^+$ T lymphocytes when exposed to α-δ-DEX. Is in this figure where the most striking observation was found. Even after B-cell elimination addition of α-δ-DEX resulted in impaired T-cell proliferation and activation. Around 50% reduction of division index and CD25 expression occurred in those samples lacking of B-cells.

In relation to the respective positive control containing αCD3 alone, PBMCs free from B lymphocytes and stimulated with αCD3 plus α-δ-DEX induced a dramatic drop on the division index of $CD4^+$ T-cells. Furthermore, there was no difference between the suppression reported by the B-cell depleted sample and whole PBMCs (Figure 3.17-A). Exactly the same trend can be observed for the activation marker CD25, which also suffered a large reduction on its expression regardless the absence of B lymphocytes (Figure 3.17-B). Again, no statistical difference was detected between the non-depleted and depleted groups containing αCD3 plus α-δ-DEX.

In a further attempt to discover if the intensity of the α-δ-DEX inhibitory effect was the same in B-cell depleted PBMCs than in whole PBMCs, a statistical analysis was carried out comparing not division index or CD25 expression levels but percentages of T-cell inhibition in relation to the αCD3 positive control. Thus, the αCD3 sample which proliferated and activated normally had 0% suppression, while the samples exposed to αCD3+α-δ-DEX were plotted as % of the reduction they caused in relation with their paired αCD3 control (Figure 3.18). From this approach, it was able to determine that although downregulation of T-cell responses occurs in PBMCs lacking of B lymphocytes, a trend to a deeper negative effect is induced by α-δ-DEX when B-cells are present within the co-culture. In the case of $CD4^+$ T-cell proliferation, there was a statistical difference of means for the % of suppression shown by the whole PBMCs sample (69.76%, SD$\pm$16.04) *versus* the B-cell depleted sample (52.98%, SD$\pm$13.0) (Figure 3.18-A). However, the significance between these two groups appeared lost (p=0.08) when the same % of suppression was quantified for T-cell activation (Figure 3.18-B). Since expression of activation markers is always more variable, a larger sample size could sustain the possibility of a stronger α-δ-DEX inhibitory effect driven by B lymphocytes.

In summary, these data indicate that $CD4^+$ T-cell responses can be significantly restricted by α-δ-DEX regardless of whether almost all of B lymphocytes are removed. However, the inhibition is stronger when B lymphocytes are present in the culture.

3.9.2 MID also inhibits T-cell responses in B-cell depleted PBMCs.

In order to clarify if such unexpected phenomenon was exclusive to α-δ-DEX, MID was investigated as a second TI type 2 mimic under the same conditions.

First, MID activity as B-cell stimulant was tested on whole PBMCs and compared against α-δ-DEX. Over a 4 day period, PBMCs were stimulated with αCD3 plus either α-δ-DEX (1 μg/ml) or MID (2 μg/ml) (section 2.3.2.2).

Even though MID failed to significantly augment B-cell proliferation compared with the αCD3 control, Figure 3.19 confirms the ability of MID to induce an effective $CD19^+$ B-cell activation almost as potent as the one induced by α-δ-DEX. Most importantly, according to the data in Figure 3.20 it was possible to confirm what was reported previously in our lab, that MID also suppresses $CD4^+$ T-cell proliferation and activation with a similar strength to α-δ-DEX.

Once established the inhibitory properties of MID as TI mimic, the same B-cell depletion experiment as the one described in section 3.9.1 was performed. B-cells were removed from PBMCs by positive selection (section 2.2.2) and stimulated with αCD3 and MID for 4 days before analysis. In addition, equivalent groups were prepared using whole PBMCs.

From Figure 3.21-A, is evident that addition of MID resulted in an impaired T-cell division index even among B-cell depleted PBMCs. In parallel, expression of the activation marker CD25 was sharply decreased by MID regardless of whether B lymphocytes were present or not within the culture (Figure 3.21-B). Similar to the experiment with α-δ-DEX, groups containing αCD3 plus MID did not show significant differences in $CD4^+$ T-cell proliferation or activation between B-cell depleted and non-depleted PBMCs.

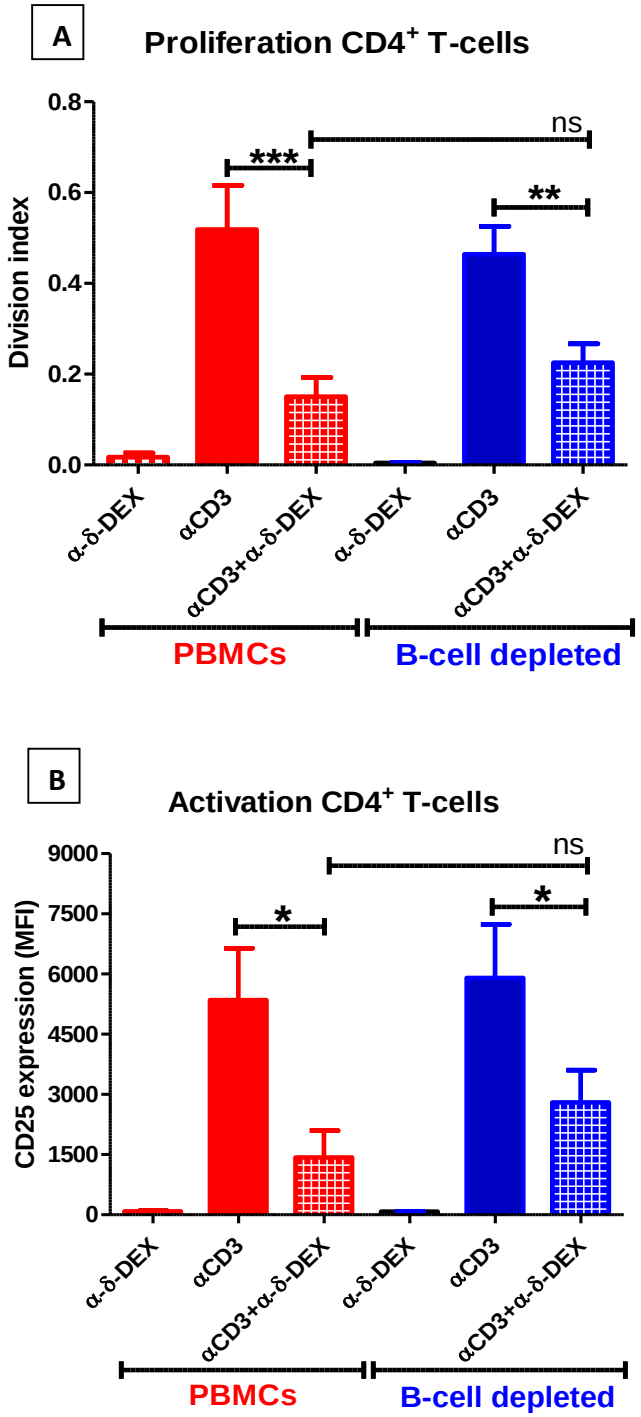

Figure 3.17: α-δ-DEX suppressive properties still occur on B-cell depleted PBMCs.

A. Proliferation CD4⁺ T-cells, reported as division index. **B. Activation CD4⁺ T-cells**, expression of the CD25 marker as median fluorescence intensity (MFI). Bars represent means and SEM. PBMCs groups n= 5; B-cell depleted n=8. One way ANOVA, Bonferroni's Multiple Comparison Test. *$p \leq 0.05$, **$p \leq 0.01$, ***$p \leq 0.001$, ns= not significant.

Whole PBMCs (in red) and B-cell depleted PBMCs (in blue) were stimulated with αCD3 (plate-bound 0.3 µg/ml) and/or α-δ-DEX (1 µg/ml). Groups containing αCD3 only represent the positive control (filled bars) under each condition.

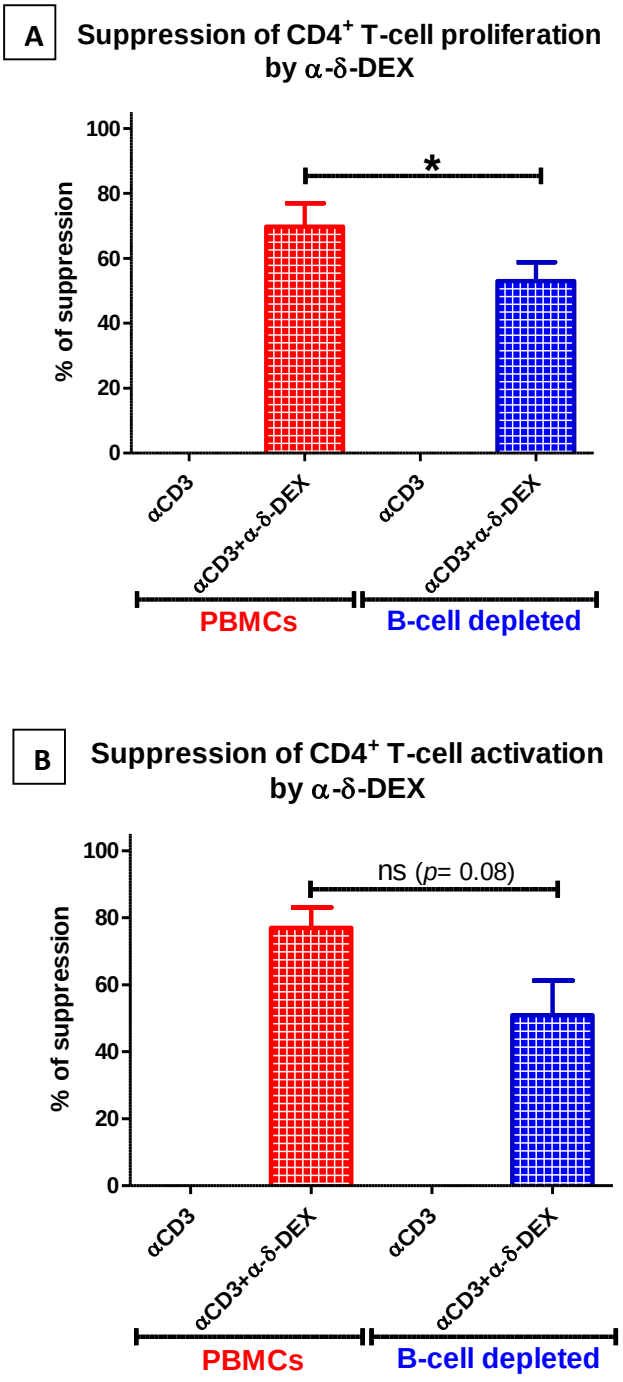

Figure 3.18: Comparison of the % of suppression between whole PBMCs and B-cell depleted PBMCs stimulated with α-δ-DEX.

A. Proliferation CD4⁺ T-cells, reported as % of suppression. **B. Activation CD4⁺ T-cells**, reported as % of suppression. Bars represent means and SEM, n= 5. Paired student *t*- test; *$p \leq 0.05$, ns= not significant.

Whole PBMCs (in red) and B-cell depleted PBMCs (in blue) were stimulated with αCD3 (plate-bound 0.3 µg/ml), with or without α-δ-DEX (1 µg/ml). Groups containing αCD3 only represent a 0% suppression baseline under each condition.

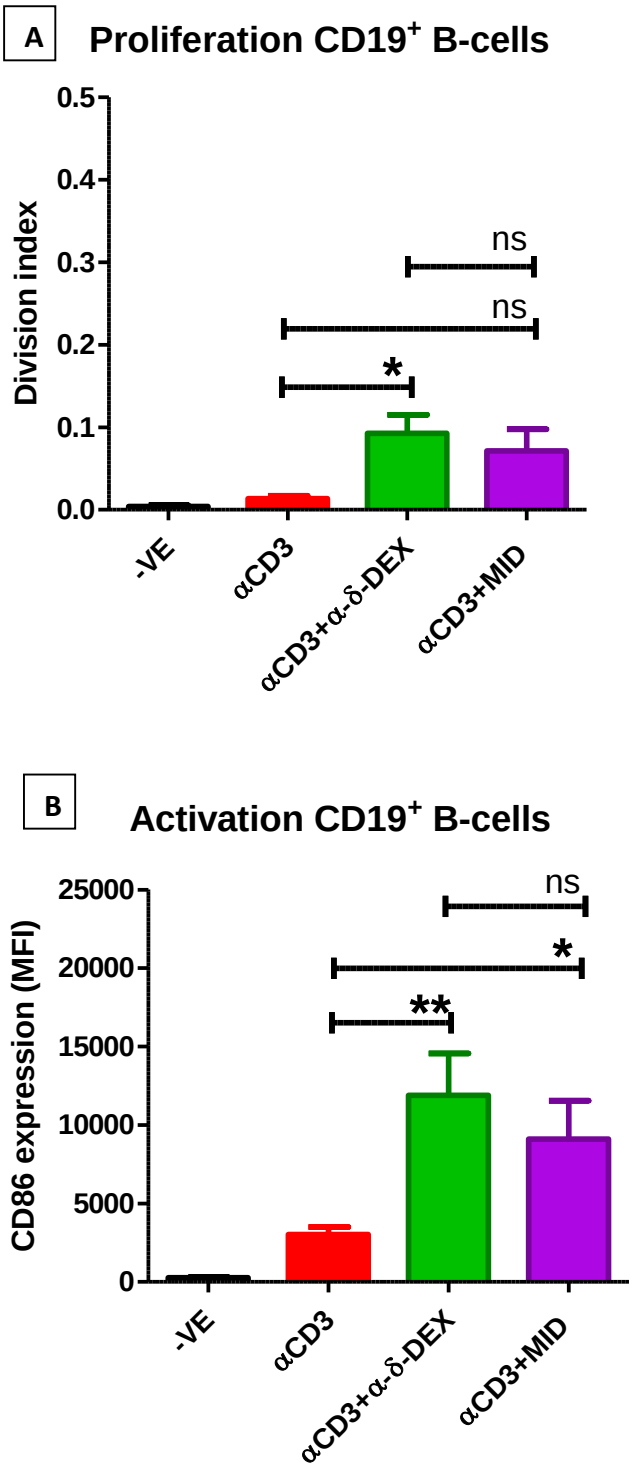

Figure 3.19: CD19⁺ B-cell activation is induced by the TI type II mimic MID.

A. Proliferation CD19⁺ B-cells, reported as division index. **B. Activation CD19⁺ B-cells**, expression of the CD86 marker as median fluorescence intensity (MFI). Bars represent means and SEM, n=5. Paired ANOVA, Bonferroni's Multiple Comparison Test. *$p \leq 0.05$, **$p \leq 0.01$, ns= not significant.

-VE= negative control, non-stimulated PBMCs. αCD3 = plate-bound 0.2 µg/ml. α-δ-DEX= 1 µg/ml. MID= 2 µg/ml.

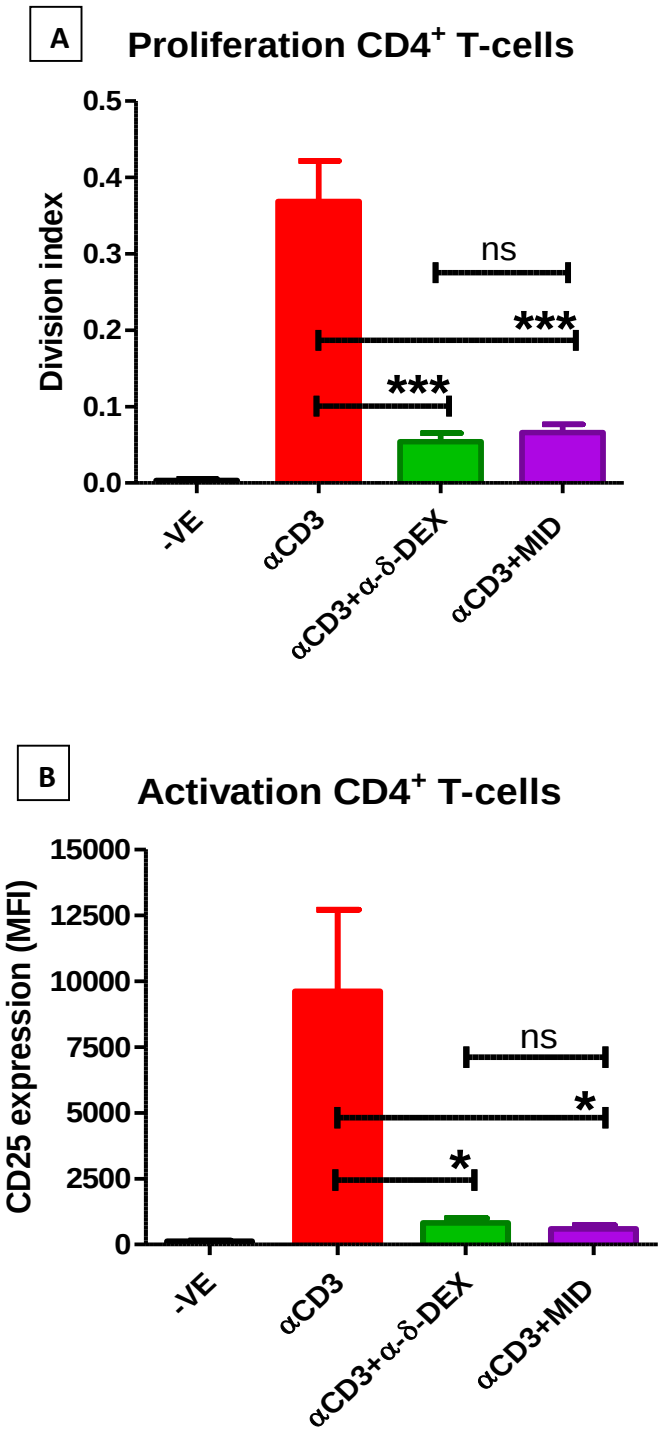

Figure 3.20: MID suppresses proliferation and activation of CD4+ T lymphocytes in a similar way as α-δ-DEX.

A. Proliferation CD4⁺ T-cells, reported as division index. **B. Activation CD4⁺ T-cells**, expression of the CD25 marker as median fluorescence intensity (MFI). Bars represent means and SEM, n=5. Paired ANOVA, Bonferroni's Multiple Comparison Test; *$p \leq 0.05$, **$p \leq 0.01$, ***$p \leq 0.001$, ns= not significant.

-VE= negative control, non-stimulated PBMCs. αCD3 = plate-bound 0.2 µg/ml. α-δ-DEX= 1 µg/ml. MID= 2 µg/ml.

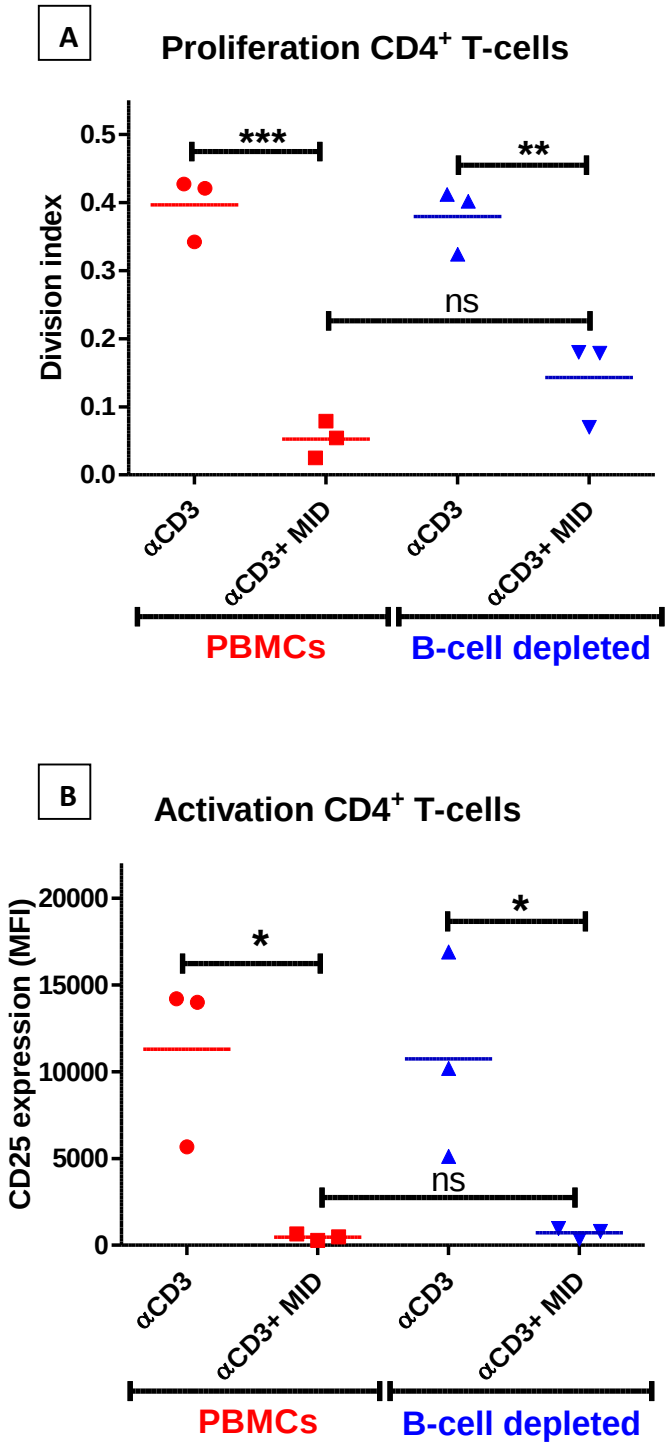

Figure 3.21: MID suppressive properties still occur on B-cell depleted PBMCs.

A. Proliferation CD4⁺ T-cells, reported as division index. **B. Activation CD4⁺ T-cells**, expression of the CD25 marker as median fluorescence intensity (MFI). Lines represent means, n= 3. Paired ANOVA, Bonferroni's Multiple Comparison Test; *$p \leq 0.05$, **$p \leq 0.01$, ***$p \leq 0.001$, ns= not significant.

Whole PBMCs (in red) and B-cell depleted PBMCs (in blue) were stimulated with αCD3 (plate-bound 0.3 µg/ml) with or without MID (2 µg/ml).

3.10 Confirmation of Depletion Efficiency and Exclusion of Rare CD19$^-$ Cells Expressing IgD

Since both TI type 2 mimics had an effect on B-cell depleted PBMCs, I returned to check the efficacy of the depletion protocol. The kit used for these experiments (section 2.2.2), positively selects for cells expressing CD19 and CD20, which are classical phenotypic markers of B lymphocytes in peripheral blood (Bisset et al. 2004).

The number of CD19$^+$ lymphocytes remaining was evaluated on day 0 immediately after performing the depletion protocol, having a successful outcome of only 0 to 0.1% events within the CD19 gate as compared with its PBMC equivalent. In correlation, no more than 1% events were found within the CD19 gate after 4 days of incubation (Figure 3.22).

Since α-δ-DEX and MID act by multiple cross-linking of surface IgD on B lymphocytes, persistence of cells expressing IgD was another investigated aspect. It was first excluded the existence of rare non B-cells which could interact with the TI mimics, being CD19$^-$ or CD20$^-$ but expressing IgD molecules on their surface. As Figure 3.23 illustrates, among PBMCs less than 0.5% events will be either CD19$^-$ or CD20$^-$ but IgD$^+$; a situation which remains unmodified irrespective of the stimulation with αCD3 plus/minus α-δ-DEX. Further confirmation of this was achieved when no events lacking the phenotypic marker CD19 but expressing IgD were discovered in any of the depleted samples on day 4 post-incubation, in the absence or presence of any stimulus (Figure 3.24). From the non-stimulated and αCD3 samples, is clear that the depletion protocol achieves almost absolute removal of CD19$^+$ and IgD$^+$ cells. Moreover, whole PBMC samples containing α-δ-DEX and MID corroborate that both TI mimics bind to IgD, as the staining of IgD molecules becomes masked.

This section allowed us to confirm the efficacy of our depletion protocol in removing almost all B lymphocytes expressing IgD on their surface. Moreover, it was possible to exclude the existence of rare cells CD19$^-$ and CD20$^-$ but IgD$^+$ which could interact with the TI mimics.

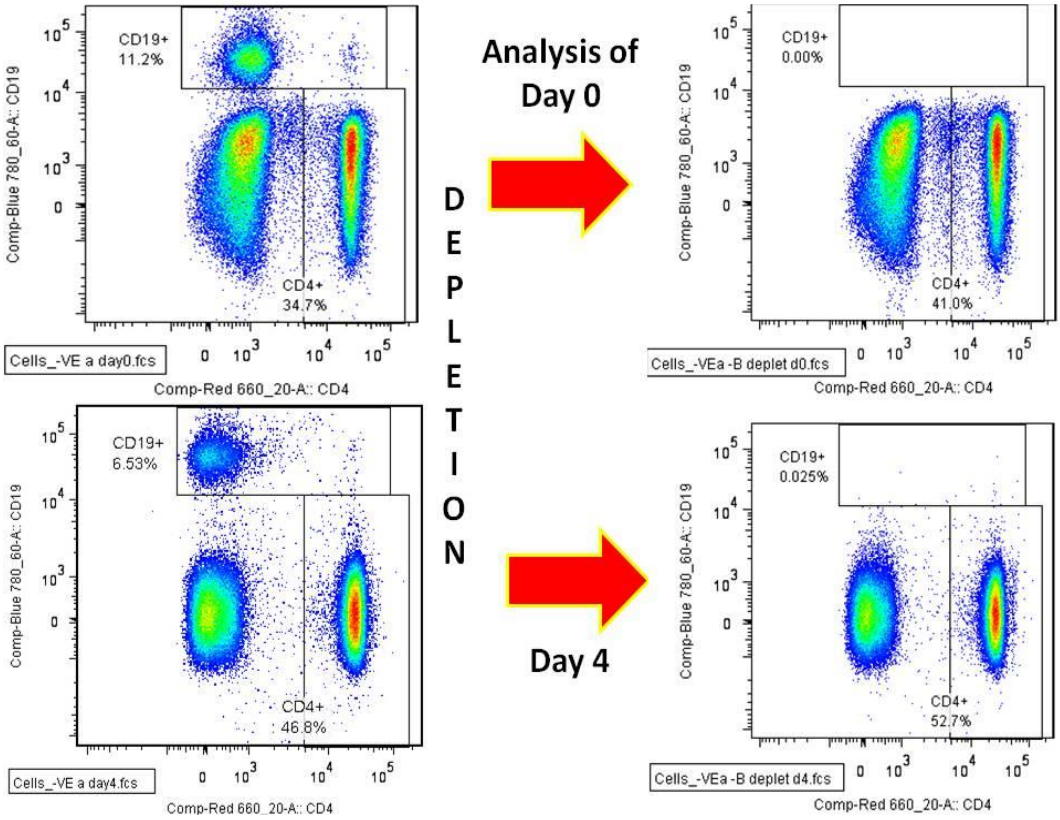

Figure 3.22: Representative dot plot examples of the efficiency of our depletion protocol at day 0 and day 4 from non-stimulated PBMCs.

Top plots illustrate PBMCs on day 0 before and after the depletion procedure. Bottom plots are representative of non-depleted PBMCs and depleted PBMCs on day 4 post-incubation. After a sequential gating strategy for exclusion of doublets and dead cells, dot plots show the final gating for selection of $CD4^+$ cells (*x*- axis= CD4-APC) *vs.*$CD19^+$ cells (*y*- axis = CD19 PE Cy-7).

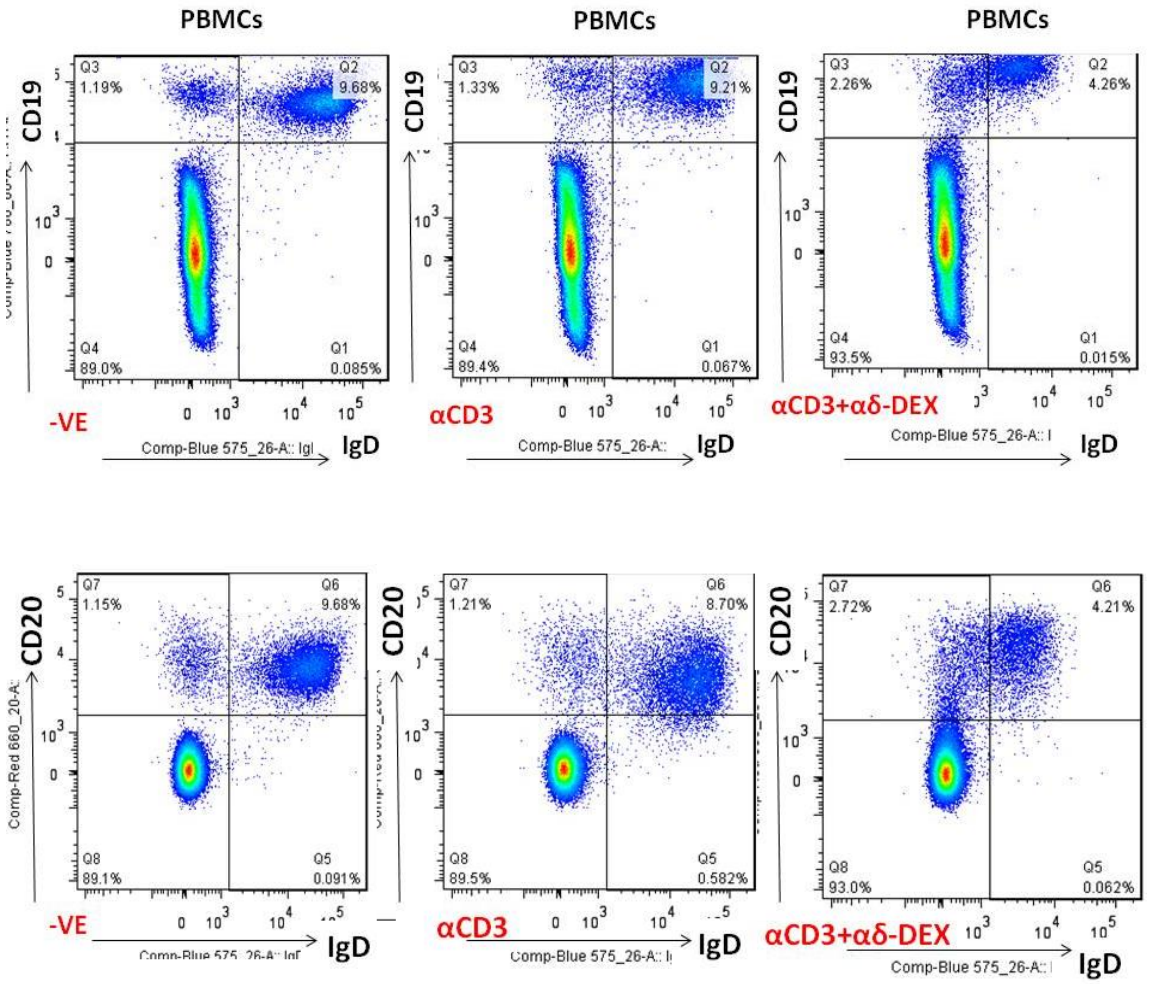

Figure 3.23: Representative dot plot examples of whole PBMCs showing less than 0.5% rare events being $CD19^-$ or $CD20^-$ but expressing IgD.

Top row illustrates whole PBMCs stained for the B-cell phenotypic marker CD19 (*y*- axis, PE Cy-7) and surface IgD (*x*- axis, PE). Bottom row shows expression of CD20 as second B lymphocyte marker (*x*- axis, APC) and IgD (*x*- axis, PE). To exclude the possibility of inducing more IgD expression after stimulation, PBMCs were inspected under different conditions: no stimulus (-VE), αCD3 plate-bound (0.2 µg/ml) or αCD3 + α-δ-DEX (1 µg/ml).

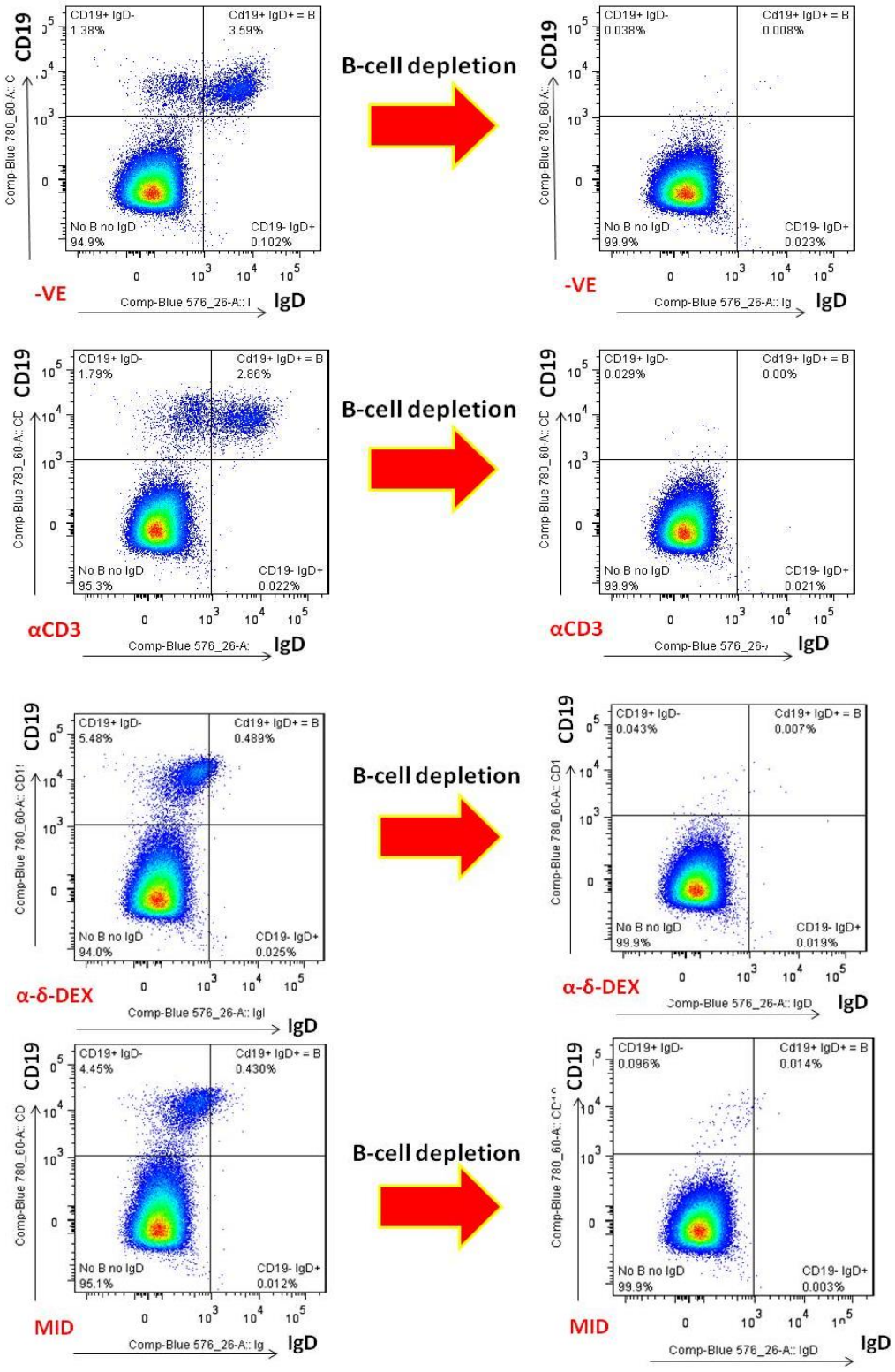

Figure 3.24: Representative dot plot examples of PBMCs before and after B-cell depletion, proving almost complete elimination of CD19⁺ IgD⁺ events.

To leave out the possibility of inducing more IgD expression after stimulation, PBMCs were inspected under different conditions: no stimulus (-VE), αCD3 plate-bound (0.2 µg/ml), α-δ-DEX (1 µg/ml) or MID (2 µg/ml). After exclusion of dead cells, dot plots show the final gates for selection of CD19⁺ cells (*y*-axis, PE Cy-7) expressing IgD (*x*- axis, PE).

3.11 IL-10 AND B-CELL DEPLETION

Based on the fact that IL-10 might have a minor effect in the α-δ-DEX suppressive mechanism (section 3.5), it was decided to explore whether over-production of IL-10 was taking place within B-cell depleted samples and was responsible for T-cell suppression. We hypothesized that if T-cell inhibition was due to large amounts of IL-10 being produced by cell populations other than B lymphocytes, then blockade of this cytokine could reverse the negative effect among B-cell depleted PBMCs.

A similar IL-10 blocking experiment to the one described in section 3.5 was designed, but this time using B-cell depleted PBMCs. A functional grade anti-IL-10 monoclonal antibody (αIL-10) at 10 µg/ml was chosen for this set of experiments due to the partial but significant restoration effect that this concentration showed for T-cell proliferation (Figure 3.7-A). Whole PBMCs and B-cell depleted PBMCs were stimulated with αCD3 plus α-δ-DEX, in the presence of either αIL-10 or its isotype control.

From the data in Figure 3.25, it can be observed how IL-10 blocking failed to restore $CD4^+$ T-cell proliferation or activation when B-cells are not present in the culture. Even though a trend could be suspected, αIL-10 did not significantly increase the division index of $CD4^+$ T lymphocytes in the presence of α-δ-DEX (Figure 3.25-A). Equally, expression of the activation marker CD25 remained low despite the addition of αIL-10 (Figure 3.25-B). No differences were reported either between the whole PBMCs groups containing αCD3+ α-δ-DEX+ αIL-10 and its B-cell depleted equivalents.

To further support the inefficacy of IL-10 blocking in the absence of B lymphocytes, exactly the same experiment was carried out using MID. Although the sample size is smaller, addition of αIL-10 resulted in partial restoration of T-cell proliferation in comparison with the isotype control (Figure 3.26-A). However, such positive effect disappeared against the sample that was only stimulated with αCD3 plus MID. Surprisingly, whole PBMCs and B-cell depleted PBMCs containing αCD3+ MID+ αIL-10 were also significantly different by their division index. In contrast, inhibition of T-cell activation was not reversed by IL-10 blocking and none of the compared groups were statistically different.

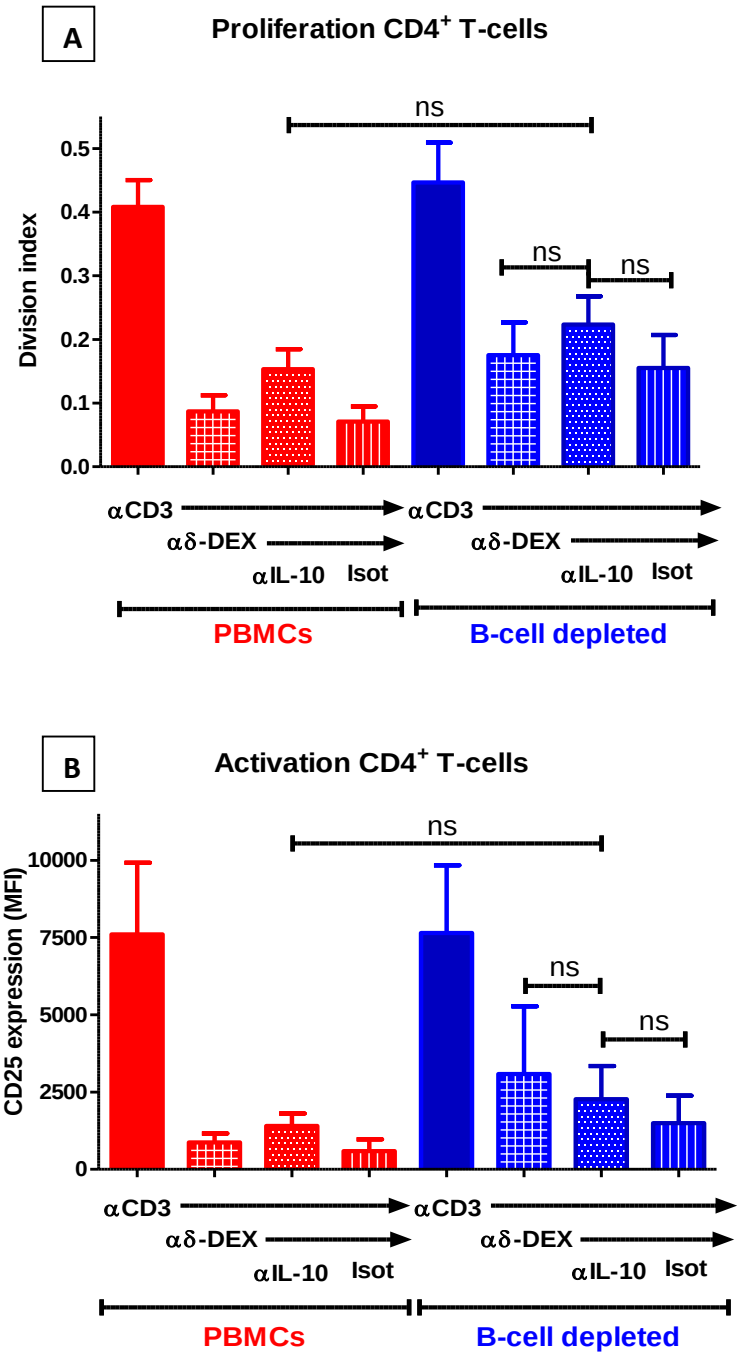

Figure 3.25: Blocking of IL-10 does not reverse α-δ-DEX effect among B-cell depleted PBMCs.

A. Proliferation CD4⁺ T-cells, reported as division index. **B. Activation CD4⁺ T-cells**, expression of the CD25 marker as median fluorescence intensity (MFI). Bars represent means and SEM, n=6. Paired ANOVA, Bonferroni's Multiple Comparison Test; ns= not significant.
Whole PBMCs (red bars) and B-cell depleted PBMCs (blue bars), were stimulated with αCD3 (plate-bound 0.3 µg/ml) plus α-δ-DEX (1 µg/ml) in the presence of either αIL-10 (10 µg/ml) or the isotype control (10 µg/ml). The groups containing αCD3 alone represent the positive controls (solid bars), while the group containing αCD3+ α-δ-DEX provides the baseline of suppression to compare against.

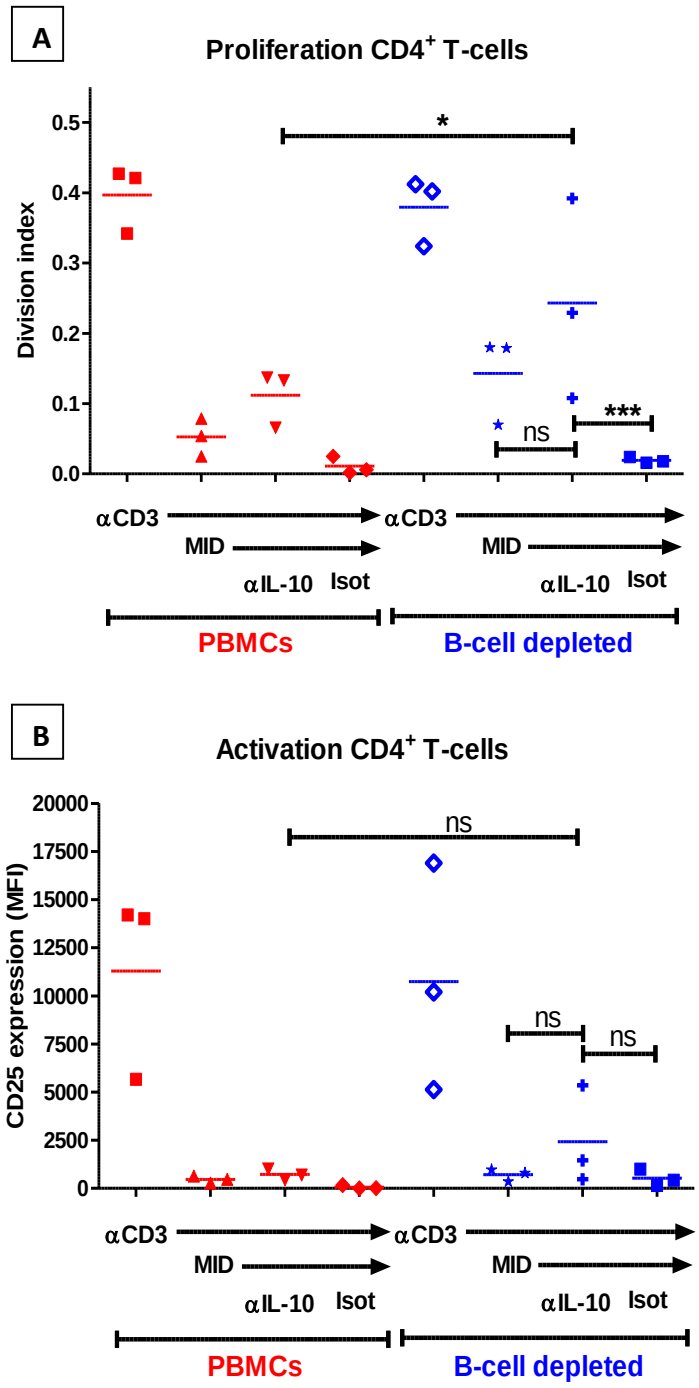

Figure 3.26: Blocking of IL-10 does not reverse MID effect among B-cell depleted PBMCs.

A. Proliferation CD4⁺ T-cells, reported as division index. **B. Activation CD4⁺ T-cells**, expression of the CD25 marker as median fluorescence intensity (MFI). Lines represent means, n=3. Paired ANOVA, Bonferroni's Multiple Comparison Test; *$p \leq 0.05$, **$p \leq 0.01$, ***$p \leq 0.001$, ns= not significant.

Whole PBMCs (red groups) and B-cell depleted PBMCs (blue groups), were stimulated with αCD3 (plate-bound 0.3 µg/ml) plus MID (2 µg/ml) in the presence of either αIL-10 (10 µg/ml) or the isotype control (10 µg/ml). The groups containing αCD3 alone represent the positive controls, while the group containing αCD3+ MID provides the baseline of suppression to compare against.

3.12 ASSESSING THE MINIMAL NUMBER OF B-CELLS REQUIRED TO ACHIEVE SUPPRESSION

To further address the ability and strength of α-δ-DEX pre-activated B lymphocytes to suppress enriched $CD4^+$ T-cells, two opposite titration experiments were performed.

The first assay was designed to determine how many TI pre-activated B-cells is the minimal number to achieve inhibition of T-cell proliferation. Following the same protocol to the one in section 3.7, α-δ-DEX pre-activated B lymphocytes were put in co-culture with enriched $CD4^+$ T lymphocytes but this time larger ratios of T to B cells were evaluated: 6:1, 18:1, 54:1, 162:1 and 486:1. Since both donors reached the maximal effect at the physiological T:B ratio of 6:1, it is possible to infer that the inhibition on T-cell proliferation is dependent on the number of α-δ-DEX pre-activated B lymphocytes (Figure 3.27-A). It is important to point out that whilst one donor was moderately repressed by low numbers of pre-activated B-cells (ratios 18:1 and 54:1) (Figure 3.27-B), the other donor remained unaffected. As we found previously (Figures 3.13 and 3.16) addition of pre-activated B lymphocytes on day one was unable to suppress the T-cell activation marker CD25 (Figure 3.27-C).

In all the experiments using α-δ-DEX pre-activated B-cells, these were added one day after T-cell stimulation was initiated with αCD3/αCD28 dynabeads (Figure 3.12). Therefore, we wondered whether the degree of inhibition could be enhanced by adding the T-cell stimulus on the same day as the α-δ-DEX pre-activated B-cells. In this assay we compared proliferation and activation of enriched $CD4^+$ T-cells stimulated one day prior addition of α-δ-DEX pre-activated B lymphocytes (day 0) *versus* T-cells stimulated on the same day of the co-culture with pre-activated B-cells (day 1). Figure 3.28-A demonstrates that TI activated B-cells are capable of dampening proliferation irrespective whether T-cell stimulation was initiated one day prior co-culture or on the same day. Interestingly and as observed in previous experiments, α-δ-DEX suppressive B-cells do not reduce CD25 expression not even when the activation stimulus was added on the same day as the T:B co-culture began (Figure 3.28-B).

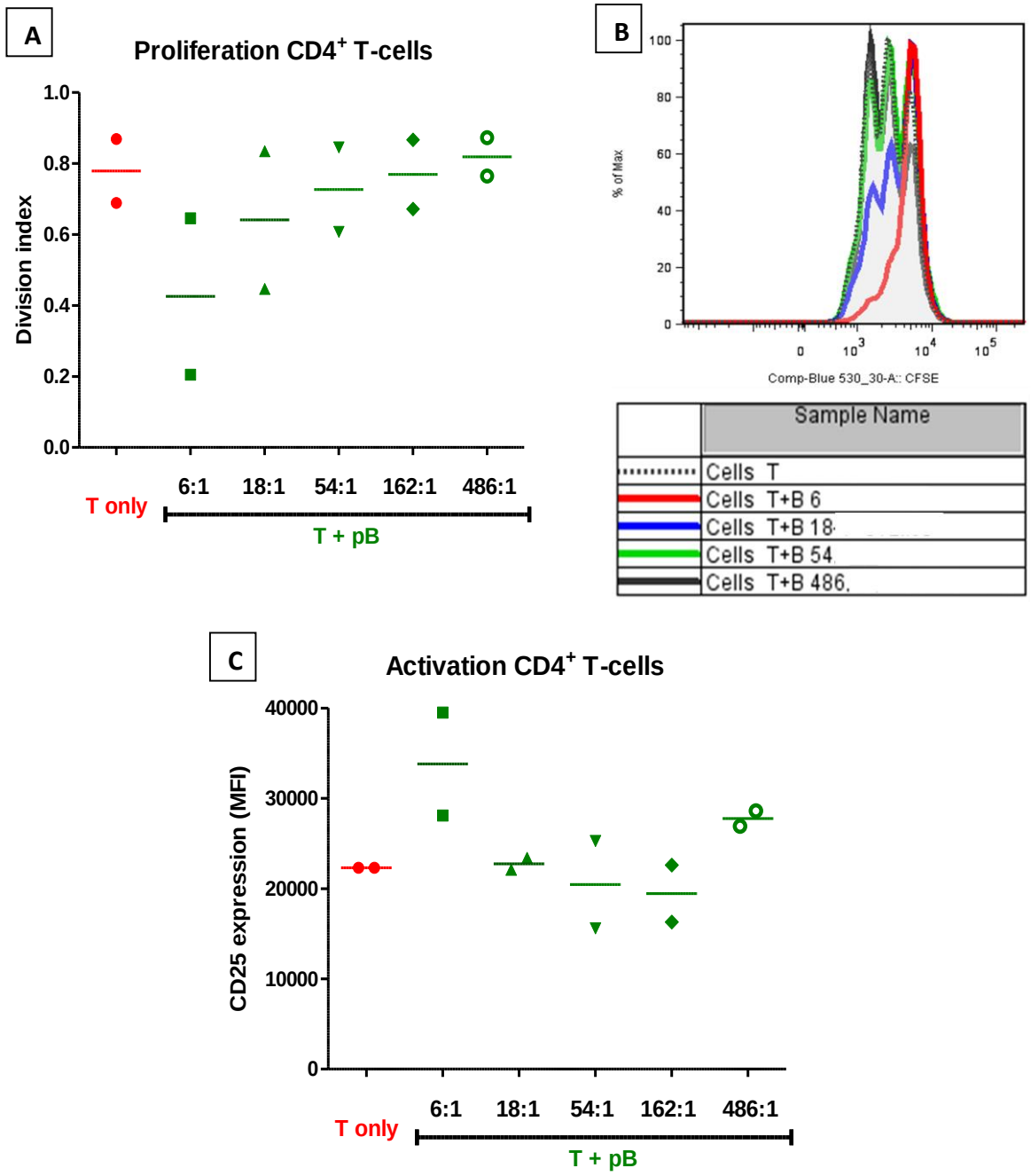

Figure 3.27: α-δ-DEX pre-activated B lymphocytes might suppress CD4⁺ T-cell proliferation even at small non-physiological numbers.

A. Proliferation of enriched CD4⁺ T-cells, reported as division index. **B. Histogram of representative example:** CD4⁺ T-cell proliferation assessed by the CFSE dilution method, the x axis represents intensity of CFSE fluorescence and the y axis % of maximum. **C. Activation of enriched CD4⁺ T-cells**, expression of the CD25 marker as median fluorescence intensity (MFI). Lines represent means, n=2.

On day 0, all conditions were stimulated with αCD3/αCD28 dynabeads (1:1 ratio). Primary CD4⁺ T and B lymphocytes were enriched by negative selection from PBMCs. In red, control group containing T-cells alone. In green, co-culture groups of CD4⁺ T-cells plus different ratios of 24 hour α-δ-DEX pre-activated B-cells: 6:1, 18:1, 54:1, 162:1 and 486:1 T-to-B cell.

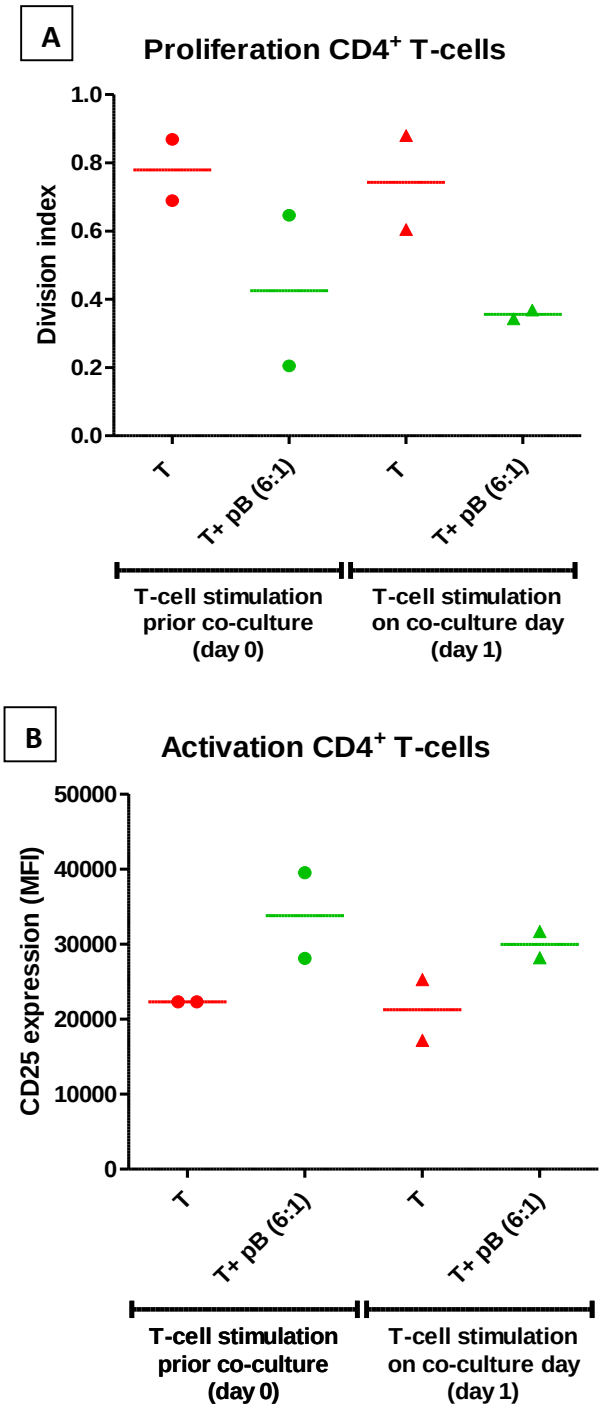

Figure 3.28: α-δ-DEX pre-activated B lymphocytes suppress CD4⁺ T-cell proliferation, even when T-cell stimulation is initiated 1 day prior co-culture. However, α-δ-DEX pre-activated B lymphocytes do not restrain CD25 expression in any situation.

A. Proliferation of enriched CD4⁺ T-cells, reported as division index. **B. Activation of enriched CD4⁺ T-cells**, expression of the CD25 marker as median fluorescence intensity (MFI). Lines represent means, n=2.
Enriched CD4⁺ T-cells were stimulated with αCD3/αCD28 dynabeads (1:1 ratio) one day prior co-culture (day 0) or on the same day (day 1). In red the control groups containing T-cells alone and in green the co-culture groups of T-cells plus α-δ-DEX pre-activated B-cells (ratio 6:1).
T= CD4⁺ T-cell, pB= α-δ-DEX pre-activated B-cell.

3.13 PURIFIED α-δ-DEX PRE ACTIVATED MONOCYTES DO NOT SUPPRESS T-CELLS

Although α-δ-DEX is a biological compound which should exclusively act on and stimulate B-cells, it was decided to perform an experiment with purified monocytes to exclude any remote chance of an effect on these accessory cells, perhaps through the dextran molecule or through a Fc receptor interaction, or through a contaminant of the α-δ-DEX preparation.

A similar protocol to the one described in section 3.7 was followed. Briefly, purified $CD4^+$ T-cells were enriched from PBMCs by negative selection on day 0 and stimulated with αCD3/αCD28 dynabeads. On the same day, PBMCs were incubated for a 24 hour period in the absence or presence of α-δ-DEX. Then, $CD14^+$ monocytes were negatively selected from those PBMCs as described in section 2.1.1. Finally, monocytes and purified T lymphocytes were co-cultured on day 1, leaving 3 more days in incubation before analysis. The right ratio between purified T-cells and monocytes was chosen again based on what the literature reports as normal range in peripheral blood of healthy adults, from all leukocytes 20-40% T-cells against 3-8% monocytes. Indeed, a ratio of 6 to 1 T-cells to monocytes was decided. Figure 3.29 illustrates a schematic representation of the methodology applied.

Data in Figure 3.30-A demonstrates the division index of αCD3/αCD28 stimulated purified $CD4^+$ T lymphocytes alone and in co-cultured with $CD14^+$ monocytes that had or had not been exposed to α-δ-DEX. Surprisingly and similarly to what we were able to detect with non pre-activated B-cells (section 3.8), even non-stimulated monocytes significantly reduced T-cell proliferation when compared against the sample containing T-cells. However, such inhibition does not seem to be associated with an α-δ-DEX effect since there was no statistical difference between the monocyte group that was incubated with α-δ-DEX and the one that was not.

As seen in previous experiments, expression of the activation marker CD25 remained unaffected regardless co-culture with monocytes (Figure 3.30-B). Again, this may have been due to an early activation from day 0 (prior co-culture), which led to an irreversible expression of the surface marker despite contact with monocytes.

In conclusion, there is no evidence to assume there is a direct α-δ-DEX influence on $CD14^+$ monocytes. But the question whether non pre-activated enriched cells (either B lymphocytes or monocytes) could develop a spontaneous suppressive phenotype *in vitro* stills remains unclear (discussed in section 3.16).

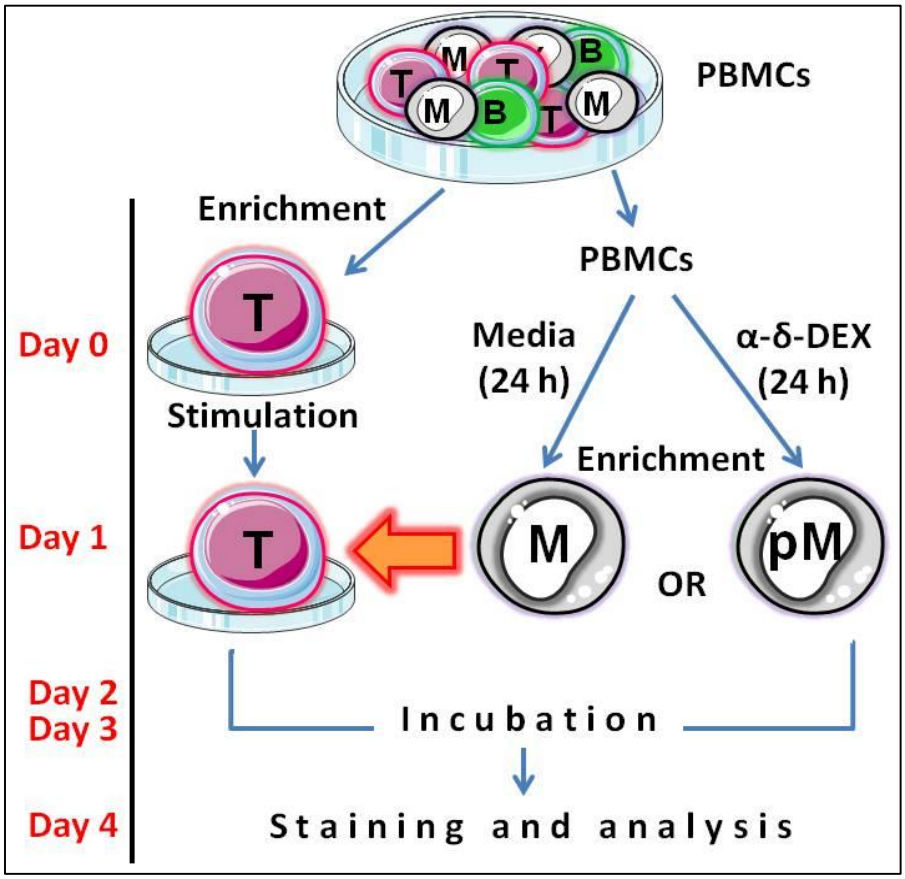

Figure 3.29: Schematic representation of the experimental protocol involving purified T lymphocytes and monocytes in the presence of α-δ-DEX.

Enriched $CD4^+$ T lymphocytes were obtained from PBMCs on day 0, followed by stimulation with αCD3/αCD28 dynabeads. On the same day, PBMCs were incubated in the presence or absence of α-δ-DEX. After a 24 hour incubation, non pre-activated monocytes and pre-activated monocytes were enriched and co-cultured with the purified $CD4^+$ T-cells. Although is not illustrated within this schema, a positive control group including T-cells alone and αCD3/αCD28 dynabeads was included.

T= $CD4^+$ T-cell, M= monocyte, pM= α-δ-DEX pre-activated monocyte.

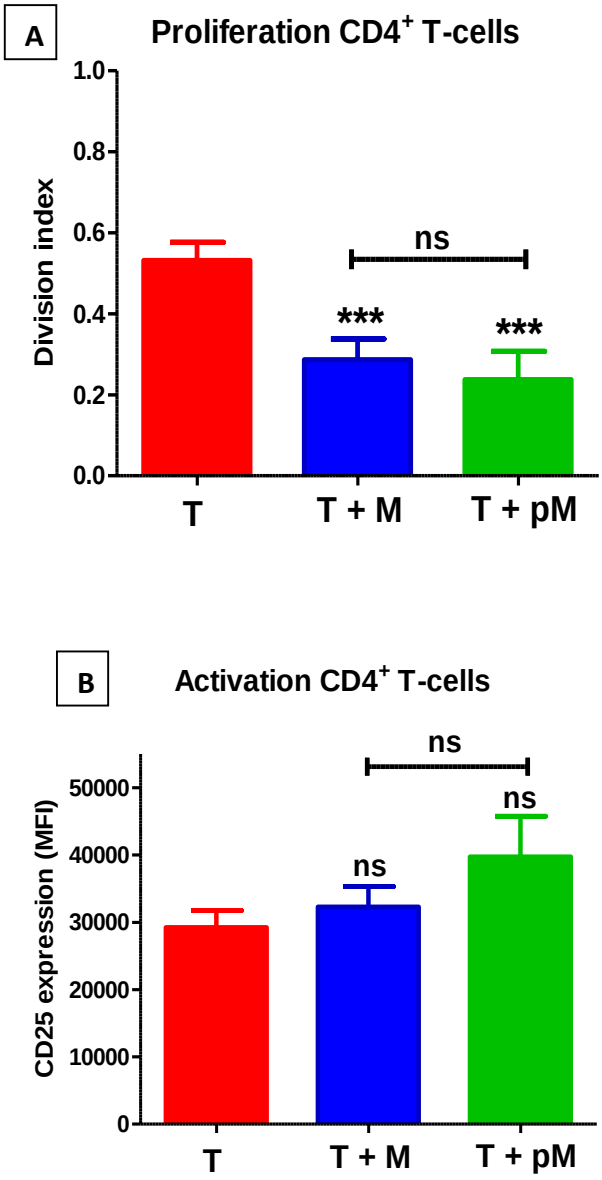

Figure 3.30: α-δ-DEX pre-activated monocytes do not suppress proliferation or activation of purified CD4⁺ T-cells.

A. Proliferation of enriched CD4⁺ T-cells, reported as division index. **B. Activation of enriched CD4⁺ T-cells**, expression of the CD25 marker as median fluorescence intensity (MFI). Bars represent means and SEM, n=7. Paired ANOVA, Bonferroni's Multiple Comparison Test; *$p \leq 0.05$, **$p \leq 0.01$, ***$p \leq 0.001$, ns= not significant.

Primary CD4⁺ T lymphocytes and monocytes were enriched by negative selection from PBMCs and all conditions were stimulated with αCD3/αCD28 dynabeads. In red, control group containing T-cells only. In blue, co-culture of T and non pre-activated monocytes. In green, co-culture of T and α-δ-DEX pre-activated monocytes.

T= CD4⁺ T-cell, M= monocyte, pM= α-δ-DEX pre-activated monocyte.

3.14 MONOCYTE DEPLETION REDUCES PROLIFERATION AND ACTIVATION BASELINE LEVELS IN THE *IN VITRO* MODEL

Although purified α-δ-DEX pre-activated B lymphocytes could exert T-cell suppression, because suppression could not be completely ablated by depletion of B-cells, we wanted to investigate whether other cells within the PBMC fraction might be involved in the suppression induced by α-δ-DEX. Monocytes are known to have suppressive properties, so we decided to further explore any possible role they might play. Although section 3.13 concluded that enriched $CD14^+$ monocytes failed to inhibit T-cell proliferation after 24 hour stimulation with α-δ-DEX, it was decided to reinforce this by performing a monocyte depletion experiment.

$CD14^+$ monocytes were depleted from the PBMC fraction using a positive selection protocol (section 2.2.2), achieving almost absolute monocyte removal (<1% $CD14^+$ cells left) (Figure 3.31-C) Whole PBMCs as well as the monocyte depletion fraction were stimulated with plate-bound αCD3, with or without α-δ-DEX (1 µg/ml) and incubated over 4 days.

In comparison with whole PBMCs, the positive control of the monocyte-depleted fraction stimulated with αCD3 alone shows a small drop in the proliferation and activation baseline levels of $CD4^+$ T-cells. This situation makes difficult to evaluate whether the α-δ-DEX-induced inhibition still occurs after monocyte removal (Figure 3.31). If individual donors and their patterns are considered we can then suggest that α-δ-DEX effect is not dependent on the presence of monocytes. However, more repeats are necessary to clarify the involvement of these cells.

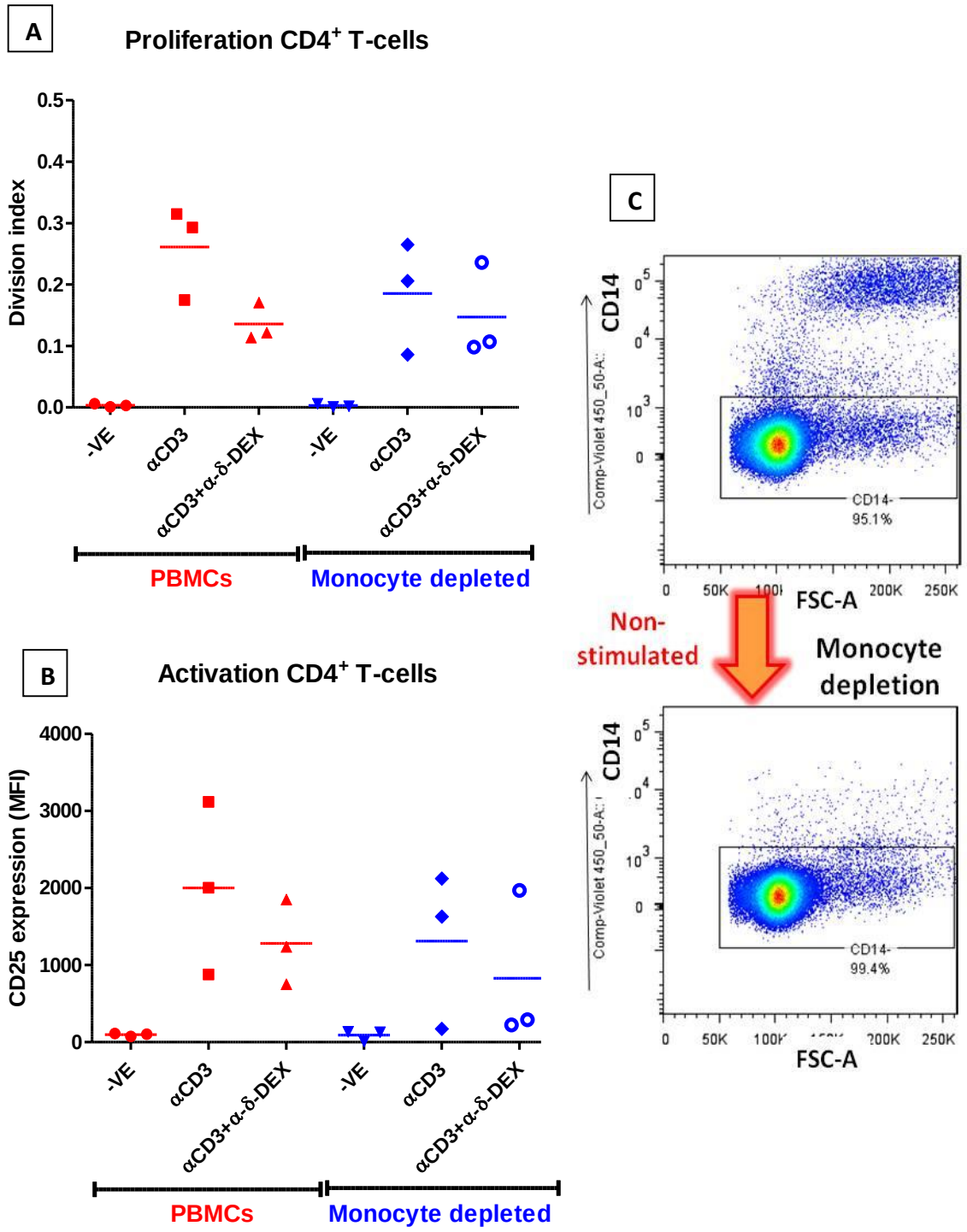

Figure 3.31: Monocyte depletion reduces proliferation and activation baseline levels in the *in vitro* model.

A. Proliferation CD4⁺ T-cells, reported as division index. **B. Activation CD4⁺ T-cells**, expression of the CD25 marker as median fluorescence intensity (MFI). **C. Representative dot plot example of the efficiency of the depletion protocol at day 4 non-stimulated cells;** x-axis FSC-A and y-axis CD14 (Pacific blue). Lines represent means, n=3.
Whole PBMCs (in red) and CD14⁺ monocyte-depleted PBMCs (in blue) were stimulated with αCD3 (plate-bound 0.3 µg/ml), with or without α-δ-DEX (1 µg/ml). Groups containing αCD3 only represent the positive control, whilst non-stimulated groups represent the negative control (-VE).

3.15 Depletion of NK Cells does Not Affect the Suppression Induced by α-δ-DEX

Searching for another candidate within the PBMC populations that could influence the activity of TI stimulated B lymphocytes, NK cells were next studied. Snapper & Mond (1996) reported that NK cells secrete IFN-γ and granulocyte-macrophage colony-stimulating factor (GM-CSF) that are essential for IgM secretion by α -δ-DEX activated B lymphocytes.

Similarly to the experiments performed in sections 3.9 and 3.14, $CD56^+$ NK cells were depleted from the PBMC fraction applying a positive selection procedure (section 2.2.2), allowing almost absolute NK removal (<1% $CD56^+$ cells left) (Figure 3.32-C). Whole PBMCs as well as the NK depletion fraction were stimulated with plate-bound αCD3, with or without α-δ-DEX (1 μg/ml) and incubated over 4 days.

From Figure 3.32 we can conclude that NK cells are not involved in the α-δ-DEX mechanism of action. Although the sample size is small, it was clear for the 3 individual donors that both proliferation and activation of $CD4^+$ T-cells were reduced if α-δ-DEX was present. As an incidental observation, it appears that removal of NK cells increases the baseline levels of T-cell division and CD25 expression after αCD3 stimulation.

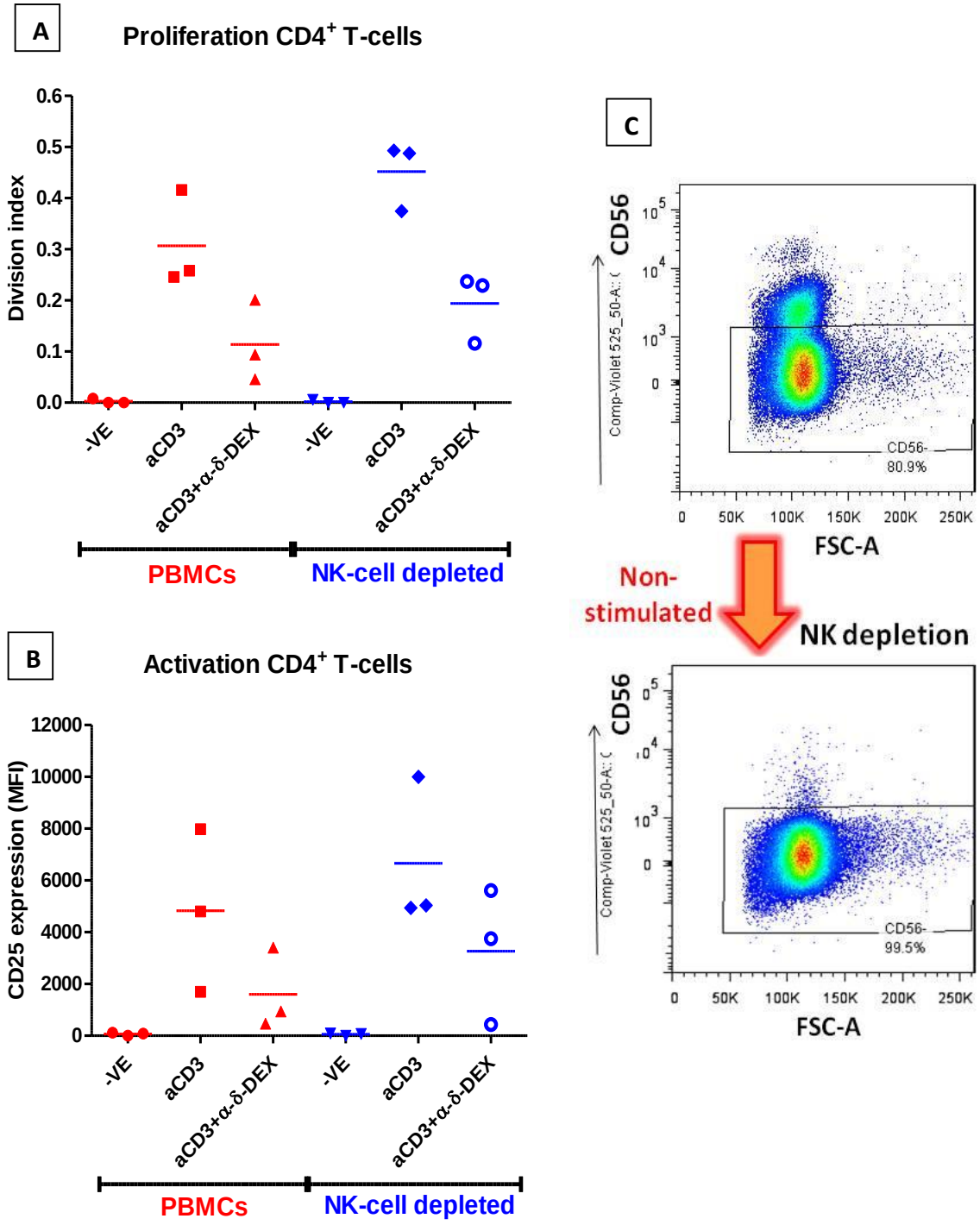

Figure 3.32: α-δ-DEX suppressive properties still occur after depletion of CD56⁺ NK cells.

A. Proliferation CD4⁺ T-cells, reported as division index. **B. Activation CD4⁺ T-cells**, expression of the CD25 marker as median fluorescence intensity (MFI). **C. Representative dot plot example of the efficiency of the depletion protocol at day 4 non-stimulated cells;** x-axis FSC-A and y-axis CD56 (Brilliant Violet 510). Lines represent means, n=3.
Whole PBMCs (in red) and CD56⁺ NK-cell depleted PBMCs (in blue) were stimulated with αCD3 (plate-bound 0.3 µg/ml) with or without α-δ-DEX (1 µg/ml). Groups containing αCD3 only represent the positive control, whilst non-stimulated groups represent the negative control (-VE).

3.16 DISCUSSION

Some antigens can induce antibody production without 'T cell help' and hence are called T-independent (TI) antigens (Mond et al. 1995) (section 1.1.5.2) Anti-IgD-conjugated dextran (α-δ-dex) and the truncated *Moraxella* IgD-binding protein (MID) are TI type II mimics that induce activation and proliferation of B lymphocytes by cross-linking of numerous B-cell receptor molecules in a similar manner to bacterial capsular polysaccharides (sections 1.1.5.2.1 and 3.1). α-δ-DEX consists on multivalent anti-IgD antibodies conjugated to a dextran molecule (Rehe et al. 1990; Brunswick et al. 1988); whilst MID consists of the IgD binding site (aminoacids 92-1200) of the outer membrane IgD-binding protein from the bacterium *Moraxella catarrhalis* (Nordström et al. 2006; Nordström et al. 2002).

It was previously observed in our lab that B-cell activation by these TI type 2 mimics resulted in inhibition of T-cell responses to TCR stimulation *in vitro* (J.B. Wing and R.A. Foster, unpublished data) (section 3.1). However, since the mechanism of action by which B lymphocytes could downregulate T lymphocytes had not been determined, the work presented in this chapter focused on assessing two main possibilities: a cell-contact dependent mechanism and the role of soluble factors.

This initial observation was corroborated, demonstrating that the TI type 2 mimic α-δ-DEX was effective in enhancing $CD19^+$ B-cell proliferation and activation but suppressing TCR-induced $CD4^+$ T-cell proliferation and activation within a PBMC culture (section 3.3). The same pattern was observed in the presence of MID, another TI type 2 mimic that was able to activate B lymphocytes while simultaneously inhibiting $CD4^+$ T lymphocytes (section 3.10.2). In this manner, we established that the phenomenon might be a general TI type 2 property rather than α-δ-DEX specific.

The B-cell molecules CD80 and CD86 (B7-1 and B7-2) can co-stimulate or downregulate T lymphocytes depending if they bind to the ligand CD28 or CTLA-4, respectively (section 1.1.4.3). In our assay, antibody blockade of CD80 and CD86 had no effect on the α-δ-DEX-mediated inhibition in 2 separate donors (section 3.4).

Whether IL-1 was involved in the mechanism of suppression was investigated because an increase in IL-1β production was demonstrated among the samples containing α-δ-DEX and αCD3 (section 3.1). However, this increase in IL-1 appears to be coincidental since IL-1 blocking using soluble IL-1RA had no impact on the suppressive effect of the B-cells (section 3.4).

IL-10 is by far the most pleiotropic anti-inflammatory cytokine because selectively inhibits the transcription factor NF-κβ (Driessler et al. 2004; Wang et al. 1995). IL-10 blocks production of pro-inflammatory cytokines and the expression of adhesion and co-stimulatory molecules on almost all cell types, reduces the antigen presenting capacity and promotes the development of T_H2 cells whilst blocking T_H1 polarisation (Asadullah et al. 2003; Moore et al. 2001). IL-10 is produced in high amounts by the immunomodulatory regulatory lymphocytic subsets Treg (Shevach 2009; McGeachy et al. 2005) and Breg (Bouaziz et al. 2010; Fillatreau et al. 2002). IL-10 is also secreted by effector lymphocytes, such as T helper T_H2 cells (section 1.1.2.1), B-effector 1 cells (section 1.1.3.1) and monocytes/macrophages (Asadullah et al. 2003). Of major relevance for this work is the well known property of IL-10 to suppress T-cell expansion by affecting secretion of IL-2, IFN-γ, IL-4 and IL-5 mainly (Taylor et al. 2006; Asadullah et al. 2003; Akdis & Blaser 1999). Taking all this into consideration, it was important to exclude IL-10 as the suppressive soluble factor in our α-δ-DEX *in vitro* model. In contrast to the negative effect on T lymphocytes, IL-10 promotes growth of B lymphocytes and function as a secondary signal to boost TI type 2 responses after BCR cross-linking. The Snapper group has demonstrated that T_H-derived IL-2, IL-3, IL-4, IL-5, IL-6, IL-10 and IFN-γ act as secondary signals to modulate Ig secretion after TI type 2 stimulation (Vos et al. 2000). If further TLR signaling occurs, this results in enhanced IL-10 secretion, extensive sustained B-cell proliferation and Ig class switching after BCR engagement (Liang et al. 2011; Bouaziz et al. 2010; Ruprecht & Lanzavecchia 2006). Under our experimental conditions, we concluded that IL-10 has, if any role at all, only a very minor role in the suppression induced by α-δ-DEX (section 3.5). There was a hint of partial reversal of the α-δ-DEX suppression of $CD4^+$ T-cell proliferation by blocking IL-10, but this was only significant at the middle of the three concentrations of αIL-10 mAb (10 μg/ml) used. However, no effect was observed in the expression of the T-cell activation marker, even with the higher concentration of αIL-10 mAb (20 μg/ml). These results suggest that IL-10 is not the responsible mechanism involved in the T-cell suppression and that its minor effect might come not from α-δ-DEX activated B-cells, but from naturally present Tregs, Bregs or accessory cells which produce IL-10 independently to the culture environment.

The next part of this chapter aimed to confirm that TI type 2 mimics induce a suppressive phenotype on IgD^+ B lymphocytes and that these cells are the ones which inhibit proliferation and activation of CD4+ T lymphocytes.

Experiments performed with purified $CD4^+$ T-cells showed that α-δ-DEX is unable of restraining αCD3/αCD28-induced proliferation and activation in the absence of other PBMCs (section 3.6). Since $CD4^+$ T lymphocytes lack IgD expression, they are not expected to respond in any way to the

presence of α-δ-DEX. Therefore, we can confidently reject any unspecific α-δ-DEX phenomenon on $CD4^+$ T lymphocytes.

During the last few years, several publications have provided evidence of an immunomodulatory role exerted by B lymphocytes, either upregulating or downregulating the intensity and quality of T-cell responses. In non pathological conditions, B-cells act as antigen presenting cells providing co-stimulation during TCR downstream activation, secreting cytokines to initiate T_H polarisation and reactivating memory T-cells (sections 1.1.3 and 1.1.4.3). Autoimmune disorders such as idiopathic thrombocytopenic purpura and systemic lupus erythamatosus are examples in which B lymphocytes activate and maintain T-cell responses even to self-antigens. In these diseases B-cell depletion with Rituximab (αCD20) was shown to be beneficial by decreasing the number of auto-reactive T-cells (producers of IL-4 and IFN-γ) whilst enhancing the number of Treg producers of IL-10 (Lund & Randall 2010). On the other hand, IL-10 producing B-cells (Bregs) act as a brake, suppressing effector T lymphocytes and promoting expansion of Tregs from naïve T-cells (Lund & Randall 2010; Fillatreau et al. 2002) (section 1.1.3.1).

One of the most relevant findings within this chapter is that addition of α-δ-DEX into a mixed PBMC culture induces a suppressive phenotype on B lymphocytes. After just 24 hour stimulation with α-δ-DEX, enriched $CD19^+/CD20^+$ B-cells are capable of restraining the proliferation of purified $CD4^+$ T-cells in co-culture (sections 3.7 and 3.8). In comparison with the enriched B lymphocytes that were not exposed to α-δ-DEX, TI type 2 activated B lymphocytes reduced the T-cell division index by a third. Unexpectedly, these pre-activated B lymphocytes failed to reduce the expression of the activation marker CD25 (discussed below). Of major importance is the fact that priming in a PBMC culture is essential, as addition of α-δ-DEX to a pure co-culture of B-cells and $CD4^+$ T-cells had no effect (sections 3.7). Indeed, this phenomenon suggests that accessory cells might be playing a role during the α-δ-DEX priming stage, perhaps by secreting cytokines or by cell-contact interactions. In contrast to the strong B-cell responses observed in PBMC cultures containing α-δ-DEX, these primed B lymphocytes had enhanced CD86 expression but did not proliferate (section 3.8), perhaps because 24 hours stimulation was not sufficient to trigger proliferation.

In relation to this, recent studies have explained that Bregs only become suppressive and secrete IL-10 after appropriate BCR engagement and secondary signals occur (Mauri & Bosma 2012). CD40-dependent cognate interactions (Yoshizaki et al. 2012; Blair et al. 2010; Fillatreau et al. 2002), the presence of IL-21 (Yoshizaki et al. 2012) and TLR activation (Yanaba et al. 2009) are examples of events which drive the generation of functional Bregs. Lampropoulou et al. (2008) demonstrated that B-cells are able to produce IL-10 and suppress $CD4^+$ T-cells after TLR-4 and

TLR-9 engagement with LPS and CpG, respectively; and that the degree of suppression was proportional to the exposure time and the concentration of the TLR agonists. Moreover, it was found that the resultant MyD88 signalling in B-cells appears to block MyD88 activation in T lymphocytes, limiting T-cell proliferation and differentiation into T_H1 and T_H17 cells in a mouse model of autoimmune encephalomyelitis (Lampropoulou et al. 2008). Thus, it might be possible that α-δ-DEX-activated B lymphocytes are receiving a secondary signal from other PBMCs present at the pre-activation stage, which in turn triggers a suppressive phenotype in B-cells.

A transfer experiment clearly demonstrated that the supernatant from 24 hour α-δ-DEX-stimulated PBMCs does not reduce proliferation or activation of enriched $CD4^+$ T-cells (section 3.8). Based on this finding, along with those in section 3.5 it is unlikely that IL-10 or any other inhibitory soluble molecules are essential for the α-δ-DEX suppression mechanism. These findings fitted with the hypothesis that cell-cell contact was required for the α-δ-DEX-mediated suppression.

A similar work to ours is the one published by (Tretter et al. 2008), which showed that large highly activated $CD25^+$ B cells stimulated with *S. aureus* Cowan I antigen (polyclonal activation) are able to inhibit proliferation of pure $CD4^+$ T-cells *in vitro via* induction of long-lasting cell division arrest and apoptosis. Although we found no evidence of T-cell apoptosis (James B. Wing, unpublished data) and expression of activation markers was also affected in the phenomena we have described in this chapter, our results are consistent with those of Tretter et al. (2008) in that constant presence and cell-contact between T and pre-activated B-cells is required to achieve suppression.

The possibility of B-cells inducing a suppressive T-cell phenotype within the PBMC culture was also addressed. Tregs constitute an effector T_H subset that can deeply suppress other effector T-cells (section 1.1.2.1). Tregs mediate suppression by secretion of anti-inflammatory cytokines (IL-10, TGF-β, IL-35), by repression of IL-2, IL-4 and IFN-γ, by cell cycle arrest or by cytolisis (Shevach 2009; Sakaguchi et al. 2008; Taylor et al. 2006). Allogeneic CD40-activated B-cells can generate human Tregs ($CD4^+$ $CD25^+$ $FoxP_3^+$ $CD45RO^+$ $CCR7^-$) from a naïve $CD4^+$ $CD25^-$ T-cell population (Tu et al. 2008). Chen et al. (2009) demonstrates that is possible to expand suppressive $FoxP3^+$ T-cells using allogeneic B-cells in co-culture, at a B-to-T cell ratio of 4:1 and adding co-stimulation with αCD28 + IL-2. Work performed in our laboratory indicated that an increase in FoxP3 expression by T-cells occurs in our α-δ-DEX model from 48 hours post-stimulation onwards. However, we concluded that induction of Tregs is not the primary mechanism of suppression, as depletion of these cells had no impact on the suppressive action of α-δ-DEX (James B. Wing, unpublished data).

To further confirm whether B lymphocytes were the only cell population able to directly suppress T-cells, the same α-δ-DEX pre-activation experiment was performed with enriched $CD14^+$ monocytes. Three monocyte subsets have been identified, each one differing in their cytokine profile and the migration/homing pattern. $CD14^{++}CD16^-$ are termed classical monocytes and account for 90% of all monocytes. The other 10% are $CD14^+CD16^+$ monocytes which can be further divided into intermediate ($CD14^{++}CD16^+$) and non-classical ($CD14^+CD16^{++}$), both secreting more TNF-α and less IL-10 as compared with the classical subset (Ziegler-Heitbrock et al. 2010; Ziegler-Heitbrock 2007; Geissmann et al. 2003). Thus, $CD14^+$ $CD16^+$ monocytes have been associated with autoimmune diseases and severe bacterial infections, such as sepsis (Ziegler-Heitbrock 2007; Fingerle et al. 1993). Like B-cells, monocytes express vesicles with MHCII molecules and present antigens to T lymphocytes (Bunbury et al. 2009).

Under the same experimental conditions as the above mentioned B-cell pre-activation experiment, purified $CD14^+$ monocytes which were exposed for 24 hours to α-δ-DEX failed to further reduce proliferation of purified $CD4^+$ T-cells as compared with the monocytes that were not exposed to the TI mimic (section 3.13). Thus, the initial hypothesis that α-δ-DEX generates a suppressive phenotype exclusively on B-cells was supported.

An unanticipated finding among this set of pre-activation experiments (sections 3.8 and 3.13) was the fact that enriched $CD19^+/CD20^+$ B lymphocytes and $CD14^+$ monocytes reduced the proliferation baseline of purified $CD4^+$ T-cells, even though they were not exposed to α-δ-DEX or any other stimulant. It is actually difficult to understand this phenomenon but might be related to exogenous conditions unrelated to the assay itself. An explanation could be that their inherent inhibitory properties become evident if taken out from their PBMC environment, in the absence of accessory cells which might normally prevent such phenotype. In the case of B-cells this is more likely due to the presence of naturally peripheral suppressive B lymphocytes which became activated under our T-B co-culture conditions. As mentioned above, Bregs circulate in blood without much activity in healthy individuals; however several stimuli or secondary signals can trigger their suppressive function (Mauri & Bosma 2012). It has been also reported that monocytes can modulate T-cells and polarise towards an anti-inflammatory lineage. For example, naïve blood $CD11b^+$ $Ly6G^-$ monocytes suppress $CD4^+/CD8^+$ T-cell proliferation induced by peptide presentation or by αCD3/αCD28 stimulation, *via* a cell contact mechanism (Slaney et al. 2011). Similarly, myeloid-derived suppressor cells which resemble inflammatory monocytes restrain antigen-driven T-cell responses by production of nitric oxide (Movahedi et al. 2008). Binding of CD83 (a glycoprotein found on activated T and B lymphocytes) to a putative CD83 receptor expressed on monocytes, initiates prostaglandin E2 secretion which in turn decreases T-cell proliferation and

production of IL-2 and IFN-γ upon αCD3/αCD28 stimulation in a PBMC culture (Chen et al. 2011). Indeed, several suppressive mechanisms could have become activated in purified B-cells or monocytes that may justify the drop in T-cell proliferation in the absence of α-δ-DEX. Although the three purified populations were obtained as untouched cells by negative selection and without using columns (section 2.2.1), one remote possibility is that the physical stress during the enrichment procedure affects how B-cells and monocytes function in co-culture with $CD4^+$ T-cells.

Another point to consider in these purification experiments is that in contrast to the assay performed with PBMCs in which both T-cell proliferation and activation were dampened, the inhibitory effect of enriched α-δ-DEX pre-activated $CD19^+/CD20^+$ B lymphocytes was only evident at the proliferation parameter. We initially attributed this finding to the experimental design, as purified $CD4^+$ T lymphocytes were activated with αCD3/αCD28 dynabeads from one day prior addition of the pre-activated B lymphocytes and so it was thought the activation signaling cascade and expression of CD25 was unstoppable (sections 3.7 and 3.8). However, this hypothesis was disproved by a subsequent experiment which showed that even when αCD3/αCD28 beads and α-δ-DEX pre-activated B-cells are put in co-culture with T-cells on the same day, the expression of CD25 does not become downregulated. Moreover, there is a tendency for upregulation on this activation marker (section 3.12). Therefore, it is likely that 24 hour α-δ-DEX-activated B lymphocytes are only able to directly restrain T-cell proliferation while the repression on activation occurs as a secondary phenomenon driven by other PBMCs in culture. Guy et al. (2013) elucidates that even though T-cell proliferation and cytokine production are both initiated as a consequence of CD3 signalling after phosphorylation of ITAMs (section 1.1.4.4), T-cell activation can occur without proliferation. Guy et al. (2013) establishes that initiation of activation starts with as few as 2 or 3 functional phosphorylated ITAMS. In contrast, proliferation requires around 10 ITAMS to activate the Notch pathway and c-Myc, which ultimately leads to a more complex cascade of cytoskeleton modifications. Alternatively it might be the case that B-cells require constant α-δ-DEX stimulation to downregulate the expression of T-cell activation markers and thus the presence of the TI type 2 mimic for only 24 hours was not sufficient. In support of this hypothesis, we observed that the amount of the B-cell activation marker CD86 expressed on enriched pre-activated cells is less than half in comparison with the amount detected on B lymphocytes that were stimulated with α-δ-DEX for 4 days in a whole PBMC culture (sections 3.3 and section 3.8).

Contrary to expectations, depletion of $CD19^+$ $CD20^+$ B lymphocytes did not prevent T-cell suppression from occurring. Addition of α-δ-DEX or MID to both whole PBMCs and B-cell depleted PBMCs resulted in a significant reduction of $CD4^+$ T-cell proliferation and activation (sections 3.9.1

and 3.9.2). However, a further analysis on these experiments found that a larger % of α-δ-DEX-induced suppression occurs when B-cells are present than when they are removed from PBMCs (section 3.9.1). Due to this unexpected observation, we assessed whether our B-cell depletion protocol was efficient enough to remove all $CD19^+/20^+$ B lymphocytes which express surface IgD. By performing a simultaneous CD19-CD20-IgD staining on day 0 and day 4 after the B-cell depletion protocol it was possible to confirm its efficacy because no more than 0.1% positive events for CD19, CD20 or IgD were detected (section 3.10).

A titration experiment using enriched $CD4^+$ T-cells and α-δ-DEX pre-activated B-cells at low ratios T-to-B cells (from 6:1 down to 486:1), showed that the suppression of T-cell proliferation is dependent on the ratio T-to-B lymphocytes. A maximal inhibitory effect is observed when more B-cells are included into the co-culture (ratio 1:6), while the effect disappears at ratios of around 18:1 to 54:1 (section 3.13). In this respect, the suppressive effect of these suppressor B lymphocytes might be more obvious as we increased the number of B-cells per T-cell. Blair et al. (2010) observed that Bregs ($CD19^+$ $CD24^{hi}$ $CD38^{hi}$) inhibit TNF-α and IFN-γ production from $CD4^+$T cells in a ratio dose dependent fashion. In similar *in vitro* settings to the ones used in this chapter, Blair et al. (2010) detected an inhibitory effect only in ratios between 1:1 and 4:1 T-to-Breg. In support, the same ratio of 4:1 PBMC-to-Breg was found to reduce the percentage of $CD8^+$ T-cells producers of IFN-γ during chronic hepatitis B infection (Das et al. 2012). Thus, our α-δ-DEX pre-activated B lymphocytes might be even more powerful in dampening T lymphocytes than these characterised Bregs.

Monocyte and NK depletion experiments were also performed due to the possible involvement of accessory cells in helping α-δ-DEX pre-activated B lymphocytes to develop a regulatory function. The monocyte depletion assay also aimed to exclude any remote chances of undesired effects on monocytes, perhaps through the dextran molecule, through Fc receptor interaction or by a contaminant contained within the α-δ-DEX preparation. Although the results obtained from this experiment do not suggest that α-δ-DEX mediated suppression is dependent on the presence of monocytes (section 3.14), this assumption should be re-confirmed with a larger sample size. Especially because in our *in vitro* settings, removal of monocytes will result in a lack of co-stimulation *via* IL-6 or CD80/CD86 molecules that may indirectly reduce the baseline of αCD3-induced T-cell proliferation and activation (Jenkins et al. 1991; Baroja et al. 1988). On the other hand, several regulatory functions have been attributed to NK cells either promoting or inhibiting T-cell responses and regulating antibody production, in particular during autoimmune disorders related to autoreactive T-cells or auto-antibodies (Lünemann et al. 2009; Liu et al. 2006; Shi et al. 2000). Moreover, IFN-γ and GM-CSF secreted by NK cells have been recognised as important

soluble factors to stimulate IgM and IgG secretion from α-δ-DEX activated B lymphocytes (Snapper & Mond 1996). In this chapter, an NK depletion assay was conclusive in showing that NK cells are not necessary to achieve α-δ-DEX-dependent inhibition on $CD4^+$ T-cells (section 3.15).

In summary, even though we were unable to explain the mechanism of action by which TI type 2 mimics α-δ-DEX and MID downregulate CD3/CD28-induced $CD4^+$ T-cell responses, we discovered that α-δ-DEX acts on B lymphocytes triggering an immunomodulatory phenotype. Soluble factors contained in supernatants, such as IL-10 are not responsible for the suppressive effect and cell-contact between $CD4^+$ T-cells and α-δ-DEX pre-activated B-cells is essential. Since these B lymphocytes only become suppressive after α-δ-DEX pre-activation in the presence of PBMCs, it is possible that accessory cells are involved in providing secondary signals to initiate a regulatory B-cell phenotype. Monocytes and NK cells do not appear to drive directly the α-δ-DEX inhibitory effect, but they do influence the baseline levels of T-cell proliferation and activation in this *in vitro* assay. Overall, our findings suggest that this suppressive α-δ-DEX phenomenon is complex and is influenced by the ratio T-to-B lymphocytes in co-culture. Moreover, the degree of the suppression varies among individual donors and seems to depend on the amount of B-cell activation induced by the TI type 2mimic. Unsolved until now was the unexpected observation in which addition of α-δ-DEX to B-cell depleted PBMC still resulted in a moderate inhibition of T-cell responses, regardless of almost absolute removal of all $CD19^+/CD20^+/IgD^+$ cells. Clearly, suppression can be mediated in some donors at quite low ratios of B cells to T cells and although our depletion appeared to remove almost all B cells expressing IgD, it is possible perhaps that a few residual cells (not detected by our FACS CD19 antibody) were the effector cells. As compared with the purified α-δ-DEX pre-activated B-cells that were stimulated for only one day, the few contaminating B cells left after the depletion and which stayed in culture for 4 days in the presence of α-δ-DEX might have expanded up slightly and exerted the residual suppressive effect.

CHAPTER 4:

N. MENINGITIDIS AND ITS OUTER MEMBRANE VESICLES SUPPRESS TCR-INDUCED T-CELL PROLIFERATION AND ACTIVATION, BUT ENHANCES T_H1 CYTOKINES AND IL-10 PRODUCTION

4.1 INTRODUCTION

As reviewed in section 1.1.5.2, T-independent (TI) antigens are those which fail to associate with MHC II molecules but are capable of inducing antibody production by cross-linking the B-cell receptor (BCR) in the absence of T-cell 'help'. Bacterial capsular polysaccharides are examples of TI type 2 antigens because they contain highly repetitive epitopes that interact simultaneously with a large number of surface immunoglobulins on B lymphocytes (Vos et al. 2000; Mond et al. 1995).

As reported in the literature, *N. meningitidis* survives in humans by evading immune responses (section 1.2.5). For example, avoids immune recognition and lysis through sialylation of lipooligosaccharides (Unkmeir, Kämmerer, et al. 2002; Estabrook et al. 1997), overcome the action of bactericidal lysosomes by preventing phagosomal maturation (Ayala et al. 1998) and induces phase variable genes to increase virulence and survival at the colonisation site (Buckee et al. 2008). In particular, the meningococcus capsule limits the adhesion with phagocytic cells and impairs complement-mediated killing by blocking antibody binding and complement deposition (Unkmeir, Kämmerer, et al. 2002; McNeil and Virji, 1997, Read et al., 1996).

The capsule from *N. meningitidis* consists of repeating carbohydrate moieties, so contains multiple identical antigenic epitopes. During natural infection, polysaccharides from this encapsulated bacterium will ligate the BCR and TLRs on B-cells, launching a TI response in addition to cytokine production from the innate immune system (Brunswick et al. 1988; Snapper & Mond 1996). Capsular polysaccharides are recognised *via* TLR-2 and TLR-4/MD-2 pathway (Zughaier 2011), providing positive downstream signalling to B-cells and other antigen presenting cells. However, a parallel downregulatory role has been identified for the *N. meningitidis* capsule. In comparison with capsule-deficient meningococci, capsulated serogroups (A, B and C) generated a weaker IL-6, IL-8 and TNF-α cytokine secretion by dendritic cells (Unkmeir, Kämmerer, et al. 2002, Giardina et al. 2001) and monocytes (Kocabas et al. 2007).

The B-cell response towards TI type 2 antigens benefits from a secondary signal (Vos et al. 2000), indeed other immunogenic components such as lipooligosaccharides (LOS) could provide this extra boost (Snapper & Mond 1996). LOS constitutes 50% of the meningococcal outer membrane but large concentrations are also secreted into the host inside vesicles (section 1.2.4.2). LOS is a major stimulus for inflammation and is responsible for the severity in septicaemia (Brandtzaeg et al. 1989) by producing large quantities of pro-inflammatory cytokines such as IL-1β, IL-6, IL-8 and TNF-α (Kolb-Mäurer et al. 2001; Unkmeir, Kämmerer, et al. 2002; Hellerud et al. 2008). LOS has a

1000-fold greater bioactivity for TLR-4 than capsular polysaccharides (Zughaier 2011) and its recognition occurs *via* the complex CD14 TLR-4/MD-2 which leads to downstream NFκβ activation (Zughaier et al. 2004; Calvano et al. 2003; Pridmore et al. 2003; Pridmore et al. 2001).

In addition to the capsule and LOS, other *Neisseria* components can enhance a TI type 2 response by providing second signal through TLRs present on APCs such as dendritic cells or monocytes, which in turn induce activation on other immune cells like lymphocytes. Using a LOS deficient meningococci strain, Sprong et al. (2001) demonstrated that non-LOS bacterial components from the outer membrane layer also induce a substantial secretion of pro-inflammatory cytokines IL-1β, TNF-α and mainly IFN-γ.

Neisseria outer membrane vesicles (OMVs) are blebs from the outer membrane, which contain mainly LOS and all the associated proteins from this layer (section 1.2.4.6). OMVs have been recognised as important immunogenic complexes and its use has been successful in the development of effective vaccines against *N. meningitidis* serogroup B (Holst et al. 2009; Giuliani et al. 2006) (section 1.2.3). For example, the novel Bexsero vaccine which is immunogenic both in adults and infants, combines OMVs with the highly immunogenic conserved surface proteins factor H binding protein (fHbp), *Neisseria* adhesin A (NadA) and *Neisseria* heparin binding antigen (NHBA) (Serruto et al. 2012). PorB is another outer membrane protein (section 1.2.4.5) which also stimulates antibody production by binding to the TLR-2/TLR-1 complex, triggering B-cell activation *via* MyD88 signalling, increasing IL-8 secretion and up-regulating expression of CD86 and MHC II molecules (Massari et al. 2006; Massari et al. 2002; Snapper et al. 1997).

We have demonstrated in Chapter 3 that TI type 2 mimics (α-δ-DEX and MID) suppress proliferation and activation of $CD4^+$ T lymphocytes whilst inducing B-cell proliferation and activation. Since some bacterial constituents are TI type 2 antigens and/or provide second signals to B-cells *via* TLR, we have hypothesized that exposure of PBMCs to paraformaldehyde fixed *N. meningitidis* could have a similar inhibitory effect.

To our knowledge, the colony opacity-associated adhesin (Opa) (section 1.2.4.4) is the only neisserial outer membrane protein that has been linked to suppression of T lymphocytes. Gray-Owen's research group has published that binding of Opa proteins to the cellular receptor CEACAM1 (carcinoembryonic antigen-related cell adhesion molecule) present on T-cells, results in a restrained proliferation and activation (Sadarangani et al. 2011; Gray-Owen & Blumberg 2006). However, this data is considered conflicting by others who believe the suppression by meningococci is only transitory and not exclusive on the Opa-CEACAM interaction (Youssef et al. 2009). In addition, recent work has shown that exposure of dendritic cells to *N. gonorrhoeae*

ablates the ability of these APCs to induce proliferation on T lymphocytes in co-culture (Zhu et al. 2012).

4.2 GENERAL METHODOLOGY

Within this chapter, the same general methodology described in Chapter 3 was applied. First, a buffy coat layer was obtained from fresh heparinised blood by density centrifugation (section 2.1). PBMCs were then washed, resuspended in RPMI media supplemented with 20% autologous plasma and stained with the proliferation dye CFSE (section 2.4). Ultimately, PBMCs were counted and added to 48-well plates at a density of $1x10^6$ cells per well in a final volume of 500 µl RPMI media supplemented with 20% autologous plasma.

T-cells were stimulated with 0.1-0.3 µg/ml plate-bound αCD3 (section 2.3.1.1) or with αCD3/αCD28 dynabeads (section 2.3.1.4) in the case of purified $CD4^+$ T-cells. The negative control for all experiments consisted of PBMCs in the absence of stimuli, whereas the positive control was represented by the sample containing T-cell activators (αCD3 or αCD3/αCD28 dynabeads). In addition to T-cell triggers, cells were exposed to different ratios of paraformaldehyde fixed *N. meningitidis:* 0.1:1, 1:1, 10:1 and 100:1 bacteria per cell.

Cell cultures were incubated at 37°C and 5% CO_2 in a humidified atmosphere for 4 days before harvesting. Extracellular immunofluorescence staining for flow cytometric analysis was performed by incubating $1x10^6$ PBMCs with the relevant antibodies (section 2.5.2).

A sequential gating strategy selected for the relevant T or B lymphocyte populations and excluded dead cells and monocytes (section 2.5.5). Like in chapter 3 (section 3.2), cell proliferation was assessed by the division index obtained from the CFSE dilution method; whilst T and B-cell activation were reported as median fluorescence intensity (MFI) of the surface markers CD25 and CD86, respectively.

Using this assay, different wild type bacterial strains, mutants and derived components (section 2.8) were studied in each of the subsections along this chapter.

Figure 4.1 describes a general overview of the experimental steps.

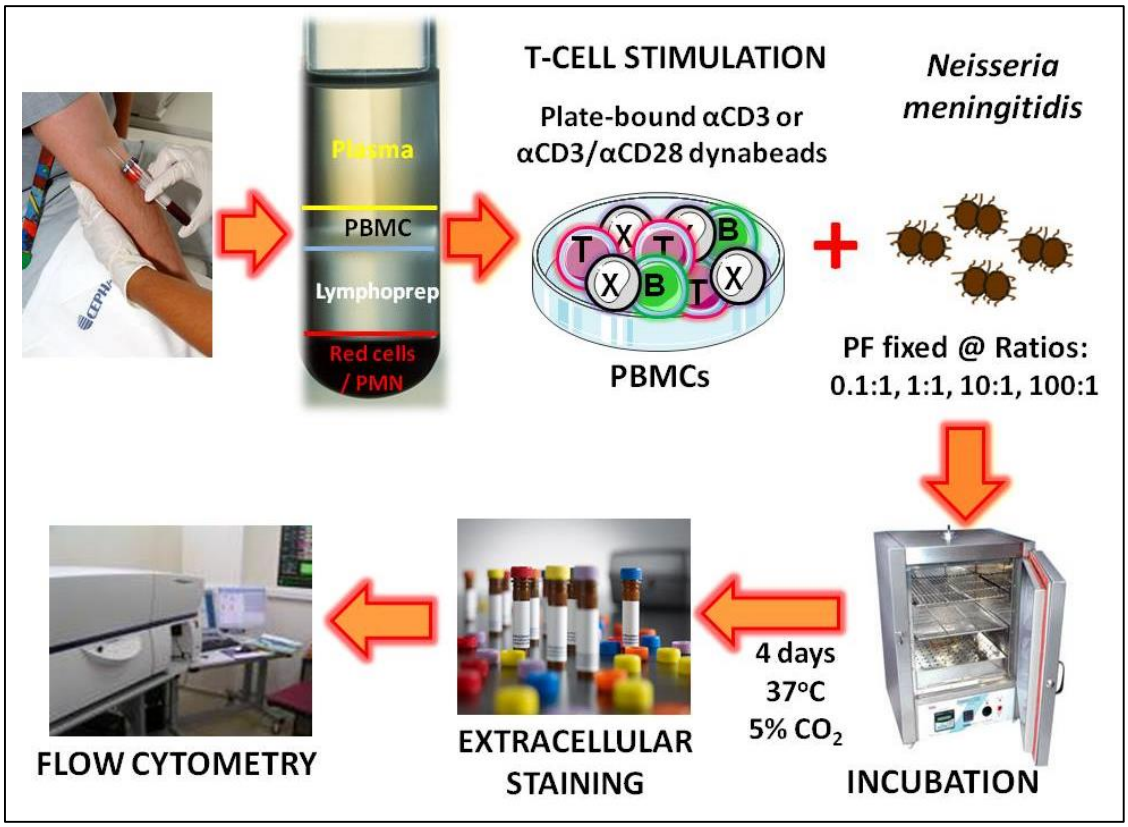

Figure 4.1: Overview of the experimental methodology applied in Chapter 4.

Human PBMCs were isolated from fresh peripheral blood using Lymphoprep™ density gradient centrifugation. T-cell stimulation was achieved with αCD3 or αCD3 + αCD28 coated dynabeads. Simultaneously, cells were exposed to paraformaldehyde (PF) fixed *N. meningitidis* at different ratios bacteria per cell: 0.1:1, 1:1, 10:1 and 100:1. Cells were plated and incubated for 96 hours at 37°C and 5% CO_2. Finally, samples were stained with the desired fluorescently-labeled antibodies and analysed by flow cytometry.

4.3 SMALL INOCULA OF WILD TYPE *N. MENINGITIDIS* SUPPRESS T-CELL PROLIFERATION AND ACTIVATION WITHOUT ACTIVATING B-CELLS

4.3.1 Small inocula of *N. meningitidis* suppress T-cell proliferation and activation.

In Chapter 3, we demonstrated how TI- type II mimics are capable of suppressing T-cell responses. Since bacterial polysaccharides are TI-type II antigens (sections 1.1.5.2 and 4.1), we hypothesized that exposure of PBMCs to paraformaldehyde fixed *N. meningitidis* could have a similar inhibitory effect.

To address this question we performed a simple experiment incubating PBMCs with plate-bound αCD3 (T-cell stimulator), in the presence or absence of wild type *N. meningitidis* (strain MC58) and at different ratios of bacteria per cell: 1:1, 10:1 and 100:1 (section 2.8.1). A sample containing αCD3 plus α-δ-DEX was also included in this experiment to compare the degree of suppression observed with TI-type II mimics.

Figure 4.2-A shows how the smallest ratio bacteria per cell (1:1) resulted in profound inhibition of $CD4^+$ T-cell division when compared with the group containing αCD3 alone, in which T-cells proliferated normally *via* TCR cross-linking. Similarly, a significant 50% reduction of division index was found with the next inoculum 10:1 bacteria per cell. In contrast, the highest bacterial count (100:1) failed to affect T-cell proliferation as no significant difference was detected against the αCD3 positive control.

Expression of the activation marker CD25 followed the same suppressive trend (Figure 4.2-B). In relation to the αCD3 control group, T-cell activation declined after exposure to low bacterial counts (1:1 and 10:1). Again, expression of CD25 seemed to be restored with the largest ratio of 100:1 bacteria per cell.

From the data in Figure 4.2 it is clear that the presence of wild type *N. meningitidis* at 1:1 and 10:1 ratios resulted in a dramatic reduction of $CD4^+$ T-cell proliferation and activation, just like the one induced by α-δ-DEX. Moreover, the smallest bacterial count 1:1 had a significantly greater effect than α-δ-DEX on restraining cell division (Figure 4.2-A).

To establish if *N. meningitidis* had a stimulatory TI- type II effect, proliferation and activation of $CD19^+$ B-cells were examined. Figure 4.3-A, illustrates clearly how small numbers of meningococci

(1:1 and 10:1 ratios) are incapable of enhancing the division index of B lymphocytes. However, the largest bacterial inoculum (100:1) intensified B-cell proliferation to a similar extent as α-δ-DEX.

Expression of the B-cell activation marker was not induced by bacterial ratios of 1:1 and 10:1 (Figure 4.3-B). A mild but significant increase of CD86 expression was detected with the largest meningococcal inoculum (100:1), although this activation was not as powerful as the one achieved with α-δ-DEX.

Histograms illustrating T and B cell responses following incubation with αCD3 with different ratios of *N. meningitidis* can be seen in Figure 4.4.

In summary, these findings suggest that the $CD4^+$ T-cell suppression observed in the presence of low numbers of fixed wild type *N. meningitidis* is unlikely to be related to an enhanced B-cell activity, as seems the case for the TI-type II mimics.

4.3.2 *N. meningitidis* and α-δ-DEX suppressive effects do not appear to be synergistic.

An experiment combining *N. meningitidis* and α-δ-DEX was designed to further confirm lack of enhancement of proliferation and activation of B lymphocytes, and to address possible synergism between them.

During 96 hours, PBMCs were stimulated with αCD3 plus either α-δ-DEX (1 μg/ml), meningococci (ratio 1:1 bacteria per cell) or both.

From Figure 4.5 (A and B) is evident that combination of α-δ-DEX and meningococcus is not synergistic in decreasing T-cell proliferation or activation than each individually, but it can be concluded that *N. meningitidis* and α-δ-DEX were at a maximal inhibitory level at the concentrations used.

In support of the conclusions made from the data shown in Figure 4.3, the combination of both stimuli did not result in more B-cell proliferation or activation than the group containing only α-δ-DEX (Figure 4.5-C and D). As previously shown, bacteria failed to trigger responses on B lymphocytes.

Although it is clear that bacteria do not induce B-cell responses, another experiment using suboptimal amounts of meningococci (ratios $\underline{\geq}$ 10:1) and of the TI mimic (reducing the concentration by half), could address whether a synergistic suppression exists between them.

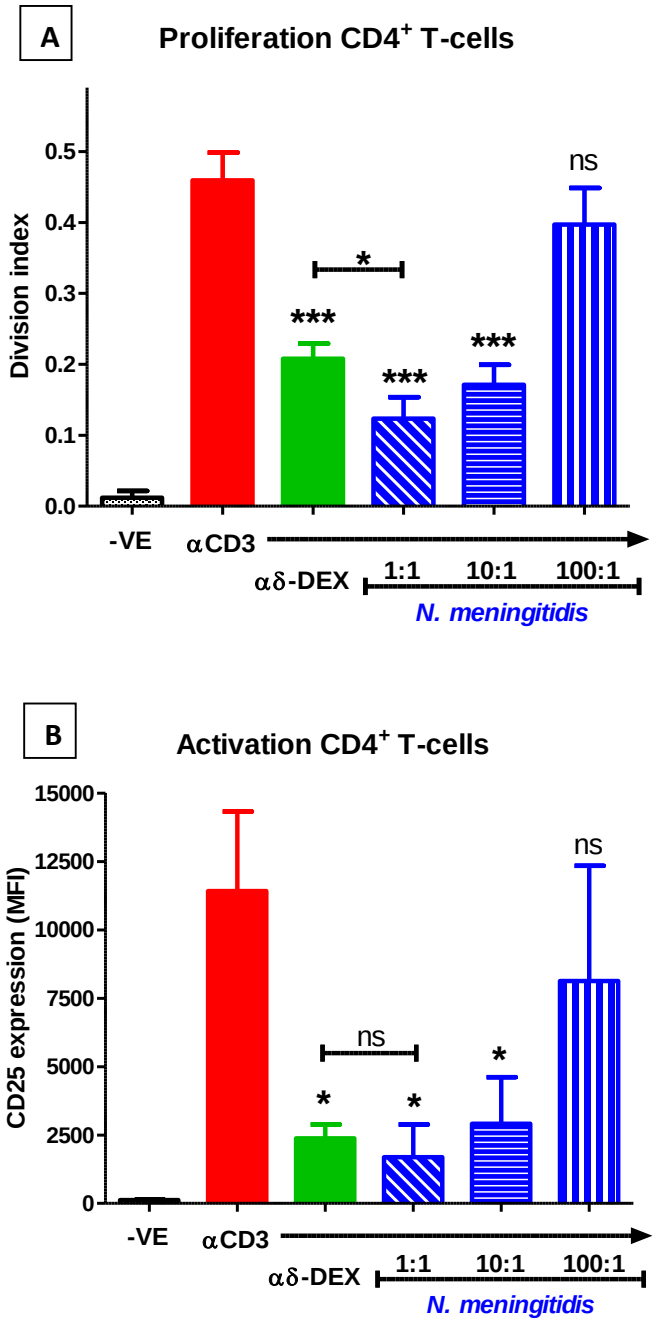

Figure 4.2: CD4⁺ T-cell proliferation and activation by TCR stimulation is suppressed by small inocula of fixed wild type *N. meningitidis.*

A. Proliferation CD4⁺ T-cells, reported as division index. **B. Activation CD4⁺ T-cells**, expression of the CD25 marker as median fluorescence intensity (MFI). Bars represent means and SEM, n=≥6. Paired ANOVA, Dunnett's Multiple Comparison Test (*vs.* αCD3) and paired student *t*-test (α-δ-DEX *vs.N. meningitidis* 1:1). **p*= 0.01-0.05, ***p*= 0.001-0.01, ****p*= ≤0.001, ns= not significant.

-VE= negative control, non-stimulated PBMCs (black bar). αCD3= T-cell stimulation (plate-bound 0.1 µg/ml). *N. meningitidis*= PF fixed, ratios 1:1, 10:1 and 100:1 bacteria per cell (blue bars). α-δ-DEX= B-cell stimulation (1 µg/ml).

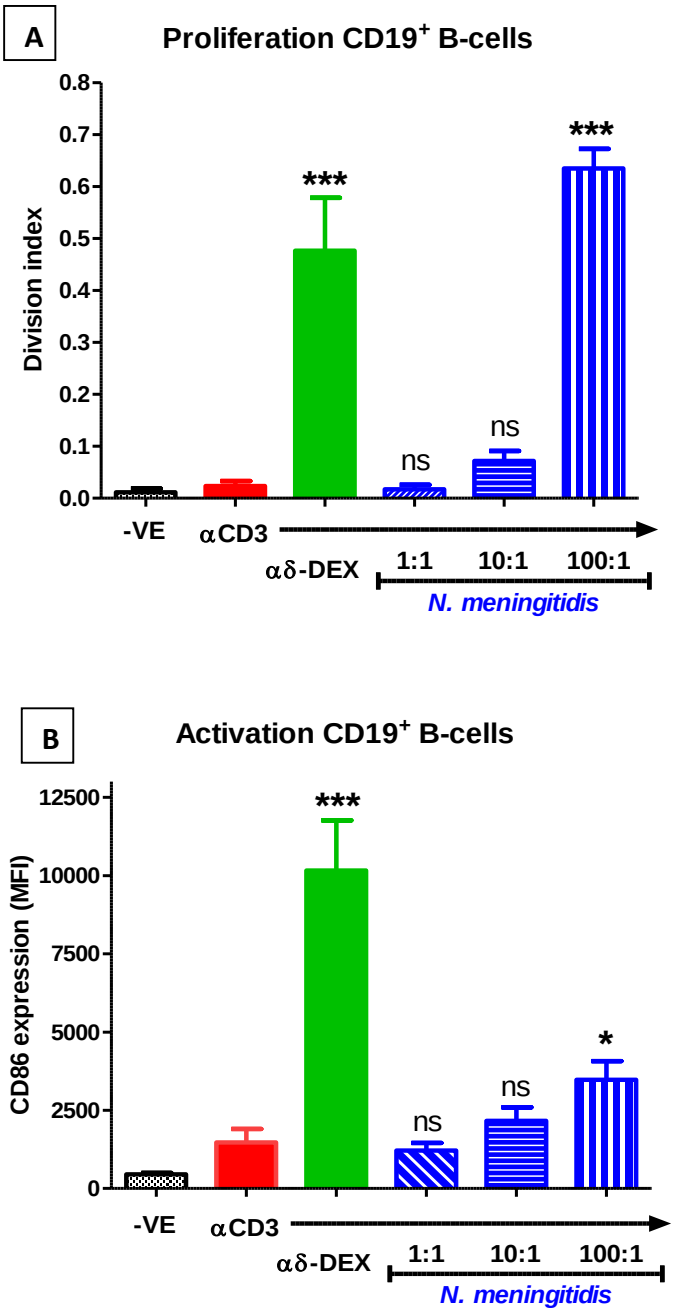

Figure 4.3: Small inocula of wild type *N. meningitidis* do not induce CD19⁺ B-cell proliferation or activation.

A. Proliferation CD19⁺ B-cells, reported as division index. **B. Activation CD19⁺ B-cells**, expression of the CD86 marker as median fluorescence intensity (MFI). Bars represent means and SEM, n=≥6. Paired ANOVA, Dunnett's Multiple Comparison Test (*vs.* αCD3). *p= 0.01-0.05, **p= 0.001-0.01, ***p= ≤0.001, ns= not significant.

-VE= negative control, non-stimulated PBMCs (black bar). αCD3= T-cell stimulation (plate-bound 0.1 µg/ml). *N. meningitidis*= PF fixed, ratios 1:1, 10:1 and 100:1 bacteria per cell (blue bars). α-δ-DEX= B-cell stimulation (1 µg/ml).

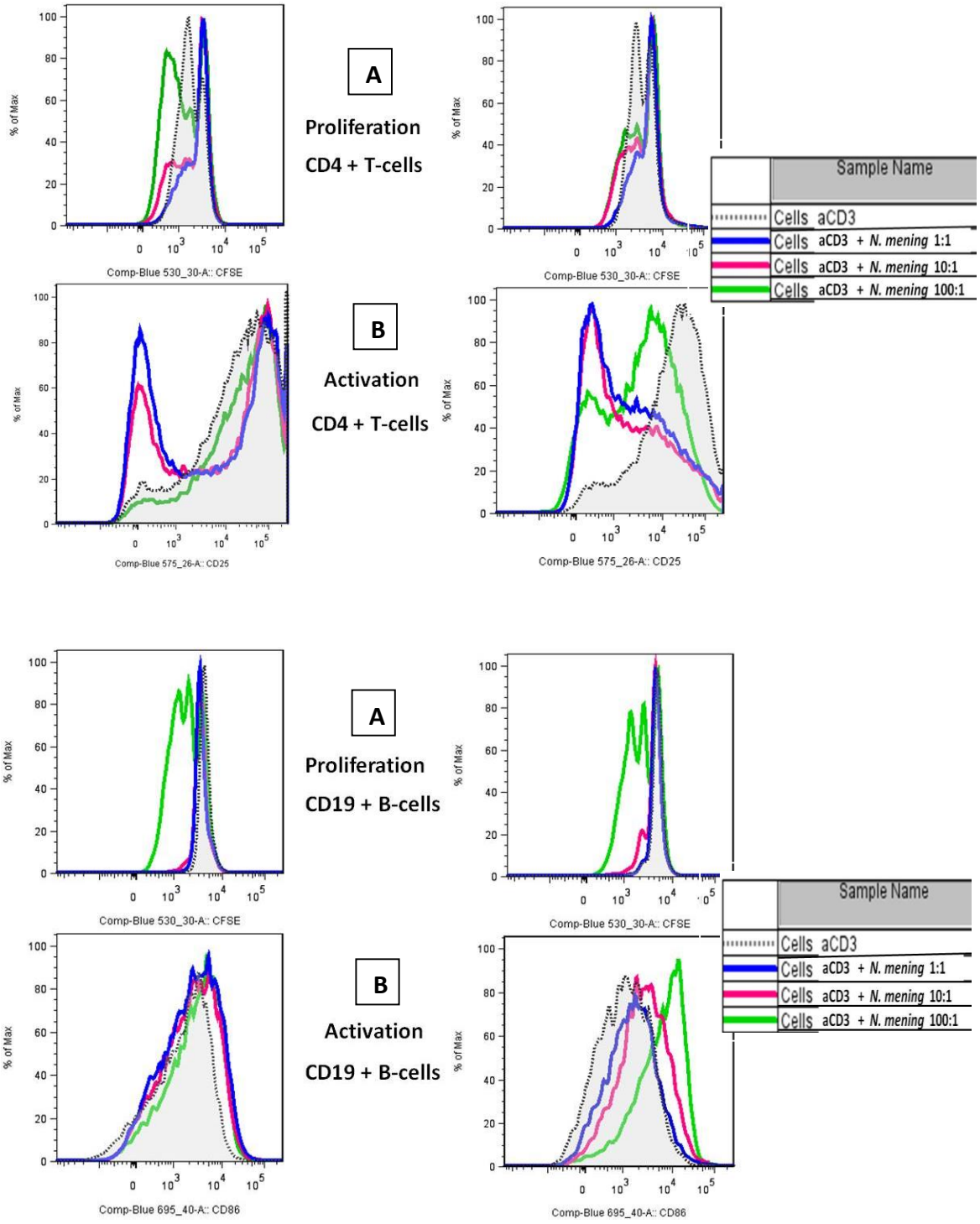

Figure 4.4: Examples of overlaid histograms illustrating T and B cell responses following incubation with αCD3 plus different ratios of *N. meningitidis*.

A. Proliferation assessed by the CFSE dilution method, the x axis represents intensity of CFSE fluorescence and the y axis % of maximum. **B. Activation as MFI of activation markers,** the x axis represents intensity of CD25-PE or CD86-PE Alexa700 fluorescence, while the y axis % of maximum.

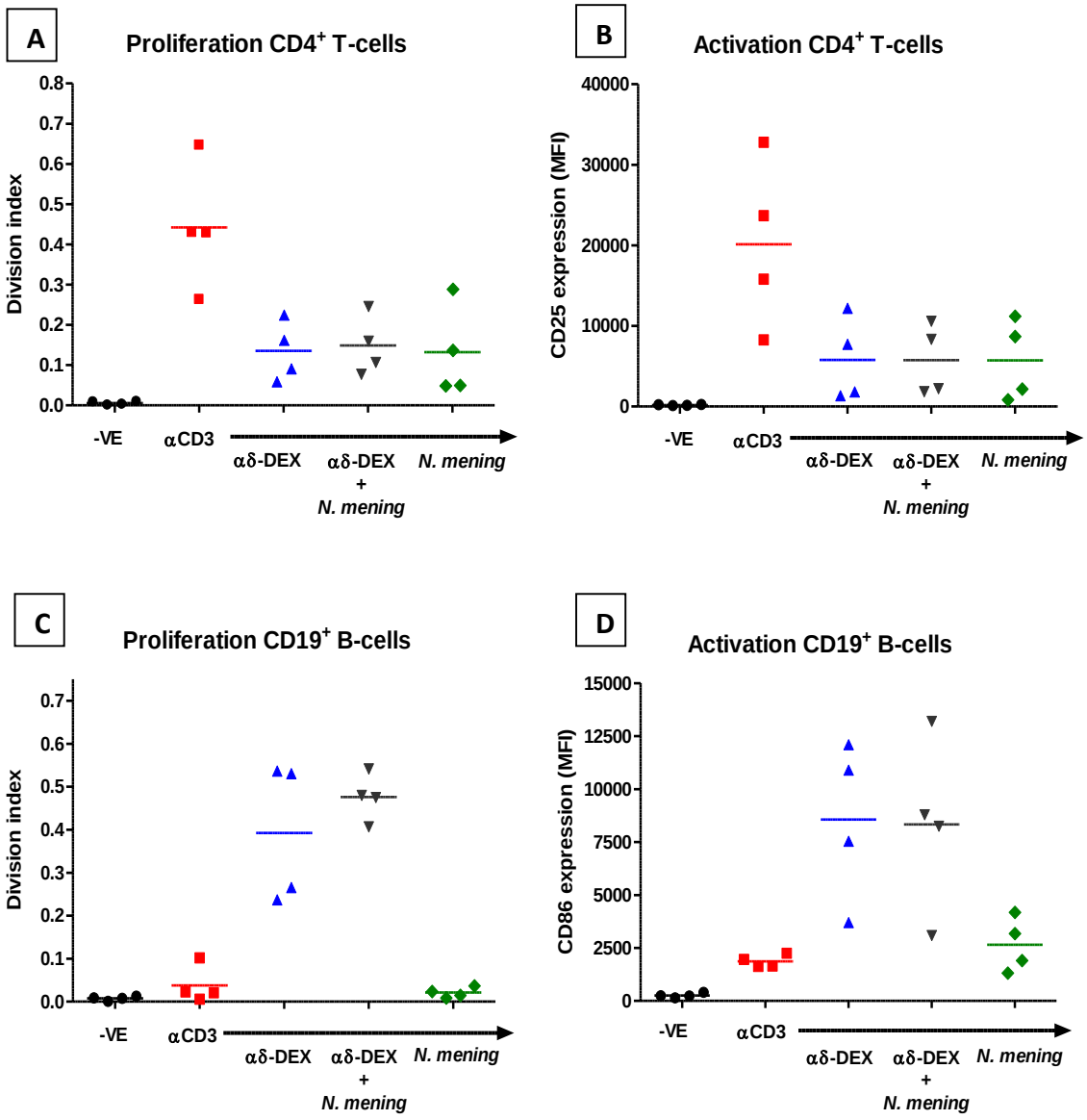

Figure 4.5: *N. meningitidis* and α-δ-DEX suppressive effects do not appear to be synergistic.

A. Proliferation CD4⁺ T-cells, reported as division index. **B. Activation CD4⁺ T-cells**, expression of the CD25 marker as median fluorescence intensity (MFI). **C. Proliferation CD19⁺ B-cells**, reported as division index. **D. Activation CD19⁺ B-cells**, expression of the CD86 marker as median fluorescence intensity (MFI). Lines represent means, n=4.

-VE= negative control, non-stimulated PBMCs. αCD3= T-cell stimulation (plate-bound 0.1 µg/ml). α-δ-DEX= B-cell stimulation (1 µg/ml). *N. meningitidis*= ratio of 1:1 bacteria per cell.

4. 4 *N. MENINGITIDIS* DOES NOT AFFECT CELL VIABILITY

To exclude *N. meningitidis* induced-cell death as the reason of the inhibitory effect, we assessed percentages of cell death using a dead/live dye which strongly stains cells with compromised membranes going into cell death (section 2.6.1). Although this method reflects the totality of dead PBMCs and does not allow us to differentiate compromised $CD4^+$ T-cells within the cell culture, we decided to include this viability dye as routine in every experiment to monitor cell death.

Figure 4.6 is representative of 14 different donors and illustrates the percentages of total cell death found on day 4 of the assay, after exposure to three different meningococcal inocula. As is evident, none of the groups containing bacteria reported a significant higher percentage of cell death in relation to the αCD3 control with no bacteria. Furthermore, the largest bacterial count (100:1) had a small but significant reduction on the % of cell death.

Therefore, we can infer that the presence of *N. meningitidis* does not appear to suppress responses of $CD4^+$ T lymphocytes by inducing cell death.

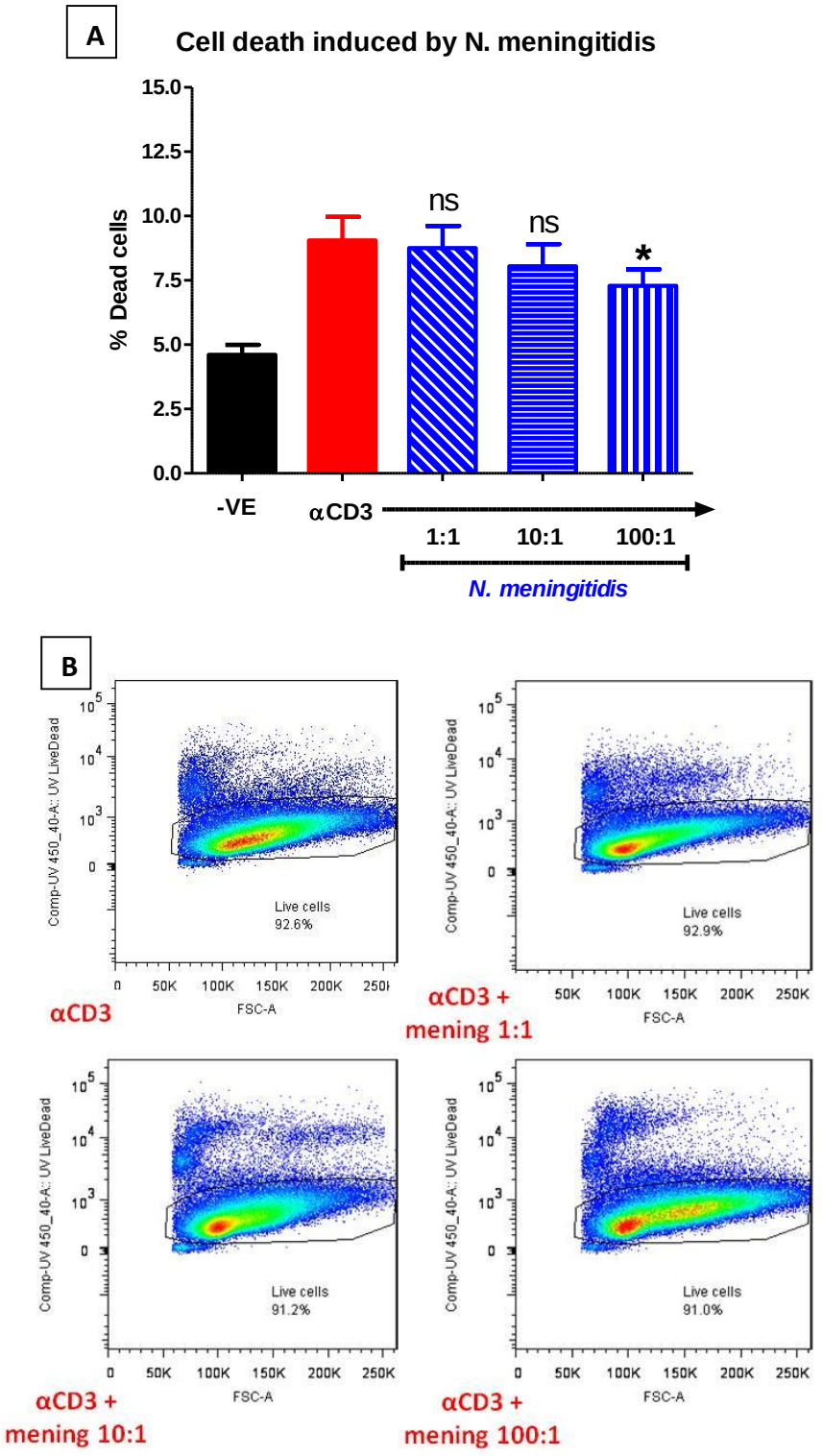

Figure 4.6: *N. meningitidis* does not affect viability of PBMCs.

A. Percentage of cell death induced by *N. meningitidis,* at ratios of 1:1, 10:1 and 100:1 bacteria per cell**.** Bars represent means and SEM, n=14. Paired ANOVA, Dunnett's Multiple Comparison Test (*vs.* αCD3). **p*= 0.01-0.05, ***p*= 0.001-0.01, ****p*= ≤0.001, ns= not significant. -VE= negative control, non-stimulated PBMCs. αCD3= T-cell stimulation (plate-bound 0.2 µg/ml). **B. Dot plot examples showing the live/dead gate applied for all conditions,** on the *y*-axis fluorescence of the UV dead/live dye and on the *x*-axis FSC-A**.** These 4 samples are representative of 1 single donor and show % of live cells within the gate.

4.5 LOS IS NOT INVOLVED IN THE MECHANISM OF SUPPRESSION

In order to discover if *Neisseria* lipooligosaccharyde (LOS) is implicated in inducing a suppressive response, we investigated the outcome of a LOS-deficient mutant strain made as a complete lpxA-knockout by insertion of a kanamycin-resistance cassette (Steeghs et al. 1998). In this way, blockade on the first step of lipid A biosynthesis occurs and the mutant lacks LPS completely (sections 1.2.4.2 and 2.8.1.1).

Although the LOS-deficient colonies were always selected by Kanamycin resistance, we further corroborated the absence of the lpxA gene by PCR. Figure 4.7 shows the expected lpxA gene bands of around 650pb for the genomic DNA extracts from the wild type strain MC58 and mutant's parental wild type strain H44/76. The largest band of around 1800pb was obtained from the LOS-deficient mutant and corresponds to the lpxA gene insertion with a Kanamycin cassette.

Having established disruption of the lpxA gene in our mutant, our basic experiment was carried out comparing the LOS-deficient mutant against its wild type parental strain H44/76 and our standard wild type strain MC58 (section 2.8.1.1). As before, bacterial ratios of 1:1, 10:1 and 100:1 were tested.

Figure 4.8 demonstrates how the LOS-deficient mutant is still effective in restraining $CD4^+$ T-cell responses in a similar manner to the wild type strains. Again, the smallest inoculum (1:1) had the largest inhibitory effect on T lymphocytes by reducing their division index by less than half in comparison with the αCD3 control group. The same negative correlation was observed with the mutant, as the largest bacterial count (100:1) was unsuccessful in stopping T-cell division (Figure 4.8-A).

This is consistent with the large reduction of T-cell activation observed after exposure to the LOS-deficient mutant at ratios of 1:1 and 10:1; an effect which disappeared at the highest ratio of 100:1 bacteria per cell (Figure 4.8-B).

In addition, no statistical differences were found among the same ratios for both of wild type strains MC58 or H44/76 and the LOS-deficient mutant, neither for proliferation nor for activation. Therefore, we can conclude that LOS does not play a critical role in the suppression mechanism induced by *N. meningitidis*.

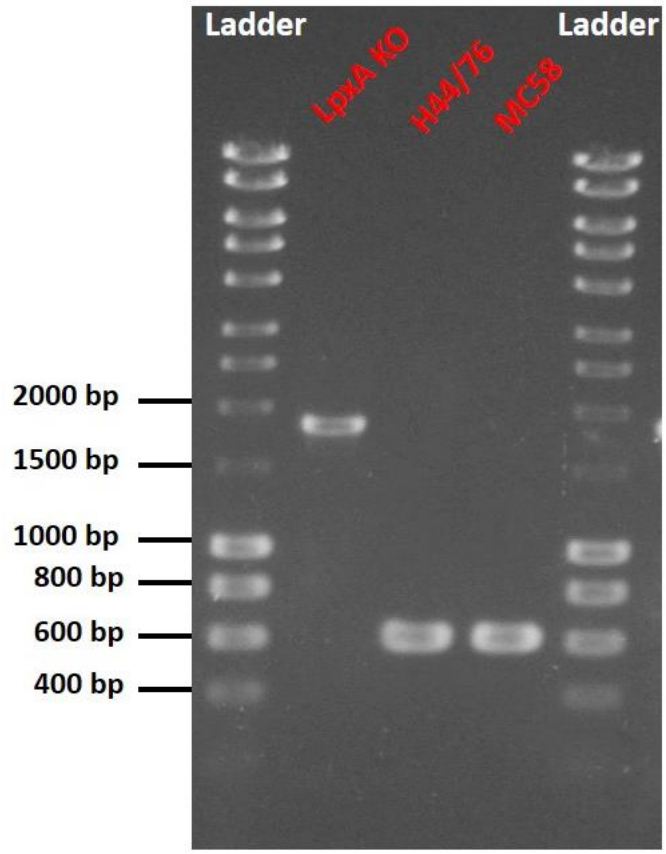

Figure 4.7: Insertion of the kanamycin cassette into the *lpxA* gene was confirmed by PCR.

From left to right: HyperLadder (Bioline), lpxA knockout mutant (LOS deficient strain), parental wild type strain H44/76, wild type strain MC58, HyperLadder (Bioline).

For the 3 strains, genomic DNA was isolated using the E.Z.N.A. Bacterial DNA protocol and following manufacturer's instructions (Bacterial DNA kit, OMEGA bio-tek). A highly specific PCR reaction was achieved using 2 µl of DNA template and a PCR cocktail (MyTaq™Mix, Bioline). Thirty PCR cycles were run under the next conditions: initial denaturation 95^{o}C for 1 minute, denaturation 95^{o}C for 15 seconds, annealing 55^{o}C for 15 seconds and extension 72^{o}C for 10 seconds. Primers for the lpxA gene segment included the insertion site for the kanamycin cassette:

lpxA_F - TGACCCTCATCCACCCGACCG ; lpxA_R- GCGGTAAAACCGTTGCGGCG.

A 1% agarose gel was loaded with the PCR products and ran for 90 minutes at 70 volts. Finally, DNA bands were stained with ethidium bromide and revealed.

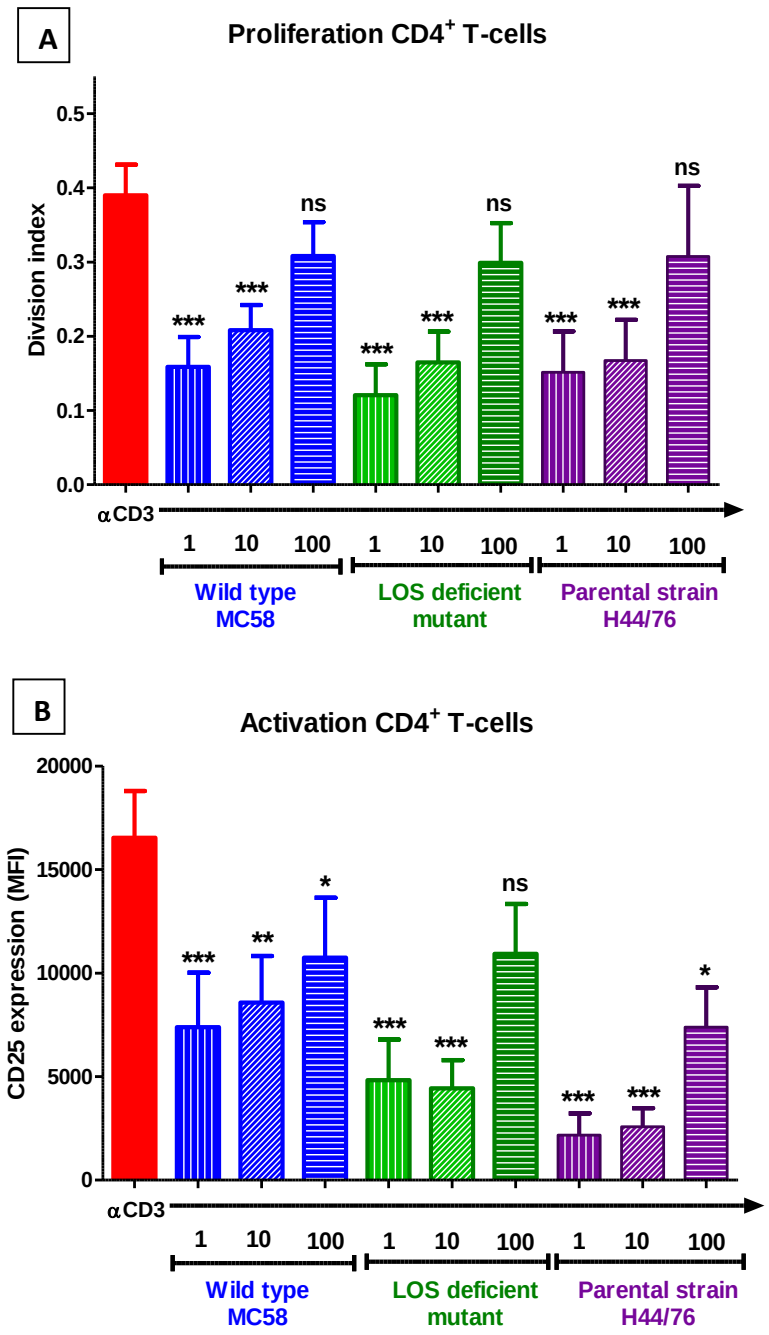

Figure 4.8: LOS is not the mechanism of suppression. LOS-deficient meningococci inhibit CD4⁺ T-cell proliferation and activation just as wild type strains do.

A. Proliferation CD4⁺ T-cells, reported as division index. **B. Activation CD4⁺ T-cells**, expression of the CD25 marker as median fluorescence intensity (MFI). Bars represent means and SEM; n=6 for MC58 and LOS mutant, n=4 for H44/76. Paired ANOVA, Dunnett's Multiple Comparison Test (*vs.* αCD3). *p= 0.01-0.05, **p= 0.001-0.01, ***p= ≤0.001, ns= not significant.
For 96 hours PBMCs were stimulated with plate-bound αCD3 (0.2 µg/ml) and exposed to PF fixed bacteria: *N. meningitidis* wild type MC58 strain (blue bars), LOS-deficient strain -lpxA knockout mutant (green bars) or parental wild type strain H44/76 (purple bars). For all groups, ratios of 1:1, 10:1 and 100:1 bacteria per cell. Red bar containing αCD3 and no bacteria is the positive control.

4.6 OMVs CONTAIN THE SUPPRESSIVE FACTOR

To discover if the suppressor element was contained within the outer membrane of the meningococcus, we conducted a more specific approach by using purified outer membrane vesicles (OMVs). OMVs are 'blebs' of the bacterial outer membrane and are primarily composed of phospholipids, LOS and outer membrane proteins (section 1.2.4.6).

Assuming that the suppressive bacterial factor could be contained inside the vesicles, different concentrations of purified OMVs from *N. meningitidis* wild type strain MC58 (section 2.8.4) were added directly to PBMCs and incubated over 4 days in the presence of T-cell stimulation (αCD3 plate-bound).

Because it is expected that secreted OMVs will contain part of the bacterial capsule and since capsular polysaccharides are the major example of TI type 2 antigens, we decided to include non-capsulated *Neisseria* OMVs within this experiment. The related non-pathogenic *N. lactamica* differs structurally from *N. meningitidis* in the absence of capsule (Kim et al. 1989); indeed, OMVs from this organism were ideal to be assessed under the same conditions. A wide range of concentrations were tested along this assay, going from 0.001 up to 50 μg/ml in the case of meningococcal OMVs and from 0.001 to 25 μg/ml for lactamica OMVs.

It is apparent from Figure 4.9-A that proliferation of $CD4^+$ T-cells was dramatically impaired by both *N.lactamica* and *N.meningitidis* OMVs irrespective of the concentration. Even the smallest concentration of OMVs (0.001 μg/ml) was sufficient to achieve significance.

Similarly, expression of the T-cell activation marker was clearly reduced by *N.meningitidis* and *N.lactamica* OMVs in a dose-dependent fashion. All concentrations, apart from the lowest reported significant differences compared to the αCD3 control group which did not contain OMVs (Figure 4.9-B)

These results indicate that purified OMVs from both *N. meningitidis* and *N. lactamica*, contain an outer membrane component capable of inhibiting T-cell proliferation and activation in a similar manner to whole fixed bacteria. In addition, *N. lactamica* OMVs allowed indirect exclusion of capsule involvement within this assay as no significant differences were found between the concentrations of OMVs from meningococcus and lactamica.

Taking an educated guess about the bacterial component responsible for inducing the suppressive mechanism, we thought on the outer membrane proteins as first candidates (sections 1.2.4.4 and

1.2.4.5). Therefore, we opted for heating the OMVs as a simple approach of protein denaturalisation and exclusion of thermolabile elements.

Data in Figure 4.10 reveals that heating of purified OMVs does not reverse the inhibitory effect on $CD4^+$ T-cell responses, neither for *N. meningitidis* nor for *N. lactamica*. In comparison with our usual αCD3 control, all groups containing heated OMVs had a significantly lower cell division index irrespective of the concentration used (Figure 4.10-A). The same phenomenon was observed for T-cell activation, as all the groups incubated with heated vesicles reported very low expression of CD25 against the positive control which was OMVs free (Figure 4.10-B).

Overall, it appears that the suppressive factor is heat stable and that high temperatures are not enough to ablate its inhibitory properties.

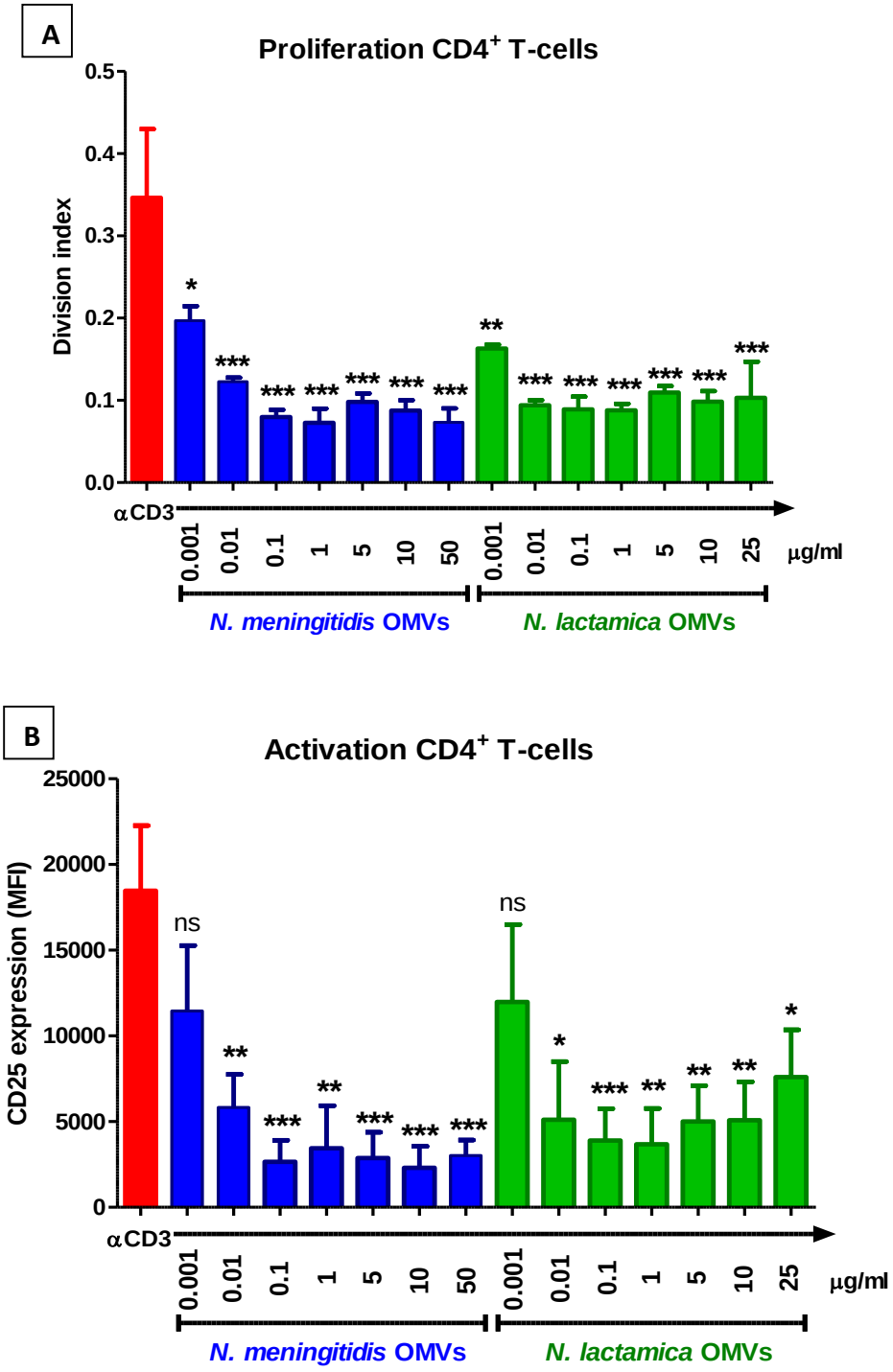

Figure 4.9: OMVs from both *N. meningitidis* and *N. lactamica* contain the suppressive factor.

A. Proliferation CD4⁺ T-cells, reported as division index. **B. Activation CD4⁺ T-cells**, expression of the CD25 marker as median fluorescence intensity (MFI). Bars represent means and SEM, n=≥4. One way ANOVA, Dunnett's Multiple Comparison Test (*vs.* αCD3). **p*= 0.01-0.05, ***p*= 0.001-0.01, ****p*= ≤0.001, ns= not significant.

For 96 hours PBMCs were stimulated with plate-bound αCD3 (0.2 µg/ml) and exposed to different concentrations of purified OMVs, from *N. meningitidis* (blue bars) or from *N. lactamica* (green bars). Red bar containing αCD3 and no OMVs represents the positive control.

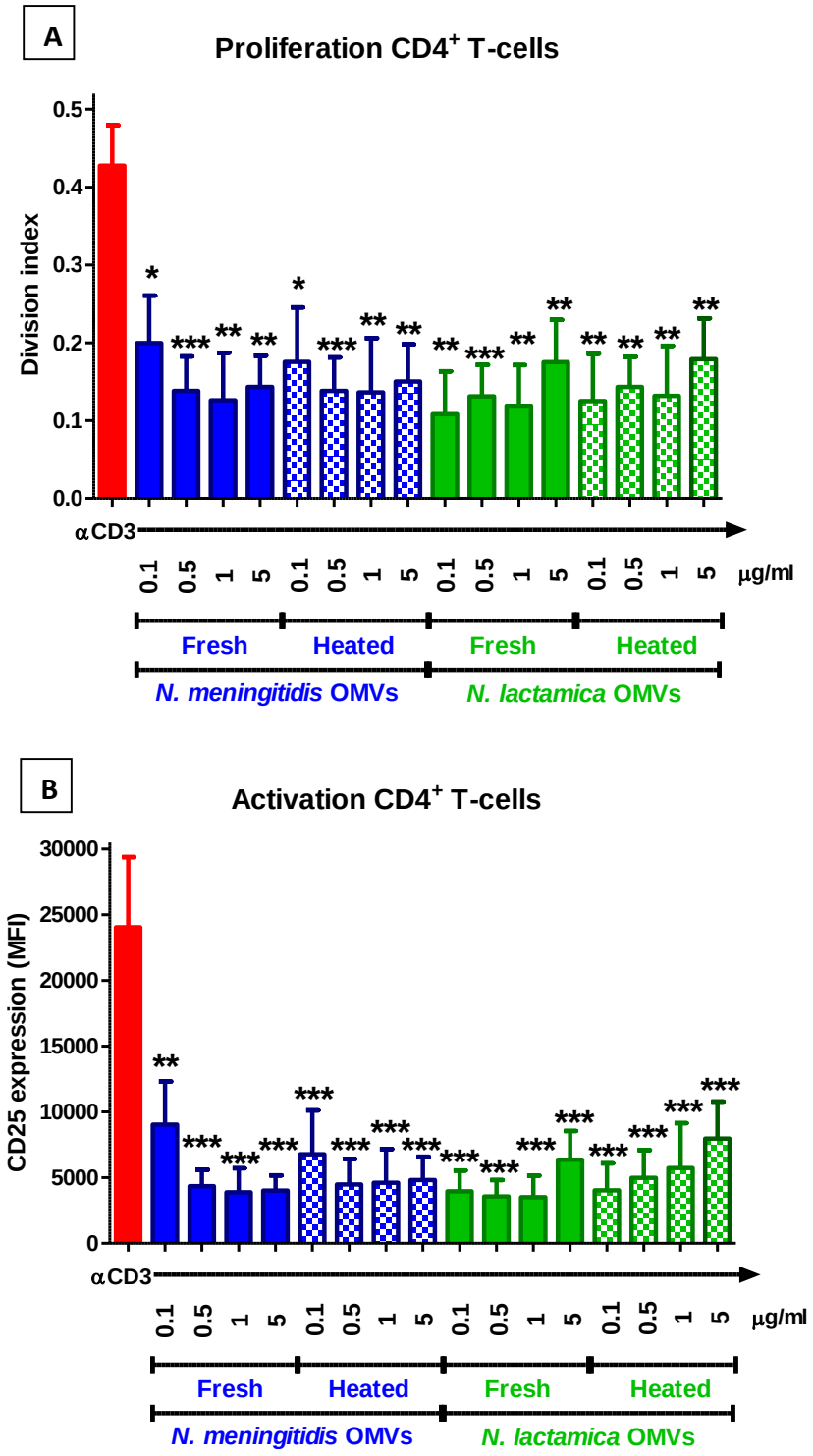

Figure 4.10: The inhibitory effect on CD4⁺ T-cells is not reversed when OMVs are heated.

A. Proliferation CD4⁺ T-cells, reported as division index. **B. Activation CD4⁺ T-cells**, expression of the CD25 marker as median fluorescence intensity (MFI). Bars represent means and SEM, n=≥4. One way ANOVA, Dunnett's Multiple Comparison Test (*vs.* αCD3) and Bonferroni's Multiple comparison test. *p= 0.01-0.05, **p= 0.001-0.01, ***p= ≤0.001, ns= not significant.

For 96 hours, PBMCs were stimulated with plate-bound αCD3 (0.2 µg/ml) and exposed to different concentrations of fresh (solid bars) or heated (square bars) purified OMVs, from *N. meningitidis* (blue bars) or from *N. lactamica* (green bars). On the day of the experiment, OMVs were heated at 100°C for 15 minutes using a dry block heater. Red bar containing αCD3 and no OMVs represents the positive control.

4.7 OPACITY PROTEIN IS NOT RESPONSIBLE FOR THE SUPPRESSION

Given the fact that purified OMVs seem to contain the bacterial component responsible for restraining T-cell proliferation and activation (section 4.6), we sought to determine whether a common surface determinant - opacity protein (Opa) is involved in the suppression. A strong Opa-CEACAM interaction is important to facilitate adherence of capsulated *Neisseria spp* to epithelial cells and invasion into the blood stream (Bradley et al. 2005). Moreover, binding of Opa with CEACAM1 has been previously reported to have inhibitory consequences in activation and proliferation on T-lymphocytes (Sadarangani et al. 2011) (section4.1)

To discover if Opa is a key element within the inhibitory mechanism, we carried out an assay to evaluate the effect of an Opa-deficient capsulated MC58/h18.18 variant (section 2.8.1.1) *versus* the wild type MC58 strain. Using αCD3-stimulated PBMCs and going from a very small inoculum of 0.1 bacteria per cell up to 100, the results from this experiment are shown in Figure 4.11.

Proliferation of $CD4^+$ T lymphocytes had a dramatic fall of between 50 to 75% for all the groups exposed to Opa-deficient bacteria in relation to the positive control (Figure 4.11-A). However there were no significant differences among the bacterial ratios of the Opa-deficient and the wild type.

A very similar trend was observed with activation (Figure 4.11-B). Again, both strains were not different when similar pairs of inocula were compared.

To further exclude a role for Opa in the inhibition another Opa-deficient strain from the same MC58 background was examined. Unlike the strain used above, this ¢2 Opa-deficient bacteria lacks of capsule (section 2.8.1.1), so we could examine a possible TI type 2 effect driven by capsular polysaccharides.

Figure 4.12-A demonstrates that cell division of T lymphocytes can be stopped by bacterial ratios from 0.1 to 10 of the non-capsulated Opa-deficient strain. Although the inoculums 1:1 and 1:10 were not significant for T-cell activation, the smallest count 0.1 significantly restrained CD25 expression Figure 4.12-B.

In conclusion, these data support that Opa is not involved in leading suppression of $CD4^+$ T lymphocytes.

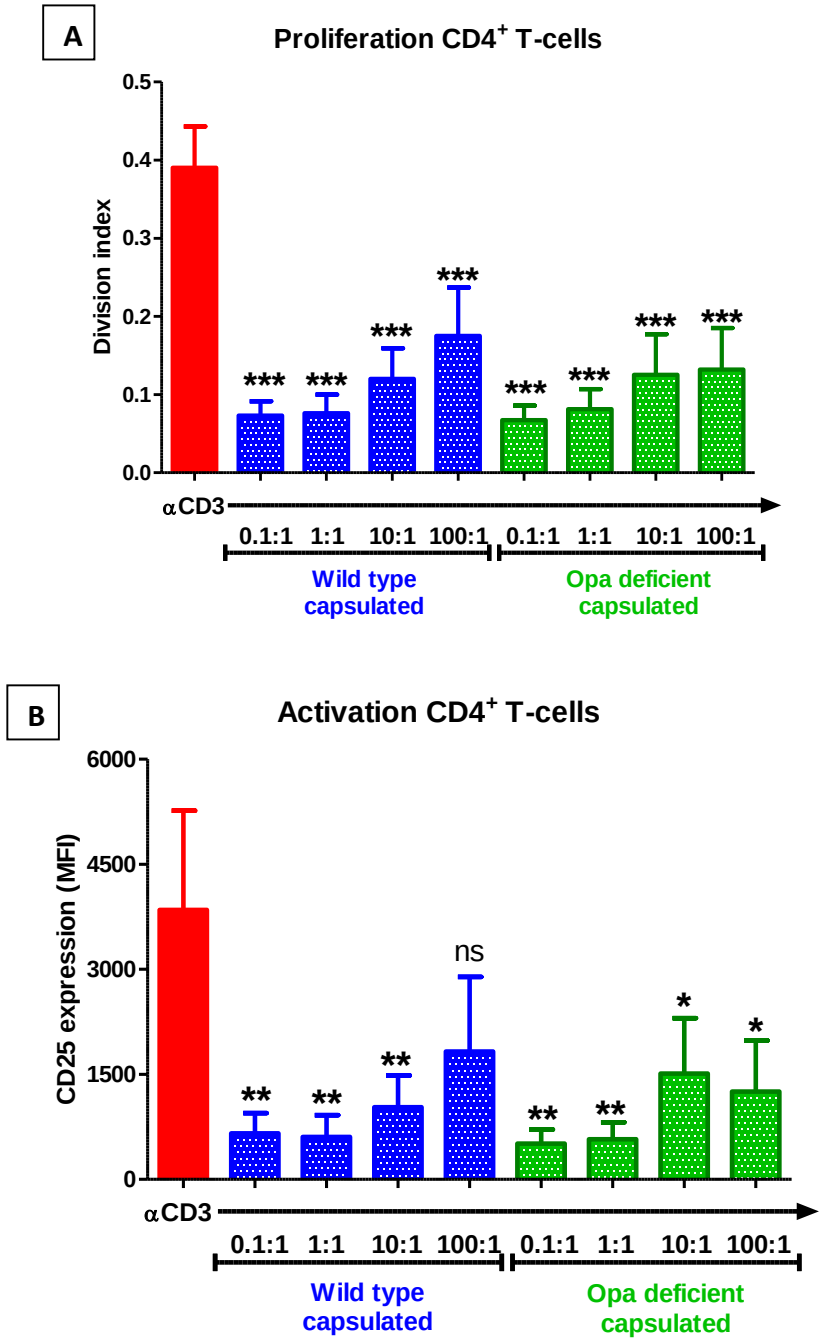

Figure 4.11: **Opa is not the bacterial factor involved in the suppression mechanism of CD4⁺ T lymphocytes (1).**

A. Proliferation CD4⁺ T-cells, reported as division index. **B. Activation CD4⁺ T-cells**, expression of the CD25 marker as median fluorescence intensity (MFI). Bars represent means and SEM; n=5. Paired ANOVA, Dunnett's Multiple Comparison Test (*vs.* αCD3). *p= 0.01-0.05, **p= 0.001-0.01, ***p= ≤0.001, ns= not significant.

For 96 hours PBMCs were stimulated with plate-bound αCD3 (0.3 µg/ml) and exposed to PF fixed bacteria, *N. meningitidis* wild type MC58 strain (blue bars) or MC58/h18.18 Opa-deficient strain (green bars). For all groups, ratios of 0.1:1, 1:1, 10:1 and 100:1 bacteria per cell. Red bar containing αCD3 and no bacteria represents the positive control.

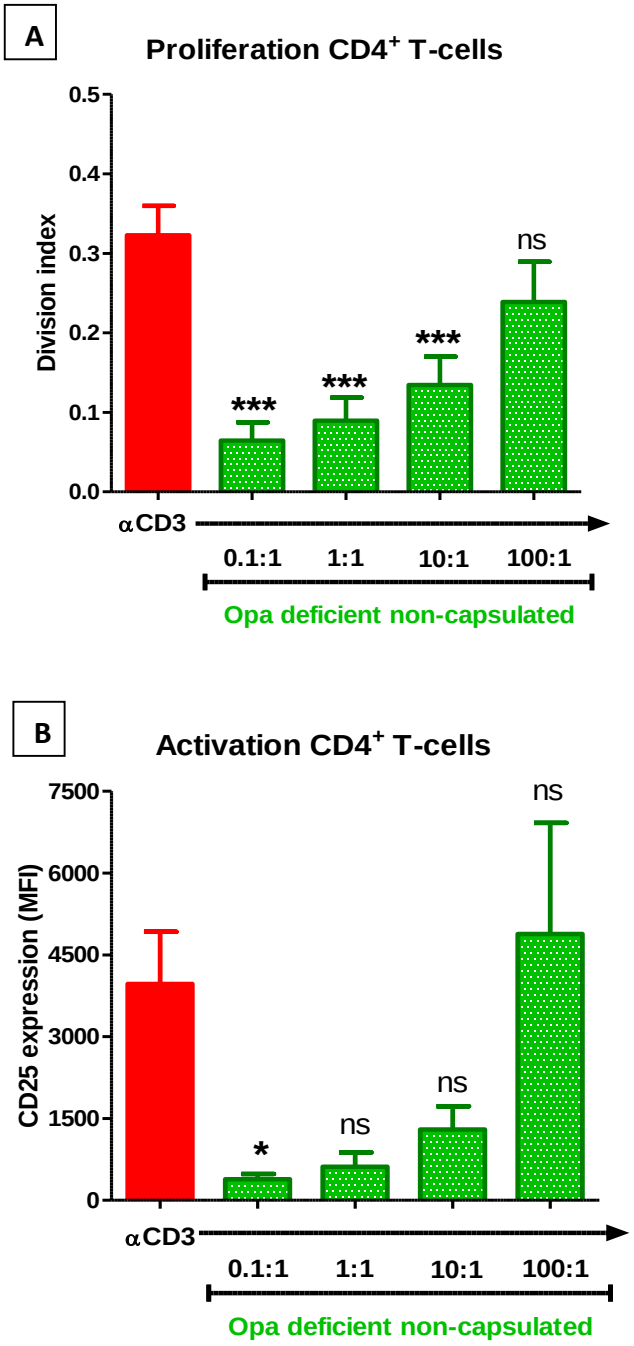

Figure 4.12: **Opa is not the bacterial factor involved in the suppression mechanism of CD4⁺ T lymphocytes (2).**

A. Proliferation CD4⁺ T-cells, reported as division index. **B. Activation CD4⁺ T-cells**, expression of the CD25 marker as median fluorescence intensity (MFI). Bars represent means and SEM; n=8. Paired ANOVA, Dunnett's Multiple Comparison Test (*vs.* αCD3). *p= 0.01-0.05, **p= 0.001-0.01, ***p= ≤0.001, ns= not significant.

For 96 hours PBMCs were stimulated with plate-bound αCD3 (0.3 µg/ml) and exposed to PF fixed non-capsulated MC58 /¢2 Opa-deficient bacteria (green bars), at different ratios: 0.1:1, 1:1, 10:1 and 100:1 bacteria per cell. Red bar containing αCD3 and no bacteria represents the positive control.

4.8 MENINGOCOCCUS DOES NOT HAVE A DIRECT SUPPRESSIVE EFFECT ON PURIFIED CD4$^+$ T-CELLS

To address the question whether bacteria acts directly on T lymphocytes, purified CD4$^+$ T-cells were incubated for 4 days with meningococci (wild type MC58 strain) at ratio of 1:1 bacteria per cell.

Primary human CD4$^+$ T-cells were enriched from fresh PBMCs using a negative selection kit (table 2.1), obtaining a final purity greater than 95% in all cases (Figure 4.13-C). Section 2.3.1.4 explains why αCD3/αCD28 dynabeads were preferred over plate-bound αCD3 to induce proliferation and activation on purified T-cells.

Figure 4.13-A shows that addition of the bacteria did not reduce the division index of purified CD4$^+$ T-cells. Similarly, expression of the activation marker was not altered by exposure to the meningococcus (Figure 4.13-B).

Indeed, we have provided evidence to confirm that *N. meningitidis* is not suppressing T-cell responses by a direct interaction.

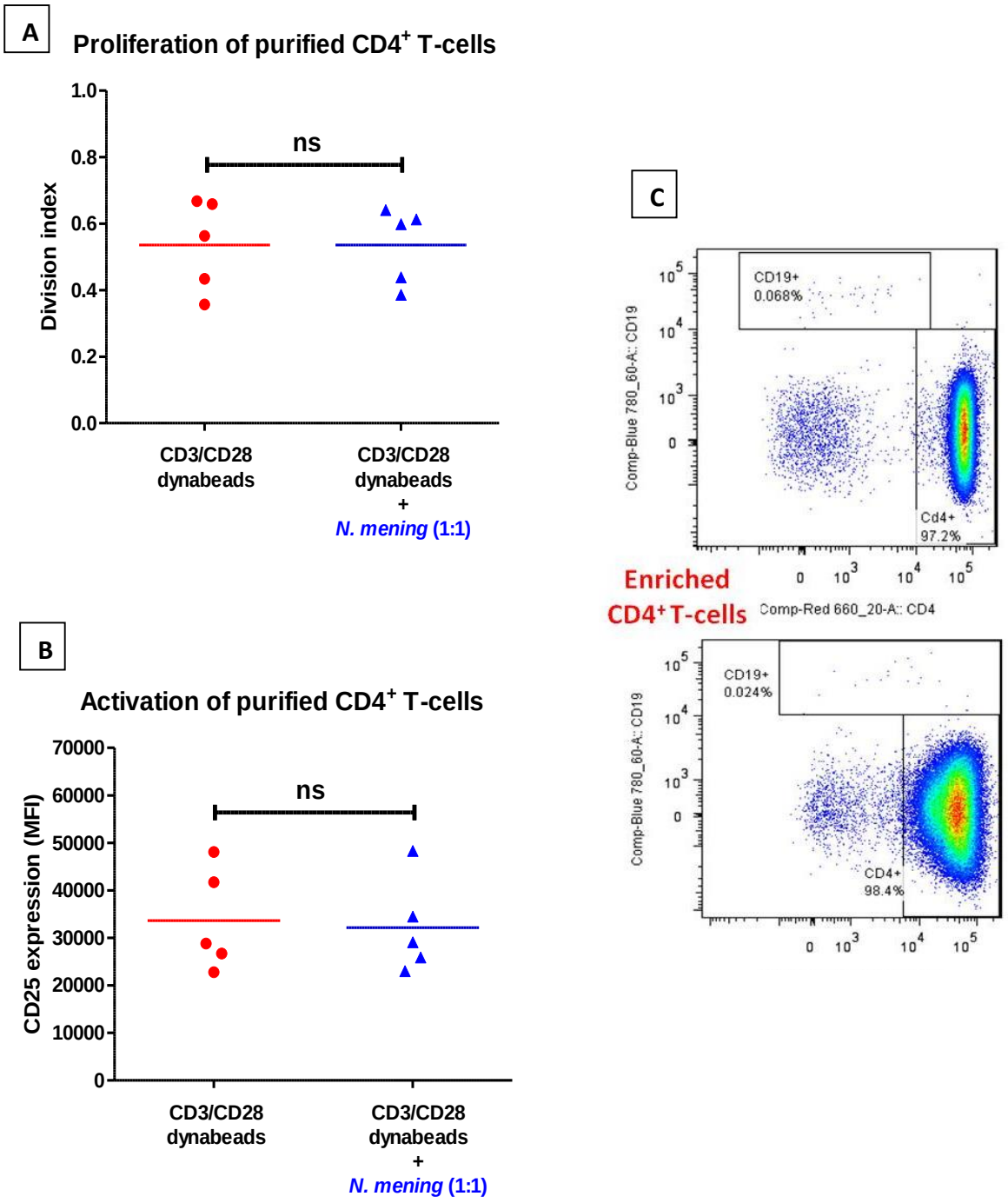

Figure 4.13: *N. meningitidis* does not have a direct suppressive effect on purified CD4⁺ T-cells.

A. Proliferation of enriched CD4⁺T-cells, reported as division index. **B. Activation of enriched CD4⁺ T-cells**, expression of the CD25 marker as median fluorescence intensity (MFI). Lines represent means, n=5. Paired student *t*-test. **p*= 0.01-0.05, ***p*= 0.001-0.01, ****p*= ≤0.001, ns= not significant. **C. Dot plot examples of primary human enriched CD4⁺ T-cells illustrating purity greater than 95%.** CD4⁺ cells (*x*- axis= CD4-APC) *vs.*CD19⁺ cells (*y*- axis = CD19 PE Cy-7). Plots are representative examples from 2 donors.

Primary CD4⁺ T-cells were enriched by negative selection from PBMCs and stimulated with αCD3/αCD28 dynabeads (1:1 ratio), in the absence or presence of PF fixed *N. meningitidis* wild type MC58 strain (1:1 bacteria per cell).

4.9 *N. MENINGITIDIS* DOES NOT INDUCE A SUPPRESSIVE PHENOTYPE ON B LYMPHOCYTES

We next explored the role of B lymphocytes within the suppression mechanism induced by meningococci. Although section 4.3 demonstrates that the presence of small bacterial counts are unable to trigger a substantial stimulation of $CD19^+$ B-cells, we carried out an experiment with purified populations to further exclude any involvement of B lymphocytes.

Figure 4.14 illustrates the methodology followed for this assay. Briefly, $CD4^+$ T-cells were negatively selected from fresh PBMCs and stimulated with αCD3/αCD28 Dynabeads on day 0. Simultaneously, PBMCs were exposed to either *N. meningitidis* (strain MC58 at ratio of 1:1) or RPMI media (as negative control) for a period of 24 hours. From those PBMCs groups, $CD19^+$ and/or $CD20^+$ B lymphocytes were enriched by negative selection (table 2.1) and then co-cultured with the purified $CD4^+$ T-cells on day 1. In co-culture, a physiological proportion of one B lymphocyte per six T lymphocytes was chosen for this assay (explained in section 3.7).

We have previously reported in section 3.8 that enriched non pre-activated B lymphocytes can stop the division index of $CD4^+$ T lymphocytes in co-culture, maybe due to spontaneous activity *in vitro* of natural B-regulatory cells. Using different volunteers and in a posterior assay, Figure 4.16-A reinforces such phenomenon as addition of non stimulated purified B-cells to a pure culture of T-cells resulted in a significant drop in proliferation. But what is relevant for this experiment is that enriched B-cells which were primed with a small inoculum of meningococci did not achieve a further inhibition (Figures 4.15 and 4.16-A).

Activation of purified $CD4^+$ T lymphocytes was not significantly affected by any of the two co-culture conditions. Neither non-stimulated nor meningococcus-stimulated B-cells reduced expression of CD25 (figures 4.15 and 4.16-B). This may be due to an early ongoing activation signalling from day 0 (prior co-culture), which led to an irreversible expression of the T-cell surface marker despite contact with B lymphocytes.

In summary, we can infer that *N. meningitidis* does not act by inducing a suppressive phenotype on B lymphocytes, as seems the case for TI type 2 mimics.

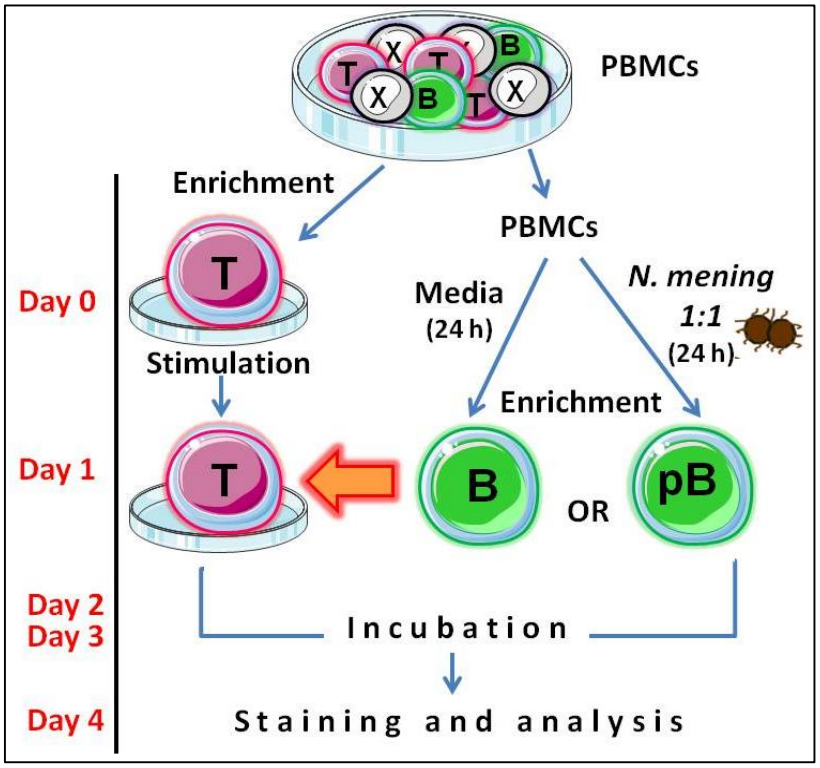

Figure 4.14: Schematic representation of the experimental protocol involving purified T and B lymphocytes in the presence of *N. meningitidis*.

Enriched $CD4^+$ T lymphocytes were obtained from PBMCs on day 0, following stimulation with αCD3/αCD28 dynabeads. On the same day, PBMCs were incubated in the presence or absence of PF *N. meningitidis* strain MC58, ratio of 1:1 bacteria per cell. After a 24 hours period, non pre-activated B-cells and pre-activated B-cells were enriched and co-cultured with the purified $CD4^+$ T-cells. Finally, 3 more days were allowed in co-culture before analysis. Although is not illustrated within this schema, a well containing only enriched T-cells plus αCD3/αCD28 dynabeads was used a positive control.

T= $CD4^+$ T-cell, B= B-cell, pB= MC58 pre-activated B-cell, X= accessory cell.

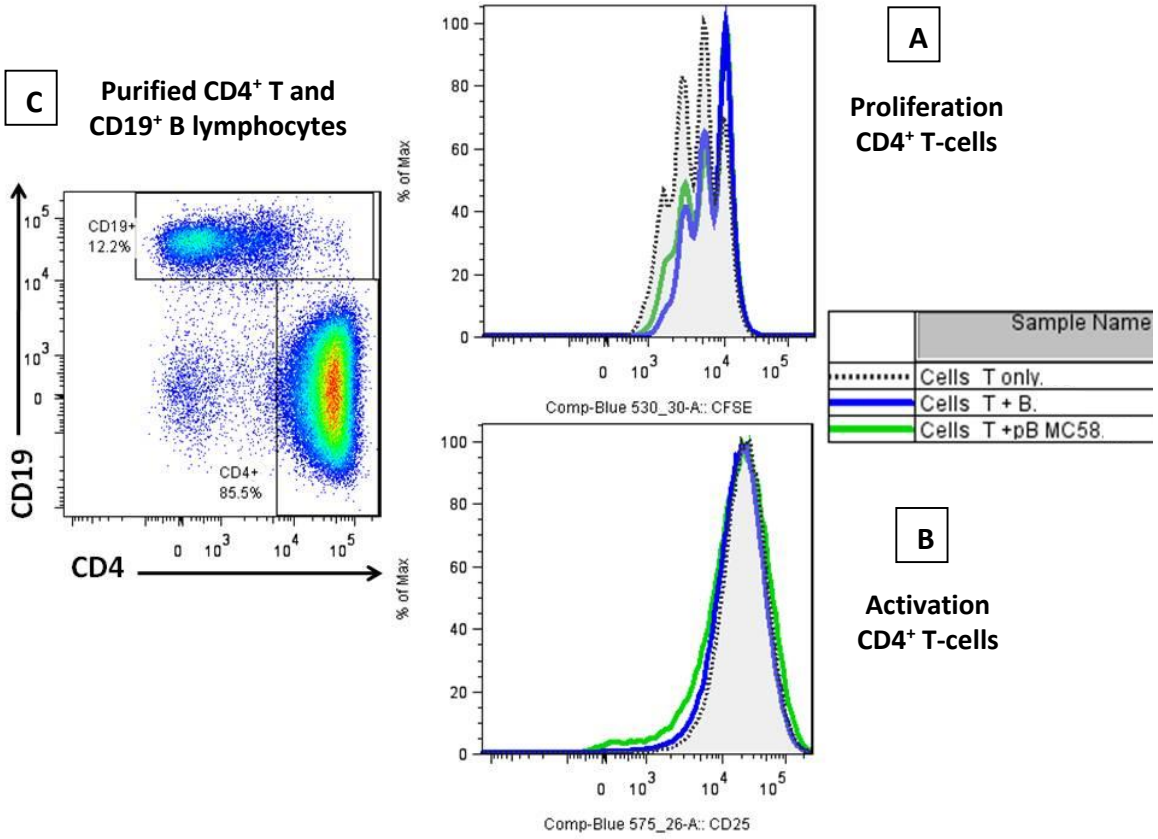

Figure 4.15: Examples of overlaid histograms illustrating T-cell responses following incubation with αCD3/αCD28 dynabeads plus non pre-activated and meningococcus pre-activated B-cells.

A. Proliferation assessed by the CFSE dilution method, the x axis represents intensity of CFSE fluorescence and the y axis % of maximum. **B. Activation as MFI of CD25 expression,** the x axis represents intensity of CD25-PE, while the y axis % of maximum. **C. Dot plot illustrating purity of enriched CD4⁺ T and CD19⁺ B lymphocytes.**

T= CD4⁺ T-cell, B= B-cell, pB= MC58 pre-activated B-cell.

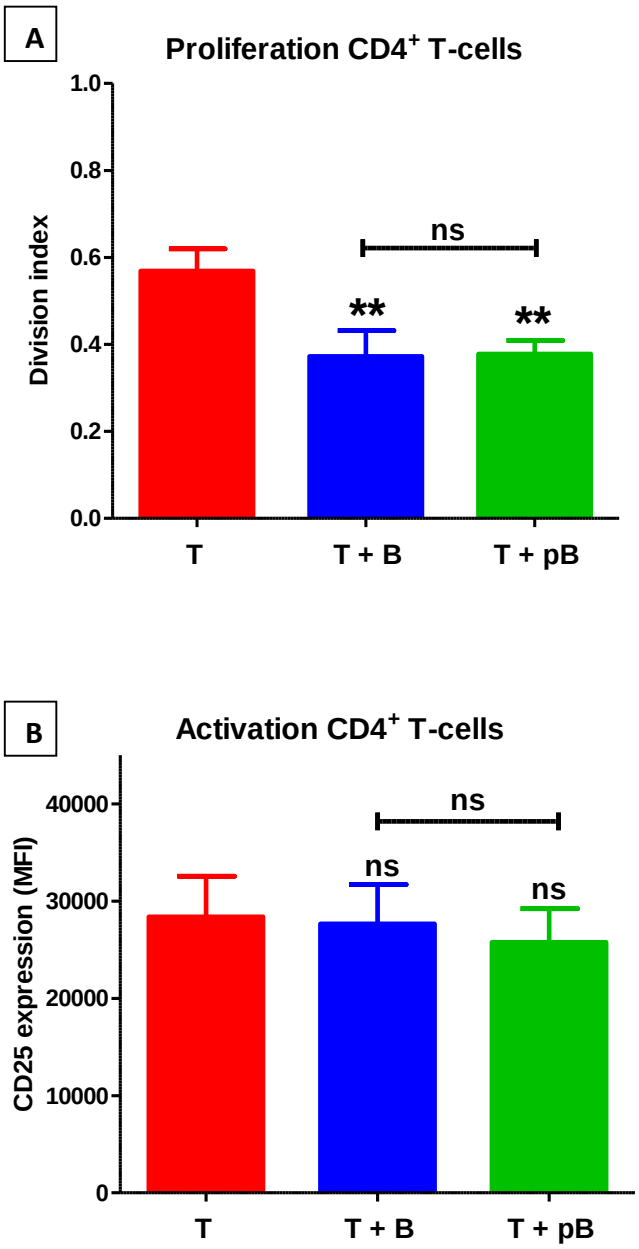

Figure 4.16: *N. meningitidis* does not induce a suppressive phenotype on B-lymphocytes.

A. Proliferation of enriched CD4⁺ T-cells, reported as division index. **B. Activation of enriched CD4⁺ T-cells**, expression of the CD25 marker as median fluorescence intensity (MFI). Bars represent means and SEM, n=8. Paired ANOVA, Bonferroni's Multiple Comparison Test; *p= 0.01-0.05, **p= 0.001-0.01, ***p= ≤0.001, ns= not significant.

All conditions were stimulated with αCD3/αCD28 dynabeads (1:1 ratio). Primary CD4⁺ T and B lymphocytes were enriched by negative selection from PBMCs. In red, control group containing T-cells alone. In blue, co-culture of T and non pre-activated B-cells. In green, co-culture of T and pre-activated B-cells, after 24 hours exposure to *N. meningitidis* (ratio 1:1).

T= CD4⁺ T-cell, B= B-cell, pB= MC58 pre-activated B-cell.

4.10 B LYMPHOCYTES ARE NOT IMPLICATED IN MENINGOCOCCUS-INDUCED SUPPRESSION

Throughout this Chapter, it has been shown that low bacterial counts of meningococci (ratios 1:1 and 10:1) do not induce proliferation or activation of B lymphocytes (section 4.3) and do not seem to generate a suppressive phenotype on those cells either (section 4.9).

To definitely exclude any role of B lymphocytes, $CD19^+$ and $CD20^+$ cells were depleted from fresh PBMCs (section 2.2.2) and incubated for 4 days with plate-bound αCD3 plus the usual bacterial ratios. Simultaneously, whole PBMCs were treated under the same conditions as comparison groups. Efficiency of this B-cell depletion was widely described in section 3.10.

As expected, removal of B lymphocytes did not reverse the negative effect of *N. meningitidis* on $CD4^+$ T-cell proliferation (Figure 4.17-A). All bacterial inocula, including the largest 100:1, diminished the division index of T lymphocytes.

From Figure 4.17-B which compares activation of T lymphocytes from B-cell depleted groups against whole PBMC, is clear that CD25 expression also declined by at least 50% in the absence of B lymphocytes irrespective of the bacterial count.

Moreover, there were no significant differences among any of the meningococcal inocula from whole PBMC or B-cell depleted PBMC, neither for proliferation nor for activation. Therefore, it is concluded that B lymphocytes are not necessary to initiate the *N. meningitidis* suppressive effect on $CD4^+$ T-cells.

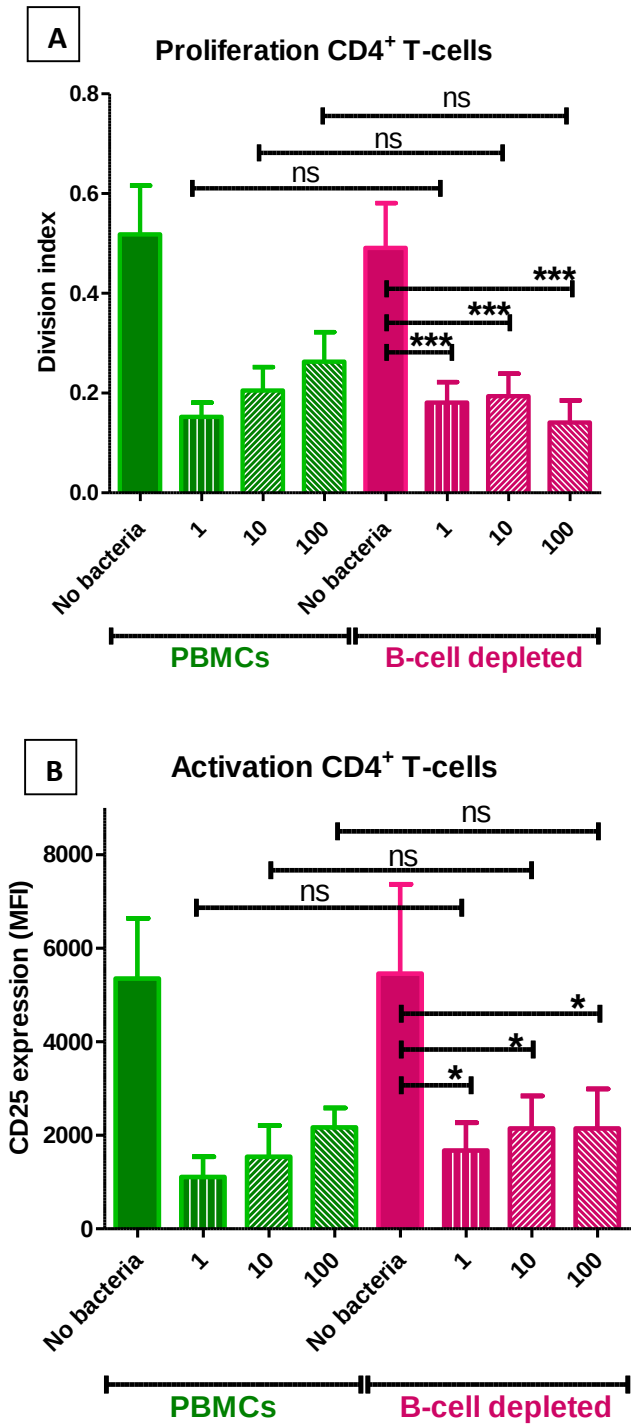

Figure 4.17: *N. meningitidis* suppressive properties still occur with B-cell depleted PBMC.

A. Proliferation CD4⁺ T-cells, reported as division index. **B. Activation CD4⁺ T-cells**, expression of the CD25 marker as median fluorescence intensity (MFI). Bars represent means and SEM, n= 5. Paired ANOVA, Bonferroni's Multiple Comparison Test. *p= 0.01-0.05, **p= 0.001-0.01, ***p= ≤0.001, ns= not significant.

During 4 days, whole PBMC (in green) and B-cell depleted PBMC (in pink) were stimulated with αCD3 (plate-bound 0.3 µg/ml) and meningococcus (strain MC58) at ratios of 1, 10 and 100 bacteria per cell. Under each condition, samples containing no bacteria represent the αCD3 positive control (filled bars).

4.11 MONOCYTES PRIMED WITH *N. MENINGITIDIS* DO NOT SUPPRESS PURIFIED CD4$^+$ T-CELLS

Since B lymphocytes did not appear to be the main cell type responding to meningococcus stimulation, at this stage it was logical to explore the role of specialised cells in bacterial recognition. Monocytes are highly capable of phagocytosis and recognition of bacterial components (sections 1.2.4 and 4.1). They also present antigenic peptides to T lymphocytes and are major producers of cytokines, thus eliciting the cooperation between the innate and acquired immune systems.

A very similar protocol to the one used in section 4.9 was followed to investigate the role of monocytes in our system. Purified CD4$^+$ T-cells were enriched from PBMCs by negative selection on day 0 and stimulated with αCD3/αCD28 dynabeads. On the same day, PBMCs were exposed to either *N. meningitidis* (strain MC58 at ratio of 1:1) or RPMI media (as negative control) for a period of 24 hours. Then, CD14$^+$ monocytes were negatively selected from those PBMCs as described in section 2.1.1. Finally, purified monocytes and purified T lymphocytes were co-cultured on day 1, leaving 3 more days in incubation before analysis. The T:monocyte ratio of 6:1 was chosen based on normal ranges within peripheral blood of healthy adults (explained in section 3.13). Figure 4.18 gives a schematic representation of the methodology applied.

Data in Figure 4.19-A demonstrates the division index of αCD3/αCD28 stimulated purified CD4$^+$ T lymphocytes alone and in co-culture with CD14$^+$ monocytes (the later with and without exposure to *N. meningitidis*). In agreement with data described in section 3.13, co-culture with non-stimulated monocytes reduced T-cell proliferation by around 50% compared to the sample containing T-cells alone. However, such inhibition does not seem to be associated with exposure to meningococci, as the monocytes exposed to the bacteria failed to induce a deeper inhibition of cell division.

Unlike previous experiments, there was a small but significant increase in activation in the sample containing meningococcus-stimulated monocytes as compared to the control group (Figure 4.19-B). No significant difference was observed between the non-stimulated and stimulated monocyte groups.

In summary, purified CD14$^+$ monocytes primed with *N. meningitidis* were incapable of restraining T-cell proliferation or activation in pure co-culture.

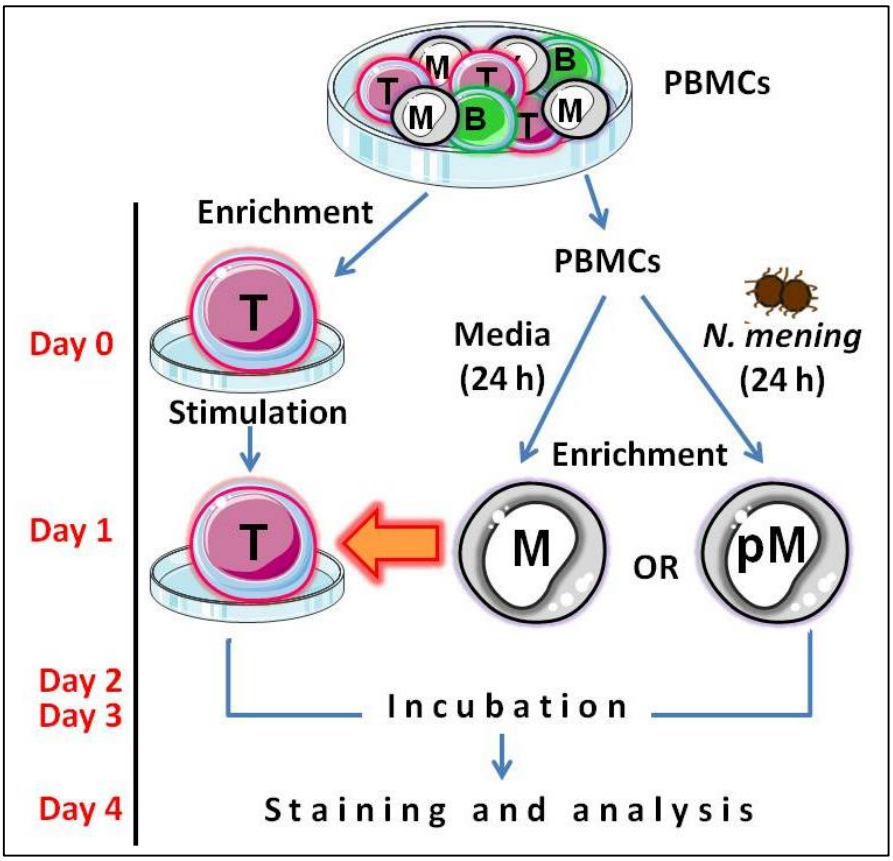

Figure 4.18: Schematic representation of the experimental protocol involving purified T lymphocytes and monocytes in the presence of *N. meningitidis*.

Enriched $CD4^+$ T lymphocytes were obtained from PBMCs on day 0, following stimulation with αCD3/αCD28 dynabeads. On the same day, PBMCs were incubated in the presence or absence of meningococcus strain MC58 ratio of 1:1 bacteria per cell, over a 24 hours period. Then, non pre-activated monocytes and pre-activated monocytes were enriched and co-cultured with the purified $CD4^+$ T-cells. Although is not illustrated within this schema, a positive control group including T-cells alone and αCD3/αCD28 dynabeads was included.

T= $CD4^+$ T-cell, M= monocyte, pM= MC58 pre-activated monocyte.

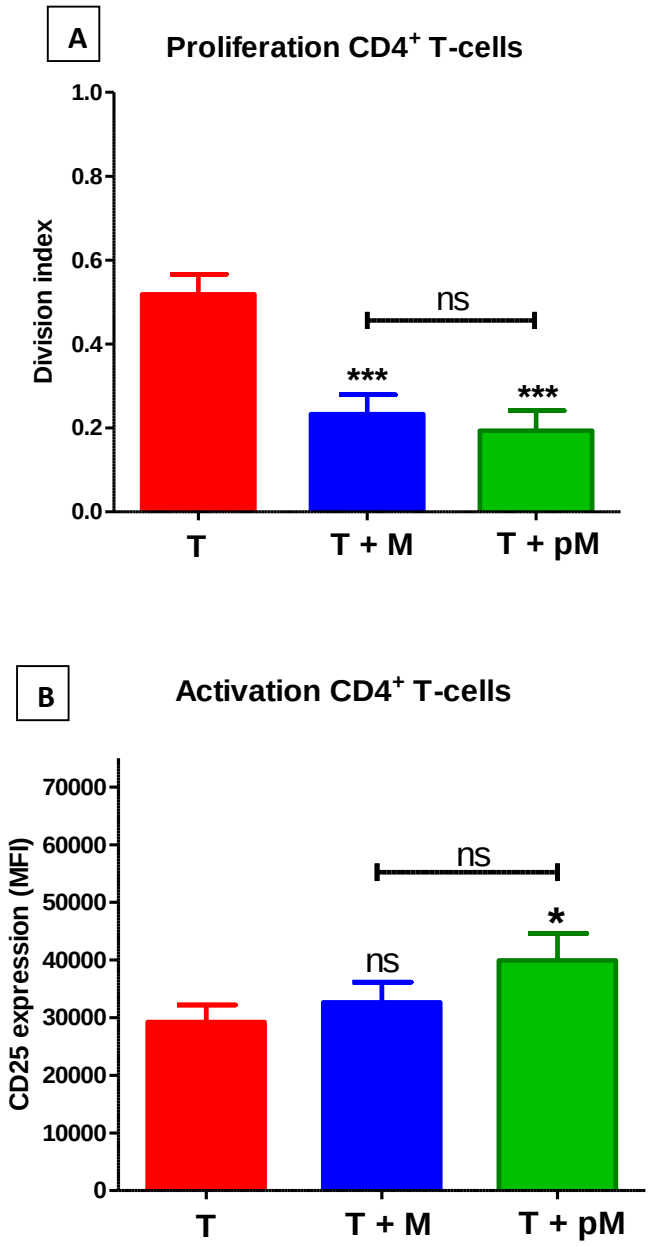

Figure 4.19: Purified CD14⁺ monocytes primed with *N. meningitidis* were incapable of restraining T-cell proliferation or activation in pure co-culture.

A. Proliferation of enriched CD4⁺ T-cells, reported as division index. **B. Activation of enriched CD4⁺ T-cells**, expression of the CD25 marker as median fluorescence intensity (MFI). Bars represent means and SEM, n=6. Paired ANOVA, Bonferroni's Multiple Comparison Test; *p= 0.01-0.05, **p= 0.001-0.01, ***p= ≤0.001, ns= not significant.

Primary CD4⁺ T lymphocytes and monocytes were enriched by negative selection from PBMCs and all conditions were stimulated with αCD3/αCD28 dynabeads. In red, control group containing T-cells only. In blue, co-culture of T and non-stimulated monocytes. In green, co-culture of T and *N. meningitidis* pre-activated monocytes.

T= CD4⁺ T-cell, M= monocyte, pM= MC58 pre-activated monocyte.

4.12 MONOCYTES ARE REQUIRED TO INDUCE T-CELL RESPONSES TO A LARGE MENINGOCOCCUS INOCULUM OF 100:1 BACTERIA PER CELL

Sections 1.2.4 and 4.1 explain that many of the *N. meningitidis spp* components are detected and trigger cell signalling *via* pattern recognition receptors, such as the membrane receptor CD14 and TLRs (TLR-1, 2 and 4) expressed on monocytes.

To further confirm that monocytes were not responsible for the inhibition after exposure to meningococcus*,* $CD14^+$ monocytes were depleted from the PBMC fraction using a positive selection protocol (section 2.2.2). In this manner, almost absolute monocyte removal (<1% $CD14^+$ cells left) was achieved (Figure 4.20-C) Whole PBMC as well as the monocyte depletion fraction were stimulated with plate-bound αCD3 and the usual PF wild type meningococci inocula 1:1, 10:1 and 100:1 bacteria per cell.

As compared with whole PBMC, the positive control (αCD3 -no bacteria) of the monocyte-depleted fraction shows a small drop in the proliferation and activation of $CD4^+$ T-cells. Therefore it is more difficult to determine the degree of suppression occurring with the smallest meningococcus ratio (Figure 4.20). If individual donors and their patterns are considered, then we can suggest that even in the absence of monocytes the suppression of T-cell responses still occurs. However, more repeats are necessary to clarify whether monocyte removal reverse the *N. meningitidis* suppressive effect at the ratio of 1:1 bacteria per cell. In contrast, the fact that monocyte depletion blocks T-cell proliferation and activation against the largest bacterial inoculum (100:1) was an evident finding (Figure 4.20).

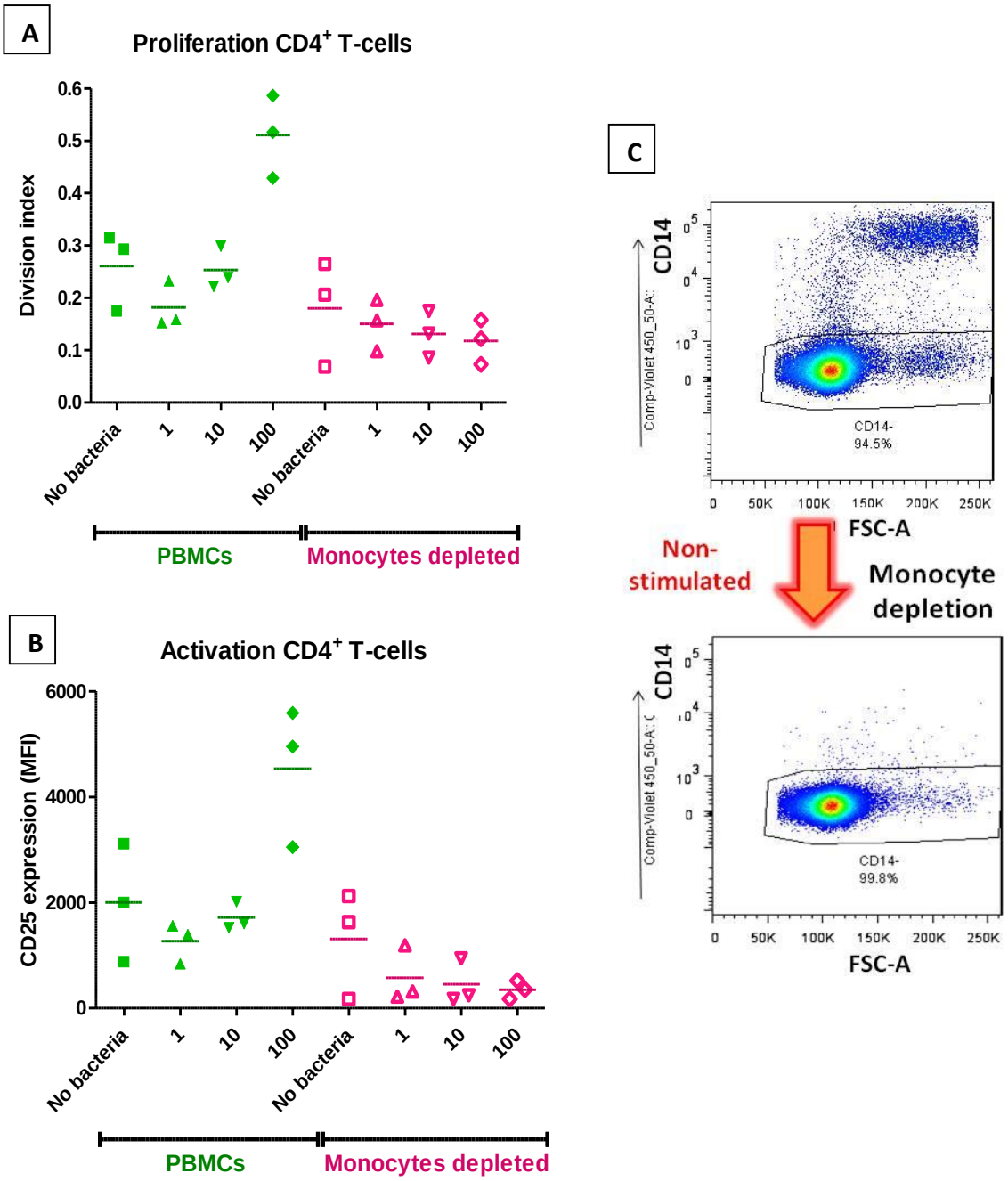

Figure 4.20: Monocytes are required to induce T-cell responses to a large meningococcus inoculum of 100:1 bacteria per cell.

A. Proliferation CD4⁺ T-cells, reported as division index. **B. Activation CD4⁺ T-cells**, expression of the CD25 marker as median fluorescence intensity (MFI). **C. Representative dot plot example of the efficiency of the depletion protocol at day 4 non-stimulated cells;** x-axis FSC-A and y-axis CD14 (Pacific blue). Lines represent means, n=3.
During 4 days, whole PBMC (in green) and monocyte depleted PBMC (in pink) were stimulated with αCD3 (plate-bound 0.3 µg/ml) and meningococcus (strain MC58) at ratios of 1, 10 and 100 bacteria per cell. Under each condition, samples containing no bacteria represent the αCD3 positive control.

4.13 *N. MENINGITIDIS* DOES NOT REQUIRE NK CELLS TO SUPPRESS CD4$^+$ T LYMPHOCYTES

NK cells were also studied because it has been reported that a distinct small fraction of NK cells can exert downregulatory actions on CD4$^+$ T lymphocytes, in a similar manner as Treg (Deniz et al. 2008).

Similarly to the experiments performed in sections 4.10 and 4.12, CD56$^+$ NK cells were depleted from the PBMC fraction applying a positive selection procedure (section 2.2.2), allowing almost absolute NK removal (<1% CD56$^+$ cells left) (Figure 4.21-C). Whole PBMC as well as the NK depletion fraction were stimulated with plate-bound αCD3 in the presence of the three different PF meningococci ratios (1:1, 10:1 and 100:1) and incubated for a period of 4 days.

Figure 4.21-A shows that in the absence of NK cells low bacterial counts of 1 and 10 restrain division of CD4$^+$ T lymphocytes, in a similar manner to whole PBMC. In contrast, the NK depletion effect is not so clear for the expression of the activation marker CD25 (Figure 4.21-B). Although more repeats are needed, if we consider individual donors and their patterns NK cells do not appear essential in suppressing T-cell activation either. A clear observation was the fact that in comparison with whole PBMC, NK depletion appears to enhance slightly T-cell proliferation and activation to αCD3 stimulation.

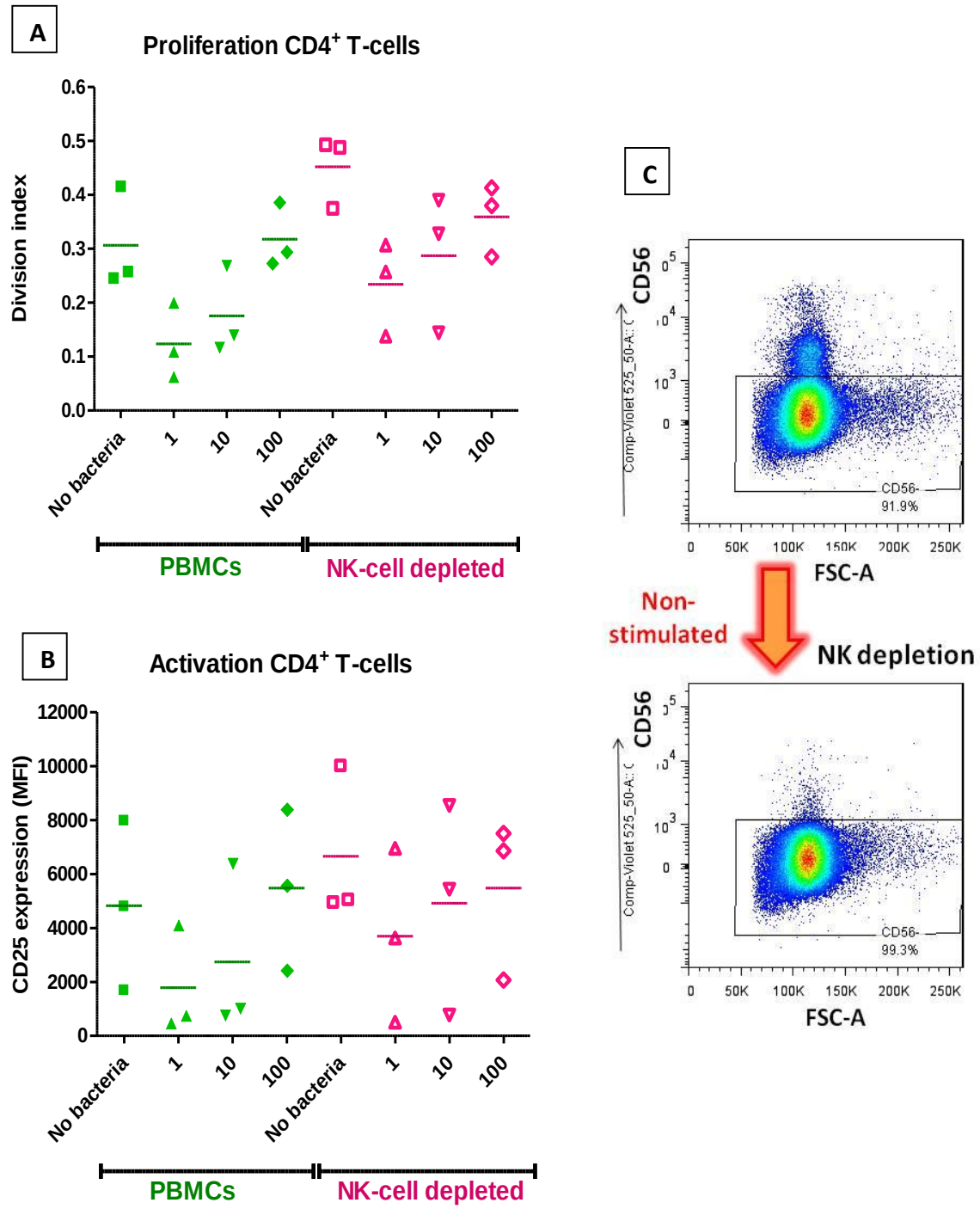

Figure 4.21: *N. meningitidis* suppressive properties still occur in NK depleted PBMC.

A. Proliferation CD4⁺ T-cells, reported as division index. **B. Activation CD4⁺ T-cells**, expression of the CD25 marker as median fluorescence intensity (MFI). **C. Representative dot plot example of the efficiency of the depletion protocol at day 4 non-stimulated cells;** x-axis FSC-A and y-axis CD56 (Brilliant Violet 510). Lines represent means, n=3.
During 4 days, whole PBMC (in green) and NK depleted PBMC (in pink) were stimulated with αCD3 (plate-bound 0.3 µg/ml) and meningococcus (strain MC58) at ratios of 1, 10 and 100 bacteria per cell. Under each condition, samples containing no bacteria represent the αCD3 positive control.

4.14 THE MECHANISM BY WHICH *N. MENINGITIDIS* SUPPRESS T LYMPHOCYTES APPEARS TO BE CELL-CONTACT DEPENDENT

To investigate whether soluble factors were intervening and whether cell contact was essential within the suppression mechanism, a supernatant transfer experiment was designed.

As usual, $CD4^+$ T lymphocytes were enriched on day 0 from fresh PBMC and stimulated with αCD3/αCD28 dynabeads. As in sections 4.9 and 4.11, PBMCs were either exposed or not to *N. meningitidis* (MC58 strain, ratio of 1:1). After 24 hours incubation, supernatants from non-stimulated PMBC or from meningococcus primed PBMC were transferred to wells containing the purified T lymphocytes. Only 200 µl of supernatant were transferred, the additional 300 µl of the usual RPMI preparation to complete a final volume of 500 µl per well, were already present from day 0 when purified $CD4^+$ T-cells were seeded. In total, from the point at which T-cells were enriched and stimulated (day 0), 4 days of incubation passed before flow cytometric analysis.

From Figure 4.22-A which represents the proliferation of that supernatant from PBMC exposed to meningococcus purified $CD4^+$ T lymphocytes, it is confirmed that the supernatant does not contain a soluble factor capable of restraining cell division. In contrast, addition of 200 µl of supernatant resulted in a significant increase of T-cell proliferation as compared with the control group. Since the supernatant from non-stimulated PBMC also showed the same trend, this is probably an incidental feature unrelated to *N. meningitidis* priming.

Neither significant reduction nor increase was observed for the expression of the activation marker CD25 in any of the groups (Figure 4.22-B). No differences were detected in samples containing supernatants *versus* the control containing purified $CD4^+$ T lymphocytes alone.

Overall we have not found evidence to suspect of a soluble suppressive factor being released by PBMCs, at least not at the initial 24 hours after exposure to *N. meningitidis.*

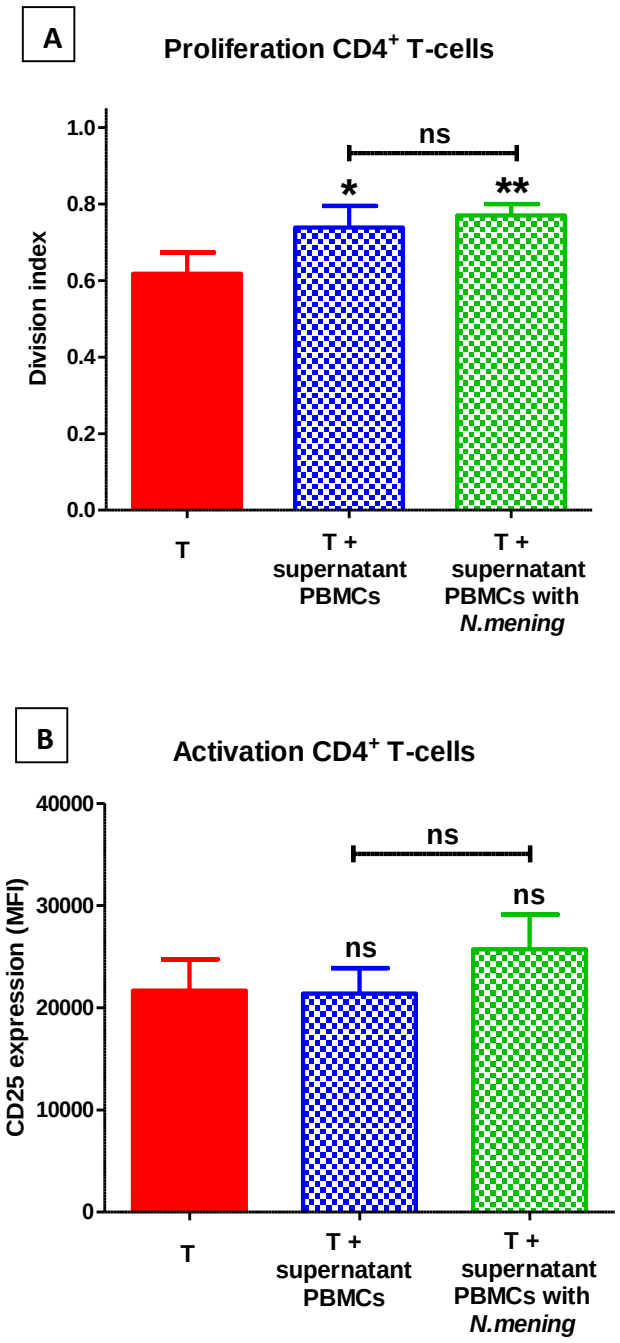

Figure 4.22: Supernatant from PBMC primed for 24 hours with *N. meningitidis* does not suppress CD4⁺ T-cell responses.

A. Proliferation of enriched CD4⁺ T-cells, reported as division index. **B. Activation of enriched CD4⁺ T-cells**, expression of the CD25 marker as median fluorescence intensity (MFI). Bars represent means and SEM, n=5. Paired ANOVA, Bonferroni's Multiple Comparison Test; *p= 0.01-0.05, **p= 0.001-0.01, ***p= ≤0.001, ns= not significant.

Primary CD4⁺ T lymphocytes were enriched by negative selection from PBMCs and all conditions were stimulated with αCD3/αCD28 dynabeads. In red (solid bar), control group containing T-cells alone. In blue, T-cells plus supernatant from non-stimulated PBMC. In green, T-cells plus supernatant from PBMC primed with *N. meningitidis* (ratio 1:1).

4.15 *N. MENINGITIDIS* ENHANCES TH1 CYTOKINES AND IL-10 PRODUCTION BUT SUPPRESSES TH2 CYTOKINES

To address whether the different ratios of *N. meningitidis* induce a change in cytokine profiles, samples from 6 randomly chosen volunteers were analysed to determine cytokines concentrations within cell culture supernatants.

PBMCs were stimulated with plate-bound αCD3 plus the usual ratios of wild type *N. meningitidis* (strain MC58): 0.1, 1, 10 and 100 bacteria per cell. Non-stimulated PBMCs were used as negative control and αCD3-stimulated PBMCs as positive control. Supernatants were collected at the time of cell harvest (after 4 days incubation) and were stored frozen at -20^{o}C until the day of analysis.

Concentrations of 10 cytokines were determined simultaneously by a multiplex cytometric bead array (section 2.7). According to the manufacturer's instructions, concentrations of IL-1β, IL-5, IL-6, IL-8, IL-10, IL-12p70, IL-13, IL-17A, IFN-γ and TNF-α were measured and reported in pg/ml. After the beginning of this study it was decided that supernatants should be tested for TGF-β, a very unstable molecule, but the supernatants had been stored in such a way that it was impossible to do this assay.

Several differences were found among the different inocula and in comparison with the positive control containing no meningococcus (Figure 4.23).

IL-1β, IL-6 and IL-8 were over-produced in the presence of *N. meningitidis* and were found to have a similar pattern. In comparison with the positive αCD3-stimulated control, samples containing 0.1:1, 1:1 and 10:1 bacteria per cell had increased levels of IL-6 and IL-8 up to 35 and 4 times more, respectively. Only the sample with the largest bacterial count of 100:1 did not show a significant rise in IL-6 or IL-8 levels. Similarly, IL-1β production was greatly augmented (~150-folds) when PBMCs were exposed to *N. meningitidis* counts equal or larger than 1:1. In contrast, both IL-5 and IL-13 concentrations decreased dramatically in all samples containing meningococci, irrespective of the size of the inoculum.

As compared with the positive control, IFN-γ and TNF-α concentrations had an upward trend proportional to the number of meningococci. TNF-α production was significantly enhanced in samples containing 10:1 and 100:1 bacteria per cell, whilst IFN-γ was only significant for the sample with the largest ratio.

Interestingly, about 3 times higher IL-10 concentrations were detected in the presence of bacterial counts of 1:1 and 10:1. The largest inoculum of 100:1 reverse this effect, as no significant difference existed between this sample and the positive control.

IL-12p70 remained unaffected, minimal concentrations were detected across all conditions (including the non-stimulated condition) and no significant differences were found. Although IL-17 appears to be reduced by small meningococci inocula, none of the groups demonstrated significant differences against the positive control.

In summary, these results suggest that bacterial counts $\leq$10:1 meningococcus induce polarisation towards T_H1 cytokines, abolishment of T_H2 responses and a simultaneous overproduction of IL-10.

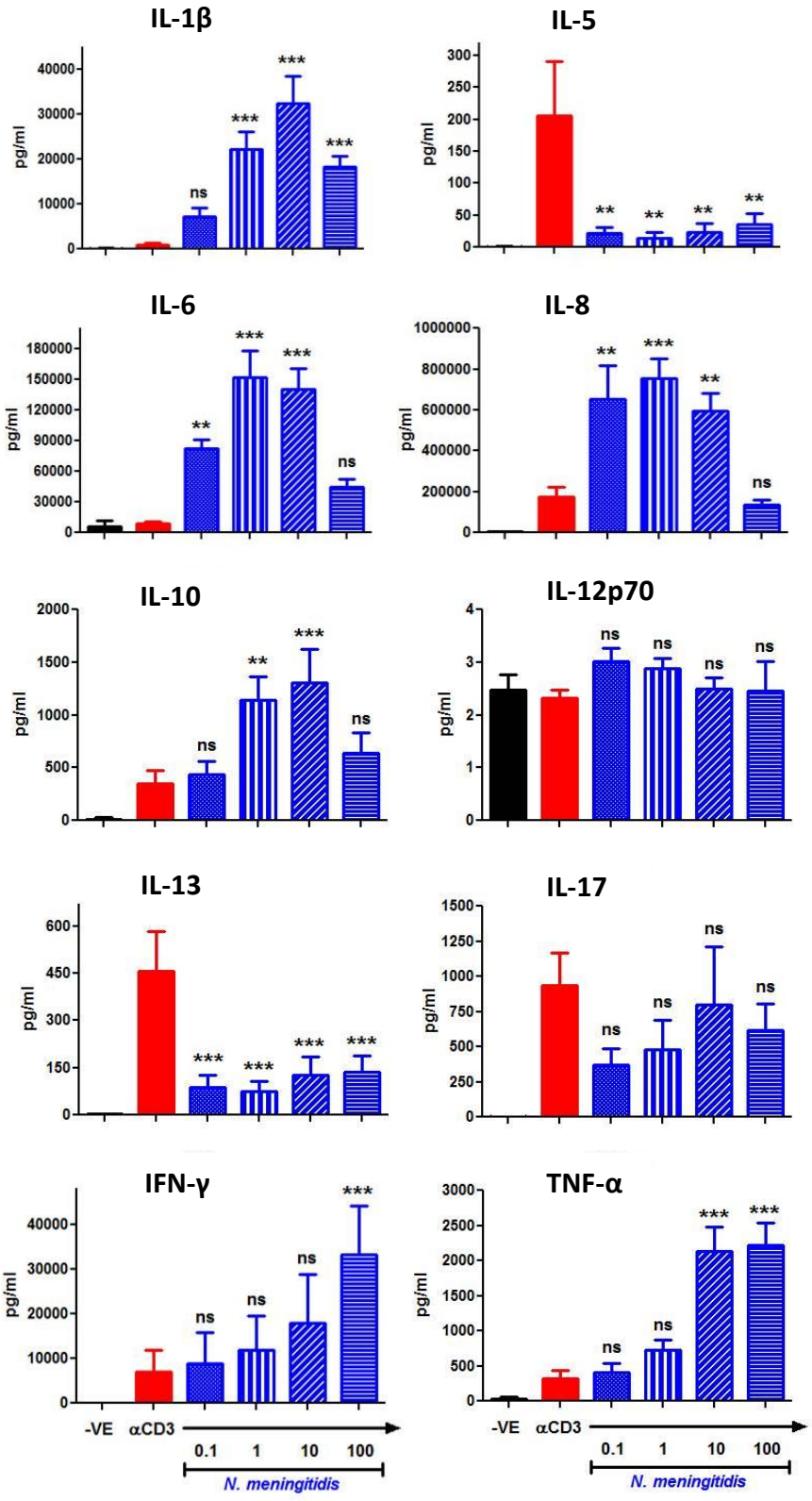

Figure 4.23: *N. meningitidis* induces T_H1 cytokines and IL-10 production, but blocks T_H2 cytokines. PBMCs were stimulated with plate-bound αCD3 plus different ratios of wild type *N. meningitidis* (strain MC58): 0.1, 1, 10 and 100 bacteria per cell. Supernatants were collected on day 4 and stored at -20°C. Cytokines assayed by Cytometric Bead Array. Bars represent means and SEM, n=6. Paired ANOVA, Dunnett's Multiple Comparison Test (*vs.* αCD3). *p= 0.01-0.05, **p= 0.001-0.01, ***p= ≤0.001, ns= not significant. –VE= non-stimulated PBMCs (black); αCD3= T-cell stimulation (red). *N. meningitidis*= PF fixed at ratios of 1:1, 10:1 and 100:1 bacteria per cell (blue).

4.16 T-CELL SUPPRESSION INDUCED BY *N. MENINGITIDIS* IS PARTIALLY REVERTED BY IL-10 BLOCKING

Since section 4.15 demonstrated an elevated IL-10 production in those samples containing small inocula of meningococcus, it was necessary to address whether the suppression was IL-10-dependent.

For this set of experiments IL-10 blocking was achieved using a functional grade anti-IL-10 monoclonal antibody (αIL-10, eBioscence clone JES3-9D7), added directly to the wells containing αCD3 plus *N. meningitidis* at 1:1 bacteria per cell. Three different concentrations of αIL-10 were tested (5, 10, 20 μg/ml) and compared against the group without αIL-10 or the positive control (αCD3-stimulated and no bacteria).

Figure 4.24-A shows that addition of αIL-10 partially restored the inhibition of $CD4^+$ T lymphocytes. Even the smallest αIL-10 concentration of 5μg/ml was sufficient to significantly increase the division index of T-cells as compared with the group containing meningococcus but not αIL-10. However, IL-10 blocking was not sufficient to completely reverse the inhibition induced by *N. meningitidis* and a significant difference persisted against the positive control that did not contain bacteria.

On the other hand, expression of the T-cell activation marker CD25 was not significantly increased by any of the αIL-10 concentrations in comparison with the sample exposed to *N. meningitidis* but without IL-10 blocking (Figure 4.24-B).

The additional control stimulated with αCD3 and IL-10 did not significantly enhanced proliferation or activation of $CD4^+$ T-cells.

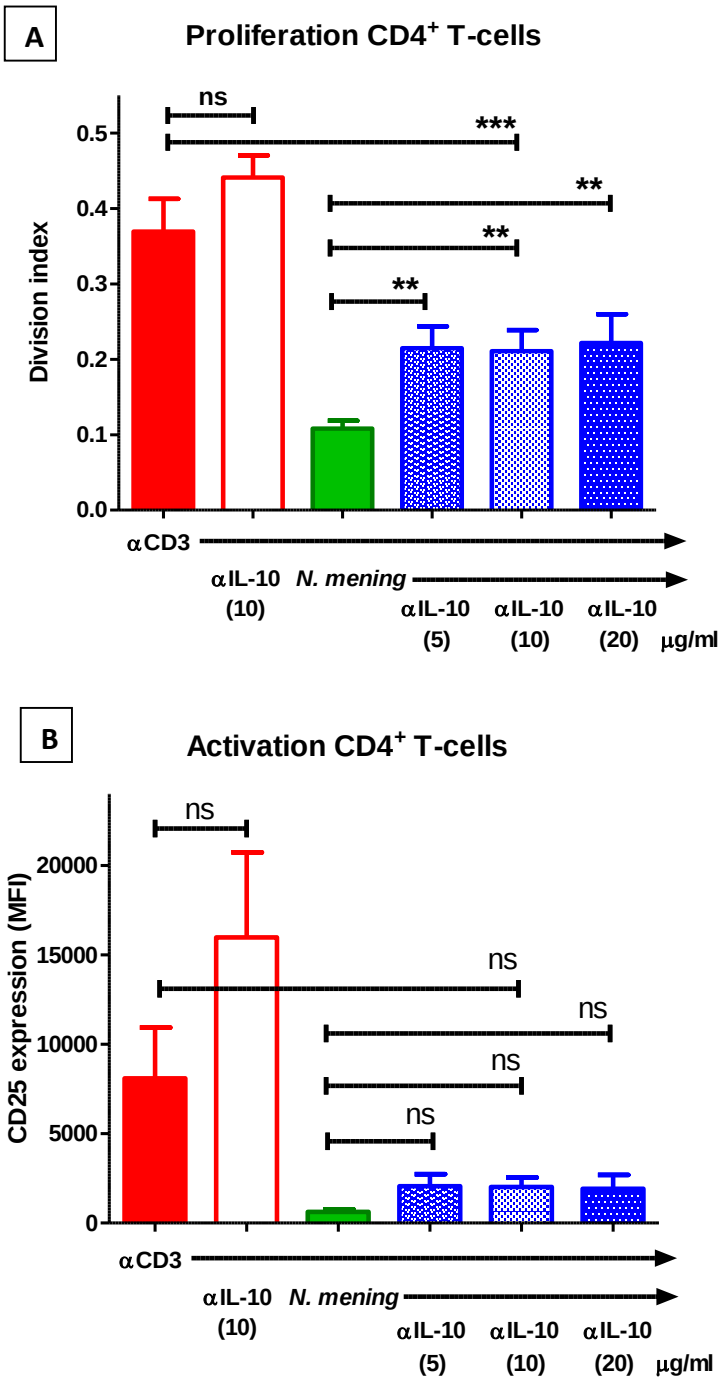

Figure 4.24: T-cell suppression induced by *N. meningitidis* was partially reverted by anti- IL-10 antibody.

A. Proliferation CD4⁺ T-cells, reported as division index. **B. Activation CD4⁺ T-cells**, expression of the CD25 marker as median fluorescence intensity (MFI). Bars represent means and SEM, n=6. Paired ANOVA, Bonferroni's Multiple Comparison Test. *$p \leq 0.05$, **$p \leq 0.01$, ***$p \leq 0.001$, ns= not significant. PBMCs were stimulated with αCD3 (plate-bound 0.2 µg/ml), in the presence of PF *N. meningitidis* (ratio 1:1) and one of the following: αIL-10 at 5, 10 or 20 µg/ml (blue bars). The group containing αCD3 only represents the positive control (red filled bar), while the group containing αCD3+*N. meningitidis* (ratio 1:1) (green filled bar) provides the baseline of suppression to compare against. The additional control sample containing αCD3+*N .meningitidis* + IL-10 at 10 µg/ml is also shown (red empty bar).

4.17 THE SUPPRESSIVE EFFECT IS NOT EXCLUSIVE TO *N. MENINGITIDIS*

We were particularly interested to determine whether the suppression phenomenon was exclusive to *N. meningitidis*. Therefore, we examined a different Gram negative organism and also a Gram positive organism in relation to the response observed with meningococcus (MC58 strain).

Over a period of 4 days, PBMCs were stimulated with plate-bound αCD3 in the presence of different bacterial counts of the Gram positive organism *Streptococcus pneumoniae*, wild type strain D39 (section 2.8.2) and the non-pathogenic Gram negative *Escherichia coli,* wild type strain ATCC 25922 (section 2.8.3).

As can be seen in Figure 4.25-A, *E. coli* had a very similar inhibitory trend in comparison to *N. meningitidis*. The smallest bacterial inoculums of 0.1 and 1 bacteria per cell were the most effective in reducing proliferation of $CD4^+$ T lymphocytes, whilst large inocula of 10 and 100 failed to stop cell division. Interestingly, the Gram positive organism *S. penumoniae* generated an inverse pattern, in which only large bacterial counts of 10 and 100 were capable of restraining T-cell proliferation.

A very similar pattern is reflected in Figure 4.25-B, again small bacterial inocula from *N. meningitidis* and *E. coli* induced a dramatic fall in T-cell activation. But again a different pattern was observed with *S. pneumoniae,* with the largest ratio of 100 bacteria per cell being the most effective in decreasing $CD4^+$ T-cell activation.

In summary, we have provided evidence to show that the suppressive effect is exhibited by bacteria other than *N. meningitidis (E.coli and S. pneumoniae),* although the resultant inhibition is dose sensitive and might vary among Gram positive and Gram negative organisms.

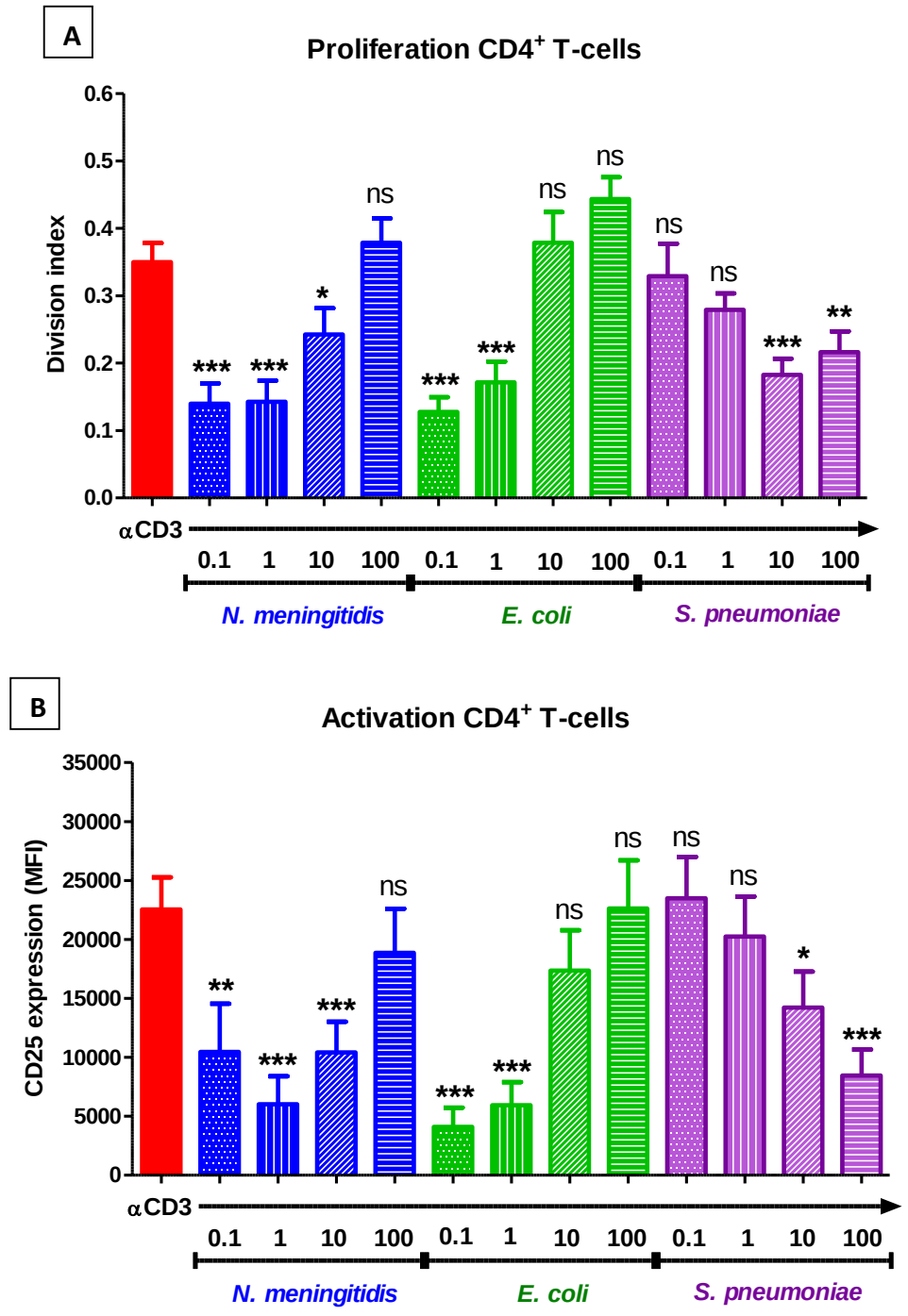

Figure 4.25: The suppressive effect is exhibited by bacteria other than *N. meningitidis (E.coli and S. pneumoniae),* although the resultant inhibition is dose sensitive and varies among organisms. A. Proliferation CD4⁺ T-cells, reported as division index. **B. Activation CD4⁺ T-cells**, expression of the CD25 marker as median fluorescence intensity (MFI). Bars represent means and SEM; n=9. Paired ANOVA, Dunnett's Multiple Comparison Test (*vs.* αCD3). *p= 0.01-0.05, **p= 0.001-0.01, ***p= ≤0.001, ns= not significant.

For 96 hours PBMCs were stimulated with plate-bound αCD3 (0.2 µg/ml) and exposed to PF fixed bacteria: *N. meningitidis* (blue bars), *E. coli* (green bars) or *S. pneumoniae* (purple bars). For all groups, ratios: 0.1:1, 1:1, 10:1 and 100:1 bacteria per cell. Red bar containing αCD3 and no bacteria is the positive control.

4.18 DISCUSSION

4.18.1 Main findings

Based on the findings from chapter 3 in which B-cell activation by TI type 2 mimics resulted in suppression of $CD4^+$ T-cell responses, the work described in this fourth Chapter intended to discover whether bacterial components or whole organisms that induce B-cell activity in a T-independent fashion could also restrain proliferation and activation of T lymphocytes.

We were able to demonstrate that paraformaldehyde fixed *N. meningitidis* is capable of inhibiting TCR-induced proliferation and activation of $CD4^+$ T-cells. A deep suppression of T-cell responses, comparable to the one observed with α-δ-DEX, occurred when αCD3-stimulated PBMCs where incubated with low bacterial counts (0.1:1, 1:1 and 10:1 bacteria per cell). However, in contrast with α-δ-DEX those bacterial inocula failed to trigger proliferation or activation of B lymphocytes (section 4.3.1). Interestingly, we found that incubation with a large bacterial count (100:1 bacteria per cell) results in a strong B-cell proliferation and activation but does not reduce proliferation or activation of $CD4^+$ T lymphocytes (section 4.3.1). It can be surmised that a large bacterial load enhances bystander pro-inflammatory activity among accessory cells and overcomes the inhibitory phenomenon. Overall, these findings suggest that the T-cell suppression observed in the presence of low numbers of *N. meningitidis* was not related to enhanced B-cell activity as seems the case for the TI-type II mimics, and so revealed the existence of another underlying mechanism of action. In support, no synergy was observed when α-δ-DEX and low counts of meningococcus were added together (section 4.3.2).

Since a range of 4.00-10.00 $x10^6$ leukocytes per ml is considered normal in human peripheral blood and from those around 40% are PBMCs, all our experiments performed with 1 $x10^6$ PBMCs per condition could offer a clinical insight regarding the different bacterial inocula used in these experiments. Hence, our ratio of 1:1 bacteria per cell (1 $x10^6$ bacteria) could be closely related to an MOI of 1 in relation to the number of PBMCs in 1 ml of blood. Moreover, our largest ratio of 100:1 bacteria per PBMC reflects the previously reported count of about 1 $x10^8$ *N. meningitidis* DNA copies per ml of plasma among patients with fulminant meningococcal septicaemia (Øvstebø et al. 2004). Of clinical relevance is the fact that the number of *Neisseria* DNA copies determined by quantitative PCR positively correlates with the severity and prognosis of systemic meningococcal disease (Darton et al. 2011; Øvstebø et al. 2004; Hackett et al. 2002).

Purified capsular polysaccharides were initially considered as the optimal model for B-cell TI type 2 activation and proliferation (Brunswick et al. 1988). However, it was later discovered that co-stimulatory pathways *via* TLR signalling, TCR cross-linking or certain cytokines were necessary to achieve Ig switching and full B-cell maturation (Peçanha et al. 1993; Peçanha et al. 1991). Recently, the Snapper group (Arjunaraja et al. 2012) discovered that polysaccharides present on whole heat inactivated meningococcus serotype C can elicit an *in vivo* primary T-independent response with mainly IgM secretion, but also a T-dependent like response with IgG secretion after secondary immunisation. They demonstrated TLR-4 involvement within the primary response, whilst CD40, CD28 and ICOS interactions were critical for the boosted secondary response. Together with other microorganisms' examples, such as *S. pnemoniae,* the expert group concludes that purified polysaccharides behave differently from those found on the surface of intact bacteria, which could trigger a late TD response due to covalent attachment to immunogenic outer membrane proteins (Snapper 2012).

In this chapter, we studied the role of polysaccharides by the use of two non-capsulated *Neisseria spp*: the non-pathogenic non-capsulated *N. lactamica*, and the capsule and Opa deficient mutant *N. meningitidis* strain ¢2. As shown in sections 4.6 and 4.7, in comparison with wild type *N. meningitidis*, capsule-lacking bacteria do not seem to reverse the detrimental effect on T-cells. Therefore it is unlikely that TI type 2 B-cell activation driven by capsular polysaccharides alone is responsible for the inhibition onCD4+ T lymphocytes.

The next question addressed for this work was related to *Neisseria* LOS and its immunogenic properties as endotoxin. Through binding with the complex CD14 TLR-4/MD-2 on antigen presenting cells and leading downstream NFkβ activation (Zughaier et al. 2004; Pridmore et al. 2003; Calvano et al. 2003; Pridmore et al. 2001), it is widely known that LOS is the main bacterial constituent to induce secretion of pro-inflammatory cytokines such as IL-1β, IL-6, IL-8 and TNF-α from monocytes and dendritic cells (Hellerud et al. 2008; Unkmeir, Kämmerer, et al. 2002; Kolb-Mäurer et al. 2001). In support of such specific and fast inflammatory response, a clinical association has been pointed out regarding the cocentration of LPS/LOS detected in plasma or cerebrospinal fluid and the severity of meningococcal disease in humans (Øvstebø et al. 2004; Brandtzaeg et al. 1989). Sprong et al. (2001) determined that 10 $x10^5$ meningococci (serogroup B wild type strain H44/76) will contain approximately 1ng of LPS and reports that bacterial counts of more than 10^7 will be the most potent stimuli for IL-1β and TNF-α production as compared with purified LPS and a LOS-deficient mutant.

In section 4.5 of this chapter, experiments performed with a LOS-deficient mutant (lpxA knockout) proved that even in absolute lack of LOS, small inocula of 1 and 10 bacteria per cell are still capable of restraining proliferation and activation of $CD4^+$ T-cells in the same fashion as the parental wild type strain. From this experiment it was also of relevance, the fact that the largest count of 100 LOS-deficient bacteria was still able to overcome the suppressive effect, refuting that LOS is responsible for a restoration in cell division and expression of the activation marker. Having said this, a large inoculum of this lpxA mutant ($10^7 – 10^8$ bacteria) should still induce some secretion of pro-inflammatory cytokines *via* TLR-2 rather than TLR-4/MD-2 (Zughaier 2011; Hellerud et al. 2008; Pridmore et al. 2001; Ingalls et al. 2001), presumably because of the presence of other outer membrane proteins (Pridmore et al. 2003).

Polysaccharides and LOS interact in conjunction and in strict regulation to escape from the immune system, and it can be postulated that the bacterium is adapted to suppress LOS-mediated immune activation to avoid recognition and killing. For example, meningococcal serogroup C capsular polysaccharide inhibits LOS-induced IL-6 and TNF-α secretion from monocytes, limiting CD14 availability and blocking NFκβ signalling (Kocabas et al. 2007). As compared with non-capsulated strains, encapsulated strains induce a weaker IL-6, IL-8 and TNF-α secretion by dendritic cells and monocytes (Kocabas et al. 2007; Unkmeir, Kämmerer, et al. 2002; Giardina et al. 2001). Therefore, although neither the capsule nor LOS appeared to be individually responsible for the T-cell inhibition observed in our system, these data should be interpreted with caution as we did not perform an experiment in which both capsule and LOS were absent.

Having excluded a direct involvement of meningococcal capsule and LOS within the inhibitory phenomenon, it was essential to investigate other bacterial components. Work published by Hellerud et al. (2008) and Sprong et al. (2001) is clear about non-LPS membrane structures that also contribute to cytokine production and TLR signalling with NFκβ activity. As discussed in sections 1.2.4 and 4.1, many *Neisseria spp.* outer membrane proteins have been recognised as immunogenic molecules and TLR agonists, so they have been suggested as possible vaccine candidates (Holst et al. 2009; Giuliani et al. 2006). PorB is the classical example of a strong specific TLR-2/TLR-1 ligand, providing intracellular signal transduction *via* NFκβ, Erk, Jnk, p38 phosphorylation and IL-8 secretion (Massari et al. 2006; Massari et al. 2002). In addition, the complex PorA/PorB has a synergistic immunogenic effect generating passive immunity (Marzoa et al. 2012). Other surface proteins that have proven induction of bactericidal antibodies include factor H binding protein (fHbp), *Neisseria* adhesin A (NadA) and *Neisserial* heparin binding antigen (NHBA), all discovered by the novel approach of reverse vaccinology (Giuliani et al. 2006) and now integrated into the 4CMenB vaccine (Serruto et al. 2012). Indeed, intact *Neisseria* outer

membrane vesicles (OMVs) which contain all those proteins across the outer membrane layer represent an excellent tool for studying immune responses.

This chapter explored whether purified *N. meningitidis* OMVs could have a similar inhibitory activity as the one observed with intact bacteria. Section 4.6 establishes that *Neisseria* vesicles contain the suppressive element and thus suggest an outer membrane location. Even in the presence of very low OMVs concentrations (from 0.001 μg/ml), a substantial detrimental effect was detected in proliferation and activation of $CD4^+$ T-cells. Moreover, heating of OMVs did not reverse the negative effect and implying that a heat stable factor is responsible. In parallel, the same experiment performed with *N. lactamica* OMVs resulted in a very similar pattern, restraining cell division of T lymphocytes and reducing expression of their activation marker from concentrations between 0.001 and 0.01 μg/ml. Since *N. lactamica* is a non-capsulated and non-pathogenic microorganism, we could propose that the immunosuppression observed is not related to the bacterial pathogenicity and certainly not to capsule or PorA expression, as they are both absent in *N. lactamica* (Troncoso et al. 2002; Kim et al. 1989).

After a literature search, only one publication was found to report suppression of T-cell responses by *Neisseria* OMVs. Our results are consistent with those of Lee et al. (2007), who observed a dose-dependent reduction of cell numbers and activation of TCR-stimulated $CD4^+$ T-cells in the presence of meningococcal and gonorrhoeal OMVs, over a period of 120 hours. However, their study was unable to detect the same phenomenon in those groups exposed to *N. lactamica* OMVs. It seems possible that this discrepancy is due to phenotypic differences among the outer membrane proteins present in the *lactamica* strain Y92 1009 that we both used. Vaughan et al. (2006) explains that some genes that encode outer membrane proteins such as Opa, are highly phase variable and so it can be expected that protein expression will vary from one batch of N*eisseria* OMVs to another. Perhaps, in our batch of *N. lactamica* OMVs the Opa frame-shift could have been `on` while for them it was `off`.

Gray-Owen's research group attributes such suppression of $CD4^+$ T-cells to binding of meningococcal Opa proteins to the cellular receptor CEACAM1 (carcinoembryonic antigen-related cell adhesion molecule 1) expressed on T-cells. Opa is a major adhesin located at the outer membrane of *Neisseria spp* and is involved in the contact with host cells and bacterial adherence (Sadarangani et al. 2011; Carbonnelle et al. 2009) (section 1.2.4.4). Opa has showed to elicit specific antibody production so is considered a good candidate antigen in vaccines against invasive meningococcal disease (Callaghan et al. 2011; Callaghan et al. 2006; Wiertz et al. 1996). In bacterial colonisation, Opa binds to CEACAMs expressed on epithelial cells and allows bacterial

trancytosis into the mucosal layer (section 1.2.2). CEACAM1 is a member of the Ig CEACAM super family and is the only one present in human lymphocytes. It contains two antagonist tyrosine residues at the cytoplasmic tail; the activation motif (ITAM) will induce positive signalling *via* tyrosine kinases, whilst the inhibitory motif (ITIM) binds to tyrosine phosphatases and blocks cell-activation cascades (Sadarangani et al. 2011). Thus, a dualistic role is attributed to this receptor and might be dependent on the CEACAM1 isoform expressed by the cell (Nagaishi et al. 2006; Chen & Shively 2004). Expression of CEACAM1 on $CD4^+$ T-cells is rapidly upregulated to the cell surface after TCR cross-linking and correlates with the degree of activation (Boulton & Gray-Owen 2002; Nakajima et al. 2002; Kammerer et al. 1998).

To our knowledge, Opa is the only protein within the *Neisseria* outer membrane layer that has been linked to a downregulation of TCR-induced $CD4^+$ T lymphocyte responses. Experiments carried out with whole gonococci and *N. gonorrhoeae* or *N. meningitidis* OMVs, have suggested that T-cell division and expression of the activation marker CD69 are restricted by an Opa-CEACAM1 interaction (Lee et al. 2007; Boulton & Gray-Owen 2002). A proposed explanatory theory is that cross-linking of CEACAM1 by Opa reclutes tyrosine phosphatases SHP-1 and SHP-2, leading to subsequent phosphorylation of ITIM and opposing T-cell activatiion (Lee et al. 2008; Chen & Shively 2004). However some published works have questioned such findings, as antibodies against Opa can enhance TCR-induced activation of T lymphocytes (Kammerer et al. 1998) and vaccines containing Opa elicit an immune response (Sadarangani et al. 2012; Callaghan et al. 2011). Recently, Youssef et al. (2009) has shown that a transitory suppression may occur, but at the end heat-killed gonococci and its OMVs will induce sustained $CD4^+$ T-cell proliferation and cytokine production irrespective of the presence or absence of Opa.

Based on such evidence and since Opa proteins are present in both *N. meningitidis* and *lactamica* (Toleman et al. 2001), we decided to investigate whether Opa-deficient meningococcus are still capable of limiting proliferation and activation of $CD4^+$ T-cells. Analysis of two *N. meningitidis* Opa-deficient strains (capsulated and non-capsulated) revealed a similar pattern to the wild type strain; proliferation and activation of T lymphocytes had a dramatic fall of between 50 to 75% among all groups exposed to small inoculums of Opa-deficient bacteria (section 4.7). Therefore, we have provided evidence to believe that Opa is not the key repressive element under our experimental conditions.

In order to clarify whether meningococcus acts directly on T lymphocytes, $CD4^+$ T-cells were enriched from PBMCs and exposed to what we had considered an inhibitory *N. meningitidis* load (ratio 1:1 bacteria per cell). In contrast to the experiments performed with whole PBMC, this assay

failed to restrain T-cell division or CD25 expression (section 4.8). Therefore, we conclude that *N. meningitidis* does not directly suppress $CD4^+$ T-cells.

Such finding differs from the ones published by Boulton & Gray-Owen (2002) who corroborated a reduction of cell division and expression of CD69 in TCR-stimulated purified $CD4^+$ T-cells after incubation with *N. gonorrhoeae* expressing a CEACAM1 specific-Opa. However, important differences can be pointed out between our assay and theirs; for example the use of live gonococci allowing infection for just 3 hours and the fact that they only observed T-cell inhibition with an inoculum larger than 50 bacteria/cell, reaching a maximal suppressive effect at 200 bacteria/ cell.

Other investigators have found that APCs can downregulate T-cells if primed with bacterial components. For example, Bryn et al. (2008), found that LPS treated monocytes restrain T-cells by induction of regulatory $Foxp3^+$ lymphocytes through a prostaglandin E_2-dependent mechanism. Similarly, exposure of dendritic cells to different MOIs of *N. gonorrhoeae* from 1 to 100 bacteria per cell and over a 24 hours period, results in a dose-dependent reduction of proliferation of purified T-cells when put in co-culture (Zhu et al. 2012). Increased IL-10 levels within supernatants and elevated PD-1 ligand expression on dendritic cells, suggested anergy and/or apoptosis induction as possible mechanisms of action (Zhu et al. 2012). In relation to the well known poor immunogenic properties of group B meningococcal polysaccharide, a recent publication found that murine B-cells treated with meningococcal polysaccharide suffered a blockade of NF-kβ, with downregulation of cyclophilin ligand interactor (TACI), B-cell activator factor (BAFFR) and the proliferation ligand (APRIL); all of which are key molecules involved in T-independent activation, Ig switching, maturation and survival of B lymphocytes (Kanswal et al. 2011). Thus, we aimed to investigate whether *N. meningitidis* could be affecting T-cells by first acting on APCs in our experimental model.

Co-culture experiments between enriched T lymphocytes and enriched B lymphocytes or monocytes were performed. Since priming of whole PBMC appeared to be essential to induce an α-δ-DEX-inhibitory phenotype on B lymphocytes (section 3.7), the same approach was taken in these assays. Thus, PBMCs were incubated with meningococci (1:1 bacteria cell) over a period of 24 hours before enrichment of $CD19^+$ and/or $CD20^+$ B-cells and $CD14^+$ monocytes. Sections 4.9 and 4.11 describe that co-culture of pure $CD4^+$ T lymphocytes with either primed B lymphocytes or primed monocytes do not reproduce the same negative phenomenon observed as with whole PBMCs. An overall reduction of cell division was clear, but this was independent of bacterial priming.

Since the responsible cell type could be difficult to discover by a co-culture approach, we then aimed for exclusion experiments in which B lymphocytes, monocytes and NK cells were depleted from PBMCs before incubation with meningococci.

Chapter 3 has already discussed in detail how B lymphocytes might acquire a repressive phenotype and downregulate TCR-induce T-cell activation. In this chapter, it was demonstrated that meningococci were still able to stop proliferation and activation even after removal of B lymphocytes (section 4.10). Indeed, it was concluded that B-cells are not implicated in the mechanism by which *N. meningitidis* suppresses $CD4^+$ T-cells.

Monocytes are essential in bridging innate and adaptive immune responses, by presenting antigens to T-cells and by secreting cytokines which stimulate T and B lymphocytes. From the total $CD14^+$ monocyte population, 10% of them will also express CD16 on their surface. This $CD16^+$ monocyte subset is known as inflammatory because secretes more TNF-α and less IL-10 as compared with the $CD16^-$ classical subset (Ziegler-Heitbrock et al. 2010; Geissmann et al. 2003). Indeed, $CD14^+$ $CD16^+$ monocytes have been associated with autoimmune diseases and severe bacterial infections (Ziegler-Heitbrock 2007). For example, expansion of $CD16^+$ monocytes has been reported in sepsis (Shalova et al. 2012; Fingerle et al. 1993). In addition, depletion of inflammatory monocytes in mice, resulted in ineffective T-independent B-cell activity towards pneumococcal polysaccharides and also $CD4^+$ T-dependent IgG response to pneumococcal proteins (Chen & Snapper 2013). The depletion protocol performed in this chapter selected and removed all $CD14^+$ monocytes and so $CD14^+$ $CD16^+$ cells were also excluded from the PBMC fraction. Under our experimental settings, *N. meningitidis* does not seem to depend on monocytes to exert its inhibitory effect, but a larger sample with a higher concentration of αCD3/αCD28 might be necessary to overcome the reduction on the baseline levels of T-cell proliferation and activation (section 4.12). From this experiment we were able to confirm that monocytes are required to induce T-cell responses to a large meningococcus inoculum. In comparison with whole PBMC, the monocyte depleted fraction did not show enhanced proliferation and CD25 expression after exposure to 100:1 bacteria per cell (section 4.12). Because monocytes will pick up several of the bacterial components *via* pattern recognition receptors, it was hypothesized that in the presence of large number of meningococci monocytes will become activated and will induce a pro-inflammatory state, activating bystander cells by cell contact and/or secretion of cytokines.

Similar to the T_H1 and T_H2 polarisation that derives from naive T helper cells (section 1.1.2.1), NK cells undergo differentiation in the presence of IL-2 or IL-4 into NK1 or NK2 subsets respectively (Peritt et al. 1998). NK1 are producers of IFN-γ, GM-CSF, TNF-α and LT; whilst NK2 produce less

IFN-γ but more IL-5 and IL-13 (Deniz et al. 2002; Peritt et al. 1998). Deniz et al. (2008) described a small fraction of NK cells more likely from the NK2 lineage which inhibit antigen specific $CD4^+$ T-cell proliferation. These regulatory NK cells were characterised by expression of inhibitory NK receptors (KIR, CD158a) and IL-10 production. Invariant NK T cells (iNKT) are a special subset of T-cells that express an invariant TCR α chain. iNKT are capable of recognising microbial glycolipid antigens, but they do not generate memory and lead to an innate-like response with secretion of IL-4 and IFN-γ (Kronenberg & Kinjo 2009). Moreover, iNKT express variable amounts of markers found classically on NK cells, such as CD56, CD16 and in particular CD161 (Montoya et al. 2007). iNKT cells become activated either by direct glycolipid recognition or by APCs which secrete cytokines after TLR engagement with bacterial components (Kinjo et al. 2011; Kronenberg & Kinjo 2009). iNKT cells may act as a bridge between the innate and adaptive systems because they can inhibit the response of $CD8^+$ T-cells (Goubier et al. 2013; Bjordahl et al. 2012) and neutrophils (Wintermeyer et al. 2009). The NK depletion experiment performed in this chapter, showed that removal of $CD56^+$ NK cells do not affect the suppression mechanism of action of *N. meningitidis.* Small bacterial counts (1:1 and 10:1) repressed proliferation of $CD4^+$ T-cells just as whole PBMC did (section 4.13)

From the above experiments we conclude that PBMCs act in a complex network to encounter and respond to microorganisms, so is not always easy to separate the individual cell contributions from the overall effect. For example, in an autoimmune murine model it was found that activation of B-cells *via* TLR-4 and TLR-9 using LPS from *E. coli*, CpG oligonucleotides or even heat-inactivated *Mycobacterium tuberculosis* suppress T-cell proliferation, but only when dendritic cells are also present (Lampropoulou et al. 2008). Indeed, the depletion experiments presented here may underestimate compensation scenarios driven by the remaining cell populations.

Since B lymphocytes, monocytes and NK cells were excluded as leading cells within the suppression mechanism, we investigated whether a soluble factor was being produced by whole PBMC in the presence of small inoculums of *N. meningitidis* and was responsible for the suppression phenomenon. However, transfer of supernatant rejected this possibility and advised a cell-contact dependent mechanism. Supernatant from PBMCs incubated with meningococci (ratio 1:1) for 24 hours, did not contain a soluble factor capable of restraining proliferation and activation of enriched $CD4^+$ T lymphocytes (section 4.14).This finding is consistent with most of the scientific evidence discussed herein, which mainly suggests cell-contact interactions among immune cells in response to bacterial antigens. However, because the supernatant used in this experiment was obtained only after 24 hours incubation with the bacterium, exists the possibility

that the suppressive factor is released at a later time point and that was not present in the 24 hour mixture.

A broad cytokine analysis from supernatants of PBMC cultures exposed to the different meningococci ratios, provided information about cytokines that could be mediating the suppression. Upon analysis of supernatants, many differences were found in the samples containing *N. meningitidis* counts ≤10:1 *versus* the highest ratio of 100:1 or the positive control containing αCD3 stimulation alone (section 4.15). Supernatants from PBMC cultures exposed to 0.1:1, 1:1 and 10:1 meningococcus per cell reported an overproduction of the pro-inflammatory cytokines IL-1β, IL-6 and the chemokine IL-8. Interestingly, levels of these 3 interleukins decreased with the largest meningococcus inoculum of 100:1. Concentrations of the classical T_H2 cytokines, IL-5 and IL-13, decreased dramatically in all samples containing meningococci irrespective of the size of the inoculum. On the other hand, IFN-γ and TNF-α production was strongly enhanced in the sample containing the largest bacterial inoculum (100:1). Using a whole blood model and a wild type *N. meningitidis* serogroup B strain, Hellerud et al. (2008) reported very similar patterns for TNF-α, IL-1β, IL-6 and IL-8 concentration in relation to a scale of 10^4 up to 10^8 bacteria per ml.

Indeed, *N. meningitidis* ratios equal to 1:1 but minor than 100:1 bacteria per cell induce a dominant T_H1 profile and block the T_H2 response (section 1.1.2.1). This T_H1 response might be required for macrophage stimulation and phagocytosis of the meningococci. Meningococcus induces dendritic cell maturation with expression of CD40 and CD86 and IL-12 production, which stimulates Th1 development (Dixon et al. 2001).

The most striking result is the large production of IL-10 in those samples containing bacterial counts of 1 and 10 bacteria per cell and so this finding remarks the possibility of an IL-10-mediated mechanism of suppression. During infectious diseases, the role of IL-10 is to keep an inflammatory balance and protect against uncontrolled responses against the pathogen. In septicaemia, in particular during the initial phase of fulminant meningococcal septic shock IL-10 levels are correlated with the severity of the inflammatory response (Bjerre et al. 2004; Derkx et al. 1995).

It has been widely discussed along this work the role of IL-10 as a pleiotropic anti-inflammatory cytokine, secreted mainly by monocytes, macrophages, Treg, Breg and T_H2 populations. IL-10 is a potent inhibitor of the most inducible pro-inflammatory interleukins and chemokines produced by T lymphocytes, monocytes, macrophages and neutrophils during inflammation. For example, IL-1β, IL-4, IL-6, IL-8, IL-12, IFN-γ and TNF-α are all down-regulated by IL-10 (Asadullah et al. 2003; Moore et al. 2001). Since IL-10 restrains the expression of co-stimulatory molecules on the surface of APCs, T-cell proliferation and secretion of T-cell cytokines are greatly affected (Asadullah et al.

2003). Moreover, IL-10 has been implicated in induction of endotoxin tolerance (Wolk et al. 2000) and T-cell un-responsiveness or anergy (Joss et al. 2000; Akdis & Blaser 1999). IL-10 also de-activates monocytes and enhances the presence of anti-inflammatory factors, such as IL-1 receptor antagonist (Moore et al. 2001; Cassatella et al. 1994). By blocking COX-2 gene expression, IL-10 blocks PGE_2 production and the subsequent extracellular matrix turnover by monocytes and macrophages (Niiro et al. 1995). In contrast, IL-10 acts as a stimulatory co-factor for B lymphocytes for proliferation, Ig production and survival (Kobayashi et al. 2002; Rousset et al. 1992). This chapter demonstrated that blocking of IL-10 using αIL-10 partially reverses the meningococcus-mediated inhibition of $CD4^+$ T-cell proliferation but not T-cell activation (section 4.16). A possible explanation is related to the fact that IL-10 only inhibits T-cell proliferation and cytokine secretion from those T lymphocytes stimulated *via* CD28, but not from the ones stimulated with CD3 alone (Joss et al. 2000; Akdis et al. 2000). IL-10 avoids tyrosine phosphorylation of CD28 (section 1.1.4.3) and therefore downstream activation (Joss et al. 2000; Akdis et al. 2000). In agreement, it is known that IL-10 blocks release of T_H1 and T_H2 cytokines after CD28 co-stimulation (Joss et al. 2000; Schandené et al. 1994). In conclusion, it might be the case that in our *in vitro* experiment IL-10 blocking resulted beneficial only for those T lymphocytes that established interactions with APCs *via* B7/CD28 molecules, and for those T lymphocytes that did not enter into an irreversible anergy state induced by IL-10.

Perhaps one of the major contributions of this chapter is the fact that the inhibitory effect is exhibited by bacteria other than *N. meningitidis* (section 4.17). Incubation with *E. coli* at counts of 0:1 and 1 bacteria per PBMC also caused a deep blockade on cell division and expression of the T-cell activation marker. Interestingly, a different pattern was observed with the Gram positive *S. pneumoniae.* The maximal inhibitory effect was obtained with an inoculum of between 10 and 100 *S. pneumoniae* per cell, indicating that T-cell down-regulation is dose-sensitive and possibly dependent on the bacterial Gram structure. In support, infection with the Gram negative *Salmonella enteric* serovar Typhi is a well documented case in which an inhibition of $CD4^+$ T lymphocytes occurs *in vitro* (Eisenstein 2001). Moreover, an *in vivo* model in mice has suggested that *Salmonella* only primes the immune system and generates an environment towards suppression, but that the real inhibitory signal and blockade of IL-2, IFN-γ and TNF-α production is evident only after exposure to a secondary combined stimulus of a flagellin peptide plus LPS (Srinivasan & McSorley 2007).

In summary, paraformaldehyde fixed *N. meningitidis* at ratios of between 0.1 and 10 bacteria per PBMC suppress TCR-mediated $CD4^+$ T cell proliferation and activation; induce a T_H1 response, suppress T_H2 cytokines and increase secretion of IL-10. Neither B lymphocytes nor monocytes nor

NK cells appear to be isolated cell types responsible for the inhibitory effect, and so the suppression may be the result of collective PBMCs interactions. Inhibition of $CD4^+$ T-cell responses *via* IL-10 seems to be only a partial mechanism of action. Therefore, other unknown down-regulatory processes might be taking place simultaneously. From the meningococci components, the capsule and LOS are not the inhibitory elements. The suppressive factor is contained inside *N. meningitidis* and *N. lactamica* outer membrane vesicles, and is not affected by temperature denaturalisation. To our knowledge, Opa is the only *N. meningitidis* component that has been reported to exert immunosupressor properties. However, meningococcus strains that lacked Opa expression were still capable of restraining T-cell responses in the *in vitro* model applied along this project. Finally, the suppression phenomenon is likely to be common to pathogens other than *N. meningitidis,* suggesting a critical component of bacterial pathogenesis involved in the `silent` colonisation of some mucosal surfaces.

CHAPTER 5:

ROLE OF NITRIC OXIDE IN TCR-INDUCED T-CELL RESPONSES

5.1 INTRODUCTION

Apart from the well known properties as vasodilator and bactericidal agent, nitric oxide (NO) is a pleiotropic intracellular messenger capable of *S*-nitrosylation of proteins (section 1.3.2). In particular, NO leads intracellular signals by activating the soluble guanylate cyclase, which converts GTP into cyclic GMP, a potent second messenger (Friebe & Koesling 2003). Thus, NO has been considered an important regulator of cell function and viability (Stamler et al. 2001). Published work has shown that nitrosylation/denitrosylation as a redox switch is dynamically regulated and can lead to activation of some proteins but inhibition of others (M. W. Foster et al. 2009; Hess et al. 2005). Thus, NO plays a role in several processes within cells, such as mitochondrial biogenesis (Nisoli et al. 2004), mitochondrial respiration and membrane potential (Brown 2001; Beltrán et al. 2000) and apoptosis *via* caspases (Mannick et al. 2001; Kim et al. 2001). NO is generated by the conversion of L-arginine to L-citrulline by a family of enzymes called nitric oxide synthases (NOS) (section 1.3.1). From these enzymes, the inducible NOS (iNOS) has been widely characterised for being responsible for NO production in macrophages, dendritic and natural killers cells; whilst the role of the endothelial NOS (eNOS) present in activated T lymphocytes has not been fully understood. The work of Nagy et al. (2003) and Ibiza et al. (2006) demonstrated NO production and eNOS expression in T-cells after TCR engagement with αCD3/αCD28 or superantigens, which leads to phosphorylation of the CD3ζ chain and ZAP-70 with subsequent downstream phosphorylation of the ERK pathway (section 1.1.4.4). The NO produced during the interaction between T lymphocytes and antigen presenting cells, acts on the redox-active Cys residue 118 of the Golgi-localised N-Ras protein, which becomes activated. N-Ras in turn causes activation of the ERK pathway, pushing the cell toward the cell death pathway (Lander et al., 1997, Ibiza et al., 2008).

Some publications focus on NO as an inhibitory molecule of T-cell responses. Reports have described that NO induces a reversible type of T-cell anergy, reducing phosphorylation of tyrosine residues in Jak3/STAT5, so T lymphocytes exposed to NO-producing cells, such as macrophages and myeloid suppressor cells, are unable to proliferate (Mazzoni et al. 2002; Bingisser et al. 1998; Strickland et al. 1996). Even in the presence of mesenchymal stem cells which generally suppress T-cell proliferation, addition of a NOS inhibitor restored not only the T-cell proliferation but also Stat5 phosphorylation (Sato et al. 2007). Macrophage-derived NO supports T-cell proliferation, but is also capable of repressing it as a regulatory feedback in the presence of Staphylococcal enterotoxins (Isobe & Nakashima 1992). In addition, balance of T_H1/T_H2 cytokines and the

resultant T-cell differentiation can be altered via cGMP depending on NO levels and its exposure time (Niedbala et al. 2006; Macphail et al. 2003). Studies have suggested that NO may regulate T-cell function but is not T_H1/T_H2 selective, neither for proliferation nor for cytokine production (Macphail et al. 2003; Bauer et al. 1997).

Infection by *N. meningitidis* and in particular some bacterial components such as lipooligosaccharide (LOS), trigger NO production in innate immune cells (section 1.2.6). However, the meningococcus can counteract the bactericidal effect of reactive nitrogen intermediates by a partial denitrification pathway (section 1.2.6.1), whereby the soluble nitrogen oxide nitrite (NO_2^-) is reduced into NO and finally expelled as N_2O (Berks et al. 1995). This mechanism allows *Neisseria* to not only avoid killing by NO-related compounds, but to supplement the microaerobic growth of the organism by utilisation of NO_2^- as a terminal electron acceptor (Anjum et al. 2002). In the NO-rich environment of the human nasopharynx, this pathway facilitates meningococcal survival and perpetuates the carrier state (Stevanin et al. 2005).

The regulation that NO exerts on T-cells in the presence of bacterial infections is a critical area which is under-investigated. Since *N. meningitidis* components stimulate NO production and NO is also produced as a result of T-cell activation, this chapter intended to study if NO donation or inhibition could have a suppressive effect on T lymphocytes and indeed explain part of the inhibitory phenomenon observed in Chapter 4. To our knowledge, there are few reports studying whether NO production after bacterial infection or *in vitro* exposure could lead to T-cell suppression. Immunosuppression has been observed in mouse models of *Salmonella* infection and NO has been attributed as a responsible compound. Immunisation with attenuated *Salmonella typhirnurium,* activates murine mature macrophages and induces a large production of NO, which results in profound suppression of T and B-cell responses to mitogens (al-Ramadi et al. 1992). During bacterial infections, IFN-γ secreted by T_H1 and NK cells is the major stimulus for NO production from macrophages (Ding et al. 1988). Consistently the NO-mediated inhibitory effect can be reversed by simultaneous addition of IL-4, anti-IFN-γ and a competitive inhibitor of NO production (al-Ramadi et al. 1992); or by depletion of NK cells producers of IFN-γ plus anti-IFN-γ (Schwacha et al. 1998). Similarly, macrophage-derived NO from mice chronically infected with *M. tuberculosis* ablated the proliferative response of $CD4^+$ T lymphocytes whilst blocking of NO synthesis restored T-cell responses in this animal model (Nabeshima et al. 1999).

5.2 METHODOLOGY

The same general methodology described in chapters 3 and 4 was applied. First, a buffy coat layer was obtained from fresh heparinised blood by density centrifugation (section 2.1). PBMCs were then washed, resuspended in RPMI media supplemented with 20% autologous plasma and stained with the proliferation dye CFSE (section 2.4). Ultimately, PBMCs were counted and added to 48-well plates at a density of $1x10^6$ cells per well in a final volume of 500 µl RPMI media supplemented with 20% autologous plasma.

T-cells were stimulated with 0.1-0.3 µg/ml plate-bound anti-CD3 (αCD3) (section 2.3.1.1), Concanavalin A (ConA) (section 2.3.1.2) or *Staphylococcus aureus* enterotoxin B (SEB) (section 2.3.1.3). Simultaneously, PBMCs were incubated in the presence or the absence of NO, using NOC-18 as NO donor (section 2.9.1) and the arginine analogs L-NMMA or L-NAME as inhibitors of NO production (section 2.9.2). The negative control for all experiments consisted of non-stimulated PBMCs, whereas the positive control was represented by the sample containing T-cell activators.

Cell cultures were incubated at 37°C and 5% CO_2 in a humidified atmosphere for 96 hours before harvesting. Extracellular immunofluorescence staining for flow cytometric analysis was performed by incubating $1x10^6$ PBMCs with the relevant antibodies (section 2.5.2).

A sequential gating strategy selected for the relevant T or B lymphocyte populations and excluded dead cells and monocytes (section 2.5.5). As in chapters 3 and 4, cell proliferation was assessed by the division index obtained from the CFSE dilution method; whilst T and B-cell activation were reported as median fluorescence index (MFI) of the surface markers CD25 and CD86, respectively.

Figure 5.1 illustrates a general overview of the experimental steps.

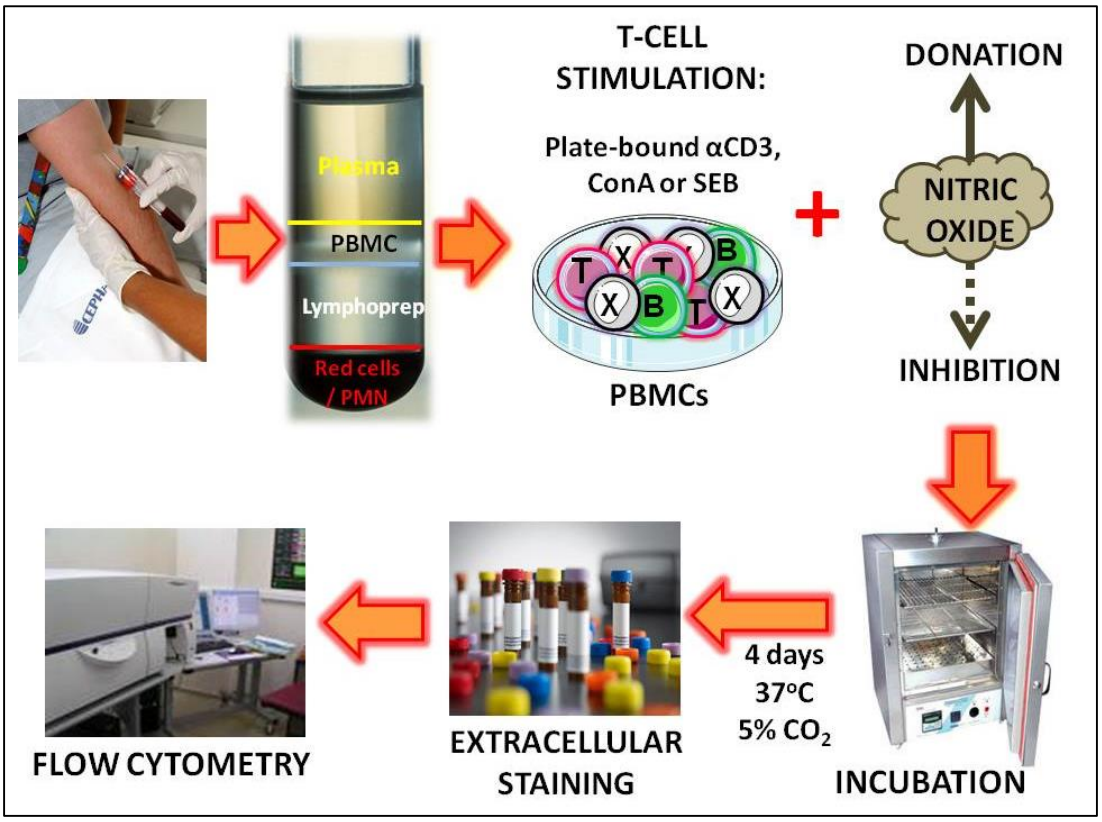

Figure 5.1: Overview of the experimental methodology applied in this chapter

Human PBMCs were isolated from fresh peripheral blood using Lymphoprep™ density gradient centrifugation. T-cell stimulation was achieved with anti-CD3 (αCD3), Concanavalin A (ConA) or *S. aureus* enterotoxin B (SEB). Simultaneously, PBMCs were incubated in the presence or the absence of NO, using NOC-18 as NO donor and L-NMMA or L-NAME as inhibitors of NO production. Cells were plated and incubated for 96 hours at 37°C and 5% CO_2. Finally, samples were stained with the desired fluorescently-labeled antibodies and analysed by flow cytometry.

5.3 NON-STIMULATED CD4$^+$ T-CELLS ARE UNRESPONSIVE TO NO DONATION OR INHIBITION

We first explored whether donation of NO or inhibition of its production could induce proliferation or activation in resting T-cells. Different concentrations of the NO donor NOC-18 (from 1.25 to 156 μM) or the NO synthase inhibitor L-NMMA (from 0.5 to 10 mM) were added to non-stimulated PBMCs and incubated for 96 hours before analysis.

Figure 5.2 illustrates that in the absence of stimulation, CD4$^+$ T lymphocytes are unresponsive to either NO donation or NO inhibition. Regardless of the concentration used, no change in the division index was observed after incubation with NOC-18 or L-NMMA. Similarly, expression of the T-cell activation marker CD25 remained unaffected in comparison with the negative control (data not shown).

The lack of response to NO donation and inhibition in resting T lymphocytes was anticipated, as the scientific evidence describes a major NO effect only after TCR cross-linking (section 5.1), Therefore, we next focus on assessing the role of NO in activated CD4$^+$ T-cells.

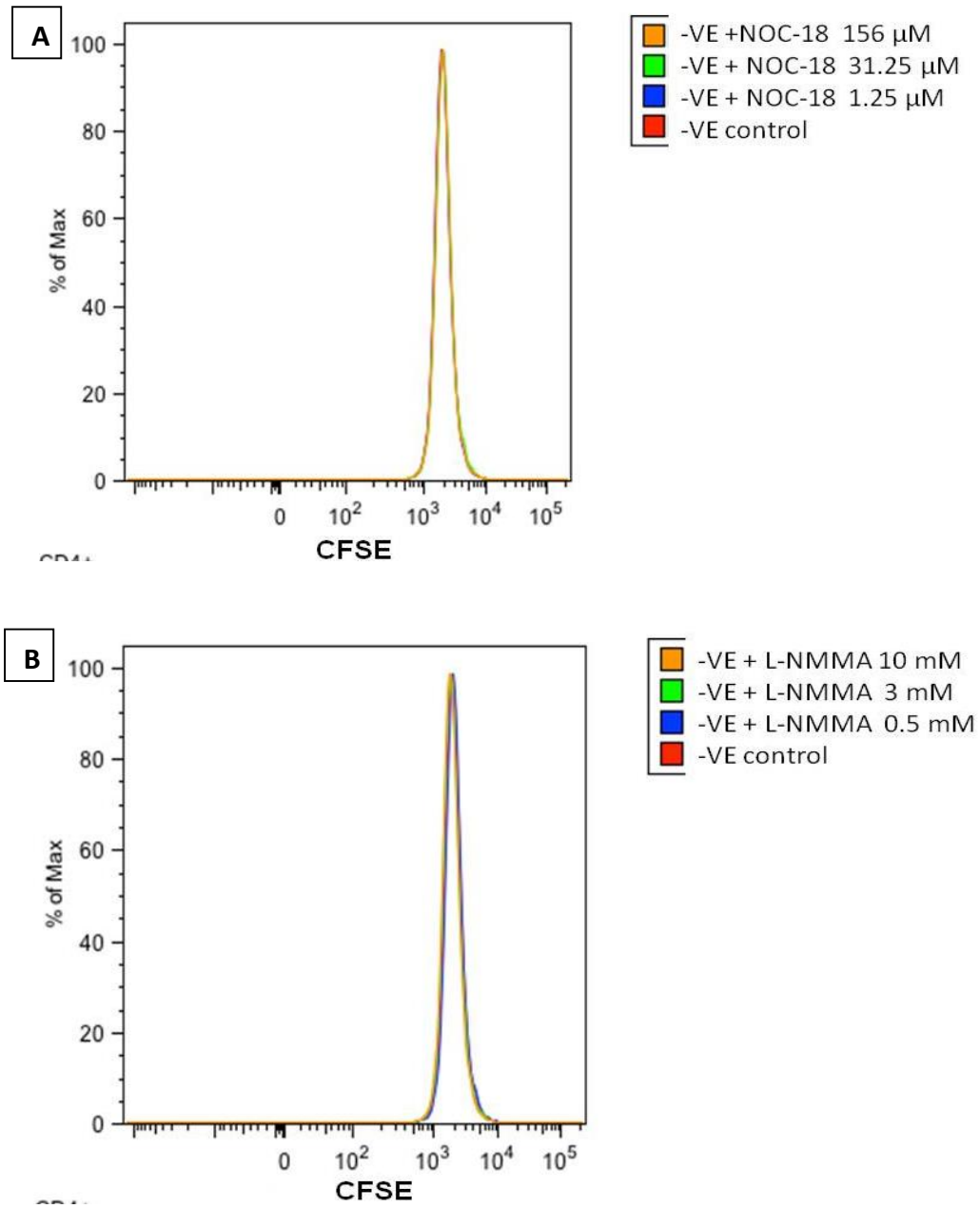

Figure 5.2: Representative proliferation histograms illustrating how non-stimulated CD4$^+$ T-cells are unresponsive to NO donation or NO inhibition.

Non-stimulated PBMCs were exposed to graded concentrations of the **NO donor NOC-18 (A)** and the **NO synthase inhibitor L-NMMA (B)**. Proliferation was assessed by the CFSE dilution method; the *x*-axis represents intensity of CFSE fluorescence and the *y*-axis % of maximum. Data is representative of two experiments.

-VE= negative control, non-stimulated PBMCs.

5.4 Effect of NO Donation in Activated T Lymphocytes

5.4.1 Selection of maximum possible concentration of NOC-18 as NO donor.

NOC-18 is a stable NO-amine complex which spontaneously releases 2 molecules of NO under cell culture conditions and has a half-life of 21 hours. Based on similar experiments with human lymphocytes using NOC-18 as NO donor (Fujiwara et al. 2006), we aimed to determine the maximum possible concentration of NOC-18 to use without inducing cell death in our assay.

PBMCs were stimulated with plate-bound αCD3 and incubated for 96 hours in the presence of graded concentrations of NOC-18. A dose curve from 5 to 1000 μM demonstrated that concentrations $\geq$500 μM reduce viability of αCD3-stimulated PBMCs, reflected by a marked loss of total cell numbers and a reduction in the percentage of live cells as measured by UV dead/live staining (Figure 5.3).

5.4.2 Effect of NO donation in T-cell proliferation.

Knowing that 300 μM was our maximum permitted concentration, cells were incubated with plate-bound αCD3 and graded amounts of NOC-18, from 1.25 to 312 μM. Although this exploratory assay did not find significant differences among the groups containing NOC-18 *versus* the αCD3 control, a dose-dependent pattern was observed towards an increment in division index of $CD4^+$ T-cells (Figure 5.4- A and B).

To assure a real influence of the NO donor in activated $CD4^+$ T lymphocytes, additional and larger experiments were carried out using αCD3, ConA and SEB as mitogenic stimuli. Due to the above results, 300 μM was chosen as the maximal optimal NOC-18 concentration capable of achieving an effect but without inducing cell death.

Although we observed a small increase in proliferation among individual samples containing the NO donor, there was no statistical evidence that NOC-18 enhanced proliferation of $CD4^+$ T-cells (Figure 5.4- C).

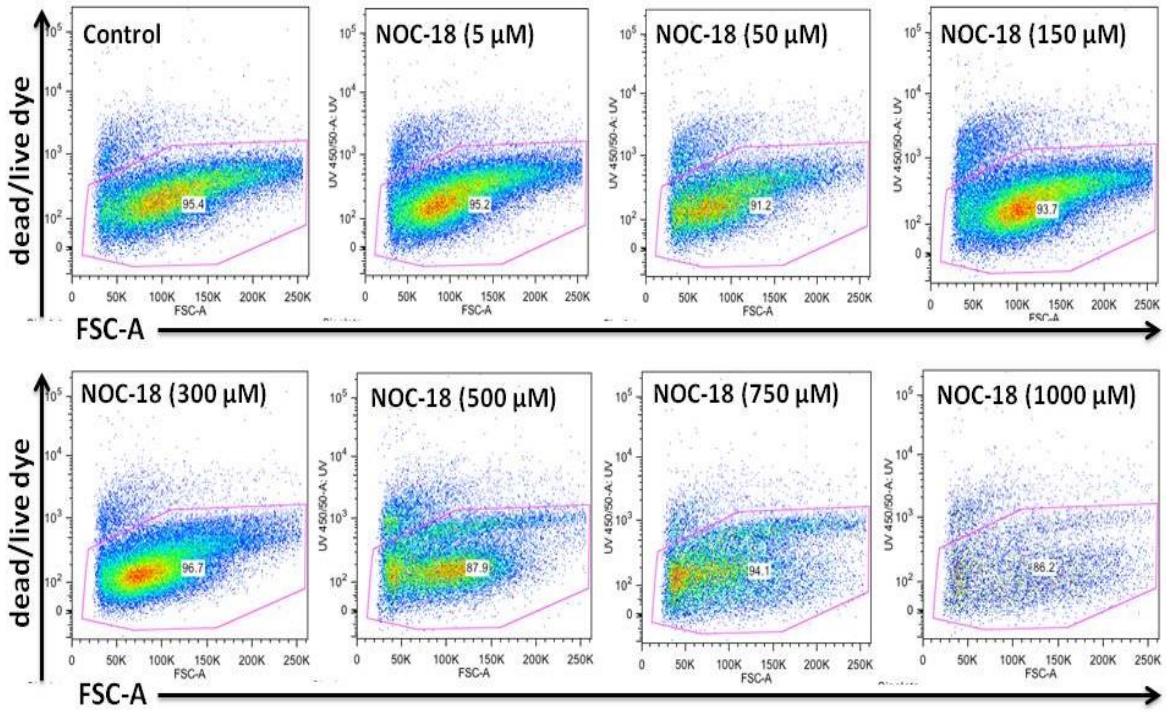

Figure 5.3: Concentrations of NOC-18 ≥500 µM induce cell death in αCD3-stimulated PBMCs.

Dot plot examples showing the dead/live gate applied for all conditions, on the *y*-axis fluorescence of the UV dead/live dye and on the *x*-axis FSC-A**.** Plots are representative of 1 single donor (out of 2 experiments) and show % of live cells within the gate.

αCD3-stimulated PBMCs were incubated with graded concentrations of NOC-18 (5, 50, 150, 300, 500, 750 and 1000 µM) over 96 hours.

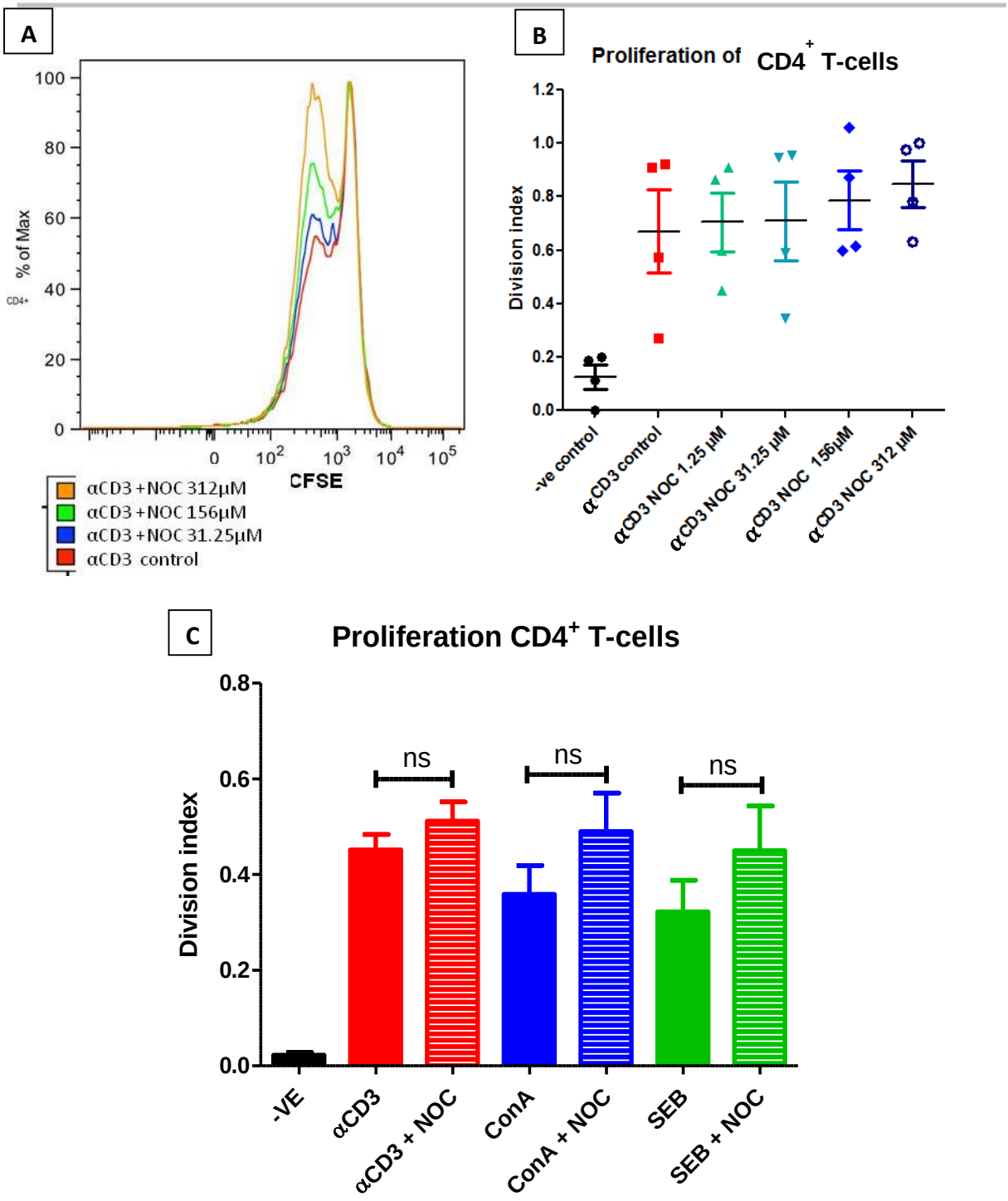

Figure 5.4: Effect of NO donation in proliferation of CD4⁺ T-cells.

A. Example of overlaid histograms illustrating T cell proliferation following incubation with αCD3 plus different NOC-18 concentrations. Proliferation assessed by the CFSE dilution method, *x*-axis represents intensity of CFSE fluorescence and *y*-axis % of maximum. **B. Proliferation CD4⁺ T-cells**, reported as division index. PBMCs were stimulated with αCD3 (0.1 μg/ml) plus graded concentrations of NOC-18. Means and SEM, n=4. **C. Proliferation CD4⁺ T-cells**, reported as division index. PBMCs were stimulated with either αCD3 (0.1 μg/ml), ConA (Concanavalin A, 5 μg/ml) or SEB (*S. aureus* enterotoxin B, 400 ng/ml); plus NOC-18 (300 μM) where indicated. Bars represent means and SEM, n=7. Paired ANOVA, Bonferroni's Multiple Comparison Test; ns= not significant.

5.4.3 $CD4^+$ T-cell activation is not significantly modified by NO donation.

Using the same experiment as the one performed in Figure 5.4-C, expression of the CD25 activation marker was also studied in the presence of NOC-18.

Supporting our previous observation on the effect of NO on T-cell proliferation, Figure 5.5-A shows that no significant differences were detected for the levels of T-cell activation among the groups containing the NO donor in comparison with the positive controls.

Even though CD25 is accepted as a good surface activation marker, Foxp3 was included as a secondary intracellular activation marker (section 2.5.3). Foxp3 is commonly used as a marker of T-regulatory cells, but it is also transiently expressed in human activated non-regulatory $CD4^+$ T lymphocytes just after TCR crosslinking (Wang et al. 2007). Foxp3 acts as an internal break in those activated cells, resulting in cellular hyporesponsiveness and reduction in the production of cytokines (Wang et al. 2007). In comparison with the sample containing αCD3 alone, Figure 5.5-B show data demonstrating that addition of NOC-18 does not modify Foxp3 expression within $CD4^+$ T-cells.

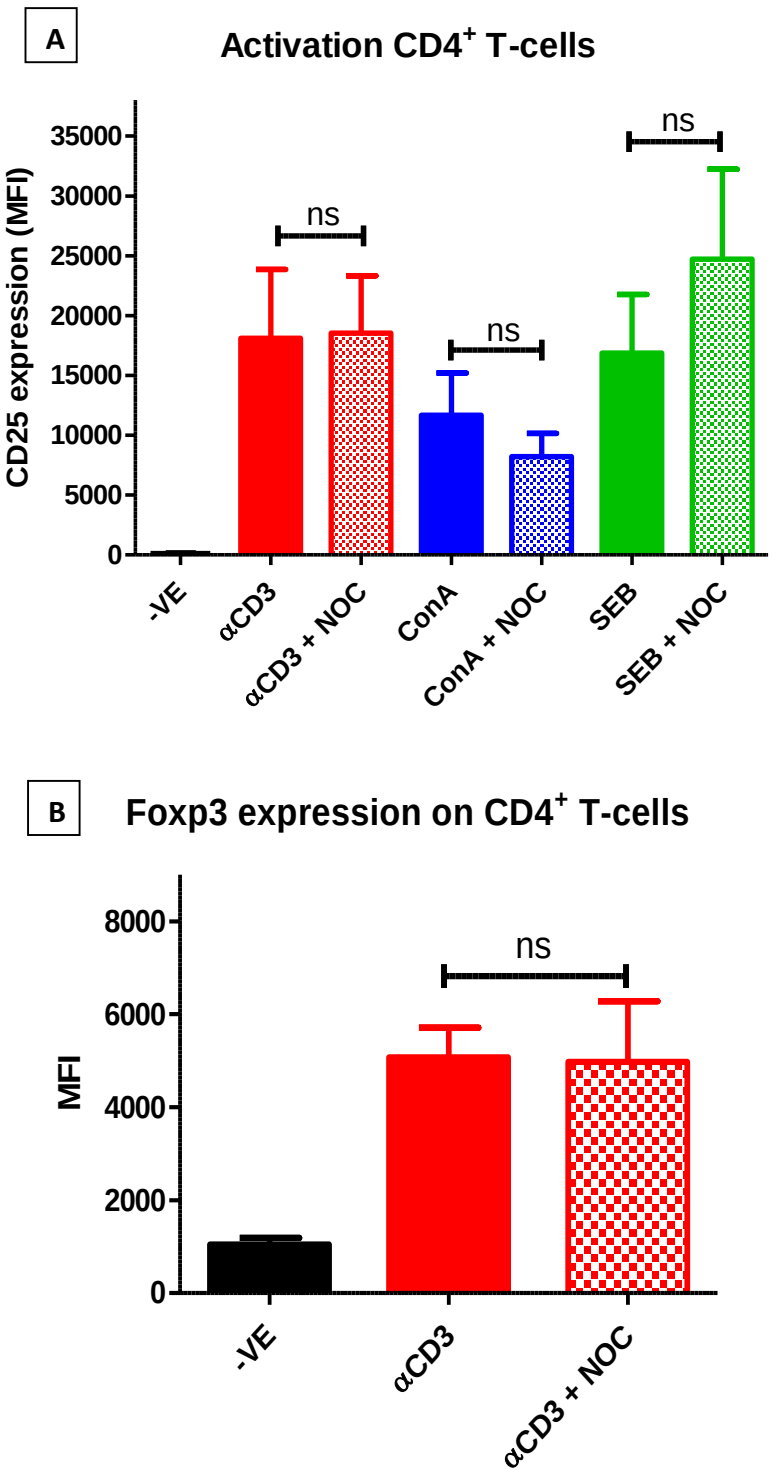

Figure 5.5: T-cell activation is not significantly modified by NO donation.

A. Activation CD4⁺ T-cells by expression of the CD25 marker, reported as median fluorescence intensity (MFI). PBMCs were stimulated with either αCD3 (0.1 µg/ml), ConA (Concanavalin A, 5 µg/ml) or SEB (*S. aureus* enterotoxin B, 400 ng/ml); plus NOC-18 (300 µM). Bars represent means and SEM, n=7. Paired ANOVA, Bonferroni's Multiple Comparison Test; ns= not significant. **B. Foxp3 expression in CD4⁺ T-cells,** reported as median fluorescence intensity (MFI). PBMCs were stimulated with αCD3 (0.1 µg/ml) plus NOC-18 (300 µM) where indicated. Bars represent means and SEM, n=7. Paired *t*-test (two tailed); ns= not significant.

5.5 INHIBITION OF NO PRODUCTION IN TCR-STIMULATED T LYMPHOCYTES

5.5.1 Selection of L-NAME as NOS inhibitor.

We next examined whether inhibition of NO production could affect TCR-induced T-cell responses. For this purpose, two L-arginine analogues (L-NMMA and L-NAME) were selected as inhibitors of NO synthases (NOS). L-arginine analogues inhibit NOS activity by competing for uptake with L-arginine in the binding site on the NOS enzyme (section 2.9.2).

Preliminary assays were performed on PBMCs stimulated with αCD3 and exposed to graded concentrations of L-NMMA (1.5, 3 and 10 mM) for 96 hours. As can be seen from Figure 5.6-B, the largest amount of L-NMMA resulted in a significant reduction in the division index of $CD4^+$ T lymphocytes in comparison with the αCD3 control.

Based on the assumption that eNOS is the predominant NOS expressed within T-cells after TCR crosslinking (Ibiza et al. 2006; Nagy et al. 2003), L-NMMA was replaced by L-NAME, which has a 10-fold higher affinity for the constitutive isoforms eNOS and nNOS than for iNOS (Danilov et al. 2005). Similar to the effect seen with L-NMMA, a small experiment on αCD3-stimulated PBMCs demonstrated that L-NAME was also capable of restraining proliferation of $CD4^+$ T-cells in a dose dependent manner (Figure 5.6-C).

5.5.2 $CD4^+$ T-cell proliferation is suppressed by blockade of NOS activity.

In order to confirm these initial findings, a subsequent and larger experiment was carried out. PBMCs were stimulated with either αCD3, the T-cell mitogen ConA or the superantigen SEB and incubated for 4 days in the presence of L-NAME at a concentration of 10mM. Figure 5.7 corroborates that the groups containing L-NAME suffered a drop in the division index of $CD4^+$ T lymphocytes of at least 50%.

Next, we wanted to know whether the suppression induced by L-NAME was evident from the beginning of the proliferative stage. Thus, four time points were investigated along the incubation period: 24, 48, 72 and 96 hours. Surprisingly, a significant difference was detected as early as 48 hours for the groups containing L-NAME (10mM) in comparison with our positive controls stimulated with αCD3 or SEB (Figure 5.8).

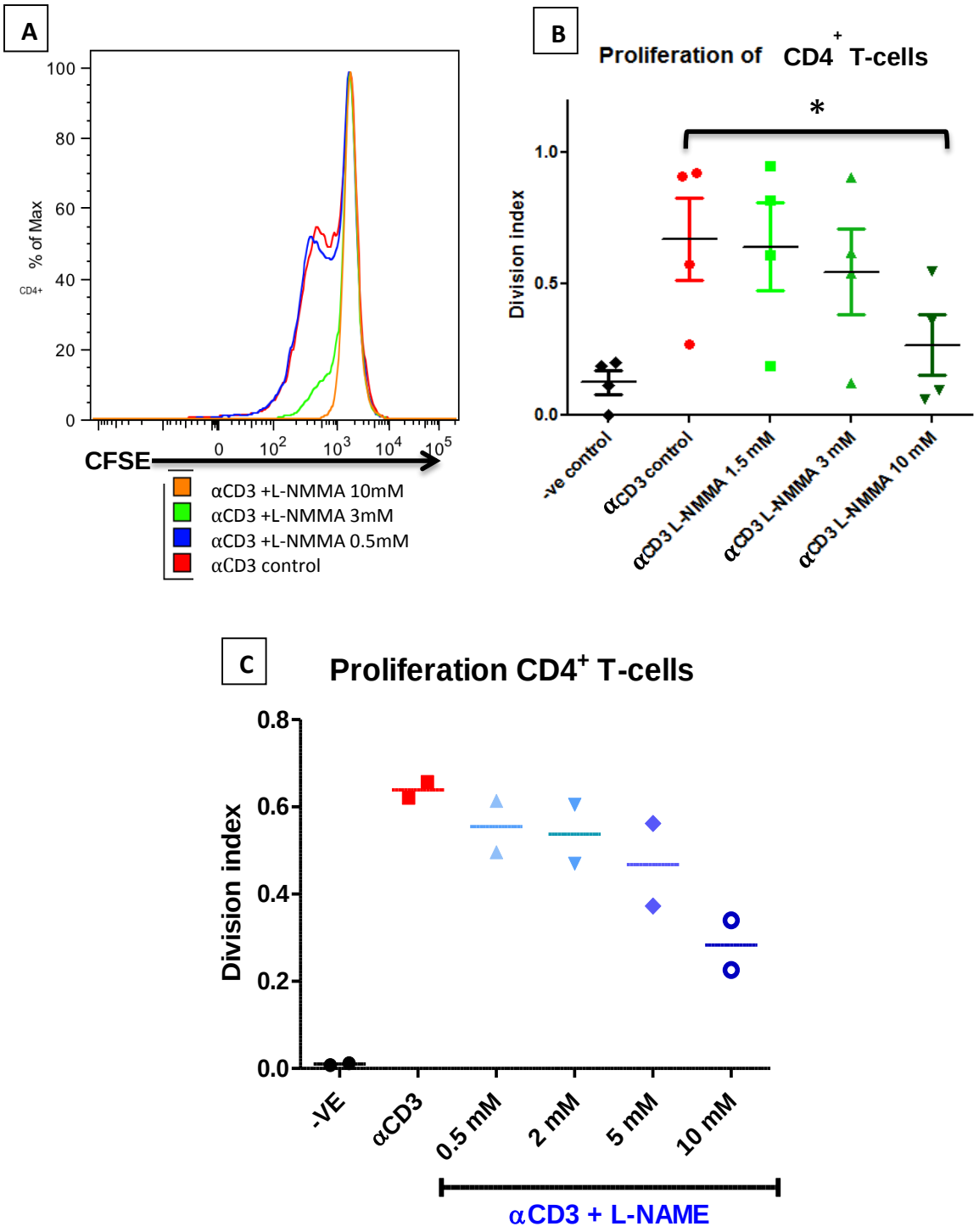

Figure 5.6: Inhibitors of NO synthases have a negative effect on T-cell division.

A. Example of overlaid histograms illustrating T-cell proliferation following incubation with αCD3 plus different L-NMMA concentrations. Proliferation assessed by the CFSE dilution method, *x*-axis represents intensity of CFSE fluorescence and *y*-axis % of maximum. **B. L-NMMA reduces proliferation of CD4⁺ T-cells in a dose dependent manner,** reported as division index**.** PBMCs were stimulated with αCD3 (0.1 µg/ml). Means and SEM, n=4. Paired ANOVA, Dunnet's Multiple Comparison Test (*vs* αCD3); **p* ≤0.05. **C. L-NAME reduces proliferation of CD4⁺ T-cells in a dose dependent manner,** reported as division index**.** PBMCs were stimulated with αCD3 (0.1 µg/ml). Means and SEM, n=2. -VE= negative control, non-stimulated PBMCs.

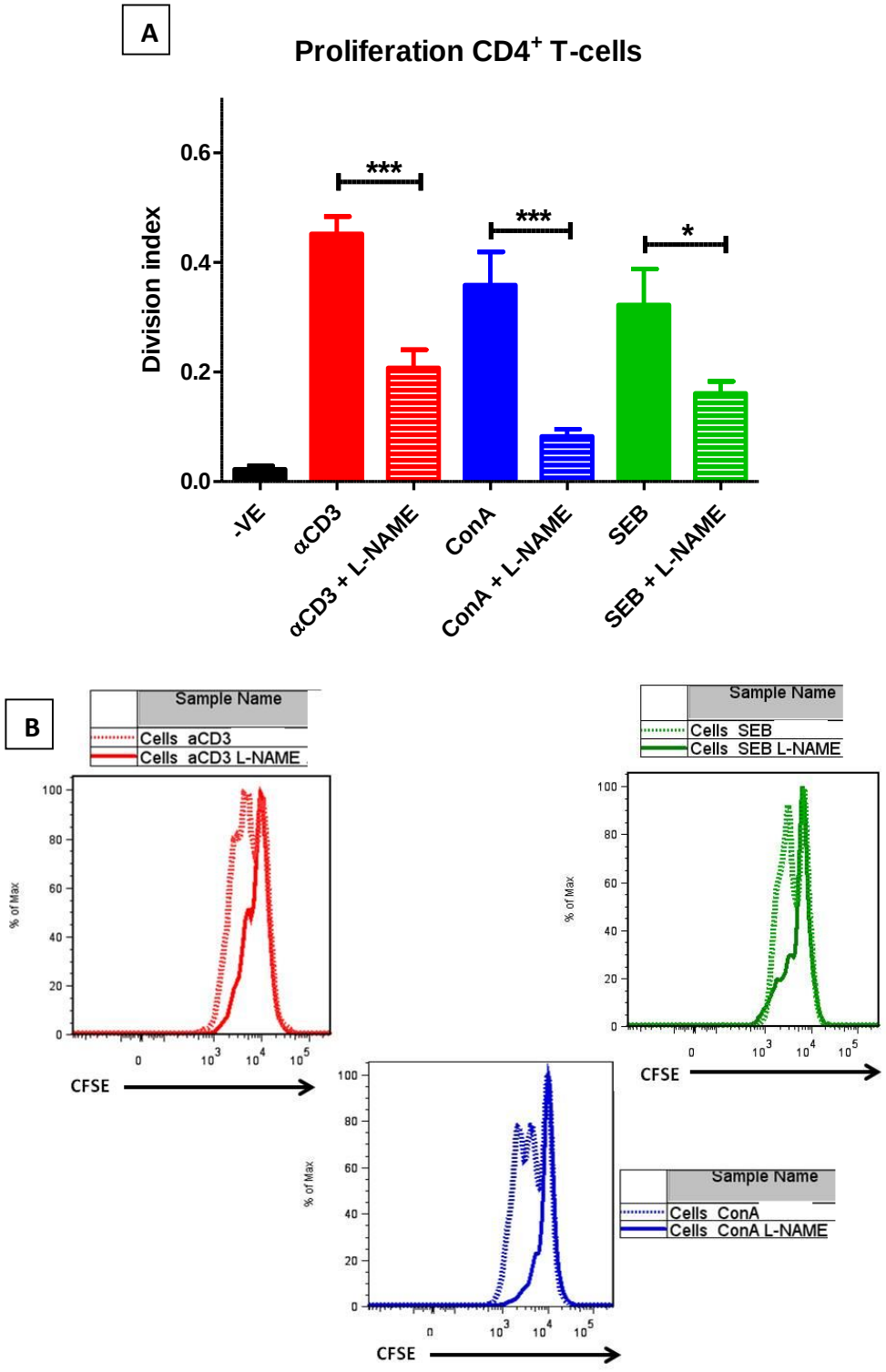

Figure 5.7: CD4⁺ T-cell proliferation is suppressed by L-NAME.

A. Proliferation CD4⁺ T-cells, reported as division index. PBMCs were stimulated with either αCD3 (0.1 µg/ml), ConA (5 µg/ml) or SEB (400 ng/ml); plus/minus L-NAME (10 mM). Bars represent means and SEM, n=7. Paired ANOVA, Bonferroni's Multiple Comparison Test; *$p \leq 0.05$, **$p \leq 0.01$, ***$p \leq 0.001$. -VE= negative control, non-stimulated PBMCs. **B. Representative examples of overlaid histograms illustrating T cell proliferation following stimulation with αCD3, ConA or SEB, plus/minus L-NAME** (10 mM). Proliferation assessed by the CFSE dilution method, *x*-axis represents intensity of CFSE fluorescence and *y*-axis % of maximum.

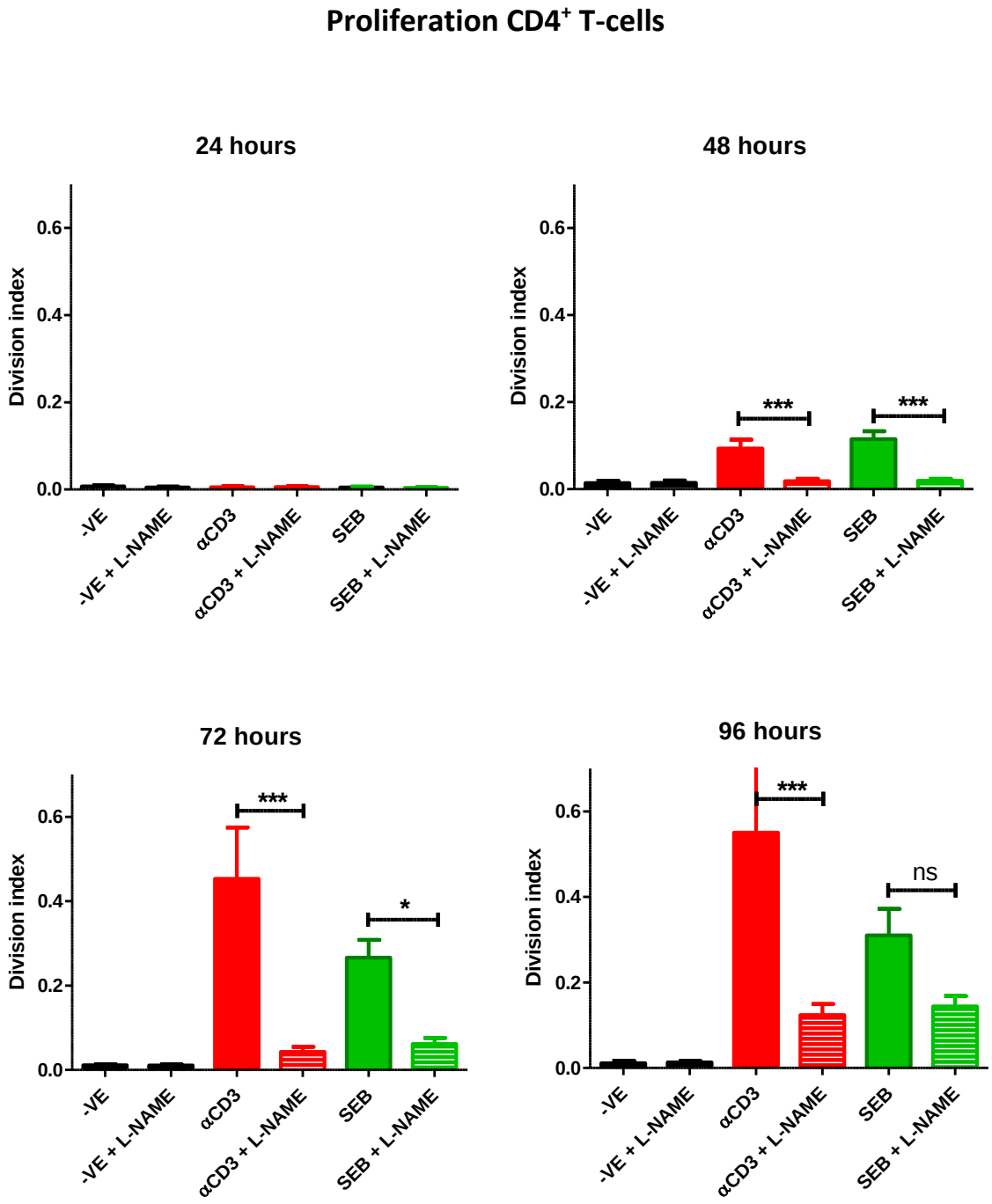

Figure 5.8: T-cell proliferation is suppressed from an early stage in the presence of L-NAME.

Proliferation of $CD4^+$ T-cells, reported as division index and at four time points (24, 48, 72 and 96 hours post-stimulation). PBMCs were stimulated with either αCD3 (0.1 µg/ml) or SEB (400 ng/ml); plus/minus L-NAME (10 mM). Bars represent means and SEM, n=6. Paired ANOVA, Bonferroni's Multiple Comparison Test; *$p \leq 0.05$, **$p \leq 0.01$, ***$p \leq 0.001$, ns= not significant.

-VE= negative control, non-stimulated PBMCs.

5.5.3 The inhibition in T-cell proliferation induced by L-NAME is partially reversed by simultaneous exposure to NOC-18.

In order to establish whether the suppression observed in activated $CD4^+$ T-cells was indeed the result of NO deprivation in the system, a complementation assay was designed. PBMCs were incubated with αCD3 plus L-NAME and in the presence of different NOC-18 concentrations (from 50 to 300 μM) for 4 days.

From data in Figure 5.9 it can be seen that the significant reduction between the αCD3 positive control and the group containing L-NAME disappears when NOC-18 is added to the culture at concentrations of 150 and 300 μM. However, such samples were not statistically different in comparison with the sample αCD3 + L-NAME.

Although different possibilities could be inferred for this phenomenon (discussed in section 5.8), this experiment cannot provide conclusive evidence that NO donation with NOC-18 can fully overcome the suppression induced by L-NAME.

5.5.4 L-NAME significantly restrains activation of SEB-stimulated $CD4^+$ T-cells.

Expression of the surface activation marker CD25 was not decreased among all of the stimulated groups. Whilst L-NAME exposure did not cause a significant reduction in CD25 expression on PBMC samples activated with αCD3 and ConA, cells incubated with SEB and L-NAME showed a significant fall in CD25 expression (Figure 5.10-A).

Regarding Foxp3 expression in αCD3-stimulated $CD4^+$ T lymphocytes; this intracellular marker remained unaffected when L-NAME was added to the culture (Figure 5.10-B).

Overall, these findings suggest that T-cell activation might not be heavily influenced by NO levels.

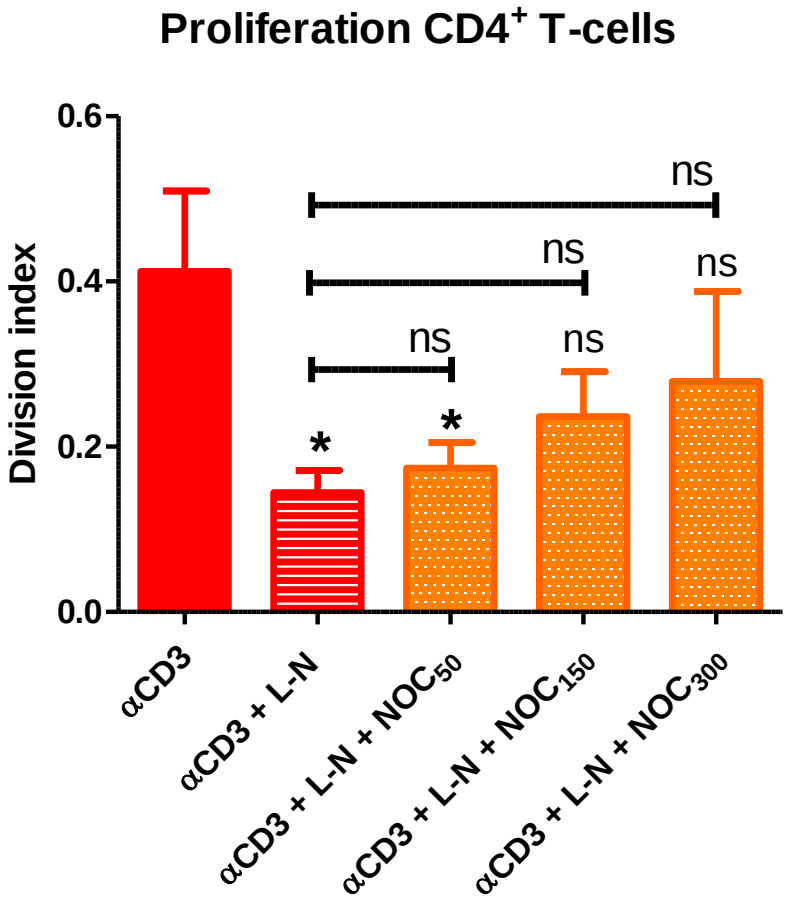

Figure 5.9: The inhibition of T-cell proliferation induced by L-NAME is partially reversed by simultaneous exposure to NOC-18.

Proliferation CD4⁺ T-cells, reported as division index. PBMCs were stimulated with αCD3 (0.1 µg/ml) and incubated for 4 days in the presence of L-NAME (10 mM) plus NOC-18 at different concentrations (50, 150 and 300 µM). Bars represent means and SEM, n=4. Paired ANOVA, Bonferroni's Multiple Comparison Test; *$p \leq 0.05$, ns= not significant.

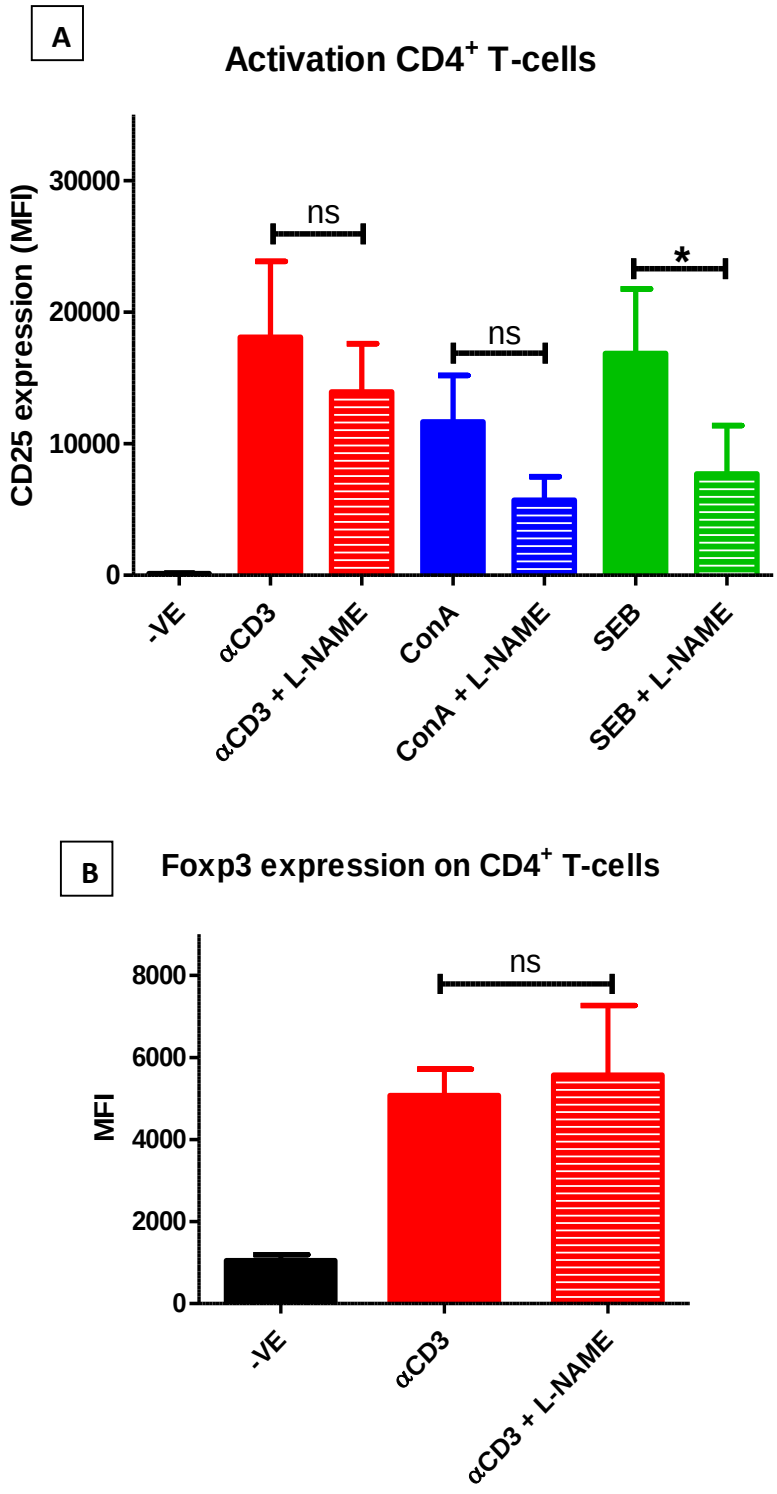

Figure 5.10: L-NAME significantly restrains CD25 expression in SEB-stimulated CD4⁺ T-cells.

A. Activation CD4⁺ T-cells by expression of the CD25 marker, reported as median fluorescence intensity (MFI). PBMCs were stimulated with either αCD3 (0.1 µg/ml), ConA (Concanavalin A, 5 µg/ml) or SEB (*S. aureus* enterotoxin B, 400 ng/ml); plus L-NAME (10 mM). Bars represent means and SEM, n=7. Paired ANOVA, Bonferroni's Multiple Comparison Test; *$p \leq 0.05$, ns= not significant. **B. Foxp3 expression in CD4⁺ T-cells,** reported as median fluorescence intensity (MFI). PBMCs were stimulated with αCD3 (0.1 µg/ml) plus L-NAME (10 mM) where indicated. Bars represent means and SEM, n=7. Paired *t*-test (two tailed); ns= not significant.

5.6 VIABILITY ASSAYS

To exclude that the reduction in T-cell proliferation observed among the samples containing the NO inhibitor was due to induction of cell death, a UV dead/live dye was included in each experiment. At 96 hours post-incubation, Figure 5.11 shows that none of the groups containing L-NAME had a higher percentage of cell death as compared with the respective positive controls (αCD3, ConA and SEB). Moreover, addition of L-NAME resulted in a positive effect for SEB stimulated cells, decreasing the % of cell death.

The UV dead/live dye used in these experiments is a general measurement of cell death, incapable of discriminating among cell populations or detecting cells that have recently entered into apoptosis. Thus, a more thorough approach was taken by performing a viability assay with TO-PRO-3 and Annexin-V, which are used to discriminate between apoptotic and necrotic cells (section 2.6.1). Cells staining positive for both Annexin-V and TO-PRO-3 are considered necrotic or late apoptotic, whilst Annexin-V positive but TO-PRO-3 negative are classified as early apoptotic populations. To further evaluate cell death that could be undetectable at 96 hours but happening at earlier stages, 3 more time points were investigated along the 4 days of incubation (24, 48 and 72 hours) (Figure 5.12). αCD3 and SEB were selected as T-cell stimuli for this set of experiments.

Although a statistical analysis was not possible with a small sample size (n=2), all groups containing L-NAME had a higher percentage of $CD4^+$ T-cell death after incubation for 24 hours, characterised by a double positive population for Annexin-V and TO-PRO-3 (data not shown). At 48, 72 and 96 hours post-stimulation, the difference between activated αCD3 and SEB samples and those also treated with L-NAME were small. In contrast, the level of cell death in L-NAME treated but non-stimulated PBMCs was much higher compared to the non-stimulated control group (Figure 5.12). The results are expressed as total % of $CD4^+$ T-cell death (Annexin V^+, TO-PRO-3^+ and double positives) for every time point.

Since these data suggested that inhibition of NO production using L-NAME may have an early cytotoxic effect on non-stimulated and activated $CD4^+$ lymphocytes, we wondered whether the increase in cell death was due to the lack of NO within the system, or if the observed phenomenon was due to cytotoxicity of L-NAME at the concentrations used in these experiments. To investigate the possibility that the observed cell death was due to a change in NO concentrations in this system, samples containing both L-NAME (10 mM) and the NO donor NOC-18 (150 µM and 300 µM) were analysed with the Annexin-V / TO-PRO-3 assay. As shown in Figure 5.13, addition of NOC-18 has no effect on the percentage of cell death observed in the presence of L-NAME, not at

24 or 96 hours post-incubation; and irrespective of whether the PBMCs were non-stimulated or αCD3-activated. However, only 2 samples per group were analysed and in comparison with the previous Annexin-V / TO-PRO-3 experiment (Figure 5.12) we did not find the marked cell death on the groups containing L-NAME after 24 hour incubation. Therefore, we concluded that larger sample sizes are necessary to determine whether the resultant increase in cell death induced by L-NAME is NO-mediated.

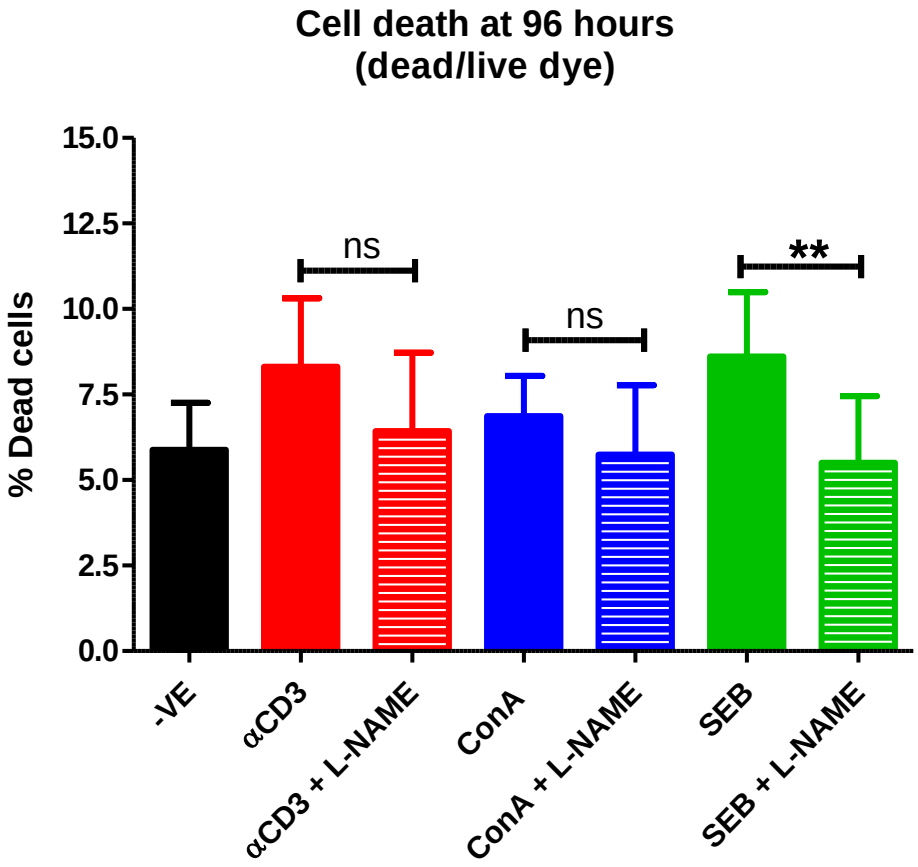

Figure 5.11: L-NAME treatment does not induce cell death and has only limited effects on stimulated CD4⁺ T-cell viability at 96 hours.

Percentage of dead cells (not within the live cells gate) applying the basis of the UV dead/live dye. PBMCs were stimulated with either αCD3 (0.1 µg/ml), ConA (5 µg/ml) or SEB (400 ng/ml); plus/minus L-NAME (10 mM) over 4 days. Bars represent means and SEM, n=7. Paired ANOVA, Bonferroni's Multiple Comparison Test; *$p \leq 0.05$, **$p \leq 0.01$, ns= not significant.

-VE= negative control; non-stimulated PBMCs.

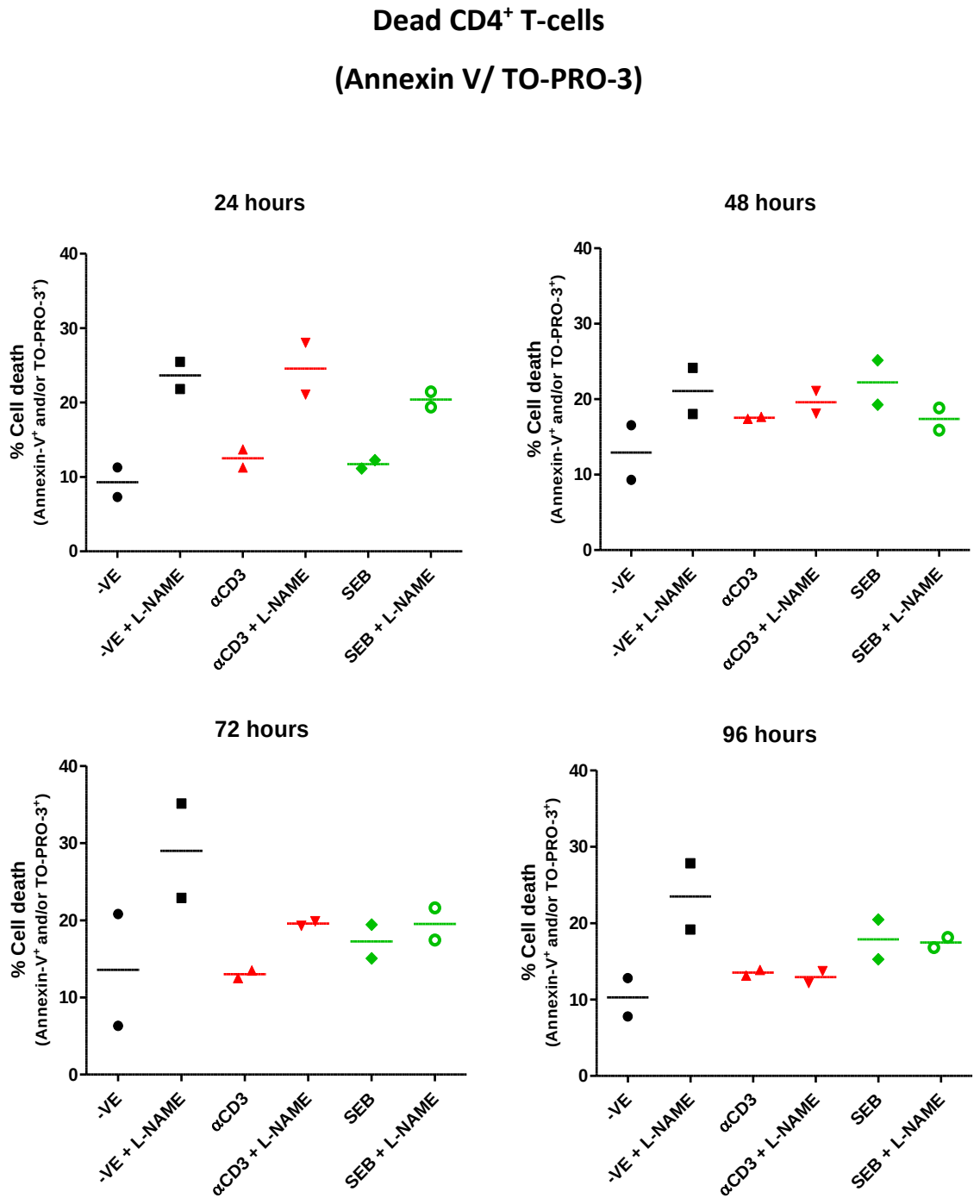

Figure 5.12: Percentage of CD4$^+$ T-cell death induced by L-NAME after 24, 48, 72 and 96 hour incubation, detected by an Annexin-V / TO-PRO-3 assay.

Non-stimulated and αCD3 (0.1 µg/ml) or SEB (400 ng/ml) activated PBMCs were exposed to L-NAME (10 mM). CD4$^+$ T-cell death was quantified as Annexin-V$^+$, TO-PRO-3$^+$ or double positives, at 24, 48, 72 and 96 hours. Results are expressed in % and means; n= 2.

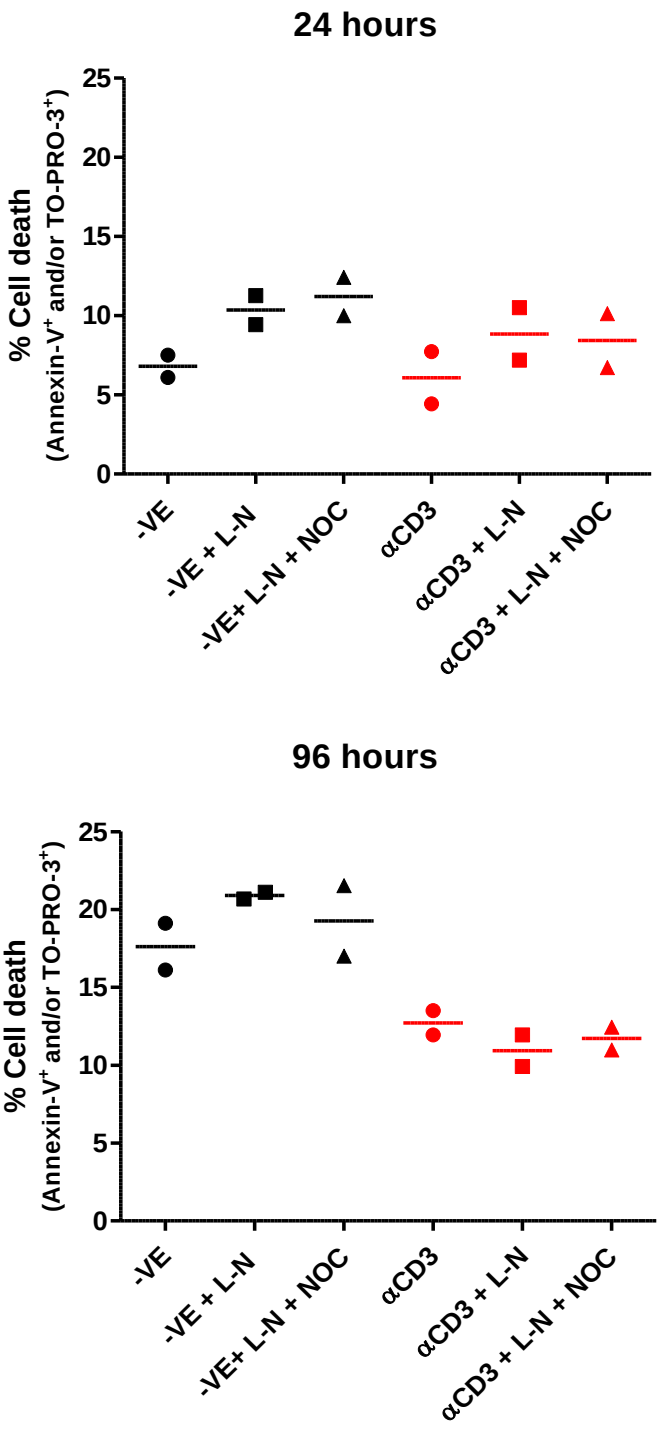

Figure 5.13: NO donation does not ameliorate CD4$^+$ T-cell death induced by L-NAME exposure.

Non-stimulated and αCD3 (0.1 µg/ml) activated PBMcs were exposed to L-NAME (10 mM) alone or in combination with NOC-18 (300 µM). CD4$^+$ T-cell death was quantified as Annexin-V$^+$, TO-PRO-3$^+$ or double positives, at 24 and 96 hours post-incubation. Results are expressed in % and means; n= 2.

5.7 CAVTRATIN, A NOVEL PEPTIDE INHIBITOR OF eNOS

Because of the issue surrounding the potential cytotoxicity of L-NAME for our PBMC culture, we sought to block NO production by other means. Given that the constitutive $Ca2^{+}$-dependent endothelial NOS (eNOS) is the primary form of NOS expressed in T-cells after TCR engagement (Ibiza et al. 2006; Nagy et al. 2003), our next step was to achieve a selective inhibition of eNOS within T lymphocytes. Recently, a novel peptide based on the caveolin-1 protein sequence, has been successfully used for selective eNOS inhibition in endothelial cells (Gratton et al. 2003; Bucci et al. 2000).

5.7.1 Cavtratin has an effect in TCR-induced T-cell responses

The caveolin-1-derived peptide named Cavtratin is a fusion protein and consists of the scaffolding domain of caveolin-1 (amino acids 82-101), attached to the homeodomain of antennapedia protein. The scaffolding domain of caveolin-1 interacts directly with eNOS and blocks its catalytic activity *via* inhibition of calmodulin binding (Kwok et al. 2009; Bucci et al. 2000; Ju et al. 1997). The homeodomain of antennapedia, a *Drosophila* transcription factor facilitates uptake of peptides or oligonucleotides into mammalian cells through a non-endocytic, nondegradative pathway (section 2.9.3).

PBMCs were stimulated with αCD3 and incubated for 4 days in the presence of different concentrations of Cavtratin or a control version of the peptide, which contains the caveolin-1 domain but lacks the internalisation sequence (section 2.9.3).

Figure 5.14-A shows that $CD4^{+}$ T-cell division is significantly enhanced by Cavtratin at 5 µM. Although the Cavtratin and the control groups were not different from each other, the proliferative effect was not seen in the group exposed to the control peptide at the same 5 µM concentration. A biphasic trend can be observed, in which low concentrations of Cavtratin are insufficient to modify T-cell proliferation, whereas concentrations higher that 5 µM may have an inhibitory effect.

In contrast, neither Cavtratin nor the control peptide were able to significantly modify expression of the activation marker CD25 in $CD4^{+}$ T lymphocytes (Figure 5.14-B). Also, no differences were found between the samples exposed to Cavtratin and the ones exposed to the control peptide.

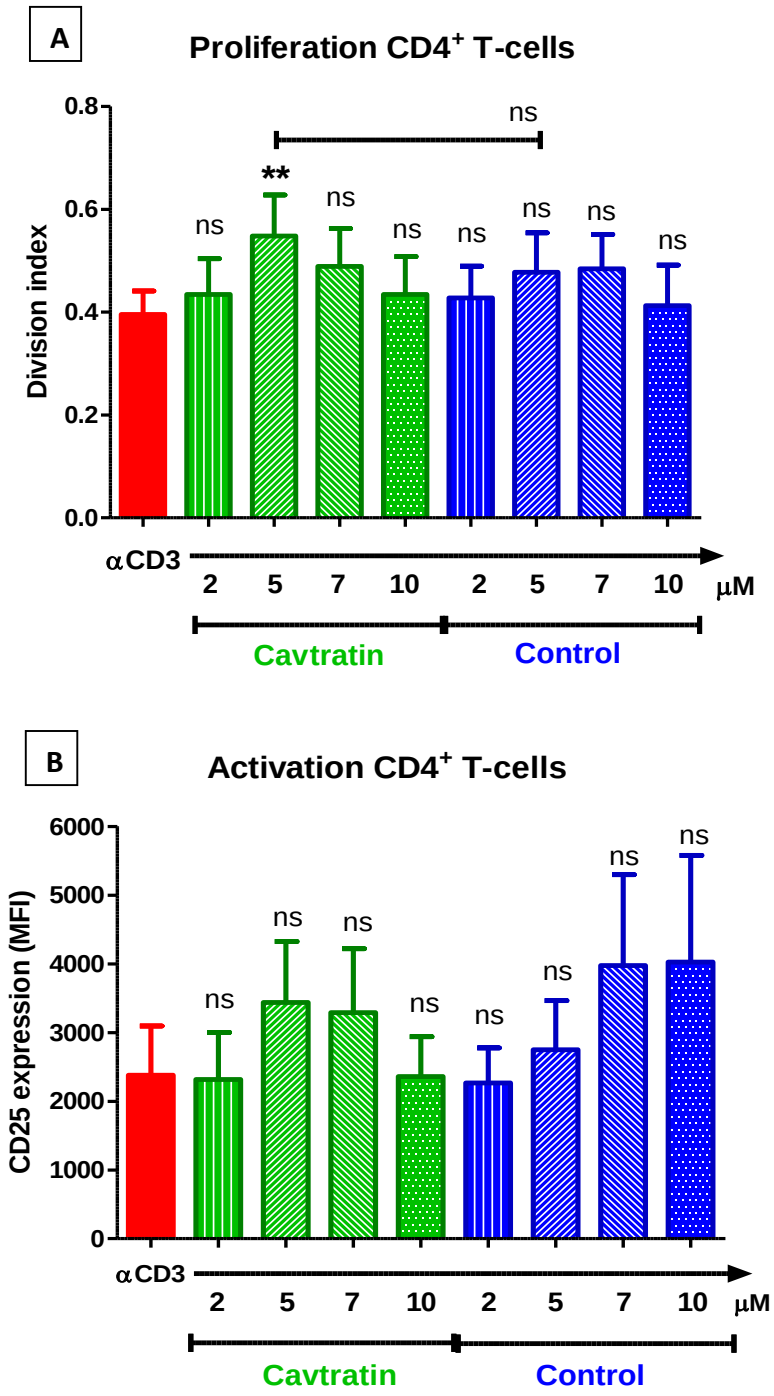

Figure 5.14: Cavtratin significantly enhances T-cell proliferation at 5 μM.

A. Proliferation of CD4⁺ T-cells, reported as division index. **B. Activation CD4⁺ T-cells**, expression of the CD25 marker, reported as median fluorescence intensity (MFI). Bars represent means and SEM, n=6. Paired ANOVA, Bonferroni's Multiple Comparison Test (all groups *vs.* αCD3 and 5μM Cavtratin *vs*. 5μM Control). *$p \leq 0.05$, **$p \leq 0.01$, ns= not significant.

PBMCs were stimulated with αCD3 (plate-bound 0.3 μg/ml) and incubated in the presence of different concentrations of Cavtratin (green bars) or the control peptide -without internalisation sequence (blue bars).

5.7.2 T-cell proliferation and activation in response to Cavtratin are confounded by the presence of DMSO

According to manufacturer's instructions both Cavtratin and the control peptide were solubilised in dimethyl sulfoxide (DMSO). Since DMSO can be cytotoxic above certain concentrations, we addressed whether the loss of a proliferative effect at Cavtratin concentrations $\geq$7 μM was induced by DMSO.

Thus, we performed an experiment incubating αCD3-stimulated PBMCs with graded concentrations of Cavtratin (2 to 10 μM) but also including a group that was exposed to DMSO alone, equal to the volume as of the largest Cavtratin concentration.

Surprisingly, DMSO significantly increases cell division index of $CD4^+$ T lymphocytes in comparison with the αCD3 control (Figure 5.15-A). Of major relevance is the fact that there is a statistical difference between the group containing Cavtratin 10 μM and the group containing the same volume of DMSO; indicating that the absence of a proliferative effect at 10 μM concentration is related to the Cavtratin action and not to the solvent DMSO.

In the case of T-cell activation, no significant differences were found for any of the groups containing Cavtratin when compared to the αCD3 control. We were also unable to detect a significant difference between the sample containing Cavtratin 10 μM and the one with DMSO alone (Figure 5.15-B).

To further assess if Cavtratin was able to restrict T-cell responses at concentrations higher than those tested, another experiment was designed by exposing αCD3-stimulated PBMCs to Cavtratin (10, 15 or 20 μM), the control peptide (10, 15 or 20 μM) or DMSO alone (equivalent volumes as Cavtratin concentrations).

Figure 5.16 shows how Cavtratin concentrations of 15 and 20 μM resulted in a deep suppression of T-cell proliferation and activation; however, the same drop occurred for the other groups containing the control peptide or DMSO alone. Therefore, this data suggests that the inhibition observed at high Cavtratin concentrations is due to the presence of DMSO.

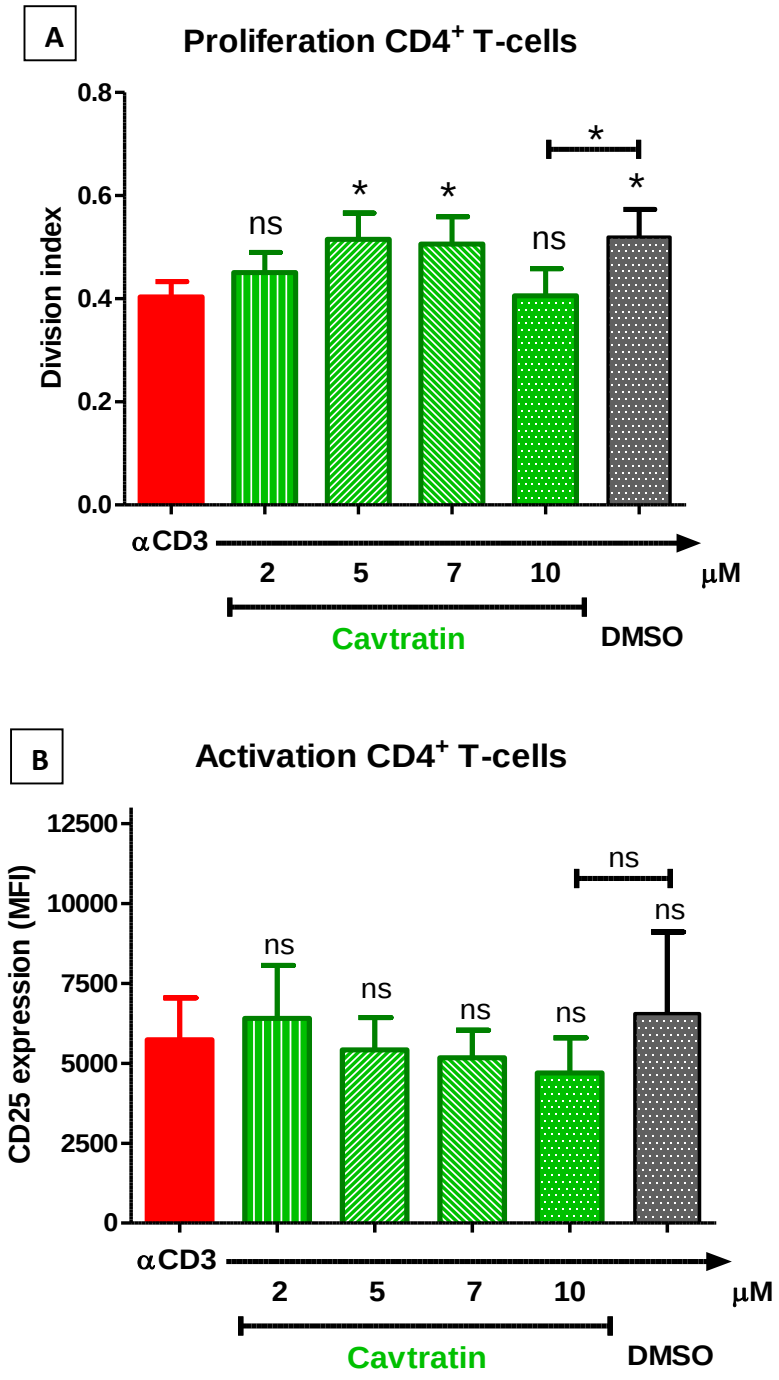

Figure 5.15: DMSO appears to mask the effect of Cavtratin.

A. Proliferation CD4⁺ T-cells, reported as division index. **B. Activation CD4⁺ T-cells**, expression of the CD25 marker as median fluorescence intensity (MFI). Bars represent means and SEM, n=12 (DMSO, n=8). Paired ANOVA, Bonferroni's Multiple Comparison Test (all groups *vs.* αCD3 and 10μM Cavtratin *vs*. DMSO Control). *$p \leq 0.05$, ns= not significant.

PBMCs were stimulated with αCD3 (plate-bound 0.3 μg/ml) and incubated in the presence of different concentrations of Cavtratin (green bars). As a further control DMSO was added to the PBMC culture at the same volume as the 10 μM concentration (gray bar).

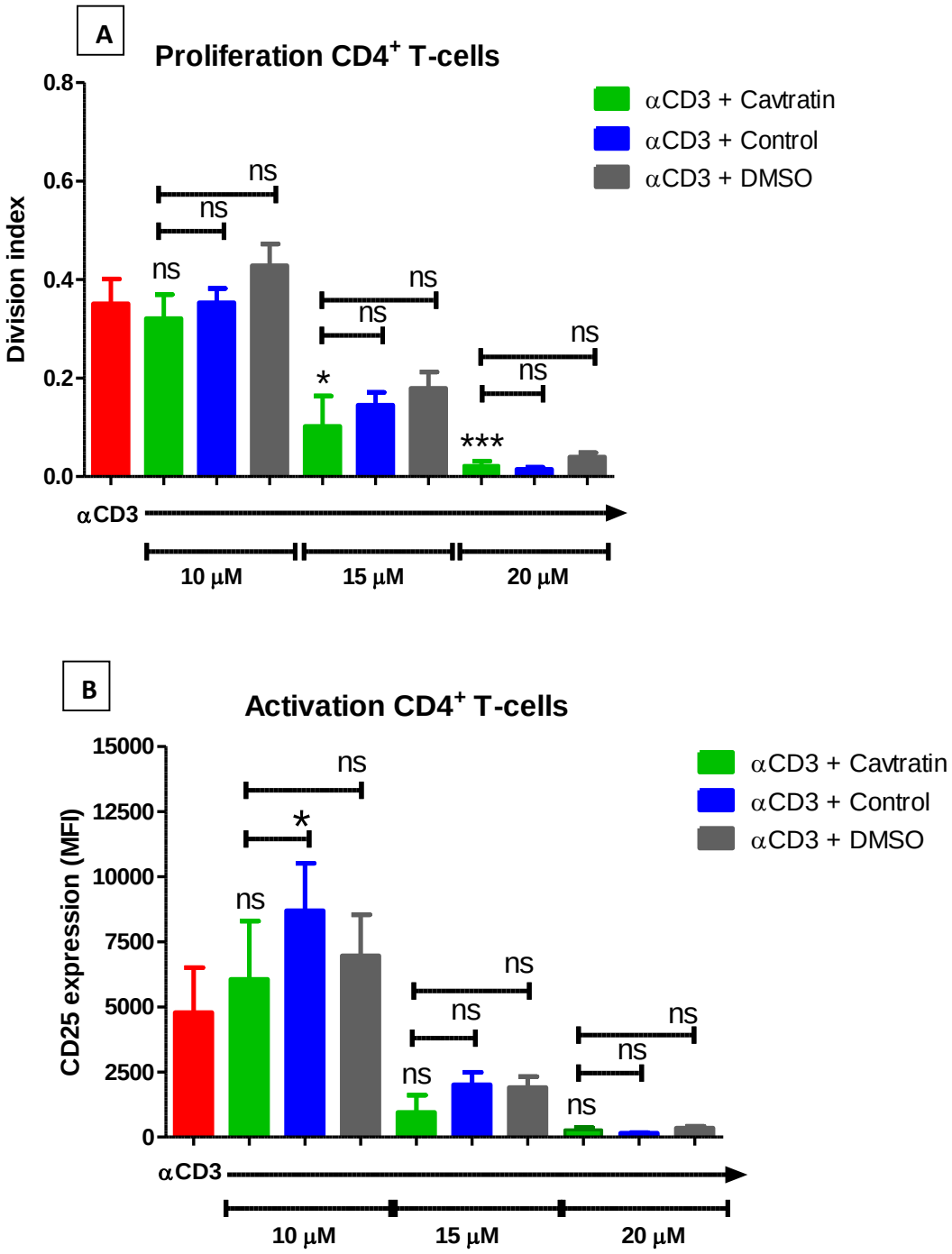

Figure 5.16: Measurements of CD4⁺ T cell proliferation and activation in response to Cavtratin are confounded by the presence of DMSO.

A. Proliferation of CD4⁺ T-cells, reported as division index. **B. Activation of CD4⁺ T-cells**, expression of the CD25 marker reported as median fluorescence intensity (MFI). Bars represent means and SEM, n= 4-6. ANOVA, Bonferroni's Multiple Comparison Test. Cavtratin groups were compared against the αCD3 control and then within their groups against the control peptide and DMSO. *$p \leq 0.05$, **$p \leq 0.01$, ***$p \leq 0.001$, ns= not significant.

PBMCs were stimulated with αCD3 (plate-bound 0.3 µg/ml) and incubated in the presence of different concentrations of Cavtratin (green bars), the control peptide -without internalisation sequence (blue bars) or the corresponding volume of DMSO (gray bars).

5.7.3 Cavtratin enhances proliferation of CD4$^+$ T lymphocytes.

To finally determine whether the effect was Cavtratin dependent and not just only a DMSO artefact, a new Cavtratin stock solution was prepared in cell culture media (RPMI 1640 + glutamine) and compared against the Cavtratin preparation in DMSO. Although it was also desired to test the control peptide, it was not possible to dissolve it in cell culture media.

Covering a larger range of doses, PBMCs were stimulated with αCD3 and exposed to 5, 10, 15 or 20 µM of the two Cavtratin preparations (in media or DMSO) over the course of 4 days.

From the data in Figure 5.17-A we can conclude that Cavtratin concentrations of 10 and 15 µM enhance proliferation of CD4$^+$ T-cells, if dissolved in cell culture media. In contrast, the Cavtratin preparation in DMSO decreased T-cell proliferation in a dose-dependent manner.

Although a similar pattern was observed for the CD25 activation marker, no significant differences were detected due to a large inter-experimental variability (Figure 5.17-B).

Overall, these experiments show that Cavtratin has a proliferative influence on CD4$^+$ T lymphocytes.

5.7.4 Cavtratin reduces cell death of PBMCs in culture.

In order to corroborate that cell death was not occurring in the conditions above tested, the % of dead cells obtained from the UV dead/live dye included in each experiment were plotted and analysed. Although the results presented in Figure 5.18 are representative of total cell death among PBMCs at 96 hours after incubation, this general viability overview allows us to detect for medium to severe cell loss.

Surprisingly, Cavtratin had a beneficial outcome reducing cell death by about one third in comparison with the αCD3 control (Figure 5.18). As expected the DMSO preparation showed a higher percentage of dead cells as the concentrations increased.

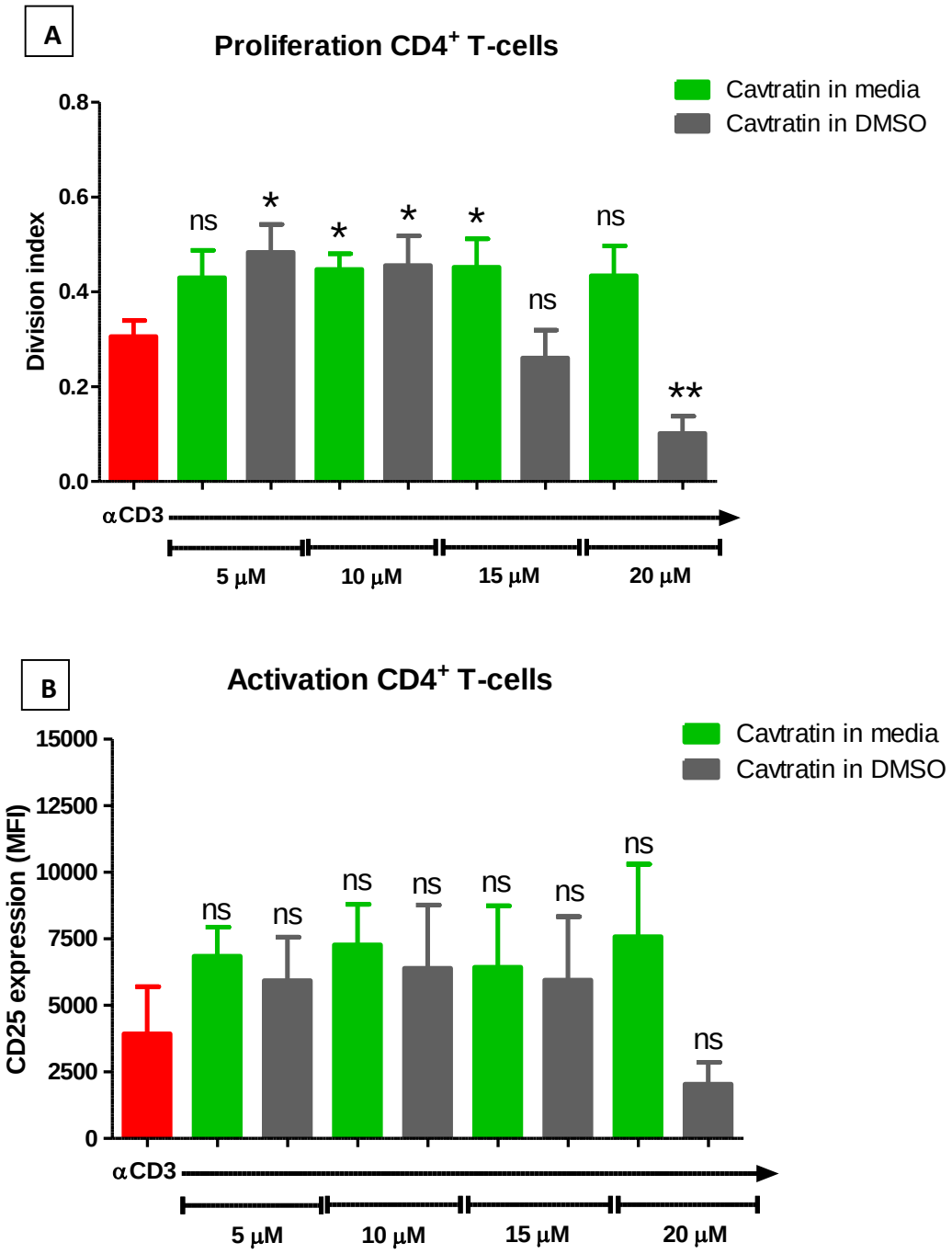

Figure 5.17: Cavtratin enhances CD4⁺ T-cell proliferation.

A. Proliferation CD4⁺ T-cells, reported as division index. **B. Activation CD4⁺ T-cells**, expression of the CD25 marker as median fluorescence intensity (MFI). Bars represent means and SEM, n= 4-5. ANOVA, Dunnett's Multiple Comparison Test (*vs.* αCD3). *$p \leq 0.05$, **$p \leq 0.01$, ns= not significant.

PBMCs were stimulated with αCD3 (plate-bound 0.3 μg/ml) and incubated in the presence of different concentrations of Cavtratin dissolved in cell culture media (green bars) or Cavtratin dissolved in DMSO (gray bars).

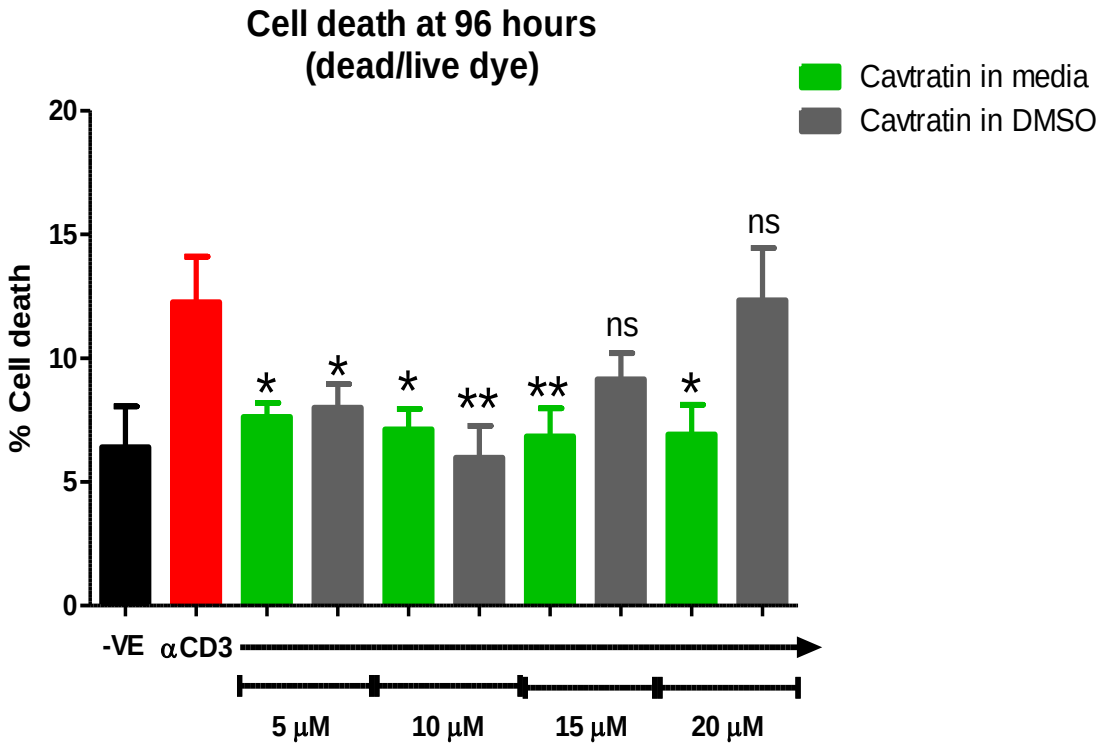

Figure 5.18: Cavtratin reduces percentage of dead PBMCs at 96 hours.

Percentage of dead cells (not within the live cells gate) applying the basis of the UV dead/live dye. Bars represent means and SEM, n= 4-5. ANOVA, Dunnett's Multiple Comparison Test (*vs.* αCD3); *$p \leq 0.05$, **$p \leq 0.01$, ns= not significant.

PBMCs were stimulated with αCD3 (plate-bound 0.3 μg/ml) and incubated for 4 days in the presence of different concentrations of Cavtratin prepared in cell culture media (green bars) or Cavtratin prepared in DMSO (gray bars). -VE= negative control, non-stimulated PBMCs.

5.8 DISCUSSION

5.8.1 Main findings

Since components of *N. meningitidis* stimulate NO production and NO is also produced at the moment of T-cell activation, the work described here is the initial approach to characterise NO-mediated T-cell activation and proliferation. The primary aim of this chapter was to determine whether NO plays a direct role in proliferation and/or activation of human primary T-cells, and to determine the effect that NO donation or inhibition has on stimulated $CD4^+$ T lymphocytes using our *in vitro* model.

Although NO production by the immune system mainly occurs in response to bacterial components and during the cell activation process, the presence of NO is also essential for maintaining a normal physiological function in resting cells (section 1.3.). In this Chapter, we demonstrated that neither the NO donor (NOC-18) nor the NOS inhibitor (L-NMMA) were able to induce any effect on non-stimulated PBMCs. Division index and expression of the activation marker CD25 in resting $CD4^+$ T lymphocytes were unaffected in the presence of different concentrations of NOC-18 and L-NMMA (section 5.3). This suggests that NO *per se* is unable to induce proliferation or activation in non-stimulated T-cells and that resting T lymphocytes are not susceptible to fluctuations in NO concentration. In support of this, several authors have proved that TCR engagement, followed by subsequent mitochondrial hyperpolarisation and Ca_2^+ release, are required events before NO production is triggered within the cell (Ibiza et al. 2006; Perl et al. 2004; Nagy et al. 2003). The fact that higher levels of eNOS mRNA have been detected in activated T-cells in comparison with non-stimulated controls (Nagy et al. 2003; Reiling et al. 1996), corroborates the idea that baseline levels of NO are minimal in non-stimulated cells.

Moving next into investigating NO donation in activated $CD4^+$ T lymphocytes, section 5.4.1 demonstrated that concentrations $\geq$500 μM of NOC-18 reduce viability of PBMCs. We determine that 300 μM of NOC-18 was the largest concentration we could use for future experiments without impacting on the viability of the PBMC populations. Although an initial experiment using graded concentrations of NOC-18 (from 1 up to 300 μM) suggested a dose-dependent enhancement of T-cell proliferation and activation, repeat experiments subsequently showed that NOC-18 (300 μM) was unable to modulate the proliferation and activation of these cells, irrespective of the T-cell stimuli used (αCD3, ConA or SEB) (sections 5.4.2 and 5.4.3).

Given the pleitropic nature of NO, it is unlikely that its administration to PBMCs is completely without effect. Since TCR engagement will induce local NO production which is sufficient to trigger TCR-activation pathways (section 1.3.7), the excessive NO released by NOC-18 might had an effect in intracellular processes different from T-cell proliferation and activation. It is also possible that NOC-18 degradation was accelerated by non T-cells contained in the PBMC culture. Because the half life of NOC-18 is about 21 hours, another possibility is that the influence of NO donation might had been transitory and disappeared by day 4 when the analysis was performed. In the presence of a NO-releasing derivative of aspirin (NCX-4016) and DETA-NO, a previous report observed a transitory reduction (of less than 48 hours) of cellular respiration in T lymphocytes, which resulted in a subsequent inhibition of αCD3/αCD28-induced proliferation and decreased IL-2, IL-4, IL-5 and IFN-γ secretion (Fiorucci et al. 2004). Similar to our findings, Macphail et al. (2003) found no difference in CD25 expression between cells exposed to a NO donor (SNAP or GSNO) and the ones that were not. Published work has proposed that low concentrations of NO donors (SNAP <10 μM; NOC-18 <10 μM) may increase proliferation/activation of T-cells and induce more NO production; whilst high concentrations (SNAP 100 and 500 μM; NOC >100 μM) may suppress proliferation/activation or even induce apoptosis (Niedbala et al. 1999). NOC-18 did not exhibit suppressive properties on stimulated cells, but was also insufficient to induce further proliferation after TCR engagement in our *in vitro* system.

From published work, it can be concluded that the response to NO in primary human $CD4^+$ T-cells does not always follow a consistent pattern and may vary among individual donors. In support, authors have determined that the dualistic effect of NO depends on the concentration, its source, time of exposure and the cellular environment of activity (Fiorucci et al. 2004; Macphail et al. 2003; Bogdan 2001). For example, Fujiwara et al. (2006) found that NOC-18 concentrations between 100 and 200 μM inhibit T-cell division and IL-2 production only if NOC-18 is given as pre-treatment for 24 hours before co-culture with stimulator cells. IL-2, IL-4 and IL-10 production from activated, human PBMCs can be inhibited by 3 different NO releasing compounds when they are administrated for a period of 24 hours, but the suppression achieved by each compound varies in strength and in the concentration required (Korhonen et al. 2008). Moreover, Nukaya et al. (1995) determined that the sensitivity to NO varies among T-cell subtypes, as the same concentration of a NO donor (0.1 μM SNP) induced a deeper inhibition of DNA synthesis in T_H2 than in T_H1 T-cells. In similar conditions to the assay performed in this chapter, Niedbala et al. (2007) found that NOC-18 (100-200 μM) enhances IL-2 production and proliferation of $CD4^+$ $CD25^-$, but not $CD4^+$ $CD25^+$, murine T lymphocytes. NO induced a T_H2-like suppressive phenotype on those $CD4^+$ cells,

increasing CD25 expression and secretion of IL-10, but lacking expression of the classic T-regs factor Foxp3.

In contrast, a dose-dependent reduction in T-cell proliferation was observed when PBMCs were exposed to the NOS inhibitors L-NAME and L-NMMA (section 5.5.1). All the stimulated groups (αCD3, ConA or SEB) containing L-NAME (10 mM) showed a significant drop in division index of $CD4^+$ T lymphocytes. This inhibitory phenomenon was evident as early as 48 hours after stimulation with αCD3 or SEB (section 5.5.2), but was only partially reversed by simultaneous NO donation with NOC-18 (150 and 300 μM) (section 5.5.3). One publication performing very similar experiments on human PBMCs and using L-NMMA at similar concentrations (1 to 8 mM), has proposed that NO is indeed an essential molecule to achieve T-cell proliferation in response to superantigens, so blockade of NO production results in abrogation of proliferation (Sriskandan et al. 1996). After several repetitions and under different stimuli (αCD3, ConA or SEB), only the SEB stimulated group containing L- NAME (10 mM) had a significant decrease in CD25 expression (section 5.5.3). Thus suggesting that NO is unlikely to be required for the expression of the activation markers CD25 and Foxp3 in non-superantigen stimulation, or that the effect might occur at early hours along the incubation period but disappears by day 4.

Many other investigators disagree and have reported that T-cell proliferation and their response to antigens is inhibited by NO donation, while L-arginine analogues increase T-cell responses (van der Veen, Dietlin, Pen, et al. 2000; van der Veen, Dietlin, Dixon Gray, et al. 2000; Brás et al. 1997; Lejeune et al. 1994; Gregory et al. 1993). Bingisser et al. (1998) and Mazzoni et al. (2002) describe that NO induces a reversible type of T-cell anergy by reducing phosphorylation of tyrosine residues in Jak3/STAT5, an essential molecule for proliferation and cycle progression in activated T-cells (Moriggl et al. 1999). In a rat model of major physical trauma, it was found that in the presence of T-cell stimulation high concentrations of endogenous NO abrogate T-cell division by arresting $CD4^+$ splenocytes in a late G1 phase, and committing those cells to subsequent apoptosis and necrosis (Valenti et al. 2005). Apart from leading apoptosis, caspases can be active in non-apoptotic T lymphocytes and modulate their proliferative capacity and IL-2 secretion upon TCR engagement with mitogens or αCD3 (Koenig et al. 2012; Kennedy et al. 1999; Wilhelm et al. 1998). Mahidhara et al. (2003) has shown that Caspase-3 activity increases with T-cell divisions and attribute a NO-dependent anti-proliferative effect to blockade of caspase activity by *S*- nitrosylation (section 1.3.6). Small concentrations of the NO donor SNAP (pulsed doses over 48 hours incubation) resulted in lower caspase-3 like activity and profound inhibition in proliferation of murine αCD3-stimulated T lymphocytes, without inducing cell death (Mahidhara et al. 2003).

For those experiments where T-cell proliferation and activation were evaluated after 96 hours incubation, a UV dead/live dye was used to quantify the percentages of viable cells among the groups containing NOC-18 and L-NAME in comparison with the controls. Despite that the UV dead/live dye did not demonstrate a significant reduction in the proportions of live cells, we performed an assay to detect cells that enter apoptosis at early stages to be undetectable by 96 hours. Data from the Annexin V / TO-PRO-3 assay suggested that stimulated and non-stimulated groups containing L-NAME (10 mM) have a small increase in the percentages of cell death after 24 hour incubation (section 5.6). Although the difference in cell death appears to be normalised after 48 hours among the activated groups containing L-NAME, the non-stimulated group had more cell death along the 96 hour incubation. These findings are inconsistent with other publications, which found they can reverse TCR-triggered cell death using NOS inhibitors (Valenti et al. 2005; Williams et al. 1998). Thus, it was suspected that either L-NAME had a direct toxic effect or that absolute lack of NO production was harmful for the PBMC culture.

To investigate the possibility that cell death was occurring due to NO deprivation, a supplementation experiment was carried out; however, simultaneous addition of NOC-18 did not impact upon the relatively higher percentage of cell death induced by L-NAME (section 5.6). In this experiment, there is the possibility that the amount of NO donated by NOC-18 might had not been sufficient to replenish the NO needs. Other possibility is that blockade of NO synthases by L-NAME might result in fast, irreversible cellular events that cannot be overcome by external NO donation.

Because in T lymphocytes NO has been found to be produced by eNOS and in response to TCR engagement (Ibiza et al. 2006; Nagy et al. 2003), we aimed to investigate the effect of a specific eNOS inhibitor in our *in vitro* system. Caveolin-1 is a cholesterol binding protein and the main constituent of the organelle caveolae; contributes to transcytosis of macromolecules, promotes the assembly and stability of plasma membrane raft microdomains and also participates in signal transduction cascades (Frank et al. 2003). Within endothelial cells and under resting conditions, eNOS is located at the caveolae where its catalytic activity remains suppressed by clamping with the major scaffolding domain of caveolin-1 (Ju et al. 1997), specifically by two threonine residues (numbers 90 and 91 in the domain sequence) and most importantly the phenylalanine residue in position 92 of the domain sequence (Bernatchez et al. 2011). Bucci et al. (2000) manufactured a peptide derived from the scaffolding domain of caveolin-1, which interferes with the Ca_2^+/calmodulin-binding region (Ju et al. 1997) (section 1.3.1) and dose-dependently inhibits eNOS activity. This peptide termed Cavtratin consists of 19 amino acids corresponding to that primary binding domain of caveolin 1 (amino acids 82-101), plus an internalisation sequence obtained

from the *Drosophila* transcription factor that facilitates peptide uptake by mammalian cells (section 2.9.3). Cavtratin has been successfully used to specifically block eNOS and subsequent NO production within blood vessels; avoiding vascular relaxation, leakage, interstitial edema and atherosclerosis in mouse models (Chidlow et al. 2009; Rodriguez-Feo et al. 2008; Lin et al. 2007; Gratton et al. 2003; Bucci et al. 2000). Although expression of caveolin-1 has been reported to be absent in human peripheral T lymphocytes (Vallejo & Hardin 2005; Alonso & Millán 2001; Fra et al. 1994), it is expected that the peptide's Ca_2^+/calmodulin suppression exerted on the lymphoid eNOS still occurs.

With the experiments carried out in section 5.7, it has been demonstrated that Cavtratin at concentrations of 10 and 15 µM increases proliferation of $CD4^+$ T lymphocytes. However, expression of CD25 was not significantly enhanced by any of the Cavtratin concentrations. Unexpectedly, Cavtratin reduced overall cell death within the PBMC culture in comparison with the αCD3 control at 96 hours post-incubation (section 5.7.4). Even though we did not directly evaluate blockade of eNOS activity, a concentration of 10 µM of the caveolin-1 derived peptide has been proved to be effective in achieving complete inhibition of eNOS activity *in vitro* (Bucci et al. 2000; Ju et al. 1997). Assessment of the Cavtratin control peptide was not conclusive so it was not possible to determine whether an internalisation sequence was required to achieve an effect in T-cells. To our knowledge, the work performed in this chapter is the first one studying a possible effect of eNOS blockade in $CD4^+$ T lymphocytes using a caveolin-1 derived peptide.

Overall, we can conclude that the role of NO in T-cells remains controversial and obscure due to the number of implicated variables. Special attention must be paid to studies done in mice that report NO-derived toxicity, since murine cells produce higher amounts of NO in comparison with human cells, further NO addition by a NO donor may result in cytotoxicity. Moreover, because human cells have small basal amounts of NO, NOS inhibition in these cells could lead to a severe NO deprivation and subsequent lack of proliferation and/or cytokine responses after exposure to antigens (Sriskandan et al. 1996).

CHAPTER 6:

DISCUSSION

Since a full discussion of the main findings has already been provided in each of the chapters of this thesis, Chapter 6 aims to summarise and understand the clinical relevance of some of the key findings from this PhD work. This chapter also discusses the limitations of the methodology employed to address and to interpreter the research questions along this project. Finally, some plans for future work are mentioned.

This thesis aimed to determine the mechanism of action of a previous finding recorded in our research group, by which T-independent (TI) type 2 mimics induce B-cell responses but simultaneously suppress T-cell proliferation and activation (Chapter 3). *N. meningitidis* is a bacterium which rarely causes invasive disease and sepsis, but perpetuates colonisation by avoiding immune recognition and killing. Because several *N. meningitidis* constituents are TI type 2 antigens and/or provide second signals to B-cells *via* TLRs, we hypothesized that exposure of PBMCs to paraformaldehyde fixed meningococcus could have a suppressive effect on T-cells (Chapter 4). Several bacterial components stimulate NO production; however *N. meningitidis* can counteract the bactericidal effect of reactive nitrogen intermediates by a partial denitrification pathway. Since NO is also produced as a result of TCR engagement, it was investigated whether a change of NO concentrations could affect T-cell proliferation and activation (Chapter 5).

6.1 MAIN FINDINGS

6.1.1 Chapter 3- Human B-cell activation with a TI type 2 antigen mimic inhibits TCR-induced T-cell proliferation and activation.

Chapter 3 reports a novel downregulatory role for T-independent (TI) type 2 activated B lymphocytes. The present study has demonstrated that B-cell activation using TI type 2 antigen mimics inhibits proliferation and activation of human $CD4^+$ T lymphocytes *in vitro*. Anti-IgD-conjugated dextran (α-δ-DEX) and the truncated Moraxella IgD-binding protein (MID) are TI type 2 mimics that induce activation and proliferation of B lymphocytes by cross-linking of numerous B-cell receptor molecules (specifically membrane-bound IgD).

αCD3-induced T-cell proliferation and expression of the activation marker CD25 become deeply suppressed when α-δ-dex or MID are present in the PBMC culture. While T-cell inhibition was

significant it was not total and T-cells were still able to deliver T-cell help as demonstrated by the synergistic activity of αCD3 and α-δ-DEX on B-cell activation and activation.

Experiments performed with purified cell populations excluded the possibility of α-δ-DEX acting directly on $CD4^+$ T lymphocytes. Furthermore, these experiments confirm that B lymphocytes exposed to α-δ-DEX for a period of 24 hours (in the presence of PBMCs) become activated and acquire a suppressive phenotype, capable of restraining proliferation of $CD4^+$ T-cells in co-culture. Interestingly, these suppressor B-cells appear to be effective even when they are present at numbers below the physiological T:B ratio.

Depletion of monocytes and NK cells confirmed that B lymphocytes are the single cell type responsible for the inhibition. Among the molecules investigated in this work, blocking of IL-10, IL-1, CD80 and CD86 did not reverse the α-δ-DEX-induced inhibitory effect.

Although the exact mechanism of action was not identified, no soluble factors appear to be playing a role in the inhibition and cell contact interactions between T and B lymphocytes are essential.

While the field of B-regulatory biology is rapidly developing, the role of B-cells as co-stimulators is better described than their inhibitory effects on T-cells. In order to control B-cell mediated autoimmunity B-cell depletion therapy has been used with some success. However, it is clear that this may also remove regulatory B-cells, with potentially unforeseen consequences. We would suggest that one key to controlling T-cell immunopathology resulting from bacterial infection or autoimmune disease may lie with the understanding and potentially the induction of B-cell suppression phenomena similar to those observed here.

6.1.2 Chapter 4- *N. meningitidis* suppress TCR-induced T-cell proliferation and activation, but enhances Th1 cytokines and IL-10 production.

Chapter 4 demonstrated that paraformaldehyde fixed *N. meningitidis* is capable of inhibiting TCR-induced proliferation and activation of $CD4^+$ T lymphocytes. A deep suppression of T-cell responses, comparable to the one observed with α-δ-DEX, occurred when αCD3-stimulated PBMCs where incubated with low bacterial counts (0.1:1, 1:1 and 10:1 bacteria per cell). Importantly and in contrast to α-δ-DEX, these meningococci inocula did not enhance B-cell responses, suggesting that the mechanism of suppression is not directed by B lymphocytes. In support, we found that incubation with a large bacterial count (100:1 bacteria per cell) results in a strong B-cell proliferation and activation but does not reduce proliferation or activation of $CD4^+$

T lymphocytes. It can be surmised that a large bacterial load enhances bystander pro-inflammatory activity among accessory cells and overcomes the inhibitory phenomenon. Importantly, enriched $CD4^+$ T lymphocytes were not affected directly by *N. meningitidis* (1:1 bacteria per cell). Incubation for 24 hours with a small inoculum of *N. meningitidis* (1:1 bacteria per cell) was unsuccessful to generate a suppressive phenotype on B lymphocytes or monocytes. Co-culture between enriched $CD4^+$ T lymphocytes and meningococcus pre-activated enriched B lymphocytes or monocytes did not reduce $CD4^+$ T-cell responses. Further confirmation was obtained when depletion of B-cells, monocytes or NK cells did not reverse the meningococcus-mediated inhibition in PBMC cultures. Supernantant from PBMCs exposed to *N. meningitidis* did not ablate T-cell division index or expression of the activation marker CD25, suggesting a cell contact mechanism. It was therefore concluded that in our *in vitro* model, PBMCs act in a complex network to encounter microorganisms and to establish cell interactions, so is not always easy to separate the individual cell contributions from the overall effect.

Strains of *N. meningitidis* deficient in capsule and lipooligosaccharides (LOS) excluded these bacterial constituents as responsible for the inhibitory phenomenon. Fresh and heated outer membrane vesicles (OMVs) from *N. meningitidis* and *N. lactamica* replicated the suppression phenomenon induced by the whole organism. From the components of the outer membrane, two Opa-deficient strains demonstrated that Opa-CEACAM interactions are not the mechanism by which *Neisseria spp* restrain T-cell responses. Although the exact meningococcus constituent was not identified, we concluded that the suppressor factor must be contained within OMVs.

A clear T_H1 cytokine profile was observed in supernatants of PBMC cultures incubated with ratios of 1:1 and 10:1 meningococci per PBMC. Increased production of IL-1β, IL-6, IL-8 and a dose dependent rise in TNF-α and IFN-γ was detected in these samples. In contrast, the classical T_H2 cytokines IL-5 and IL-13 were greatly reduced. Unexpectedly, the PBMC groups containing bacterial inocula of 1:1 and 10:1 had significant higher levels of IL-10, in comparison with controls and the inocula at the extremes of the range. However, blocking of IL-10 resulted in only partial restoration of T-cell proliferation and reveals the existence of another underlying mechanism of action.

In conclusion, this chapter confirms that bacteria are capable of immunomodulation. This regulatory activity may be relevant to the pathogenesis of a number of bacterial infections and could potentially be an immune evasion mechanism used by pathogens. Or perhaps a mechanism evolved by the host to limit T-cell mediated immune pathology induced by bacteria.

6.1.3 Chapter 5- Role of nitric oxide in TCR-induced T-cell responses

Chapter 5 provides preliminary data about the role of NO in $CD4^+$ T-cell responses. The primary aim was to determine whether NO plays a direct role in proliferation and/or activation of human primary T-cells, and to determine the effect that NO donation or inhibition has on $CD4^+$ T lymphocytes using our *in vitro* model.

The first finding was that neither the NO donor (NOC-18) nor the NOS inhibitor (L-NMMA) were able to induce any effect on non-stimulated PBMCs. Division index and expression of the activation marker CD25 in resting $CD4^+$ T lymphocytes are unaffected in the presence of different concentrations of NOC-18 and L-NMMA. Therefore, NO donation and inhibition was studied in polyclonal activated T-cells, using αCD3, concanavalin A or the superantigen SEB.

NO donation with the NO slow-releasing compound NOC-18, at concentrations from 1 up to 300 μM, suggested a dose-dependent enhancement of T-cell proliferation and activation. However, repeat experiments using the maximum concentration of NOC-18 (300 μM) which does not compromise cell viability, show no significant differences irrespective of the T-cell stimuli used. Since the half life of NOC-18 is about 21 hours, the influence of NO donation might had been transitory and disappeared by day 4 when the analysis was performed.

NO inhibition with the arginine analogue L-NAME (10 mM) resulted in a significant reduction of T-cell proliferation across all stimuli. However, an annexin-V/topro-3 assay found that L-NAME induces cell death at early time points, perhaps by a cytotoxic mechanism.

Work published by Nagy et al. (2003) and Ibiza et al. (2006) have demonstrated NO production and eNOS expression in T-cells after TCR engagement with αCD3/αCD28 or superantigens. In order to be more specific and to achieve blockade of NO from T lymphocytes, the novel specific eNOS inhibitor derived from the caveolin-1 structure (named Cavtratin) was tested. Cavtratin concentrations of 10 and 15 μM increase significantly the division index of $CD4^+$ T lymphocytes, but do not enhance expression of the activation marker CD25. Moreover, addition of Cavtratin significantly reduced the percentage of cell death as compared with the αCD3 control.

The regulation that NO exerts on T-cells in the presence of bacterial infections is a critical area which is under-investigated, therefore the findings herein presented could potentially open a new research field. For example, the work performed in this chapter is the first one studying a possible effect of a caveolin-1 derived peptide in $CD4^+$ T lymphocytes.

6.2 METHODOLOGICAL CRITICISMS

6.2.1 Chapter 3- Human B-cell activation with a TI type 2 antigen mimic inhibits TCR-induced T-cell proliferation and activation.

There is the possibility that the B-cell depletion protocol leave a small number of B lymphocytes behind. Since the depletion kit works by positively selecting $CD19^+$ and $CD20^+$ cells, these antigens should had not been used to assess purity of the depleted fraction. Although a simultaneous staining with CD19 and IgD demonstrated that <0.05% IgD^+ events remain in the culture after the depletion protocol, further and final confirmation of the efficiency of the B-cell depletion protocol should be addressed using other B-cell phenotypic markers (for example, CD22 or CD45). A similar situation occurred for the monocyte and NK cell depletion procedures, where the classical markers CD14 and CD56 were used to remove these populations. Therefore, alternative antigens should be targeted to assess purity of these depleted fractions.

The degree by which α-δ-DEX pre-activated B-cells suppress T-cells varies among donors and depend on the T:B ratio. This situation rises a new research question regarding the susceptibility of B lymphocytes to acquire inhibitory properties. Naturally occurring regulatory B-cells ($CD19^{high}$ $CD24^{high}$ $CD38^{high}$) might also mask our findings and we should try to exclude them from our initial sample. Perhaps removal of already activated B lymphocytes could provide a non-stimulated population that respond better to α-δ-DEX stimulation.

6.2.2 Chapter 4- *N. meningitidis* suppress TCR-induced T-cell proliferation and activation, but enhances Th1 cytokines and IL-10 production.

All the experiments performed in this chapter included paraformaldehyde fixed bacteria. Therefore, we cannot assure that our observations can be extrapolated into an infection model with live bacteria. However, since fresh OMVs also ablated T-cell responses we could suggest that the suppressor factor is indeed a constituent located at the bacterial outer membrane layer, and not the result of bacterial metabolism.

6.2.3 Chapter 5- Role of nitric oxide in TCR-induced T-cell responses

One of the main disadvantages in this chapter is that NO released was not evaluated. Therefore, it is difficult to confirm that NOC-18 was actually donating NO and that L-NAME was actually blocking NO production. More importantly, the effect of the NO donor or inhibitor might have more emphasis on one particular cell population in the PBMC culture. Monocytes/macrophages are major producers of NO and fluctuations in NO concentrations might deeply influence their behavior and their interaction with T lymphocytes.

Recently, (Tomassian et al. 2011) reported expression of caveolin-1 in murine T lymphocytes and demonstrated that caveolin-1 is required for the TCR-induced responses of $CD8^+$, but not $CD4^+$ T-cells. In comparison with wild type mice, $CD8^+$ T lymphocytes from caveolin-1 knockout mice showed less TNF-α and IFN-γ production, together with a defective proliferation and poor viral clearance. In human peripheral blood cells, caveolin-1 expression has only been detected in T cell leukemia cell lines (Hatanaka et al. 1998). Thus, it is necessary to prove that the proliferative effect observed in the presence of Cavtratin is the pure result of eNOS inhibition and not a secondary intervention with caveolin-1 signalling pathways in T-cells or in other cells. A study performed by Ohnuma et al. (2007) reported that caveolin-1 expressed in APCs binds to its ligand (CD26) on T-cells and provides co-stimulatory signalling similar to the one of CD28. Using recombinant immunoglobulin-caveolin-1 fusion proteins it was identified that the *N*-terminal domain (amino acids 1-82) of caveolin-1 is the one that binds to CD26 and triggers T-cell proliferation and NF-κβ activation in a TCR/CD3-dependent manner (Ohnuma et al. 2007).

6.2.4 Overall considerations

Within the methods of the immunological assay that was developed within this PhD project there is room for human error and variability at some points.

Donor variability turned out to be the major factor to take into consideration along this project. The numerical outcomes vary among individuals and they can even vary from day to day. Many external factors can influence immune responses. Perhaps, the subjects from whom blood was taken might have been experiencing a sub-clinical response to infection of some kind at the time, which might have influenced the subsequent behavior of their lymphocytes *in vitro*.

Across the experiments of this work, inter-donor variability was found regardless of the stimuli used, in particular for T and B-cell activation markers. Although exact numerical outcomes for fold change in proliferation and expression of activation markers vary among individuals, it is important to focus on how the response patterns with different stimuli are consistent across all the experiments.

Another factor of variability correlates with the antibodies used over the time period in which this project took place. Even when manufacturers remain the same, antibodies exhibit significant variation in bioactivity among clones and lot numbers (Li et al. 2010). A clear example of this variability was the T-cell proliferation and activation baselines induced by different clones and lots of αCD3 mAb.

Isolated PBMCs may behave differently *in vitro* than *in vivo*. Since all experiments from this research project were done *in vitro,* suitable animal models might provide a more natural environment allowing integral immune system cooperation. In addition, this project focused on $CD4^+$ lymphocytes only so it would be interesting to study whether $CD8^+$ T-cells respond in the same way.

6.3 Future Work and Clinical Considerations

6.3.1 Chapter 3- Human B-cell activation with a TI type 2 antigen mimic inhibits TCR-induced T-cell proliferation and activation.

Expression of B-cell co-stimulatory molecules can vary along the incubation time after stimulation is started. Therefore, measurement of these molecules at different time points may provide information about the mechanism of action. B7-H4 is an inducible molecule member of the B7 family, expressed on activated monocytes, dendritic cells, T and B lymphocytes (Sica et al. 2003); whereas the putative receptor for B7-H4 is expressed only on activated T lymphocytes (Sica et al. 2003; Zang et al. 2003). B7-H4 is a negative regulator for CD4 and CD8 T lymphocytes, blocking phosphorylation of the MAP kinases, ERK, p38 and JNK (Wang et al. 2012). Signaling through this molecule inhibits proliferation, cell cycle progression and production of cytokines; as well as

impairs cytotoxicity functions (Sica et al. 2003; Zang et al. 2003). Recent publications have suggested that B7-H4 is involved in the suppression observed in tumours (Kryczek et al. 2006; Leung & Suh 2013). In this context, it could be that α-δ-DEX-activated B lymphocytes express B7-H4 and by this mechanism restrain activation and proliferation of $CD4^+$ T-cells. In our *in vitro* model, blockade of B7-H4 using a specific monoclonal antibody should determine if this molecule is playing a role in the suppression.

6.3.2 Chapter 4- *N. meningitidis* suppress TCR-induced T-cell proliferation and activation, but enhances Th1 cytokines and IL-10 production.

The fact that paraformaldehyde fixed *N. meningitidis* was capable of suppressing $CD4^+$ T-cell proliferation and activation, indicates that *in vivo* the presence of dead/attenuated microorganisms (perhaps after treatment with bacteriostatic antibiotics) could still exert an immunomodulatory effect on T lymphocytes. Øvstebø et al. (2004) has reported that a big difference exists between the total numbers of live and dead meningococci detected by quantitative blood cultures *versus* quantitative PCR. Moreover, several patients could have negative blood cultures and yet detectable amounts of LPS and neisserial DNA by PCR (Øvstebø et al. 2004). This work proposes that dead microorganisms and circulating LPS contribute importantly to the clinical outcome and prognosis in fulminant meningococcemia.

Results showing that OMVs suppress proliferation and activation of $CD4^+$ T lymphocytes represent a pinpoint to look at in relation to the new OMVs vaccines. Therefore, dissecting the OMV constituents to find the bacterial molecule responsible for the suppression phenomenon is an imperative future step for us.

Because IL-10 production was increased by inocula of 1:1 and 10:1 meningococci per PBMC, results obvious to exclude any role of Treg and Breg in the suppression mechanism. Perhaps small bacterial counts induce activation of these regulatory lymphocytes.

Finally to determine whether this suppressive phenomenon is common to several microorganisms, it would be interesting to perform our assays with different pathogenic and commensal bacteria.

6.2.3 Chapter 5- Role of nitric oxide in TCR-induced T-cell responses

The first attempt will be to evaluate NO concentrations from supernatants. A NO-sensitive electrode and the chemiluminescense method allow measurement of NO and oxidative NO products (NO_2-, NO_3- and *S*-nitrosothiols). In addition, the use of the fluorescent NO-sensitive probe DAF-FM by flow cytometry could help to investigate whether T lymphocytes are directly influenced by NO donation/inhibition.

A functional assay to evaluate the secretion of cytokines could reveal whether NO has a preference over one particular T-cell type (T_H1 or T_H2 subsets). Complementary evaluation of pro and anti-inflammatory cytokines, such as TNF-α, IL-1, IL-6 and IL-10 will provide extra information about the mechanism of action by which Cavtratin may enhance T-cell proliferation.

Apart from *N. meningitidis*, other microorganisms such as *Salmonella* and *Escherichia coli* can metabolise NO by a denitrification system (Laver et al. 2010). Therefore, it is important to investigate whether NO fluctuations affect the performance of T lymphocytes against bacterial infection. For example, *Moraxella catarrhalis* produces NO *via* its nitrite reductase (AniA) during infection of airway epithelial cells. This bacterial NO pushes the cell towards the cell death pathway by increasing IL-1α and TNF-α production, activating caspase-3 activity and reducing levels of anti-apoptotic proteins (Mocca & Wang 2012).

REFERENCES

Abu-Soud, H.M., Yoho, L.L. & Stuehr, D.J., 1994. Calmodulin controls neuronal nitric-oxide synthase by a dual mechanism. Activation of intra- and interdomain electron transfer. *The Journal of biological chemistry*, 269(51), pp.32047–50.

Akdis, C. a et al., 2000. A molecular basis for T cell suppression by IL-10: CD28-associated IL-10 receptor inhibits CD28 tyrosine phosphorylation and phosphatidylinositol 3-kinase binding. *FASEB journal : official publication of the Federation of American Societies for Experimental Biology*, 14(12), pp.1666–8.

Akdis, C. a & Blaser, K., 1999. IL-10-induced anergy in peripheral T cell and reactivation by microenvironmental cytokines: two key steps in specific immunotherapy. *FASEB journal : official publication of the Federation of American Societies for Experimental Biology*, 13(6), pp.603–9.

Akdis, M. et al., 2004. Immune responses in healthy and allergic individuals are characterized by a fine balance between allergen-specific T regulatory 1 and T helper 2 cells. *The Journal of Experimental Medicine*, 199(11), pp.1567–1575.

Akira, S., Uematsu, S. & Takeuchi, O., 2006. Pathogen recognition and innate immunity. *Cell*, 124(4), pp.783–801.

Allen, R.C. et al., 1993. CD40 ligand gene defects responsible for X-linked hyper-IgM syndrome. *Science (New York, N.Y.)*, 259(5097), pp.990–3.

Alonso, M. a & Millán, J., 2001. The role of lipid rafts in signalling and membrane trafficking in T lymphocytes. *Journal of cell science*, 114(Pt 22), pp.3957–65.

al-Ramadi, B.K. et al., 1992. Immunosuppression induced by nitric oxide and its inhibition by interleukin-4. *European journal of immunology*, 22(9), pp.2249–54.

Alugupalli, K.R. et al., 2007. MyD88- and Bruton's tyrosine kinase-mediated signals are essential for T cell-independent pathogen-specific IgM responses. *Journal of immunology (Baltimore, Md. : 1950)*, 178(6), pp.3740–9.

Anjum, M.F. et al., 2002. Nitric oxide metabolism in *Neisseria meningitidis*. *Journal of bacteriology*, 184(11), pp.2987–93.

Arjunaraja, S. et al., 2012. The nature of an in vivo anti-capsular polysaccharide response is markedly influenced by the composition and/or architecture of the bacterial subcapsular domain. *Journal of immunology (Baltimore, Md. : 1950)*, 188(2), pp.569–77.

Arnelle, D.R. & Stamler, J.S., 1995. NO+, NO, and NO- donation by *S*-nitrosothiols: implications for regulation of physiological functions by *S*-nitrosylation and acceleration of disulfide formation. *Archives of biochemistry and biophysics*, 318(2), pp.279–85.

Asadullah, K., Sterry, W. & Volk, H.D., 2003. Interleukin-10 therapy--review of a new approach. *Pharmacological reviews*, 55(2), pp.241–69.

ATCC, 2012. Escherichia coli (Migula) Castellani and Chalmers (ATCC® 25922. , p.http://www.lgcstandards–atcc.org/products/all/2592.

Ayala, P. et al., 1998. Infection of epithelial cells by pathogenic neisseriae reduces the levels of multiple lysosomal constituents. *Infection and immunity*, 66(10), pp.5001–7.

Azenabor, A. a, Kennedy, P. & York, J., 2009. Free intracellular Ca2+ regulates bacterial lipopolysaccharide induction of iNOS in human macrophages. *Immunobiology*, 214(2), pp.143–52.

Bajpai, U.D. et al., 2000. Bruton's tyrosine kinase links the B cell receptor to nuclear factor kappaB activation. *The Journal of experimental medicine*, 191(10), pp.1735–44.

Banki, K. et al., 1999. Elevation of mitochondrial transmembrane potential and reactive oxygen intermediate levels are early events and occur independently from activation of caspases in Fas signaling. *Journal of immunology (Baltimore, Md. : 1950)*, 162(3), pp.1466–79.

Baroja, M.L. et al., 1988. Cooperation between an anti-T cell (anti-CD28) monoclonal antibody and monocyte-produced IL-6 in the induction of T cell responsiveness to IL-2. *Journal of immunology (Baltimore, Md. : 1950)*, 141(5), pp.1502–7.

Barr, T. a et al., 2007. TLR-mediated stimulation of APC: Distinct cytokine responses of B cells and dendritic cells. *European journal of immunology*, 37(11), pp.3040–53.

Barth, K.R., Isabella, V.M. & Clark, V.L., 2009. Biochemical and genomic analysis of the denitrification pathway within the genus *Neisseria*. *Microbiology (Reading, England)*, 155(Pt 12), pp.4093–103.

Bauer, H. et al., 1997. Nitric oxide inhibits the secretion of T-helper 1- and T-helper 2-associated cytokines in activated human T cells. *Immunology*, 90(2), pp.205–11.

Beauchemin, N. et al., 1999. Redefined nomenclature for members of the carcinoembryonic antigen family. *Experimental cell research*, 252(2), pp.243–9.

Van de Beek, D. et al., 2004. Clinical features and prognostic factors in adults with bacterial meningitis. *The New England journal of medicine*, 351(18), pp.1849–59.

Van de Beek, D. et al., 2006. Community-acquired bacterial meningitis in adults. *The New England journal of medicine*, 354(1), pp.44–53.

Bekeredjian-Ding, I. & Jego, G., 2009. Toll-like receptors--sentries in the B-cell response. *Immunology*, 128(3), pp.311–23.

Beltrán, B. et al., 2000. The effect of nitric oxide on cell respiration: A key to understanding its role in cell survival or death. *Proceedings of the National Academy of Sciences of the United States of America*, 97(26), pp.14602–7.

Benson, M.J. et al., 2007. All-trans retinoic acid mediates enhanced T reg cell growth, differentiation, and gut homing in the face of high levels of co-stimulation. *The Journal of experimental medicine*, 204(8), pp.1765–74.

Berks, B.C. et al., 1995. Enzymes and associated electron transport systems that catalyse the respiratory reduction of nitrogen oxides and oxyanions. *Biochimica et biophysica acta*, 1232(3), pp.97–173.

Bernatchez, P. et al., 2011. A noninhibitory mutant of the caveolin-1 scaffolding domain enhances eNOS-derived NO synthesis and vasodilation in mice. *The Journal of clinical investigation*, 121(9), pp.3747–55.

Bettelli, E. et al., 2008. Induction and effector functions of T(H)17 cells. *Nature*, 453(7198), pp.1051–7.

Billiar, T.R. et al., 1990. Modulation of nitrogen oxide synthesis in vivo: NG-monomethyl-L-arginine inhibits endotoxin-induced nitrate/nitrate biosynthesis while promoting hepatic damage. *Journal of leukocyte biology*, 48(6), pp.565–9.

Bingisser, R.M. et al., 1998. Macrophage-derived nitric oxide regulates T cell activation via reversible disruption of the Jak3/STAT5 signaling pathway. *Journal of immunology (Baltimore, Md. : 1950)*, 160(12), pp.5729–34.

Bisset, L.R. et al., 2004. Reference values for peripheral blood lymphocyte phenotypes applicable to the healthy adult population in Switzerland. *European journal of haematology*, 72(3), pp.203–12.

Bjerre, a. et al., 2000. Cellular activating properties and morphology of membrane-bound and purified meningococcal lipopolysaccharide. *Journal of Endotoxin Research*, 6(6), pp.437–445.

Bjerre, A. et al., 2004. Plasma interferon-gamma and interleukin-10 concentrations in systemic meningococcal disease compared with severe systemic Gram-positive septic shock. *Critical care medicine*, 32(2), pp.433–8.

Bjordahl, R.L. et al., 2012. iNKT cells suppress the CD8+ T cell response to a murine Burkitt's-like B cell lymphoma. *PloS one*, 7(8), p.e42635.

Blair, P. a et al., 2010. CD19(+)CD24(hi)CD38(hi) B cells exhibit regulatory capacity in healthy individuals but are functionally impaired in systemic Lupus Erythematosus patients. *Immunity*, 32(1), pp.129–40.

Bogdan, C., 2001. Nitric oxide and the immune response. *Nature immunology*, 2(10), pp.907–16.

Bos, M.P. et al., 2002. Carcinoembryonic antigen family receptor recognition by gonococcal Opa proteins requires distinct combinations of hypervariable Opa protein domains. *Infection and immunity*, 70(4), pp.1715–23.

Bouaziz, J.-D. et al., 2010. IL-10 produced by activated human B cells regulates CD4(+) T-cell activation in vitro. *European journal of immunology*, 40(10), pp.2686–91.

Boulanger, M.J. & Murphy, M.E.P., 2002. Crystal structure of the soluble domain of the major anaerobically induced outer membrane protein (AniA) from pathogenic *Neisseria*: a new class of copper-containing nitrite reductases. *Journal of molecular biology*, 315(5), pp.1111–27.

Boulton, I.C. & Gray-Owen, S.D., 2002. Neisserial binding to CEACAM1 arrests the activation and proliferation of CD4+ T lymphocytes. *Nature immunology*, 3(3), pp.229–36.

Bradley, C.J. et al., 2005. Critical determinants of the interactions of capsule-expressing *Neisseria meningitidis* with host cells: the role of receptor density in increased cellular targeting via the outer membrane Opa proteins. *Cellular microbiology*, 7(10), pp.1490–503.

Brandtzaeg, P. et al., 2001. Invited review: *Neisseria meningitidis* lipopolysaccharides in human pathology. *Journal of Endotoxin Research*, 7(6), pp.401–420.

Brandtzaeg, P. et al., 1989. Plasma endotoxin as a predictor of multiple organ failure and death in systemic meningococcal disease. *The Journal of infectious diseases*, 159(2), pp.195–204.

Brás, a et al., 1997. Nitric oxide regulates clonal expansion and activation-induced cell death triggered by staphylococcal enterotoxin B. *Infection and immunity*, 65(10), pp.4030–7.

Braun, J.M. et al., 2002. Proinflammatory responses to lipo-oligosaccharide of *Neisseria meningitidis* immunotype strains in relation to virulence and disease. *The Journal of infectious diseases*, 185(10), pp.1431–8.

Bredt, D.S. & Snyder, S.H., 1990. Isolation of nitric oxide synthetase, a calmodulin-requiring enzyme. *Proceedings of the National Academy of Sciences of the United States of America*, 87(2), pp.682–5.

Breitfeld, D. et al., 2000. Follicular B helper T cells express CXC chemokine receptor 5, localize to B cell follicles, and support immunoglobulin production. *The Journal of experimental medicine*, 192(11), pp.1545–52.

Bronte, V. et al., 2005. Boosting antitumor responses of T lymphocytes infiltrating human prostate cancers. *The Journal of experimental medicine*, 201(8), pp.1257–68.

Brookes, P.S. et al., 2000. Concentration-dependent effects of nitric oxide on mitochondrial permeability transition and cytochrome c release. *The Journal of biological chemistry*, 275(27), pp.20474–9.

Brown, G.C., 2001. Regulation of mitochondrial respiration by nitric oxide inhibition of cytochrome *c* oxidase. *Biochimica et biophysica acta*, 1504(1), pp.46–57.

Brown, G.C. & Cooper, C.E., 1994. Nanomolar concentrations of nitric oxide reversibly inhibit synaptosomal respiration by competing with oxygen at cytochrome oxidase. *FEBS letters*, 356(2-3), pp.295–8.

Brunswick, M. et al., 1988. Picogram quantities of anti-Ig antibodies coupled to dextran induce B cell proliferation. *Journal of immunology (Baltimore, Md. : 1950)*, 140(10), pp.3364–72.

Bryn, T. et al., 2008. LPS-activated monocytes suppress T-cell immune responses and induce FOXP3+ T cells through a COX-2-PGE2-dependent mechanism. *International immunology*, 20(2), pp.235–45.

Bucci, M. et al., 2000. In vivo delivery of the caveolin-1 scaffolding domain inhibits nitric oxide synthesis and reduces inflammation. *Nature medicine*, 6(12), pp.1362–7.

Buckee, C.O. et al., 2008. Role of selection in the emergence of lineages and the evolution of virulence in *Neisseria meningitidis*. *Proceedings of the National Academy of Sciences of the United States of America*, 105(39), pp.15082–7.

Buhl, A.M. & Cambier, J.C., 1999. Phosphorylation of CD19 Y484 and Y515, and linked activation of phosphatidylinositol 3-kinase, are required for B cell antigen receptor-mediated activation of Bruton's tyrosine kinase. *Journal of immunology (Baltimore, Md. : 1950)*, 162(8), pp.4438–46.

Bunbury, A. et al., 2009. Functional analysis of monocyte MHC class II compartments. *FASEB journal : official publication of the Federation of American Societies for Experimental Biology*, 23(1), pp.164–71.

Busch, T. et al., 2000. Nasal, pulmonary and autoinhaled nitric oxide at rest and during moderate exercise. *Intensive care medicine*, 26(4), pp.391–9.

Calame, K.L., 2001. Plasma cells: finding new light at the end of B cell development. *Nature immunology*, 2(12), pp.1103–8.

Call, M.E. et al., 2002. The organizing principle in the formation of the T cell receptor-CD3 complex. *Cell*, 111(7), pp.967–79.

Callaghan, M.J. et al., 2011. Potential of recombinant opa proteins as vaccine candidates against hyperinvasive meningococci. *Infection and immunity*, 79(7), pp.2810–8.

Callaghan, M.J., Jolley, K. a & Maiden, M.C.J., 2006. Opacity-associated adhesin repertoire in hyperinvasive *Neisseria meningitidis*. *Infection and immunity*, 74(9), pp.5085–94.

Calvano, J.E. et al., 2003. Modulation of the lipopolysaccharide receptor complex (CD14, TLR4, MD-2) and toll-like receptor 2 in systemic inflammatory response syndrome-positive patients with and without infection: relationship to tolerance. *Shock (Augusta, Ga.)*, 20(5), pp.415–9.

Carbonnelle, E. et al., 2009. Meningococcal interactions with the host. *Vaccine*, 27 Suppl 2, pp.B78–89.

Carpenter, A.C. & Bosselut, R., 2010. Decision checkpoints in the thymus. *Nature immunology*, 11(8), pp.666–73.

Carrol, E.D. et al., 2005. A predominantly anti-inflammatory cytokine profile is associated with disease severity in meningococcal sepsis. *Intensive care medicine*, 31(10), pp.1415–9.

Cartwright, K. a et al., 1987. The Stonehouse survey: nasopharyngeal carriage of meningococci and *Neisseria lactamica*. *Epidemiology and infection*, 99(3), pp.591–601.

Cassatella, M.A. et al., 1994. Interleukin 10 (IL-10) upregulates IL-1 receptor antagonist production from lipopolysaccharide-stimulated human polymorphonuclear leukocytes by delaying mRNA degradation. *The Journal of experimental medicine*, 179(5), pp.1695–9.

Cassell, D.J. & Schwartz, R.H., 1994. A quantitative analysis of antigen-presenting cell function: activated B cells stimulate naive CD4 T cells but are inferior to dendritic cells in providing costimulation. *The Journal of experimental medicine*, 180(5), pp.1829–40.

Caugant, D. a, 2008. Genetics and evolution of *Neisseria meningitidis*: importance for the epidemiology of meningococcal disease. *Infection, genetics and evolution : journal of molecular epidemiology and evolutionary genetics in infectious diseases*, 8(5), pp.558–65.

Caugant, D.A. et al., 1994. Asymptomatic carriage of *Neisseria meningitidis* in a randomly sampled population. *Journal of clinical microbiology*, 32(2), pp.323–30.

Cerutti, A. et al., 1998. CD40 ligand and appropriate cytokines induce switching to IgG, IgA, and IgE and coordinated germinal center and plasmacytoid phenotypic differentiation in a human monoclonal IgM+IgD+ B cell line. *Journal of immunology (Baltimore, Md. : 1950)*, 160(5), pp.2145–57.

Chakravortty, D. & Hensel, M., 2003. Inducible nitric oxide synthase and control of intracellular bacterial pathogens. *Microbes and infection / Institut Pasteur*, 5(7), pp.621–7.

Chatila, T. a et al., 1987. Requirement for mitogen, T cell-accessory cell contact, and interleukin 1 in the induction of resting T-cell proliferation. *Clinical immunology and immunopathology*, 44(2), pp.235–47.

Chen, C. & Shively, J.E., 2004. The cell-cell adhesion molecule carcinoembryonic antigen-related cellular adhesion molecule 1 inhibits IL-2 production and proliferation in human T cells by association with *Src* homology protein-1 and down-regulates IL-2 receptor. *Journal of immunology (Baltimore, Md. : 1950)*, 172(6), pp.3544–52.

Chen, L. et al., 2011. CD83-stimulated monocytes suppress T-cell immune responses through production of prostaglandin E2. *Proceedings of the National Academy of Sciences of the United States of America*, 108(46), pp.18778–83.

Chen, L.C. et al., 2009. Direct expansion of human allospecific FoxP3+CD4+ regulatory T cells with allogeneic B cells for therapeutic application. *Journal of immunology (Baltimore, Md. : 1950)*, 183(6), pp.4094–102.

Chen, Q. & Snapper, C.M., 2013. Inflammatory monocytes are critical for induction of a polysaccharide-specific antibody response to an intact bacterium. *Journal of immunology (Baltimore, Md. : 1950)*, 190(3), pp.1048–55.

Cheng, P.C. et al., 1999. MHC class II antigen processing in B cells: accelerated intracellular targeting of antigens. *Journal of immunology (Baltimore, Md. : 1950)*, 162(12), pp.7171–80.

Chesnut, R.W. & Grey, H.M., 1981. Studies on the capacity of B cells to serve as antigen-presenting cells. *Journal of immunology (Baltimore, Md. : 1950)*, 126(3), pp.1075–9.

Chidlow, J.H. et al., 2009. Endothelial caveolin-1 regulates pathologic angiogenesis in a mouse model of colitis. *Gastroenterology*, 136(2), pp.575–84.e2.

Chlichlia, K. et al., 1998. Caspase activation is required for nitric oxide-mediated, CD95(APO-1/Fas)-dependent and independent apoptosis in human neoplastic lymphoid cells. *Blood*, 91(11), pp.4311–20.

Choi, B.-S. et al., 2009. Differential impact of L-arginine deprivation on the activation and effector functions of T cells and macrophages. *Journal of leukocyte biology*, 85(2), pp.268–77.

Choi, Y.W. et al., 1989. Interaction of Staphylococcus aureus toxin “superantigens” with human T cells. *Proceedings of the National Academy of Sciences of the United States of America*, 86(22), pp.8941–5.

Chow, J.C. et al., 1999. Toll-like receptor-4 mediates lipopolysaccharide-induced signal transduction. *The Journal of biological chemistry*, 274(16), pp.10689–92.

Claus, H. et al., 2002. Many carried meningococci lack the genes required for capsule synthesis and transport. *Microbiology (Reading, England)*, 148(Pt 6), pp.1813–9.

Cleeter, M.W. et al., 1994. Reversible inhibition of cytochrome c oxidase, the terminal enzyme of the mitochondrial respiratory chain, by nitric oxide. Implications for neurodegenerative diseases. *FEBS letters*, 345(1), pp.50–4.

Constant, S. et al., 1995. B lymphocytes can be competent antigen-presenting cells for priming CD4+ T cells to protein antigens in vivo. *Journal of immunology (Baltimore, Md. : 1950)*, 155(8), pp.3734–41.

Corless, C.E. et al., 2001. Simultaneous detection of *Neisseria meningitidis, Haemophilus influenzae*, and *Streptococcus pneumoniae* in suspected cases of meningitis and septicemia using real-time PCR. *Journal of clinical microbiology*, 39(4), pp.1553–8.

Cornall, R.J. et al., 1998. Polygenic autoimmune traits: Lyn, CD22, and SHP-1 are limiting elements of a biochemical pathway regulating BCR signaling and selection. *Immunity*, 8(4), pp.497–508.

Coureuil, M. et al., 2009. Meningococcal type IV pili recruit the polarity complex to cross the brain endothelium. *Science (New York, N.Y.)*, 325(5936), pp.83–7.

Coutinho, A. et al., 1974. Mechanism of thymus-independent immunocyte triggering. Mitogenic activation of B cells results in specific immune responses. *The Journal of experimental medicine*, 139(1), pp.74–92.

Cowley, S.C., Myltseva, S. V & Nano, F.E., 1996. Phase variation in Francisella tularensis affecting intracellular growth, lipopolysaccharide antigenicity and nitric oxide production. *Molecular microbiology*, 20(4), pp.867–74.

Crawford, A. et al., 2006. Primary T cell expansion and differentiation in vivo requires antigen presentation by B cells. *Journal of immunology (Baltimore, Md. : 1950)*, 176(6), pp.3498–506.

Cruz-Ramos, H. et al., 2002. NO sensing by FNR: regulation of the *Escherichia coli* NO-detoxifying flavohaemoglobin, Hmp. *The EMBO journal*, 21(13), pp.3235–44.

Cucak, H. et al., 2009. Type I interferon signaling in dendritic cells stimulates the development of lymph-node-resident T follicular helper cells. *Immunity*, 31(3), pp.491–501.

Culotta, E. & Koshland, D.E., 1992. NO news is good news. *Science (New York, N.Y.)*, 258(5090), pp.1862–5.

Dal Porto, J.M. et al., 2004. B cell antigen receptor signaling 101. *Molecular immunology*, 41(6-7), pp.599–613.

Danilov, A.I. et al., 2005. Effects of long term NOS inhibition on disease and the immune system in MOG induced EAE. *Nitric oxide : biology and chemistry / official journal of the Nitric Oxide Society*, 13(3), pp.188–95.

Dardalhon, V. et al., 2008. IL-4 inhibits TGF-beta-induced Foxp3+ T cells and, together with TGF-beta, generates IL-9+ IL-10+ Foxp3(-) effector T cells. *Nature immunology*, 9(12), pp.1347–55.

Darton, T.C. et al., 2011. Bacterial genomic detection within cerebrospinal fluid of patients with meningococcal disease is influenced by microbial and host characteristics. *Clinical infectious diseases : an official publication of the Infectious Diseases Society of America*, 53(5), pp.463–7.

Das, A. et al., 2012. IL-10-producing regulatory B cells in the pathogenesis of chronic hepatitis B virus infection. *Journal of immunology (Baltimore, Md. : 1950)*, 189(8), pp.3925–35.

DelaTorre, a, Schroeder, R. a & Kuo, P.C., 1997. Alteration of NF-kappa B p50 DNA binding kinetics by S-nitrosylation. *Biochemical and biophysical research communications*, 238(3), pp.703–6.

Delves, P.J. & Roitt, I.M., 2000. The immune system. First of two parts. *The New England journal of medicine*, 343(1), pp.37–49.

Deniz, G. et al., 2002. Human NK1 and NK2 subsets determined by purification of IFN-gamma-secreting and IFN-gamma-nonsecreting NK cells. *European journal of immunology*, 32(3), pp.879–84.

Deniz, G. et al., 2008. Regulatory NK cells suppress antigen-specific T cell responses. *Journal of immunology (Baltimore, Md. : 1950)*, 180(2), pp.850–7.

Depoil, D. et al., 2008. CD19 is essential for B cell activation by promoting B cell receptor-antigen microcluster formation in response to membrane-bound ligand. *Nature immunology*, 9(1), pp.63–72.

Derkx, B. et al., 1995. High levels of interleukin-10 during the initial phase of fulminant meningococcal septic shock. *The Journal of infectious diseases*, 171(1), pp.229–32.

Van Deuren, M. et al., 1995. Correlation between proinflammatory cytokines and antiinflammatory mediators and the severity of disease in meningococcal infections. *The Journal of Infectious Diseases*, 172, pp.433–439.

Dimmeler, S. et al., 1998. Nitric oxide inhibits APO-1/Fas-mediated cell death. *Cell growth & differentiation : the molecular biology journal of the American Association for Cancer Research*, 9(5), pp.415–22.

Ding, A.H., Nathan, C.F. & Stuehr, D.J., 1988. Release of reactive nitrogen intermediates and reactive oxygen intermediates from mouse peritoneal macrophages. Comparison of activating cytokines and evidence for independent production. *Journal of immunology (Baltimore, Md. : 1950)*, 141(7), pp.2407–12.

Dintzis, R.Z., Middleton, M.H. & Dintzis, H.M., 1983. Studies on the immunogenicity and tolerogenicity of T-independent antigens. *Journal of immunology (Baltimore, Md. : 1950)*, 131(5), pp.2196–203.

Dixon, G.L. et al., 2001. Dendritic cell activation and cytokine production induced by group B *Neisseria meningitidis*: interleukin-12 production depends on lipopolysaccharide expression in intact bacteria. *Infection and immunity*, 69(7), pp.4351–7.

Donda, a et al., 2000. Locally inducible CD66a (CEACAM1) as an amplifier of the human intestinal T cell response. *European journal of immunology*, 30(9), pp.2593–603.

Dong, C. & Martinez, G.J., 2010. T cells: the usual subsets. *Nature Reviews: Immunology*, p.77030. Available at: http://www.nature.com/nri/posters/tcellsubsets/index.html [Accessed May 1, 2011].

Dopter, C., 1909. Etude de quelques germs isoles du rhino-pharynx, voisans du meningocoque (parameningocoques). *C R Soc Biol (París)*, p.74.

Driessler, F. et al., 2004. Molecular mechanisms of interleukin-10-mediated inhibition of NF-kappaB activity: a role for p50. *Clinical and experimental immunology*, 135(1), pp.64–73.

Dustin, M.L., 2008. T-cell activation through immunological synapses and kinapses. *Immunological reviews*, 221, pp.77–89.

Dziarski, R., 1982. Preferential induction of autoantibody secretion in polyclonal activation by peptidoglycan and lipopolysaccharide. I. In vitro studies. *Journal of immunology (Baltimore, Md. : 1950)*, 128(3), pp.1018–25.

Eisenstein, T.K., 2001. Implications of *Salmonella*-induced nitric oxide (NO) for host defense and vaccines: NO, an antimicrobial, antitumor, immunosuppressive and immunoregulatory molecule. *Microbes and infection / Institut Pasteur*, 3(14-15), pp.1223–31.

Elgueta, R. et al., 2009. Molecular mechanism and function of CD40/CD40L engagement in the immune system. *Immunological reviews*, 229(1), pp.152–72.

Eriksson, S. et al., 2000. *Salmonella typhimurium* mutants that downregulate phagocyte nitric oxide production. *Cellular microbiology*, 2(3), pp.239–50.

Erwin, P. a et al., 2006. Subcellular targeting and differential *S*-nitrosylation of endothelial nitric-oxide synthase. *The Journal of biological chemistry*, 281(1), pp.151–7.

Estabrook, M.M., Griffiss, J.M. & Jarvis, G.A., 1997. Sialylation of *Neisseria meningitidis* lipooligosaccharide inhibits serum bactericidal activity by masking lacto-N-neotetraose. *Infection and immunity*, 65(11), pp.4436–44.

Eyerich, S. et al., 2009. Th22 cells represent a distinct human T cell subset involved in epidermal immunity and remodeling. *The Journal of clinical investigation*, 119(12), pp.3573–85.

Fantini, M.C. et al., 2004. Cutting edge: TGF-beta induces a regulatory phenotype in CD4+CD25- T cells through Foxp3 induction and down-regulation of Smad7. *Journal of immunology (Baltimore, Md. : 1950)*, 172(9), pp.5149–53.

Fillatreau, S. et al., 2002. B cells regulate autoimmunity by provision of IL-10. *Nature immunology*, 3(10), pp.944–50.

Fingerle, G. et al., 1993. The novel subset of CD14+/CD16+ blood monocytes is expanded in sepsis patients. *Blood*, 82(10), pp.3170–6.

Fiorucci, S. et al., 2004. Nitric oxide regulates immune cell bioenergetic: a mechanism to understand immunomodulatory functions of nitric oxide-releasing anti-inflammatory drugs. *Journal of immunology (Baltimore, Md. : 1950)*, 173(2), pp.874–82.

Florquin, S. et al., 1994. The protective role of endogenously synthesized nitric oxide in staphylococcal enterotoxin B-induced shock in mice. *The Journal of experimental medicine*, 180(3), pp.1153–8.

Fluckiger, A.C. et al., 1998. Btk/Tec kinases regulate sustained increases in intracellular Ca2+ following B-cell receptor activation. *The EMBO journal*, 17(7), pp.1973–85.

Fontenot, J.D., Gavin, M. a & Rudensky, A.Y., 2003. Foxp3 programs the development and function of CD4+CD25+ regulatory T cells. *Nature immunology*, 4(4), pp.330–6.

Forsgren, a et al., 2001. Isolation and characterization of a novel IgD-binding protein from *Moraxella catarrhalis*. *Journal of immunology (Baltimore, Md. : 1950)*, 167(4), pp.2112–20.

Foster, M.W., Hess, D.T. & Stamler, J.S., 2009. Protein S-nitrosylation in health and disease: a current perspective. *Trends in molecular medicine*, 15(9), pp.391–404.

Foster, R. a et al., 2009. Evidence of a functional B-cell immunodeficiency in adults who experience serogroup C meningococcal disease. *Clinical and vaccine immunology : CVI*, 16(5), pp.692–8.

Fra, A.M. et al., 1994. Detergent-insoluble glycolipid microdomains in lymphocytes in the absence of caveolae. *The Journal of biological chemistry*, 269(49), pp.30745–8.

Frank, P.G. et al., 2003. Caveolin, caveolae, and endothelial cell function. *Arteriosclerosis, thrombosis, and vascular biology*, 23(7), pp.1161–8.

Franzoso, S. et al., 2008. Human monocytes/macrophages are a target of *Neisseria meningitidis* Adhesin A (NadA). *Journal of leukocyte biology*, 83(5), pp.1100–10.

Frasch, C.E., Zollinger, W.D. & Poolman, J.T., 1985. Serotype antigens of *Neisseria meningitidis* and a proposed scheme for designation of serotypes. *Reviews of infectious diseases*, 7(4), pp.504–10.

Freeman, G.J. et al., 2000. Engagement of the PD-1 immunoinhibitory receptor by a novel B7 family member leads to negative regulation of lymphocyte activation. *The Journal of experimental medicine*, 192(7), pp.1027–34.

Friebe, A. & Koesling, D., 2003. Regulation of nitric oxide-sensitive guanylyl cyclase. *Circulation research*, 93(2), pp.96–105.

Fujimoto, M. et al., 2000. CD19 regulates intrinsic B lymphocyte signal transduction and activation through a novel mechanism of processive amplification. *Immunologic research*, 22(2-3), pp.281–98.

Fujiwara, T. et al., 2006. Immunoregulation and apoptosis induction of nitric oxide in the human mixed lymphocytes culture. *Transplantation proceedings*, 38(10), pp.3211–3.

Fulton, D. et al., 1999. Regulation of endothelium-derived nitric oxide production by the protein kinase Akt. *Nature*, 399(6736), pp.597–601.

Fusco, P.C. et al., 1997. Preclinical evaluation of a novel group B meningococcal conjugate vaccine that elicits bactericidal activity in both mice and nonhuman primates. *The Journal of infectious diseases*, 175(2), pp.364–72.

Ganley-Leal, L.M., Liu, X. & Wetzler, L.M., 2006. Toll-like receptor 2-mediated human B cell differentiation. *Clinical immunology (Orlando, Fla.)*, 120(3), pp.272–84.

Gao, S. et al., 2004. Docking of endothelial nitric oxide synthase (eNOS) to the mitochondrial outer membrane: a pentabasic amino acid sequence in the autoinhibitory domain of eNOS targets a proteinase K-cleavable peptide on the cytoplasmic face of mitochondria. *The Journal of biological chemistry*, 279(16), pp.15968–74.

Garside, P. et al., 1998. Visualization of specific B and T lymphocyte interactions in the lymph node. *Science (New York, N.Y.)*, 281(5373), pp.96–9.

Garthwaite, J., 2008. Concepts of neural nitric oxide-mediated transmission. *The European journal of neuroscience*, 27(11), pp.2783–802.

Gauld, S.B. et al., 2002. Differential roles for extracellularly regulated kinase-mitogen-activated protein kinase in B cell antigen receptor-induced apoptosis and CD40-mediated rescue of WEHI-231 immature B cells. *Journal of immunology (Baltimore, Md. : 1950)*, 168(8), pp.3855–64.

Geisberger, R., Lamers, M. & Achatz, G., 2006. The riddle of the dual expression of IgM and IgD. *Immunology*, 118(4), pp.429–37.

Geissmann, F., Jung, S. & Littman, D.R., 2003. Blood monocytes consist of two principal subsets with distinct migratory properties. *Immunity*, 19(1), pp.71–82.

Genaro, a M. et al., 1995. Splenic B lymphocyte programmed cell death is prevented by nitric oxide release through mechanisms involving sustained Bcl-2 levels. *The Journal of clinical investigation*, 95(4), pp.1884–90.

Geppert, T.D. & Lipsky, P.E., 1987. Accessory cell independent proliferation of human T4 cells stimulated by immobilized monoclonal antibodies to CD3. *Journal of immunology (Baltimore, Md. : 1950)*, 138(6), pp.1660–6.

Gergely, P. et al., 2002. Mitochondrial hyperpolarization and ATP depletion in patients with systemic lupus erythematosus. *Arthritis and rheumatism*, 46(1), pp.175–90.

Ghafourifar, P. et al., 1999. Mitochondrial nitric-oxide synthase stimulation causes cytochrome c release from isolated mitochondria. Evidence for intramitochondrial peroxynitrite formation. *The Journal of biological chemistry*, 274(44), pp.31185–8.

Giardina, P.C. et al., 2001. Construction of acetate auxotrophs of *Neisseria meningitidis* to study host-meningococcal endotoxin interactions. *The Journal of biological chemistry*, 276(8), pp.5883–91.

Gibaldi, M., 1993. What is nitric oxide and why are so many people studying it? *Journal of clinical pharmacology*, 33(6), pp.488–96.

Giuliani, M.M. et al., 2006. A universal vaccine for serogroup B meningococcus. *Proceedings of the National Academy of Sciences of the United States of America*, 103(29), pp.10834–9.

Giulivi, C., Poderoso, J.J. & Boveris, A., 1998. Production of nitric oxide by mitochondria. *The Journal of biological chemistry*, 273(18), pp.11038–43.

Glockzin, S. et al., 1999. Activation of the cell death program by nitric oxide involves inhibition of the proteasome. *The Journal of biological chemistry*, 274(28), pp.19581–6.

Goldbach-Mansky, R., 2012. Immunology in clinic review series; focus on autoinflammatory diseases: update on monogenic autoinflammatory diseases: the role of interleukin (IL)-1 and an emerging role for cytokines beyond IL-1. *Clinical and experimental immunology*, 167(3), pp.391–404.

Gomes, B. et al., 2006. The cGMP/protein kinase G pathway contributes to dihydropyridine-sensitive calcium response and cytokine production in TH2 lymphocytes. *The Journal of biological chemistry*, 281(18), pp.12421–7.

Gorringe, A.R. & Pajón, R., 2012. Bexsero: a multicomponent vaccine for prevention of meningococcal disease. *Human vaccines & immunotherapeutics*, 8(2), pp.174–83.

Gorringe, A.R. et al., 2009. Phase I safety and immunogenicity study of a candidate meningococcal disease vaccine based on *Neisseria lactamica* outer membrane vesicles. *Clinical and vaccine immunology : CVI*, 16(8), pp.1113–20.

Gotschlich, E.C., Liu, T.Y. & Artenstein, M.S., 1969. Human immunity to the meningococcus. 3. Preparation and immunochemical properties of the group A, group B, and group C meningococcal polysaccharides. *The Journal of experimental medicine*, 129(6), pp.1349–65.

Goubier, A. et al., 2013. Invariant NKT cells suppress CD8(+) T-cell-mediated allergic contact dermatitis independently of regulatory CD4(+) T cells. *The Journal of investigative dermatology*, 133(4), pp.980–7.

Goud, S.N., Kaplan, A.M. & Subbarao, B., 1990. Primary antibody responses to thymus-independent antigens in the lungs and hilar lymph nodes of mice. *Infection and immunity*, 58(7), pp.2035–41.

Gramaglia, I. et al., 2000. The OX40 costimulatory receptor determines the development of CD4 memory by regulating primary clonal expansion. *Journal of Immunology*, 165(6), pp.3043–3050.

Gratton, J.P. et al., 2003. Selective inhibition of tumor microvascular permeability by cavtratin blocks tumor progression in mice. *Cancer cell*, 4(1), pp.31–9.

Gray-Owen, S.D. et al., 1997. CD66 carcinoembryonic antigens mediate interactions between Opa-expressing *Neisseria gonorrhoeae* and human polymorphonuclear phagocytes. *The EMBO journal*, 16(12), pp.3435–45.

Gray-Owen, S.D. & Blumberg, R.S., 2006. CEACAM1: contact-dependent control of immunity. *Nature reviews. Immunology*, 6(6), pp.433–46.

Green, J.M. et al., 1994. Absence of B7-dependent responses in CD28-deficient mice. *Immunity*, 1(6), pp.501–8.

Gregory, S.H. et al., 1993. Reactive nitrogen intermediates suppress the primary immunologic response to *Listeria*. *Journal of immunology (Baltimore, Md. : 1950)*, 150(7), pp.2901–9.

Grimaldi, C.M., Hicks, R. & Diamond, B., 2005. B cell selection and susceptibility to autoimmunity. *Journal of immunology (Baltimore, Md. : 1950)*, 174(4), pp.1775–81.

Grisham, M.B., Granger, D.N. & Lefer, D.J., 1998. Modulation of leukocyte-endothelial interactions by reactive metabolites of oxygen and nitrogen: relevance to ischemic heart disease. *Free radical biology & medicine*, 25(4-5), pp.404–33.

Grommé, M. & Neefjes, J., 2002. Antigen degradation or presentation by MHC class I molecules via classical and non-classical pathways. *Molecular immunology*, 39(3-4), pp.181–202.

Guy, C.S. et al., 2013. Distinct TCR signaling pathways drive proliferation and cytokine production in T cells. *Nature immunology*, 14(3), pp.262–70.

Hackett, S.J. et al., 2002. Meningococcal bacterial DNA load at presentation correlates with disease severity. *Archives of disease in childhood*, 86(1), pp.44–6.

Hammerschmidt, S. et al., 1996. Capsule phase variation in *Neisseria meningitidis* serogroup B by slipped-strand mispairing in the polysialyltransferase gene (siaD): correlation with bacterial invasion and the outbreak of meningococcal disease. *Molecular microbiology*, 20(6), pp.1211–20.

Hara, M.R. et al., 2005. S-nitrosylated GAPDH initiates apoptotic cell death by nuclear translocation following Siah1 binding. *Nature cell biology*, 7(7), pp.665–74.

Harari, A. et al., 2009. Distinct profiles of cytotoxic granules in memory CD8 T cells correlate with function, differentiation stage, and antigen exposure. *Journal of virology*, 83(7), pp.2862–71.

Harrington, L.E. et al., 2005. Interleukin 17-producing CD4+ effector T cells develop via a lineage distinct from the T helper type 1 and 2 lineages. *Nature immunology*, 6(11), pp.1123–32.

Harris, D.P. et al., 2005. Cutting edge: the development of IL-4-producing B cells (B effector 2 cells) is controlled by IL-4, IL-4 receptor alpha, and Th2 cells. *Journal of immunology (Baltimore, Md. : 1950)*, 175(11), pp.7103–7.

Harris, D.P. et al., 2000. Reciprocal regulation of polarized cytokine production by effector B and T cells. *Nature immunology*, 1(6), pp.475–82.

Harrison, O.B. et al., 2013. Description and nomenclature of *Neisseria meningitidis* capsule locus. *Emerging infectious diseases*, 19(4), pp.566–73.

Harrison, L.H., Trotter, C.L. & Ramsay, M.E., 2009. Global epidemiology of meningococcal disease. *Vaccine*, 27 Suppl 2, pp.B51–63.

Hatanaka, M. et al., 1998. Expression of caveolin-1 in human T cell leukemia cell lines. *Biochemical and biophysical research communications*, 253(2), pp.382–7.

"Health Protection Agency," 2012. Guidance for public health management of meningococcal disease in the UK. , p.59.

Hellerud, B.C. et al., 2008. Stages of meningococcal sepsis simulated in vitro, with emphasis on complement and Toll-like receptor activation. *Infection and immunity*, 76(9), pp.4183–9.

Henry, Y. & Guissani, a, 1999. Interactions of nitric oxide with hemoproteins: roles of nitric oxide in mitochondria. *Cellular and molecular life sciences : CMLS*, 55(8-9), pp.1003–14.

Herzenberg, L.A., 2000. B-1 cells: the lineage question revisited. *Immunological reviews*, 175, pp.9–22.

Hess, D.T. et al., 2005. Protein S-nitrosylation: purview and parameters. *Nature reviews. Molecular cell biology*, 6(2), pp.150–66.

Heufler, C. et al., 1996. Interleukin-12 is produced by dendritic cells and mediates T helper 1 development as well as interferon-gamma production by T helper 1 cells. *European journal of immunology*, 26(3), pp.659–68.

Heurlier, K. et al., 2008. The nitric oxide (NO)-sensing repressor NsrR of *Neisseria meningitidis* has a compact regulon of genes involved in NO synthesis and detoxification. *Journal of bacteriology*, 190(7), pp.2488–95.

Hilkens, C.M. et al., 1997. Human dendritic cells require exogenous interleukin-12-inducing factors to direct the development of naive T-helper cells toward the Th1 phenotype. *Blood*, 90(5), pp.1920–6.

Hirahara, K. et al., 2013. Mechanisms underlying helper T-cell plasticity: Implications for immune-mediated disease. *The Journal of allergy and clinical immunology*, 131(5), pp.1276–87.

Holst, J. et al., 2009. Properties and clinical performance of vaccines containing outer membrane vesicles from *Neisseria meningitidis*. *Vaccine*, 27 Suppl 2, pp.B3–12.

Holten, E., 1979. Serotypes of *Neisseria meningitidis* isolated from patients in Norway during the first six months of 1978. *Journal of clinical microbiology*, 9(2), pp.186–8.

Householder, T.C. et al., 1999. cis- and trans-acting elements involved in regulation of aniA, the gene encoding the major anaerobically induced outer membrane protein in *Neisseria gonorrhoeae*. *Journal of bacteriology*, 181(2), pp.541–51.

Householder, T.C. et al., 2000. Gonococcal nitric oxide reductase is encoded by a single gene, norB, which is required for anaerobic growth and is induced by nitric oxide. *Infection and immunity*, 68(9), pp.5241–6.

Huet, S. et al., 1987. Role in T-cell activation for HLA class I molecules from accessory cells: further distinction between activation signals delivered to T cells via CD2 and CD3 molecules. *Proceedings of the National Academy of Sciences of the United States of America*, 84(20), pp.7222–6.

Hutloff, A. et al., 1999. ICOS is an inducible T-cell co-stimulator structurally and functionally related to CD28. *Nature*, 397(6716), pp.263–6.

Ianaro, a et al., 1994. A nitric oxide synthase inhibitor reduces inflammation, down-regulates inflammatory cytokines and enhances interleukin-10 production in carrageenin-induced oedema in mice. *Immunology*, 82(3), pp.370–5.

Ibiza, S. et al., 2008. Endothelial nitric oxide synthase regulates N-Ras activation on the Golgi complex of antigen-stimulated T cells. *Proceedings of the National Academy of Sciences of the United States of America*, 105(30), pp.10507–12.

Ibiza, S. et al., 2006. Endothelial nitric oxide synthase regulates T cell receptor signaling at the immunological synapse. *Immunity*, 24(6), pp.753–65.

Ignarro, L.J. et al., 1987. Endothelium-derived relaxing factor produced and released from artery and vein is nitric oxide. *Proceedings of the National Academy of Sciences of the United States of America*, 84(24), pp.9265–9.

Ignarro, L.J. et al., 1993. Oxidation of nitric oxide in aqueous solution to nitrite but not nitrate: comparison with enzymatically formed nitric oxide from L-arginine. *Proceedings of the National Academy of Sciences of the United States of America*, 90(17), pp.8103–7.

Iijima, N. et al., 2008. Dendritic cells and B cells maximize mucosal Th1 memory response to herpes simplex virus. *The Journal of experimental medicine*, 205(13), pp.3041–52.

Imboden, J.B. & Weiss, a, 1987. The T-cell antigen receptor regulates sustained increases in cytoplasmic free Ca2+ through extracellular Ca2+ influx and ongoing intracellular Ca2+ mobilization. *The Biochemical journal*, 247(3), pp.695–700.

Ingalls, R.R., Lien, E. & Golenbock, D.T., 2001. Membrane-associated proteins of a lipopolysaccharide-deficient mutant of *Neisseria meningitidis* activate the inflammatory response through toll-like receptor 2. *Infection and immunity*, 69(4), pp.2230–6.

Into, T. et al., 2008. Regulation of MyD88-dependent signaling events by S nitrosylation retards toll-like receptor signal transduction and initiation of acute-phase immune responses. *Molecular and cellular biology*, 28(4), pp.1338–47.

Isobe, K. & Nakashima, I., 1992. Feedback suppression of staphylococcal enterotoxin-stimulated T-lymphocyte proliferation by macrophages through inductive nitric oxide synthesis. *Infection and immunity*, 60(11), pp.4832–7.

Jaimes, E. a et al., 2001. Countervailing influence of tumor necrosis factor-alpha and nitric oxide in endotoxemia. *Journal of the American Society of Nephrology : JASN*, 12(6), pp.1204–10.

Janeway, C.A., 1992. The T cell receptor as a multicomponent signalling machine: CD4/CD8 coreceptors and CD45 in T cell activation. *Annual review of immunology*, 10, pp.645–74.

Janeway, C.A. & Medzhitov, R., 2002. Innate immune recognition. *Annual review of immunology*, 20(2), pp.197–216.

Janssen-Heininger, Y.M., Poynter, M.E. & Baeuerle, P.A., 2000. Recent advances towards understanding redox mechanisms in the activation of nuclear factor kappaB. *Free radical biology & medicine*, 28(9), pp.1317–27.

Jarva, H. et al., 2005. Binding of the complement inhibitor C4bp to serogroup B *Neisseria meningitidis*. *Journal of immunology (Baltimore, Md. : 1950)*, 174(10), pp.6299–307.

JCVI, 2013. JCVI interim position statement on use of Bexsero® meningococcal B vaccine in the UK.https://www.gov.uk/government/uploads/system/uploads/attachment_data/file/224896/JCVI_interim_statement_on_meningococcal_B_vaccination_for_web.pdf

Jenkins, M.K. et al., 1991. CD28 delivers a costimulatory signal involved in antigen-specific IL-2 production by human T cells. *Journal of immunology (Baltimore, Md. : 1950)*, 147(8), pp.2461–6.

Jensen, D.E., Belka, G.K. & Du Bois, G.C., 1998. S-Nitrosoglutathione is a substrate for rat alcohol dehydrogenase class III isoenzyme. *The Biochemical journal*, 331 (Pt 2, pp.659–68.

Johnston, R.J. et al., 2009. Bcl6 and Blimp-1 are reciprocal and antagonistic regulators of T follicular helper cell differentiation. *Science (New York, N.Y.)*, 325(5943), pp.1006–10.

Joss, a et al., 2000. IL-10 directly acts on T cells by specifically altering the CD28 co-stimulation pathway. *European journal of immunology*, 30(6), pp.1683–90.

Ju, H. et al., 1997. Direct interaction of endothelial nitric-oxide synthase and caveolin-1 inhibits synthase activity. *The Journal of biological chemistry*, 272(30), pp.18522–5.

Kaiko, G.E. et al., 2008. Immunological decision-making: how does the immune system decide to mount a helper T-cell response? *Immunology*, 123(3), pp.326–38.

Källström, H. et al., 1997. Membrane cofactor protein (MCP or CD46) is a cellular pilus receptor for pathogenic *Neisseria*. *Molecular Microbiology*, 25, pp.639–647.

Kammerer, R. et al., 1998. Biliary glycoprotein (CD66a), a cell adhesion molecule of the immunoglobulin superfamily, on human lymphocytes: structure, expression and involvement in T cell activation. *European journal of immunology*, 28(11), pp.3664–74.

Kanswal, S. et al., 2011. Suppressive effect of bacterial polysaccharides on BAFF system is responsible for their poor immunogenicity. *Journal of immunology (Baltimore, Md. : 1950)*, 186(4), pp.2430–43.

Kawai, T. & Akira, S., 2011. Toll-like receptors and their crosstalk with other innate receptors in infection and immunity. *Immunity*, 34(5), pp.637–50.

Kennedy, N.J. et al., 1999. Caspase activation is required for T cell proliferation. *The Journal of experimental medicine*, 190(12), pp.1891–6.

Kerwin, J.F. & Heller, M., 1994. The arginine-nitric oxide pathway: a target for new drugs. *Medicinal research reviews*, 14(1), pp.23–74.

Khan, A.Q., Lees, A. & Snapper, C.M., 2004. Differential regulation of IgG anti-capsular polysaccharide and antiprotein responses to intact *Streptococcus pneumoniae* in the presence of cognate CD4+ T cell help. *Journal of immunology (Baltimore, Md. : 1950)*, 172(1), pp.532–9.

Khan, W.N. et al., 1995. Defective B cell development and function in Btk-deficient mice. *Immunity*, 3(3), pp.283–99.

Khan, W.N., 2001. Regulation of B lymphocyte development and activation by Bruton's tyrosine kinase. *Immunologic research*, 23(2-3), pp.147–56.

Kilbourn, R.G. et al., 1990. Reversal of endotoxin-mediated shock by NG-methyl-L-arginine, an inhibitor of nitric oxide synthesis. *Biochemical and biophysical research communications*, 172(3), pp.1132–8.

Kim, J.J., Mandrell, R.E. & Griffiss, J.M., 1989. *Neisseria lactamica* and *Neisseria meningitidis* share lipooligosaccharide epitopes but lack common capsular and class 1, 2, and 3 protein epitopes. *Infection and immunity*, 57(2), pp.602–8.

Kim, K.M. & Reth, M., 1995. The B cell antigen receptor of class IgD induces a stronger and more prolonged protein tyrosine phosphorylation than that of class IgM. *The Journal of experimental medicine*, 181(3), pp.1005–14.

Kim, P.K. et al., 2001. The regulatory role of nitric oxide in apoptosis. *International immunopharmacology*, 1(8), pp.1421–41.

Kinjo, Y. et al., 2011. Invariant natural killer T cells recognize glycolipids from pathogenic Gram-positive bacteria. *Nature immunology*, 12(10), pp.966–74.

Kirchner, M., Heuer, D. & Meyer, T.F., 2005. CD46-independent binding of neisserial type IV pili and the major pilus adhesin, PilC, to human epithelial cells. *Infection and immunity*, 73(5), pp.3072–82.

Knowles, R.G. & Moncada, S., 1994. Nitric oxide synthases in mammals. *The Biochemical journal*, 298 (Pt 2, pp.249–58.

Knuf, M. et al., 2013. Immunogenicity and safety of the quadrivalent meningococcal serogroups A, C, W-135 and Y tetanus toxoid conjugate vaccine (MenACWY-TT) in 2-10-year-old children: results of an open, randomised, controlled study. *European journal of pediatrics*, 172(5), pp.601–12.

Kobayashi, N., Nagumo, H. & Agematsu, K., 2002. IL-10 enhances B-cell IgE synthesis by promoting differentiation into plasma cells, a process that is inhibited by CD27/CD70 interaction. *Clinical and experimental immunology*, 129(3), pp.446–52.

Kocabas, C. et al., 2007. *Neisseria meningitidis* type C capsular polysaccharide inhibits lipooligosaccharide-induced cell activation by binding to CD14. *Cellular microbiology*, 9(5), pp.1297–310.

Koenig, A. et al., 2012. Proliferating γδ T cells manifest high and spatially confined caspase-3 activity. *Immunology*, 135(4), pp.276–86.

Kolb-Mäurer, A. et al., 2001. Interaction of *Neisseria meningitidis* with human dendritic cells. *Infection and immunity*, 69(11), pp.6912–22.

Korhonen, R. et al., 2008. Nitric oxide-releasing compounds inhibit the production of interleukin-2, -4 and -10 in activated human lymphocytes. *Basic & clinical pharmacology & toxicology*, 103(4), pp.322–8.

Kornelisse, R.F. et al., 1996. The role of nitric oxide in bacterial meningitis in children. *The Journal of infectious diseases*, 174(1), pp.120–6.

Kozjak-Pavlovic, V. et al., 2009. Bacterial porin disrupts mitochondrial membrane potential and sensitizes host cells to apoptosis. *PLoS pathogens*, 5(10), p.e1000629.

Kronenberg, M. & Kinjo, Y., 2009. Innate-like recognition of microbes by invariant natural killer T cells. *Current opinion in immunology*, 21(4), pp.391–6.

Kryczek, I. et al., 2006. B7-H4 expression identifies a novel suppressive macrophage population in human ovarian carcinoma. *The Journal of experimental medicine*, 203(4), pp.871–81.

Kwok, W. et al., 2009. Caveolin-1 mediates endotoxin inhibition of endothelin-1-induced endothelial nitric oxide synthase activity in liver sinusoidal endothelial cells. *AJP: Gastrointestinal and Liver Physiology*, 297(5), pp.G930–G939.

Kwon, S., Newcomb, R.L. & George, S.C., 2001. Mechanisms of synergistic cytokine-induced nitric oxide production in human alveolar epithelial cells. *Nitric oxide : biology and chemistry / official journal of the Nitric Oxide Society*, 5(6), pp.534–46.

Lampropoulou, V. et al., 2008. TLR-activated B cells suppress T cell-mediated autoimmunity. *Journal of immunology (Baltimore, Md. : 1950)*, 180(7), pp.4763–73.

Lander, H.M. et al., 1997. A molecular redox switch on p21(ras). Structural basis for the nitric oxide-p21(ras) interaction. *The Journal of biological chemistry*, 272(7), pp.4323–6.

Langrish, C.L. et al., 2005. IL-23 drives a pathogenic T cell population that induces autoimmune inflammation. *The Journal of experimental medicine*, 201(2), pp.233–40.

Lanie, J. a et al., 2007. Genome sequence of Avery's virulent serotype 2 strain D39 of *Streptococcus pneumoniae* and comparison with that of unencapsulated laboratory strain R6. *Journal of bacteriology*, 189(1), pp.38–51.

Latchman, Y. et al., 2001. PD-L2 is a second ligand for PD-1 and inhibits T cell activation. *Nature immunology*, 2(3), pp.261–8.

Laver, J.R. et al., 2010. Bacterial nitric oxide detoxification prevents host cell S-nitrosothiol formation: a novel mechanism of bacterial pathogenesis. *FASEB journal : official publication of the Federation of American Societies for Experimental Biology*, 24(1), pp.286–95.

Lécuyer, H., Nassif, X. & Coureuil, M., 2012. Two strikingly different signaling pathways are induced by meningococcal type IV pili on endothelial and epithelial cells. *Infection and immunity*, 80(1), pp.175–86.

Lee, H.S.W. et al., 2007. Neisserial outer membrane vesicles bind the coinhibitory receptor carcinoembryonic antigen-related cellular adhesion molecule 1 and suppress CD4+ T lymphocyte function. *Infection and immunity*, 75(9), pp.4449–55.

Lee, H.S.W., Ostrowski, M.A. & Gray-Owen, S.D., 2008. CEACAM1 dynamics during neisseria gonorrhoeae suppression of CD4+ T lymphocyte activation. *Journal of immunology (Baltimore, Md. : 1950)*, 180(10), pp.6827–35.

Lee, S.W. et al., 2005. PilT is required for PI(3,4,5)P3-mediated crosstalk between *Neisseria* gonorrhoeae and epithelial cells. *Cellular microbiology*, 7(9), pp.1271–84.

Lejeune, P. et al., 1994. Nitric oxide involvement in tumor-induced immunosuppression. *Journal of immunology (Baltimore, Md. : 1950)*, 152(10), pp.5077–83.

Leon, C.G. et al., 2008. Discovery and development of toll-like receptor 4 (TLR4) antagonists: a new paradigm for treating sepsis and other diseases. *Pharmaceutical research*, 25(8), pp.1751–61.

Leung, J. & Suh, W.-K., 2013. Host B7-H4 Regulates Antitumor T Cell Responses through Inhibition of Myeloid-Derived Suppressor Cells in a 4T1 Tumor Transplantation Model. *Journal of immunology (Baltimore, Md. : 1950)*.

Li, F. et al., 2010. Cell culture processes for monoclonal antibody production. *mAbs*, 2(5), pp.466–479.

Li, Z. et al., 1997. Phosphatidylinositol 3-kinase-gamma activates Bruton's tyrosine kinase in concert with Src family kinases. *Proceedings of the National Academy of Sciences of the United States of America*, 94(25), pp.13820–5.

Liang, Y. et al., 2011. Toll-like receptor 2 induces mucosal homing receptor expression and IgA production by human B cells. *Clinical immunology (Orlando, Fla.)*, 138(1), pp.33–40.

Lin, M.I. et al., 2007. Caveolin-1-deficient mice have increased tumor microvascular permeability, angiogenesis, and growth. *Cancer research*, 67(6), pp.2849–56.

Ling, E.M. et al., 2004. Relation of CD4+CD25+ regulatory T-cell suppression of allergen-driven T-cell activation to atopic status and expression of allergic disease. *Lancet*, 363(9409), pp.608–15.

Linsley, P.S., Brady, W., Grosmaire, L., et al., 1991. Binding of the B cell activation antigen B7 to CD28 costimulates T cell proliferation and interleukin 2 mRNA accumulation. *The Journal of experimental medicine*, 173(3), pp.721–30.

Linsley, P.S., Brady, W., Urnes, M., et al., 1991. CTLA-4 is a second receptor for the B cell activation antigen B7. *The Journal of experimental medicine*, 174(3), pp.561–9.

Linsley, P.S. et al., 1992. Immunosuppression in vivo by a soluble form of the CTLA-4 T cell activation molecule. *Science (New York, N.Y.)*, 257(5071), pp.792–5.

Linton, P.-J. et al., 2003. Costimulation via OX40L expressed by B cells is sufficient to determine the extent of primary CD4 cell expansion and Th2 cytokine secretion in vivo. *The Journal of experimental medicine*, 197(7), pp.875–83.

Lissenden, S. et al., 2000. Identification of transcription activators that regulate gonococcal adaptation from aerobic to anaerobic or oxygen-limited growth. *Molecular microbiology*, 37(4), pp.839–55.

Liu, R. et al., 2006. Autoreactive T cells mediate NK cell degeneration in autoimmune disease. *Journal of immunology (Baltimore, Md. : 1950)*, 176(9), pp.5247–54.

Liu, Y.J. et al., 1996. Within germinal centers, isotype switching of immunoglobulin genes occurs after the onset of somatic mutation. *Immunity*, 4(3), pp.241–50.

Lu, Y.-C., Yeh, W.-C. & Ohashi, P.S., 2008. LPS/TLR4 signal transduction pathway. *Cytokine*, 42(2), pp.145–51.

Lünemann, A., Lünemann, J.D. & Münz, C., 2009. Regulatory NK-cell functions in inflammation and autoimmunity. *Molecular medicine (Cambridge, Mass.)*, 15(9-10), pp.352–8.

Lund, F.E. & Randall, T.D., 2010. Effector and regulatory B cells: modulators of CD4+ T cell immunity. *Nature reviews. Immunology*, 10(4), pp.236–47.

Lundberg, J.O. & Weitzberg, E., 1999. Nasal nitric oxide in man. *Thorax*, 54(10), pp.947–52.

Lyons, a B., 2000. Analysing cell division in vivo and in vitro using flow cytometric measurement of CFSE dye dilution. *Journal of immunological methods*, 243(1-2), pp.147–54.

Lyons, a B. & Parish, C.R., 1994. Determination of lymphocyte division by flow cytometry. *Journal of immunological methods*, 171(1), pp.131–7.

Macaulay, A.E. et al., 1997. Antigen-specific B cells preferentially induce CD4+ T cells to produce IL-4. *Journal of immunology (Baltimore, Md. : 1950)*, 158(9), pp.4171–9.

Mackinnon, F.G. et al., 1993. Demonstration of lipooligosaccharide immunotype and capsule as virulence factors for *Neisseria meningitidis* using an infant mouse intranasal infection model. *Microbial pathogenesis*, 15(5), pp.359–66.

Macphail, S.E. et al., 2003. Nitric oxide regulation of human peripheral blood mononuclear cells: critical time dependence and selectivity for cytokine versus chemokine expression. *Journal of immunology (Baltimore, Md. : 1950)*, 171(9), pp.4809–15.

Mahidhara, R.S. et al., 2003. Nitric oxide-mediated inhibition of caspase-dependent T lymphocyte proliferation. *Journal of leukocyte biology*, 74(3), pp.403–11.

Maiden, M.C. et al., 1998. Multilocus sequence typing: a portable approach to the identification of clones within populations of pathogenic microorganisms. *Proceedings of the National Academy of Sciences of the United States of America*, 95(6), pp.3140–5.

Mannick, J.B. et al., 1999. Fas-induced caspase denitrosylation. *Science (New York, N.Y.)*, 284(5414), pp.651–4.

Mannick, J.B. et al., 2001. S-Nitrosylation of mitochondrial caspases. *The Journal of cell biology*, 154(6), pp.1111–6.

Mannick, J.B., Miao, X.Q. & Stamler, J.S., 1997. Nitric oxide inhibits Fas-induced apoptosis. *The Journal of biological chemistry*, 272(39), pp.24125–8.

Marie, J.C. et al., 2005. TGF-beta1 maintains suppressor function and Foxp3 expression in CD4+CD25+ regulatory T cells. *The Journal of experimental medicine*, 201(7), pp.1061–7.

Marzoa, J. et al., 2012. Induction of immune responses by purified outer membrane protein complexes from *Neisseria meningitidis*. *Vaccine*, 30(13), pp.2387–95.

Masignani, V. et al., 2001. Mu-like Prophage in serogroup B *Neisseria meningitidis* coding for surface-exposed antigens. *Infection and immunity*, 69(4), pp.2580–8.

Massari, P. et al., 2002. Cutting edge: Immune stimulation by neisserial porins is toll-like receptor 2 and MyD88 dependent. *Journal of immunology (Baltimore, Md. : 1950)*, 168(4), pp.1533–7.

Massari, P. et al., 2006. Meningococcal porin PorB binds to TLR2 and requires TLR1 for signaling. *Journal of immunology (Baltimore, Md. : 1950)*, 176(4), pp.2373–80.

Massari, P., Ho, Y. & Wetzler, L.M., 2000. *Neisseria meningitidis* porin PorB interacts with mitochondria and protects cells from apoptosis. *Proceedings of the National Academy of Sciences of the United States of America*, 97(16), pp.9070–5.

Masters, B.S. et al., 1996. Neuronal nitric oxide synthase, a modular enzyme formed by convergent evolution: structure studies of a cysteine thiolate-liganded heme protein that hydroxylates L-arginine to produce NO. as a cellular signal. *FASEB journal : official publication of the Federation of American Societies for Experimental Biology*, 10(5), pp.552–8.

Matsushita, T. et al., 2008. Regulatory B cells inhibit EAE initiation in mice while other B cells promote disease progression. *Journal of Clinical Investigation*, 118(10), pp.3420–3430.

Matsuzaki, T. et al., 1997. Nuclear staining for laser confocal microscopy. *Acta Histochemica Et Cytochemica*, 30, pp.309–314.

Mauri, C. & Bosma, A., 2012. Immune regulatory function of B cells. *Annual review of immunology*, 30, pp.221–41.

Mazzoni, A. et al., 2002. Myeloid suppressor lines inhibit T cell responses by an NO-dependent mechanism. *Journal of immunology (Baltimore, Md. : 1950)*, 168(2), pp.689–95.

McGeachy, M.J., Stephens, L.A. & Anderton, S.M., 2005. Natural recovery and protection from autoimmune encephalomyelitis: contribution of CD4+CD25+ regulatory cells within the central nervous system. *Journal of immunology (Baltimore, Md. : 1950)*, 175(5), pp.3025–32.

McGuinness, B.T. et al., 1991. Point mutation in meningococcal por A gene associated with increased endemic disease. *Lance*, 337, pp.514–7.

McHeyzer-Williams, L.J. & McHeyzer-Williams, M.G., 2005. Antigen-specific memory B cell development. *Annual review of immunology*, 23(9), pp.487–513.

McHeyzer-Williams, M.G., 1989. Combinations of interleukins 2, 4 and 5 regulate the secretion of murine immunoglobulin isotypes. *European journal of immunology*, 19(11), pp.2025–30.

McNeil, G. & Virji, M., 1997. Phenotypic variants of meningococci and their potential in phagocytic interactions: the influence of opacity proteins, pili, PilC and surface sialic acids. *Microbial pathogenesis*, 22(5), pp.295–304.

Melino, G. et al., 1997. S-nitrosylation regulates apoptosis. *Nature*, 388(6641), pp.432–3.

Merz, a J., Enns, C. a & So, M., 1999. Type IV pili of pathogenic *Neisseriae* elicit cortical plaque formation in epithelial cells. *Molecular microbiology*, 32(6), pp.1316–32.

Messmer, U.K. et al., 1994. P53 Expression in Nitric Oxide-Induced Apoptosis. *FEBS letters*, 355(1), pp.23–6.

Miller, E., Salisbury, D. & Ramsay, M., 2002. Planning, registration, and implementation of an immunisation campaign against meningococcal serogroup C disease in the UK: a success story. *Vaccine*, 20 Suppl 1, pp.S58–67.

Mizoguchi, A. & Bhan, A.K., 2006. A case for regulatory B cells. *Journal of immunology (Baltimore, Md. : 1950)*, 176(2), pp.705–10.

Mocca, B. & Wang, W., 2012. Bacterium-generated nitric oxide hijacks host tumor necrosis factor alpha signaling and modulates the host cell cycle in vitro. *Journal of bacteriology*, 194(15), pp.4059–68.

Mond, J.J., Lees, A. & Snapper, C.M., 1995. T cell-independent antigens type 2. *Annual review of immunology*, 13, pp.655–92.

Monks, C.R. et al., 1998. Three-dimensional segregation of supramolecular activation clusters in T cells. *Nature*, 395(6697), pp.82–6.

Montoya, C.J. et al., 2007. Characterization of human invariant natural killer T subsets in health and disease using a novel invariant natural killer T cell-clonotypic monoclonal antibody, 6B11. *Immunology*, 122(1), pp.1–14.

Moore, K.W. et al., 2001. Interleukin-10 and the interleukin-10 receptor. *Annual review of immunology*, 19, pp.683–765.

Moriggl, R. et al., 1999. Stat5 is required for IL-2-induced cell cycle progression of peripheral T cells. *Immunity*, 10(2), pp.249–59.

Mosmann, T.R. et al., 1986. Two types of murine helper T cell clone. I. Definition according to profiles of lymphokine activities and secreted proteins. *Journal of immunology (Baltimore, Md. : 1950)*, 136(7), pp.2348–57.

Mosmann, T.R. & Sad, S., 1996. The expanding universe of T-cell subsets: Th1, Th2 and more. *Immunology today*, 17(3), pp.138–46.

Movahedi, K. et al., 2008. Identification of discrete tumor-induced myeloid-derived suppressor cell subpopulations with distinct T cell-suppressive activity. *Blood*, 111(8), pp.4233–44.

Muenzner, P. et al., 2000. Carcinoembryonic antigen family receptor specificity of *Neisseria meningitidis* Opa variants influences adherence to and invasion of proinflammatory cytokine-activated endothelial cells. *Infection and immunity*, 68(6), pp.3601–7.

Nabeshima, S. et al., 1999. T-Cell hyporesponsiveness induced by activated macrophages through nitric oxide production in mice infected with *Mycobacterium tuberculosis*. *Infection and immunity*, 67(7), pp.3221–6.

Nagaishi, T. et al., 2006. Role of CEACAM1 as a regulator of T cells. *Annals of the New York Academy of Sciences*, 1072, pp.155–75.

Nagy, G. et al., 2004. Nitric oxide-dependent mitochondrial biogenesis generates Ca2+ signaling profile of lupus T cells. *Journal of immunology (Baltimore, Md. : 1950)*, 173(6), pp.3676–83.

Nagy, G., Koncz, A. & Perl, A., 2003. T cell activation-induced mitochondrial hyperpolarization is mediated by Ca2+- and redox-dependent production of nitric oxide. *Journal of immunology (Baltimore, Md. : 1950)*, 171(10), pp.5188–97.

Nakajima, A. et al., 2002. Activation-induced expression of carcinoembryonic antigen-cell adhesion molecule 1 regulates mouse T lymphocyte function. *Journal of immunology (Baltimore, Md. : 1950)*, 168(3), pp.1028–35.

Nakamura, K., Brauweiler, A. & Cambier, J.C., 2000. Effects of Src homology domain 2 (SH2)-containing inositol phosphatase (SHIP), SH2-containing phosphotyrosine phosphatase (SHP)-1, and SHP-2 SH2 decoy proteins on Fc gamma RIIB1-effector interactions and inhibitory functions. *Journal of immunology (Baltimore, Md. : 1950)*, 164(2), pp.631–8.

Nakamura, T. et al., 1997. Polarization of IL-4- and IFN-gamma-producing CD4+ T cells following activation of naive CD4+ T cells. *Journal of immunology (Baltimore, Md. : 1950)*, 158(3), pp.1085–94.

Namork, E. & Brandtzaeg, P., 2002. Fatal meningococcal septicaemia with “blebbing” meningococcus. *Lancet*, 360(9347), p.1741.

Nassif, X. et al., 1994. Roles of pilin and PilC in adhesion of *Neisseria meningitidis* to human epithelial and endothelial cells. *Proceedings of the National Academy of Sciences of the United States of America*, 91(9), pp.3769–73.

Niedbala, W. et al., 1999. Effects of nitric oxide on the induction and differentiation of Th1 cells. *European journal of immunology*, 29(8), pp.2498–505.

Niedbala, W. et al., 2007. Nitric oxide induces CD4+CD25+ Foxp3 regulatory T cells from CD4+CD25 T cells via p53, IL-2, and OX40. *Proceedings of the National Academy of Sciences of the United States of America*, 104(39), pp.15478–83.

Niedbala, W. et al., 2002. Nitric oxide preferentially induces type 1 T cell differentiation by selectively up-regulating IL-12 receptor beta 2 expression via cGMP. *Proceedings of the National Academy of Sciences of the United States of America*, 99(25), pp.16186–91.

Niedbala, W., Cai, B. & Liew, F.Y., 2006. Role of nitric oxide in the regulation of T cell functions. *Annals of the rheumatic diseases*, 65 Suppl 3, pp.iii37–40.

Niiro, H. et al., 1995. Inhibition by interleukin-10 of inducible cyclooxygenase expression in lipopolysaccharide-stimulated monocytes: its underlying mechanism in comparison with interleukin-4. *Blood*, 85(12), pp.3736–45.

Nisoli, E. et al., 2004. Mitochondrial biogenesis by NO yields functionally active mitochondria in mammals. *Proceedings of the National Academy of Sciences of the United States of America*, 101(47), pp.16507–12.

Nisoli, E. et al., 2003. Mitochondrial biogenesis in mammals: the role of endogenous nitric oxide. *Science (New York, N.Y.)*, 299(5608), pp.896–9.

Nordström, T. et al., 2006. The IgD-binding domain of the *Moraxella* IgD-binding protein MID (MID962-1200) activates human B cells in the presence of T cell cytokines. *Journal of leukocyte biology*, 79(2), pp.319–29.

Nordström, T., Forsgren, A. & Riesbeck, K., 2002. The immunoglobulin D-binding part of the outer membrane protein MID from *Moraxella catarrhalis* comprises 238 amino acids and a tetrameric structure. *The Journal of biological chemistry*, 277(38), pp.34692–9.

Nukaya, I. et al., 1995. Suppression of cytokine production in T helper type 2 cells by nitric oxide in comparison with T helper type 1 cells. *Microbiology and immunology*, 39(9), pp.709–14.

Obukhanych, T. V & Nussenzweig, M.C., 2006. T-independent type II immune responses generate memory B cells. *The Journal of experimental medicine*, 203(2), pp.305–10.

Ohnuma, K. et al., 2007. Caveolin-1 triggers T-cell activation via CD26 in association with CARMA1. *The Journal of biological chemistry*, 282(13), pp.10117–31.

Oliver, K.J. et al., 2002. *Neisseria lactamica* protects against experimental meningococcal infection. *Infection and immunity*, 70(7), pp.3621–6.

Van der Oost, J. et al., 1994. The heme-copper oxidase family consists of three distinct types of terminal oxidases and is related to nitric oxide reductase. *FEMS microbiology letters*, 121(1), pp.1–9.

Øvstebø, R. et al., 2004. Use of robotized DNA isolation and real-time PCR to quantify and identify close correlation between levels of *Neisseria meningitidis* DNA and lipopolysaccharides in plasma and cerebrospinal fluid from patients with systemic meningococcal disease. *Journal of clinical microbiology*, 42(7), pp.2980–7.

Ozaki, K. et al., 2002. A critical role for IL-21 in regulating immunoglobulin production. *Science (New York, N.Y.)*, 298(5598), pp.1630–4.

Pace, D., Pollard, A.J. & Messonier, N.E., 2009. Quadrivalent meningococcal conjugate vaccines. *Vaccine*, 27 Suppl 2, pp.B30–41.

Pacelli, R. et al., 1995. Nitric oxide potentiates hydrogen peroxide-induced killing *of Escherichia coli*. *The Journal of experimental medicine*, 182(5), pp.1469–79.

Palacios, R., 1985. Mechanisms by which accessory cells contribute in growth of resting T lymphocytes initiated by OKT3 antibody. *European Journal of Immunology*, 15, pp.645–651.

Palmer, R.M., Ferrige, A.G. & Moncada, S., 1987. Nitric oxide release accounts for the biological activity of endothelium-derived relaxing factor. *Nature*, 327, pp.524–526.

Park, C.S. et al., 2000. Differential and constitutive expression of neuronal, inducible, and endothelial nitric oxide synthase mRNAs and proteins in pathologically normal human tissues. *Nitric oxide : biology and chemistry / official journal of the Nitric Oxide Society*, 4(5), pp.459–71.

Park, H. et al., 2005. A distinct lineage of CD4 T cells regulates tissue inflammation by producing interleukin 17. *Nature immunology*, 6(11), pp.1133–41.

Park, H.-S. et al., 2004. Inhibition of apoptosis signal-regulating kinase 1 by nitric oxide through a thiol redox mechanism. *The Journal of biological chemistry*, 279(9), pp.7584–90.

Pasare, C. & Medzhitov, R., 2005. Control of B-cell responses by Toll-like receptors. *Nature*, 438(7066), pp.364–8.

Peçanha, L.M. et al., 1991. Dextran-conjugated anti-Ig antibodies as a model for T cell-independent type 2 antigen-mediated stimulation of Ig secretion in vitro. I. Lymphokine dependence. *Journal of immunology (Baltimore, Md. : 1950)*, 146(3), pp.833–9.

Peçanha, L.M. et al., 1993. Dextran-conjugated anti-IgD antibodies inhibit T cell-mediated IgE production but augment the synthesis of IgM and IgG. *Journal of immunology (Baltimore, Md. : 1950)*, 150(6), pp.2160–8.

Perfetto, S.P. et al., 2006. Amine reactive dyes: an effective tool to discriminate live and dead cells in polychromatic flow cytometry. *Journal of Immunological Methods*, 313, pp.199–208.

Peritt, D. et al., 1998. Differentiation of human NK cells into NK1 and NK2 subsets. *Journal of immunology (Baltimore, Md. : 1950)*, 161(11), pp.5821–4.

Perl, A. et al., 2004. Mitochondrial hyperpolarization: a checkpoint of T-cell life, death and autoimmunity. *Trends in immunology*, 25(7), pp.360–7.

Petros, A. et al., 1994. Effects of a nitric oxide synthase inhibitor in humans with septic shock. *Cardiovascular research*, 28(1), pp.34–9.

Pike, B.L. & Nossal, G.J., 1984. A reappraisal of “T-independent” antigens. I. Effect of lymphokines on the response of single adult hapten-specific B lymphocytes. *Journal of immunology (Baltimore, Md. : 1950)*, 132(4), pp.1687–95.

Pipkorn, U., Karlsson, G. & Enerbäck, L., 1988. A brush method to harvest cells from the nasal mucosa for microscopic and biochemical analysis. *Journal of immunological methods*, 112(1), pp.37–42.

Pizza, M. et al., 2000. Identification of vaccine candidates against serogroup B meningococcus by whole-genome sequencing. *Science*, 287(5459), pp.1816–1820.

Premack, B. a & Gardner, P., 1992. Signal transduction by T-cell receptors: mobilization of Ca and regulation of Ca-dependent effector molecules. *The American journal of physiology*, 263(6 Pt 1), pp.C1119–40.

Del Prete, G.F. et al., 1991. Purified protein derivative of *Mycobacterium tuberculosis* and excretory-secretory antigen(s) of *Toxocara canis* expand in vitro human T cells with stable and opposite (type 1 T helper or type 2 T helper) profile of cytokine production. *The Journal of clinical investigation*, 88(1), pp.346–50.

Pridmore, a C. et al., 2001. A lipopolysaccharide-deficient mutant of *Neisseria meningitidis* elicits attenuated cytokine release by human macrophages and signals via toll-like receptor (TLR) 2 but not via TLR4/MD2. *The Journal of infectious diseases*, 183(1), pp.89–96.

Pridmore, A.C. et al., 2003. Activation of toll-like receptor 2 (TLR2) and TLR4/MD2 by *Neisseria* is independent of capsule and lipooligosaccharide (LOS) sialylation but varies widely among LOS from different strains. *Infection and immunity*, 71(7), pp.3901–8.

Quezada, S. a et al., 2004. CD40/CD154 interactions at the interface of tolerance and immunity. *Annual review of immunology*, 22, pp.307–28.

Rawlings, D.J. et al., 1993. Mutation of unique region of Bruton’s tyrosine kinase in immunodeficient XID mice. *Science*, 261, pp.358–361.

Rayner, C.F. et al., 1995. The effect of variations in the expression of pili on the interaction of *Neisseria meningitidis* with human nasopharyngeal epithelium. *The Journal of Infectious Diseases*, 171, pp.113–121.

Read, R.C. et al., 1996. The (alpha2-->8)-linked polysialic acid capsule of group B *Neisseria meningitidis* modifies multiple steps during interaction with human macrophages. *Infection and immunity*, 64(8), pp.3210–7.

Rees, D.D. et al., 1990. Characterization of three inhibitors of endothelial nitric oxide synthase in vitro and in vivo. *British journal of pharmacology*, 101(3), pp.746–52.

Rehe, G.T. et al., 1990. Activation of human B lymphocytes by nanogram concentrations of anti-IgM-dextran conjugates. *European Journal of Immunology*, 20, pp.1837–1842.

Reiling, N. et al., 1996. Nitric oxide synthase: expression of the endothelial, Ca2+/calmodulin-dependent isoform in human B and T lymphocytes. *European journal of immunology*, 26(3), pp.511–6.

Reimold, a M. et al., 2001. Plasma cell differentiation requires the transcription factor XBP-1. *Nature*, 412(6844), pp.300–307.

Reynaert, N.L. et al., 2004. Nitric oxide represses inhibitory *kappaB* kinase through S-nitrosylation. *Proceedings of the National Academy of Sciences of the United States of America*, 101(24), pp.8945–50.

Riley, J.L., 2009. PD-1 signaling in primary T cells. *Immunological reviews*, 229(1), pp.114–25.

Riley, J.L. & June, C.H., 2005. The CD28 family: a T-cell rheostat for therapeutic control of T-cell activation. *Blood*, 105(1), pp.13–21.

Rissoan, M.C. et al., 1999. Reciprocal control of T helper cell and dendritic cell differentiation. *Science (New York, N.Y.)*, 283(5405), pp.1183–6.

Rivera, A. et al., 2001. Role of B cells as antigen-presenting cells in vivo revisited: antigen-specific B cells are essential for T cell expansion in lymph nodes and for systemic T cell responses to low antigen concentrations. *International immunology*, 13(12), pp.1583–93.

Robb, R.J., Greene, W.C. & Rusk, C.M., 1984. Low and high affinity cellular receptors for interleukin 2. Implications for the level of Tac antigen. *The Journal of experimental medicine*, 160(4), pp.1126–46.

Robinson, K. et al., 2002. Characterization of humoral and cellular immune responses elicited by meningococcal carriage. *Infection and immunity*, 70(3), pp.1301–9.

Rock, J.D. et al., 2007. Regulation of denitrification genes in *Neisseria meningitidis* by nitric oxide and the repressor NsrR. *Journal of bacteriology*, 189(3), pp.1138–44.

Rock, J.D. et al., 2005. The pathogen *Neisseria meningitidis* requires oxygen, but supplements growth by denitrification. Nitrite, nitric oxide and oxygen control respiratory flux at genetic and metabolic levels. *Molecular microbiology*, 58(3), pp.800–9.

Rodriguez-Feo, J. a et al., 2008. Caveolin-1 influences vascular protease activity and is a potential stabilizing factor in human atherosclerotic disease. *PloS one*, 3(7), p.e2612.

Rosenstein, N.E. et al., 2001. Meningococcal disease. *The New England journal of medicine*, 344(18), pp.1378–88.

Rousset, F. et al., 1992. Interleukin 10 is a potent growth and differentiation factor for activated human B lymphocytes. *Proceedings of the National Academy of Sciences of the United States of America*, 89(5), pp.1890–3.

Rouvier, E., Luciani, M.F. & Golstein, P., 1993. Fas involvement in Ca(2+)-independent T cell-mediated cytotoxicity. *The Journal of experimental medicine*, 177(1), pp.195–200.

Rowe, H. a et al., 2007. Co-ordinate action of bacterial adhesins and human carcinoembryonic antigen receptors in enhanced cellular invasion by capsulate serum resistant *Neisseria meningitidis. Cellular microbiology*, 9(1), pp.154–68.

Rudd, C.E., Taylor, A. & Schneider, H., 2009. CD28 and CTLA-4 coreceptor expression and signal transduction. *Immunological reviews*, 229(1), pp.12–26.

Ruprecht, C.R. & Lanzavecchia, A., 2006. Toll-like receptor stimulation as a third signal required for activation of human naive B cells. *European journal of immunology*, 36(4), pp.810–6.

Russell, J.H. & Ley, T.J., 2002. Lymphocyte-mediated cytotoxicity. *Annual review of immunology*, 20(6), pp.323–70.

Sadarangani, M. et al., 2012. Construction of Opa-positive and Opa-negative strains of *Neisseria meningitidis* to evaluate a novel meningococcal vaccine. *PloS one*, 7(12), p.e51045.

Sadarangani, M., Pollard, A.J. & Gray-Owen, S.D., 2011. Opa proteins and CEACAMs: pathways of immune engagement for pathogenic *Neisseria*. *FEMS microbiology reviews*, 35(3), pp.498–514.

Sakaguchi, S. et al., 1995. Immunologic self-tolerance maintained by activated T cells expressing IL-2 receptor alpha-chains (CD25). Breakdown of a single mechanism of self-tolerance causes various autoimmune diseases. *Journal of immunology (Baltimore, Md. : 1950)*, 155(3), pp.1151–64.

Sakaguchi, S. et al., 2008. Regulatory T cells and immune tolerance. *Cell*, 133(5), pp.775–87.

Salerno, J.C. et al., 1997. An autoinhibitory control element defines calcium-regulated isoforms of nitric oxide synthase. *The Journal of biological chemistry*, 272(47), pp.29769–77.

Sandau, K. & Brüne, B., 1996. The dual role of S-nitrosoglutathione (GSNO) during thymocyte apoptosis. *Cellular signalling*, 8(3), pp.173–7.

Sato, K. et al., 2007. Nitric oxide plays a critical role in suppression of T-cell proliferation by mesenchymal stem cells. *Blood*, 109(1), pp.228–34.

Scarselli, M. et al., 2006. *Neisseria meningitidis* NhhA is a multifunctional trimeric autotransporter adhesin. *Molecular microbiology*, 61(3), pp.631–44.

Schandené, L. et al., 1994. B7/CD28-dependent IL-5 production by human resting T cells is inhibited by IL-10. *Journal of immunology (Baltimore, Md. : 1950)*, 152(9), pp.4368–74.

Schapiro, J.M., Libby, S.J. & Fang, F.C., 2003. Inhibition of bacterial DNA replication by zinc mobilization during nitrosative stress. *Proceedings of the National Academy of Sciences of the United States of America*, 100(14), pp.8496–501.

Schmitt, C. et al., 2007. A functional two-partner secretion system contributes to adhesion of *Neisseria meningitidis* to epithelial cells. *Journal of bacteriology*, 189(22), pp.7968–76.

Schwacha, M.G., Meissler, J.J. & Eisenstein, T.K., 1998. Salmonella typhimurium infection in mice induces nitric oxide-mediated immunosuppression through a natural killer cell-dependent pathway. *Infection and immunity*, 66(12), pp.5862–6.

Schwartz, R.H., 1990. A cell culture model for T lymphocyte clonal anergy. *Science (New York, N.Y.)*, 248(4961), pp.1349–56.

Sedy, J.R. et al., 2005. B and T lymphocyte attenuator regulates T cell activation through interaction with herpesvirus entry mediator. *Nature immunology*, 6(1), pp.90–8.

Sena, L.A. et al., 2013. Mitochondria are required for antigen-specific T cell activation through reactive oxygen species signaling. *Immunity*, 38(2), pp.225–36.

Serrato, J.A. et al., 2004. Heterogeneous conditions in dissolved oxygen affect N-glycosylation but not productivity of a monoclonal antibody in hybridoma cultures. *Biotechnology and Bioengineering*, 88, pp.176–188.

Serruto, D. et al., 2012. The new multicomponent vaccine against meningococcal serogroup B, 4CMenB: immunological, functional and structural characterization of the antigens. *Vaccine*, 30 Suppl 2, pp.B87–97.

Shalova, I.N. et al., 2012. CD16 regulates TRIF-dependent TLR4 response in human monocytes and their subsets. *Journal of immunology (Baltimore, Md. : 1950)*, 188(8), pp.3584–93.

Shevach, E.M., 2009. Mechanisms of foxp3+ T regulatory cell-mediated suppression. *Immunity*, 30(5), pp.636–45.

Shi, F.D. et al., 2000. Natural killer cells determine the outcome of B cell-mediated autoimmunity. *Nature immunology*, 1(3), pp.245–51.

Shih, T.-A.Y. et al., 2002. Role of BCR affinity in T cell dependent antibody responses in vivo. *Nature immunology*, 3(6), pp.570–5.

Shultz, P.J. & Raij, L., 1992. Endogenously synthesized nitric oxide prevents endotoxin-induced glomerular thrombosis. *The Journal of clinical investigation*, 90(5), pp.1718–25.

Sica, G.L. et al., 2003. B7-H4, a molecule of the B7 family, negatively regulates T cell immunity. *Immunity*, 18(6), pp.849–61.

Siliciano, R.F. et al., 1985. Activation of cytolytic T lymphocyte and natural killer cell function through the T11 sheep erythrocyte binding protein. *Nature*, 317(6036), pp.428–30.

Slaney, C.Y. et al., 2011. Naïve blood monocytes suppress T-cell function. A possible mechanism for protection from autoimmunity. *Immunology and cell biology*, 89(1), pp.7–13.

Smith-Garvin, J.E., Koretzky, G. a & Jordan, M.S., 2009. T cell activation. *Annual review of immunology*, 27, pp.591–619.

Snape, M.D. et al., 2008. Immunogenicity of a tetravalent meningococcal glycoconjugate vaccine in infants: a randomized controlled trial. *JAMA : the journal of the American Medical Association*, 299(2), pp.173–84.

Snapper, C.M. et al., 1992. Induction of IgG3 secretion by interferon gamma: a model for T cell-independent class switching in response to T cell-independent type 2 antigens. *The Journal of experimental medicine*, 175(5), pp.1367–71.

Snapper, C.M., 2012. Mechanisms underlying in vivo polysaccharide-specific immunoglobulin responses to intact extracellular bacteria. *Annals of the New York Academy of Sciences*, 1253, pp.92–101.

Snapper, C.M. et al., 1995. Multivalent, but not divalent, antigen receptor cross-linkers synergize with CD40 ligand for induction of Ig synthesis and class switching in normal murine B cells. A redefinition of the TI-2 vs T cell-dependent antigen dichotomy. *Journal of immunology (Baltimore, Md. : 1950)*, 154(3), pp.1177–87.

Snapper, C.M. et al., 1997. Neisserial porins may provide critical second signals to polysaccharide-activated murine B cells for induction of immunoglobulin secretion. *Infection and immunity*, 65(8), pp.3203–8.

Snapper, C.M. & Mond, J.J., 1996. A model for induction of T cell-independent humoral immunity in response to polysaccharide antigens. *Journal of immunology (Baltimore, Md. : 1950)*, 157(6), pp.2229–33.

Sonoda, E. et al., 1989. Transforming growth factor beta induces IgA production and acts additively with interleukin 5 for IgA production. *The Journal of experimental medicine*, 170(4), pp.1415–20.

Sprong, T. et al., 2001. Contributions of *Neisseria meningitidis* LPS and non-LPS to proinflammatory cytokine response. *Journal of leukocyte biology*, 70(2), pp.283–8.

Srinivasan, A. & McSorley, S.J., 2007. Pivotal advance: exposure to LPS suppresses CD4+ T cell cytokine production in Salmonella-infected mice and exacerbates murine typhoid. *Journal of leukocyte biology*, 81(2), pp.403–11.

Sriskandan, S., Evans, T.J. & Cohen, J., 1996. Bacterial superantigen-induced human lymphocyte responses are nitric oxide dependent and mediated by IL-12 and IFN-gamma. *Journal of immunology (Baltimore, Md. : 1950)*, 156(7), pp.2430–5.

Stamler, J.S. et al., 1992. S-nitrosylation of proteins with nitric oxide: synthesis and characterization of biologically active compounds. *Proceedings of the National Academy of Sciences of the United States of America*, 89(1), pp.444–8.

Stamler, J.S., Lamas, S. & Fang, F.C., 2001. Nitrosylation. the prototypic redox-based signaling mechanism. *Cell*, 106(6), pp.675–83.

Stassen, M., Schmitt, E. & Bopp, T., 2012. From interleukin-9 to T helper 9 cells. *Annals of the New York Academy of Sciences*, 1247, pp.56–68.

Staudt, V. et al., 2010. Interferon-regulatory factor 4 is essential for the developmental program of T helper 9 cells. *Immunity*, 33(2), pp.192–202.

Steeghs L, den Hartog R, den Boer A, Zomer B, Roholl P, van der L.P., 1998. Meningitis bacterium is viable without endotoxin. *Nature.*, 392(6675), pp.449–50.

Steeghs, L. et al., 1997. Isolation and characterization of the *Neisseria meningitidis* lpxD-fabZ-lpxA gene cluster involved in lipid A biosynthesis. *Gene*, 190(2), pp.263–70.

Stephens, D.S., Greenwood, B. & Brandtzaeg, P., 2007. Epidemic meningitis, meningococcaemia, and *Neisseria meningitidis*. *Lancet*, 369(9580), pp.2196–210.

Stephens, D.S. & McGee, Z.A., 1981. Attachment of *Neisseria meningitidis* to human mucosal surfaces: influence of pili and type of receptor cell. *The Journal of infectious diseases*, 143(4), pp.525–32.

Stevanin, T.M. et al., 2007. Metabolism of nitric oxide by *Neisseria meningitidis* modifies release of NO-regulated cytokines and chemokines by human macrophages. *Microbes and infection / Institut Pasteur*, 9(8), pp.981–7.

Stevanin, T.M., Moir, J.W.B. & Read, R.C., 2005. Nitric oxide detoxification systems enhance survival of *Neisseria meningitidis* in human macrophages and in nasopharyngeal mucosa. *Infection and immunity*, 73(6), pp.3322–9.

Stockinger, B. et al., 1996. B cells solicit their own help from T cells. *The Journal of experimental medicine*, 183(3), pp.891–9.

Strickland, D., Kees, U.R. & Holt, P.G., 1996. Regulation of T-cell activation in the lung: alveolar macrophages induce reversible T-cell anergy in vitro associated with inhibition of interleukin-2 receptor signal transduction. *Immunology*, 87(2), pp.250–8.

Stuber, E., Strober, W. & Neurath, M., 1996. Blocking the CD40L-CD40 interaction in vivo specifically prevents the priming of T helper 1 cells through the inhibition of interleukin 12 secretion. *The Journal of experimental medicine*, 183(2), pp.693–8.

Stuehr, D.J., 1997. Structure-function aspects in the nitric oxide synthases. *Annual review of pharmacology and toxicology*, 37, pp.339–59.

Sulzer, B. & Perelson, a S., 1997. Immunons revisited: binding of multivalent antigens to B cells. *Molecular immunology*, 34(1), pp.63–74.

Sundrani, R. et al., 2000. Nitric oxide synthase inhibition increases venular leukocyte rolling and adhesion in septic rats. *Critical care medicine*, 28(8), pp.2898–903.

Takeda, K. et al., 1996. Essential role of Stat6 in IL-4 signalling. *Nature*, 380, pp.627–630.

Tan, L.K.K., Carlone, G.M. & Borrow, R., 2010. Advances in the development of vaccines against *Neisseria meningitidis*. *The New England journal of medicine*, 362(16), pp.1511–20.

Tauseef, I., Ali, Y.M. & Bayliss, C.D., 2013. Phase variation of PorA, a major outer membrane protein, mediates escape of bactericidal antibodies by *Neisseria meningitidis*. *Infection and immunity*, 81(4), pp.1374–80.

Taylor, A. et al., 2006. Mechanisms of immune suppression by interleukin-10 and transforming growth factor-beta: the role of T regulatory cells. *Immunology*, 117(4), pp.433–42.

Taylor, B.S. et al., 1998. Multiple NF-kappaB enhancer elements regulate cytokine induction of the human inducible nitric oxide synthase gene. *The Journal of biological chemistry*, 273(24), pp.15148–56.

Tettelin, H. et al., 2000. Complete genome sequence of *Neisseria meningitidis* serogroup B strain MC58. *Science (New York, N.Y.)*, 287(5459), pp.1809–15.

Theilen, U. et al., 2008. Management of invasive meningococcal disease in children and young people: summary of SIGN guidelines. *BMJ (Clinical research ed.)*, 336(7657), pp.1367–70.

Thomsen, a R. et al., 1996. Exhaustion of CTL memory and recrudescence of viremia in lymphocytic choriomeningitis virus-infected MHC class II-deficient mice and B cell-deficient mice. *Journal of immunology (Baltimore, Md. : 1950)*, 157(7), pp.3074–80.

Toleman, M., Aho, E. & Virji, M., 2001. Expression of pathogen-like Opa adhesins in commensal *Neisseria*: genetic and functional analysis. *Cellular microbiology*, 3(1), pp.33–44.

Tomassian, T. et al., 2011. Caveolin-1 orchestrates TCR synaptic polarity, signal specificity, and function in CD8 T cells. *Journal of immunology (Baltimore, Md. : 1950)*, 187(6), pp.2993–3002.

Tretter, T. et al., 2008. Induction of CD4+ T-cell anergy and apoptosis by activated human B cells. *Blood Neisseria meningitidis,* 112(12), pp.4555–64.

Trifari, S. et al., 2009. Identification of a human helper T cell population that has abundant production of interleukin 22 and is distinct from T(H)-17, T(H)1 and T(H)2 cells. *Nature immunology*, 10(8), pp.864–71.

Troncoso, G. et al., 2002. Analysis of *Neisseria lactamica* antigens putatively implicated in acquisition of natural immunity to *Neisseria meningitidis*. *FEMS immunology and medical microbiology*, 34(1), pp.9–15.

Tu, W. et al., 2008. Efficient generation of human alloantigen-specific CD4+ regulatory T cells from naive precursors by CD40-activated B cells. *Blood*, 112(6), pp.2554–62.

Tunbridge, A.J. et al., 2006. Inhibition of macrophage apoptosis by *Neisseria meningitidis* requires nitric oxide detoxification mechanisms. *Infection and immunity*, 74(1), pp.729–33.

Turner, C.A., Mack, D.H. & Davis, M.M., 1994. Blimp-1, a novel zinc finger-containing protein that can drive the maturation of B lymphocytes into immunoglobulin-secreting cells. *Cell*, 77(2), pp.297–306.

Tuveson, D.A. et al., 1993. CD19 of B cells as a surrogate kinase insert region to bind phosphatidylinositol 3-kinase. *Science*, 260, pp.986–989.

Unkmeir, A., Latsch, K., et al., 2002. Fibronectin mediates Opc-dependent internalization of *Neisseria meningitidis* in human brain microvascular endothelial cells. *Molecular microbiology*, 46(4), pp.933–46.

Unkmeir, A., Kämmerer, U., et al., 2002. Lipooligosaccharide and polysaccharide capsule: virulence factors of *Neisseria meningitidis* that determine meningococcal interaction with human dendritic cells. *Infection and immunity*, 70(5), pp.2454–62.

Urwin, R. et al., 2004. Distribution of surface protein variants among hyperinvasive meningococci: implications for vaccine design. *Infection and immunity*, 72(10), pp.5955–62.

Ushmorov, a et al., 1999. Nitric-oxide-induced apoptosis in human leukemic lines requires mitochondrial lipid degradation and cytochrome C release. *Blood*, 93(7), pp.2342–52.

Valenti, L.M. et al., 2005. High levels of endogenous nitric oxide produced after burn injury in rats arrest activated T lymphocytes in the first G1 phase of the cell cycle and then induce their apoptosis. *Experimental cell research*, 306(1), pp.150–67.

Vallejo, J. & Hardin, C.D., 2005. Expression of caveolin-1 in lymphocytes induces caveolae formation and recruitment of phosphofructokinase to the plasma membrane. *FASEB journal : official publication of the Federation of American Societies for Experimental Biology*, 19(6), pp.586–7.

Vaughan, T.E. et al., 2006. Proteomic analysis of *Neisseria lactamica* and *Neisseria meningitidis* outer membrane vesicle vaccine antigens. *Vaccine*, 24(25), pp.5277–93.

Vayuvegula, B. et al., 1990. Role of monocytes in anti-CD3-induced T-cell DNA synthesis: effect of chloroquine and monensin on anti-CD3-induced human T-cell activation. *Journal of clinical immunology*, 10(5), pp.247–54.

Vazquez-Torres, A., Jones-Carson, J. & Balish, E., 1995. Nitric oxide production does not directly increase macrophage candidacidal activity. *Infection and immunity*, 63(3), pp.1142–4.

Van der Veen, R.C., Dietlin, T. a, Pen, L., et al., 2000. Antigen presentation to Th1 but not Th2 cells by macrophages results in nitric oxide production and inhibition of T cell proliferation: interferon-gamma is essential but insufficient. *Cellular immunology*, 206(2), pp.125–35.

Van der Veen, R.C., Dietlin, T. a, Dixon Gray, J., et al., 2000. Macrophage-derived nitric oxide inhibits the proliferation of activated T helper cells and is induced during antigenic stimulation of resting T cells. *Cellular immunology*, 199(1), pp.43–9.

Van der Veen, R.C. et al., 1999. Nitric oxide inhibits the proliferation of T-helper 1 and 2 lymphocytes without reduction in cytokine secretion. *Cellular immunology*, 193(2), pp.194–201.

Vendel, A.C. et al., 2009. B and T lymphocyte attenuator regulates B cell receptor signaling by targeting Syk and BLNK. *Journal of immunology (Baltimore, Md. : 1950)*, 182(3), pp.1509–17.

De Vera, M.E. et al., 1996. Transcriptional regulation of human inducible nitric oxide synthase (NOS2) gene by cytokines: initial analysis of the human NOS2 promoter. *Proceedings of the National Academy of Sciences of the United States of America*, 93(3), pp.1054–9.

Vermes, I. et al., 1995. A novel assay for apoptosis. Flow cytometric detection of phosphatidylserine expression on early apoptotic cells using fluorescein labelled Annexin V. *Journal of Immunological Methods*, 184, pp.39–51.

Vermes, I., Haanen, C. & Reutelingsperger, C., 2000. Flow cytometry of apoptotic cell death. *Journal of Immunological Methods*, 243(1-2), pp.167–190.

Vieusseux, 1806. Memoire sur la maladie qui a regne a Geneve au printemps de 1805. *J Med Chir Pharm*, 11, pp.163–182.

Villadangos, J. a, 2001. Presentation of antigens by MHC class II molecules: getting the most out of them. *Molecular Immunology*, 38(5), pp.329–346.

Virji, M. et al., 1995. Opc- and pilus-dependent interactions of meningococci with human endothelial cells: molecular mechanisms and modulation by surface polysaccharides. *Molecular Microbiology*, 18, pp.741–754.

Virji, M. et al., 1991. The role of pili in the interactions of pathogenic *Neisseria* with cultured human endothelial cells. *Molecular microbiology*, 5(8), pp.1831–41.

Vos, Q. et al., 2000. B-cell activation by T-cell-independent type 2 antigens as an integral part of the humoral immune response to pathogenic microorganisms. *Immunological reviews*, 176, pp.154–70.

De Vries, F.P. et al., 1998. *Neisseria meningitidis* producing the Opc adhesin binds epithelial cell proteoglycan receptors. *Molecular microbiology*, 27(6), pp.1203–12.

Walker, C. et al., 1991. T cell subsets and their soluble products regulate eosinophilia in allergic and nonallergic asthma. *Journal of immunology (Baltimore, Md. : 1950)*, 146(6), pp.1829–35.

Wang, J. et al., 2007. Transient expression of FOXP3 in human activated nonregulatory CD4+ T cells. *European journal of immunology*, 37(1), pp.129–38.

Wang, P. et al., 1995. Interleukin (IL)-10 inhibits nuclear factor kappa B (NF kappa B) activation in human monocytes. IL-10 and IL-4 suppress cytokine synthesis by different mechanisms. *The Journal of biological chemistry*, 270(16), pp.9558–63.

Wang, X. et al., 2012. B7-H4 Treatment of T Cells Inhibits ERK, JNK, p38, and AKT Activation. *PloS one*, 7(1), p.e28232.

Watanabe, N. et al., 2003. BTLA is a lymphocyte inhibitory receptor with similarities to CTLA-4 and PD-1. *Nature immunology*, 4(7), pp.670–9.

Van de Waterbeemd, B. et al., 2012. Identification and optimization of critical process parameters for the production of NOMV vaccine against *Neisseria meningitidis*. *Vaccine*, 30(24), pp.3683–90.

Weichselbaum, A., 1887. Uber die aetiologie der akuten meningitis cerebro-spinalis. *Fortschr Med*, 5, pp.573–583.

Wetzler, L.M., 1994. Immunopotentiating ability of neisserial major outer membrane proteins. Use as an adjuvant for poorly immunogenic substances and potential use in vaccines. *Annals of the New York Academy of Sciences*, 730, pp.367–70.

Whitmire, J.K. et al., 2009. Requirement of B cells for generating CD4+ T cell memory. *Journal of immunology (Baltimore, Md. : 1950)*, 182(4), pp.1868–76.

WHO, 2012. Bacterial Meningitis. Available at: http://www.who.int/nuvi/meningitis/en/.

WHO, 2013. Weekly epidemiological record Relevé épidémiologique hebdomadaire. , (12), pp.129–136.

Wiertz, E.J. et al., 1996. T-cell responses to outer membrane proteins of *Neisseria meningitidis*: comparative study of the Opa, Opc, and PorA proteins. *Infection and immunity*, 64(1), pp.298–304.

Wilhelm, S., Wagner, H. & Häcker, G., 1998. Activation of caspase-3-like enzymes in non-apoptotic T cells. *European journal of immunology*, 28(3), pp.891–900.

Williams, J.G., Pappu, K. & Campbell, S.L., 2003. Structural and biochemical studies of p21Ras S-nitrosylation and nitric oxide-mediated guanine nucleotide exchange. *Proceedings of the National Academy of Sciences of the United States of America*, 100(11), pp.6376–81.

Williams, M.S. et al., 1998. Nitric oxide synthase plays a signaling role in TCR-triggered apoptotic death. *Journal of immunology (Baltimore, Md. : 1950)*, 161(12), pp.6526–31.

Wink, D. a et al., 1991. DNA deaminating ability and genotoxicity of nitric oxide and its progenitors. *Science (New York, N.Y.)*, 254(5034), pp.1001–3.

Winkler, F. et al., 2001. Differential expression of nitric oxide synthases in bacterial meningitis: role of the inducible isoform for blood-brain barrier breakdown. *The Journal of infectious diseases*, 183(12), pp.1749–59.

Wintermeyer, P. et al., 2009. Invariant natural killer T cells suppress the neutrophil inflammatory response in a mouse model of cholestatic liver damage. *Gastroenterology*, 136(3), pp.1048–59.

Wolk, K. et al., 2000. Impaired antigen presentation by human monocytes during endotoxin tolerance. *Blood*, 96(1), pp.218–23.

Wong, H.R. et al., 1996. Nitric oxide production in critically ill patients. *Archives of disease in childhood*, 74(6), pp.482–9.

Van der Woude, M.W. & Bäumler, A.J., 2004. Phase and antigenic variation in bacteria. *Clinical microbiology reviews*, 17(3), pp.581–611, table of contents.

Xie, Q.W. et al., 1992. Cloning and characterization of inducible nitric oxide synthase from mouse macrophages. *Science*, 256, pp.225–228.

Xu, H. et al., 2008. The modulatory effects of lipopolysaccharide-stimulated B cells on differential T-cell polarization. *Immunology*, 125(2), pp.218–28.

Yanaba, K. et al., 2008. A regulatory B cell subset with a unique CD1dhiCD5+ phenotype controls T cell-dependent inflammatory responses. *Immunity*, 28(5), pp.639–50.

Yanaba, K. et al., 2009. The development and function of regulatory B cells expressing IL-10 (B10 cells) requires antigen receptor diversity and TLR signals. *Journal of immunology (Baltimore, Md. : 1950)*, 182(12), pp.7459–72.

Yazdankhah, S.P. & Caugant, D.A., 2004. Neisseria meningitidis: an overview of the carriage state. *Journal of Medical Microbiology*, 53(Pt 9), pp.821–832.

Yoshida, T. et al., 2010. Memory B and memory plasma cells. *Immunological reviews*, 237(1), pp.117–39.

Yoshizaki, A. et al., 2012. Regulatory B cells control T-cell autoimmunity through IL-21-dependent cognate interactions. *Nature*, 491(7423), pp.264–8.

Youssef, A.-R. et al., 2009. Opa+ and Opa- isolates of *Neisseria meningitidis* and *Neisseria gonorrhoeae* induce sustained proliferative responses in human CD4+ T cells. *Infection and immunity*, 77(11), pp.5170–80.

Zang, X. et al., 2003. B7x: a widely expressed B7 family member that inhibits T cell activation. *Proceedings of the National Academy of Sciences of the United States of America*, 100(18), pp.10388–92.

Zembowicz, a & Vane, J.R., 1992. Induction of nitric oxide synthase activity by toxic shock syndrome toxin 1 in a macrophage-monocyte cell line. *Proceedings of the National Academy of Sciences of the United States of America*, 89(6), pp.2051–5.

Zhu, W. et al., 2012. *Neisseria gonorrhoeae* suppresses dendritic cell-induced, antigen-dependent CD4 T cell proliferation. *PloS one*, 7(7), p.e41260.

Ziegler-Heitbrock, L. et al., 2010. Nomenclature of monocytes and dendritic cells in blood. *Blood*, 116(16), pp.e74–80.

Ziegler-Heitbrock, L., 2007. The CD14+ CD16+ blood monocytes: their role in infection and inflammation. *Journal of leukocyte biology*, 81(3), pp.584–92.

Zughaier, S.M., 2011. *Neisseria meningitidis* capsular polysaccharides induce inflammatory responses via TLR2 and TLR4-MD-2. *Journal of leukocyte biology*, 89(3), pp.469–80.

Zughaier, S.M. et al., 2004. *Neisseria meningitidis* lipooligosaccharide structure-dependent activation of the macrophage CD14/Toll-like receptor 4 pathway. *Infection and immunity*, 72(1), pp.371–80.